National Library of Canada

Acquisitions and Bibliographic Services Branch

395 Wellington Street
Ottawa, Ontario
K1A 0N4

Bibliothèque nationale du Canada

Direction des acquisitions et des services bibliographiques

395, rue Wellington
Ottawa (Ontario)
K1A 0N4

Your file Votre référence

Our file Notre référence

NOTICE

The quality of this microform is heavily dependent upon the quality of the original thesis submitted for microfilming. Every effort has been made to ensure the highest quality of reproduction possible.

If pages are missing, contact the university which granted the degree.

Some pages may have indistinct print especially if the original pages were typed with a poor typewriter ribbon or if the university sent us an inferior photocopy.

Reproduction in full or in part of this microform is governed by the Canadian Copyright Act, R.S.C. 1970, c. C-30, and subsequent amendments.

AVIS

La qualité de cette microforme dépend grandement de la qualité de la thèse soumise au microfilmage. Nous avons tout fait pour assurer une qualité supérieure de reproduction.

S'il manque des pages, veuillez communiquer avec l'université qui a conféré le grade.

La qualité d'impression de certaines pages peut laisser à désirer, surtout si les pages originales ont été dactylographiées à l'aide d'un ruban usé ou si l'université nous a fait parvenir une photocopie de qualité inférieure.

La reproduction, même partielle, de cette microforme est soumise à la Loi canadienne sur le droit d'auteur, SRC 1970, c. C-30, et ses amendements subséquents.

Canada

THERMOKARST SEDIMENTOLOGY OF THE TUKTOYAKTUK COASTLANDS, NWT

by

Julian Baird Murton

A Thesis

Submitted to the School of Graduate Studies and Research

in Partial Fulfilment of the Requirements for the

Degree of Doctor of Philosophy in

Geology

Ottawa-Carleton Geoscience Centre

University of Ottawa

Ottawa, Ontario

ISBN 0-315-82537-5

Canada

UNIVERSITÉ D'OTTAWA
UNIVERSITY OF OTTAWA

DOCTOR OF PHILOSOPHY
(GEOLOGY)

UNIVERSITY OF OTTAWA
Ottawa, Ontario

TITLE: Thermokarst sedimentology of the Tuktoyaktuk Coastlands, NWT

AUTHOR: Julian Baird Murton, BSc (Universities of London and Leicester)

SUPERVISOR: Dr H.M. French

NUMBER OF PAGES: ix, 193

EXAMINING COMMITTEE: Dr R.W. Arnott (University of Ottawa)
Dr N. Eyles (University of Toronto)
Dr F.A. Michel (Carleton University)
Dr J-S. Vincent (Geological Survey of Canada)

ABSTRACT

Thermokarst sedimentology is the study of the sedimentary processes and facies associated with thermokarst. Using facies analysis, oxygen isotopes and observations of processes in the Tuktoyaktuk Coastlands, this thesis (1) classifies frozen ground according to its cryostructures and cryofacies; (2) describes thermokarst facies, facies associations and sedimentary structures; (3) examines the sedimentary processes associated with thermokarst; (4) proposes thermokarst facies models; and (5) proposes criteria for identifying thermokarst-modified sediments.

The thermokarst sedimentary system of the Tuktoyaktuk Coastlands comprises uplands, slopes and basins. Beneath ice-rich uplands, downwearing thermokarst produces a thick (≤c. 2.5m) thaw layer in which sediments melt-out from underlying permafrost. Ice-rich slopes are subdivided into steep icy slopes and retrogressive thaw slumps, the former occurring where the percentage of excess ice in upland materials is less than c.30-40%, the latter where it exceeds this value. As slopes retreat by backwearing thermokarst, upland materials are redeposited by alluvial and colluvial processes. Thermokarst basins form where back- and downwearing thermokarst coincide. In deep non-oriented basins containing thermokarst lakes, three stages of basin infilling are identified. The first occurs during early and rapid basin expansion, when intense backwearing thermokarst at basin margins transports large quantities of upland materials into the basins. This pulse of resedimentation initiates sublacustrine benches. The second stage begins as the rate of basin expansion diminishes, reducing the influx of clastic sediment into lakes; thus the tops of sublacustrine benches are reworked and the main depositional process changes to suspension settling in basin centres. The final stage, commencing as lakes drain, involves basin infilling by peat accumulation and by gelifluction and aeolian deposition.

Two sedimentary structures relating to thermokarst are frost-fissure pseudomorphs and thermokarst involutions. Frost-fissure pseudomorphs develop through thaw-modification processes: slow subsidence, thermal erosion, refreezing, loading, buoyancy, spreading, folding, shearing and mass movement. Thermokarst involutions form primarily by water-escape or by loading and buoyancy. Involutions within a thick palaeothaw layer probably reflect the massive scale of soft-sediment deformation that accompanies regional thermokarst, and they provide a potential analogue for some Pleistocene involutions in the mid-latitudes.

Five criteria identify thermokarst-modified sediments in the Tuktoyaktuk Coastlands: (1) organic-rich (and sandy) diamicton; (2) granular mud aggregates in stratified facies; (3) impure sand (+/-diamicton); (4) frost-fissure pseudomorphs; and (5) thermokarst involutions.

ACKNOWLEDGEMENTS

I most warmly thank Dr H.M. French, my supervisor, for his patient support, guidance, encouragement and editorial acumen. And I am grateful to Drs R.W. Arnott, C.R. Burn, D.G. Harry, J.R. Mackay, F.A. Michel, W.H. Pollard, D.R. Sharpe, J. Shaw, W.W. Shilts and J-S. Vincent, and to S.R. Dallimore, P.A. Egginton, J.A. Heginbottom, D.A. Hodgson, F.M. Nixon and B. Wang for interesting discussions and/or for freely sharing their knowledge of the Tuktoyaktuk Coastlands. Drs J.V. Matthews Jr. and A. Martell identified organic material. G. Mrazek translated some of the Russian literature. B.P. Lowe and A.D. Green stalwartly assisted with fieldwork during 1990 and 1991 respectively, and E.W. Hearn gave much valuable advice regarding the diagrams.

The project was supported by NSERC grant A-8367 (H.M. French); University of Ottawa scholarships (1988-1991); the Geological Survey of Canada; the Inuvik Research Centre, Science Institute of the Northwest Territories; and the Polar Continental Shelf Project, Energy Mines and Resources Canada (project 37-75).

TABLE OF CONTENTS

LIST OF FIGURES

LIST OF TABLES

Chapter 1. INTRODUCTION

"Dans l'étude sur le Pléistocène ... le problème du karste thermique est passé inaperçu. L'importance de ce problème est considérable, parce qu'il nous permet de mieux comprendre les phénomènes de Pléistocène et surtout parce que beaucoup de structures et de formes périglaciaires sont en réalité le résultat du thermokarst." (Dylik, 1964)

"Despite a large literature describing landforms, processes, sediments and structures found in a wide range of variably defined 'periglacial' environments, few studies present rigorous facies and structural criteria for identification of cold climates in the rock record."
(Eyles and Clark, 1985)

1.1 Permafrost

1.1.1 Introduction

Ground that remains at or below 0°C for at least two years is defined as permafrost (Permafrost Subcommittee, ACGR, 1988). Underlying c.50% of Canada and c.20% of the Earth's land surface (Stearns, 1966; Brown, 1970, p.7), permafrost contains variable amounts of ice. Where the ice volume exceeds the pore volume that the ground would naturally have when unfrozen, the permafrost is termed "ice-rich" (i.e. it contains excess ice). It is the thaw of such ice-rich permafrost that is the subject of this thesis.

1.1.2 Permafrost sedimentology

Permafrost is central to geocryology (e.g. Kudriavtsev, 1978), the study of frozen ground (both seasonally frozen ground and permafrost), excluding glaciers (Washburn, 1980a, p.2). Geocryology has many facets: thermodynamic studies of ground freezing and thawing

(e.g. Williams and Smith, 1989, p.174-201), the mechanics of frozen ground (e.g. Vialov, 1965; Tsytovich, 1975), engineering design and construction techniques relating to permafrost (e.g. Johnston, 1981), periglacial geomorphology (e.g. French, 1976; Washburn, 1980a; Clark, 1988; Dixon and Abrahams, 1992), ground-ice studies (e.g. Shumskii, 1959; Mackay, 1972a) and palaeoclimatic reconstructions (e.g. Jahn, 1975; Washburn, 1980b; Boardman, 1987; Ballantyne and Harris, in press). Another facet, straddling the boundary between geocryology and geology, is that of cryolithology (cf. Katasonov, 1978).

Cryolithology has been defined as the study of the genesis, structure and composition of earth materials with temperatures below 0°C (Permafrost Subcommittee, 1988). However, no definition is universally accepted (Popov, 1978a; 1978b; Popov and Katasonov, 1978). For example, Katasonov (1978) restricts cryolithology to the study of frozen, mainly Quaternary, sediments. Popov (1978a; 1978b), on the other hand, regards it as a geological discipline dealing with cryogenic phenomena, specifically cryodiagenesis and cryogenic weathering, in the Earth's crust. And Bates and Jackson (1987, p.158) define it as "the study of the development, nature, and structure of underground ice, especially ice in permafrost regions". To avoid such terminological dispute and to emphasise the sedimentary importance of permafrost, the author proposes the term **permafrost sedimentology**. This subject considers (1) the depositional and diagenetic processes during, or as a result of, permafrost aggradation and degradation, and (2) the resulting facies, both frozen and unfrozen.

The permafrost sedimentology of modern permafrost areas has been poorly investigated. North American geomorphologists and Quaternary geologists working in these areas have focussed on geomorphological and thermal processes (e.g. French, 1976; Smith, 1976; Washburn, 1980a), permafrost aggradation and ground ice (e.g. Mackay, 1972a; 1985; French et al., 1982; Harry, 1988), cryostratigraphy (e.g. French et al., 1982; Harry and French, 1988) and Quaternary history (e.g. Rampton, 1982; 1988; Vincent, 1983; 1989; Dinter

et al., 1990). Rarely has permafrost aggradation (see e.g. Mackay, 1974a; French et al., 1984) or degradation (see e.g. Harry, 1982, p.126-130; Hopkins and Kidd, 1988) been considered in a in sedimentological framework. Likewise, sedimentologists have written little about permafrost sedimentology (Eyles and Eyles, 1992; see e.g. Daly and Cooper, 1976; Young and Long, 1976; Deynoux, 1982; Williams and Tonkin, 1985), a fact conspicuous in several major texts (e.g. Reineck and Singh, 1980; Leeder, 1982; Reading, 1986; Boggs, 1987; Walker and James, 1992), whose treatment of permafrost is either absent or inadequate. Also in Russia where cryolithologists have written extensively about permafrost sedimentology (see e.g. Katasonov, 1969; 1978; Popov, 1978a; 1978b; Popov et al., 1985a), one may question if the level of facies analysis compares to that routinely applied in non-permafrost environments (see e.g. Miall, 1978; Brookfield and Ahlbrandt, 1983; Ashley et al., 1985). In view of these deficiencies, permafrost sedimentology merits further scrutiny.

This thesis examines one aspect of permafrost sedimentology, namely that relating to thermokarst.

1.2 **Thermokarst**

1.2.1 Introduction

Thermokarst denotes thaw of ice-rich material, a process that usually causes subsidence of the ground surface (cf. Dylik, 1968). Although thermokarst *sensu stricto* differs from thermal erosion - the process whereby ice-rich material is thermally and mechanically eroded by moving water (cf. Permafrost Subcommittee, ACGR, 1988), thermokarst *sensu lato* includes the latter (Dylik, 1971), because subsidence and thermal erosion often coincide. This thesis therefore considers thermokarst in the broad sense.

Thermokarst may be periglacial or glacial. Periglacial thermokarst occurs where ice-rich permafrost degrades (e.g. French, 1975; 1976, p.105-133), and glacial thermokarst where

glacier ice either stagnates (e.g. Clayton, 1964; Healy, 1975; Fleisher, 1986; McKenzie and Goodwin, 1987; Johnson, 1992) or is thermaliy eroded (e.g. Eyles and Rogerson, 1977). But these types are sometimes difficult or impossible to distinguish, for example where the origin of massive ice and icy sediments is uncertain or where periglacial and glacial ground ice (Section 1.5.3) coexist in areas of "retarded" deglaciation (e.g. Astakhov and Isayeva, 1988; French and Harry, 1990; Section 1.5.4).

1.2.2 Thermokarst terrain

Thermokarst terrain varies from basin-studded plateaus (e.g. Soloviev, 1973; Williams and Yeend, 1979) through irregular and hummocky areas (e.g. Ermolaev, 1932, in French, 1976, p.105; Dylik, 1968) to thermokarst plains patterned by drained-lake basins (e.g. Rampton, 1988, Fig.21). Depressions are abundant, ranging in size from small ditches above partially melted ice wedges to large, coalescent thermokarst basins or valleys (e.g. Kachurin, 1962; Rampton, 1974; French, 1976, p.105-133). Other thermokarst landforms include thermokarst mounds (e.g. Péwé, 1954; Shumskii and Vyturin, 1966; French, 1975), badlands (e.g. French, 1974), retrogressive thaw slumps (e.g. Mackay, 1966; Lewkowicz, 1988), thermo-erosional niches (e.g. Czudek and Demek, 1970), caves, melt-dolines, gullies, natural bridges (e.g. Clayton, 1964; Healy, 1975) and oriented thermokarst lakes (e.g. Black, 1969; Harry and French, 1983).

1.2.3 The causes of thermokarst

Thermokarst ensues where a disturbance to the thermal regime of ice-rich ground initiates thaw. In the case of ground ice (Section 1.5.3), the disturbance (geomorphic, biotic or climatic) causes the thaw layer to thicken or thin (see e.g. French, 1987, Fig.10.5). For example, because vegetation modifies the effects of summer heat on underlying ground, by

shading and evapotranspiration, thereby lowering the mean annual soil temperature (Williams and Smith, 1989, p.71-79), disturbances like forest fire will increase the thaw depth (e.g. Mackay, 1977). Thermokarst may also result from trampling of vegetation or from thinning of the active layer by mass movement or construction activity (e.g. Popov, 1956; Mackay, 1970; French, 1975; 1987). These site-specific disturbances initiate **local thermokarst**. Climatic warming, by contrast, engenders **regional thermokarst** (Dylik, 1968). For example, regional thermokarst during the climatic warming at the end of the Late Wisconsinan Glaciation formed much of the present thermokarst terrain in Canada, Alaska and Siberia (e.g. Rampton, 1974; Tomirdiaro, 1982; Carter, 1988; Harry et al., 1988).

1.2.4 The importance of thermokarst

Thermokarst terrain is widespread in lowlands of arctic Canada, Alaska and Siberia that are underlain by ice-rich permafrost (e.g. Mackay, 1963; Sellmann, et al., 1975; Danilova, 1978; Tomirdiaro, 1982; Harry and French, 1983; Carter, 1988). Thermokarst is also common in modern glaciated areas such as the SW Yukon (e.g. Watson, 1980) and Antarctica (Healy, 1975), and in areas of "retarded" deglaciation, for example NW Siberia (e.g. Kaplanskaya and Tarnogradskiy, 1986; Astakhov and Isayeva, 1988).

In areas of ice-rich terrain, potential thermokarst activity augments the costs of building infrastructures (e.g. Ferrians, et al., 1969; Johnston, 1981; Williams, 1986). Problems may occur where thermokarst is induced artificially (e.g. French, 1975; Eyles and Rogerson, 1977; Lawson, 1986), for example by inadequately insulating heated structures (e.g. Brown, 1970, p.55-81) or by removing superficial materials (e.g. Péwé, 1954; French, 1975; 1987).

Construction activity on ice-rich terrain is as likely to encounter primordially frozen ground as thermokarst sediments that are ice-rich, ice-poor or unfrozen. Because the geotechnical properties of these sediments relate to their depositional processes (cf. Boulton

and Paul, 1976), an understanding of the origin of the sediments is important in predicting their geotechnical properties, so reducing the costs of site investigation or reparation.

In areas of ice-rich permafrost such as Yakutia, Siberia (Soloviev, 1973; Tomirdiaro, 1982); N Alaska (e.g. Sellmann et al., 1975; Carter, 1988); islands of western arctic Canada (e.g. French, 1974); the Yukon Coastal Plain (e.g. Rampton, 1982; Harry et al., 1988); and the Tuktoyaktuk Coastlands, thermokarst is widely regarded as a major process of landscape evolution. As thermokarst consumes ice-rich upland and polycyclic surfaces (Section 3.2), new, lower surfaces flooring thermokarst basins develop (Chapter 5). Basins may coalesce to form thermokarst valleys (e.g. Czudek and Demek, 1970; Rampton, 1974) and plains. Eventually, with the development of ice wedges and an icy layer at the top of permafrost (e.g. Soloviev, 1973; Cheng, 1983; Burn, 1986), the new surface itself may become ice-rich (e.g. Hussey and Michelson, 1966; Lawson, 1983) and in turn experience thermokarst. The evolution of thermokarst landscapes may thus involve repeated cycles of thermokarst and permafrost aggradation (cf. Czudek and Demek, 1970; Soloviev, 1973; Harry et al., 1988).

Where ice-rich permafrost once existed, its last and most evident traces would have formed during an episode of thermokarst. In a Pleistocene context thermokarst likely affected many cold, non-glacial lowlands capped by fine-grained sediments (cf. Gravenor and Kupsch, 1959; Dylik, 1964; French, 1979; Maarleveld, 1981). For example, during the Dimlington Stadial (c.26-13 ka BP), permafrost aggraded in some areas of Britain south of the glacial limit (e.g. Williams, 1975; Worsley, 1987). Where it aggraded through old, fine-grained till sheets overlying sands and gravels, as in SE Suffolk (see Rose and Allen, 1977), it probably hosted excess ice. Climatic amelioration following the Dimlington Stadial may then have initiated regional thermokarst. While there is some evidence of this, for example in E England (e.g. Sparks et al., 1972; West et al., 1974; Bryant and Carpenter, 1987; Burton, 1987; Worsley, 1987), it would be premature, however, to conclude that thermokarst was an important process

until possible thermokarst sediments and terrain here are compared with *bona fide* ones in areas of modern permafrost.

The final reason why thermokarst is important concerns global warming (e.g. Woodcock, 1991). Should this continue, thermokarst is likely to intensify and spread (e.g. Harris, 1986, p.72; Smith, 1986), likely damaging overlying settlements and large engineering structures. Moreover, thawing may release large volumes of methane (e.g. Nisbet, 1989), and potentially exacerbate global warming.

1.2.5 Thermokarst sedimentology

The study of thermokarst has been unbalanced. Examined mainly in terms of geomorphology and Quaternary history (see e.g. Rampton, 1974; French, 1976, p.105-133; Washburn, 1980a, p.268-276), thermokarst has seldom been considered as a field of sedimentology (cf.Dylik, 1963a), except by glacial sedimentologists (see e.g. Shaw, 1985, p.38-45; Dreimanis, 1989, p.45-46; Paul and Eyles, 1990). Relatively little has been reported about thermokarst sedimentary processes and facies from ice-rich permafrost environments (see e.g. Mackay, 1963, p.61-63, Fig. 20; Katasonov, 1969; Rampton, 1982, p.32-33,43; 1988, p.54, 74-75; Sher et al., 1979, p.57-58; 88-93; Ivanov, 1984, p.94-96), still less in a manner explicitly sedimentological (cf. Dylik, 1965, p.3; see e.g. Hopkins and Kidd, 1988). Yet because the sedimentological consequences of thermokarst are both numerous and geographically widespread (Chapters 3-7), it seems timely to distinguish the field of **thermokarst sedimentology**. This is the study of sedimentary processes and facies associated with thermokarst.

Thermokarst sedimentology should be studied first in areas where thermokarst processes and sediments are juxtaposed with ice-rich material. Only when this has been done is it prudent to consider ancient thermokarst environments. Strangely, the opposite has

occurred, the periglacial half of the subject having developed most in non-permafrost regions, particularly in central and NW Europe (see e.g. Dylik, 1963a; 1964; Maarleveld, 1981; Vandenberghe and Broek, 1982; Vandenberghe, 1983a; 1983b). Yet in such regions it is difficult to know if excess ice previously existed, and if it did, in what form and quantity, problems compounded by the destructive nature of thermokarst. Consequently, thermokarst sedimentology, as it stands, is largely inferential - more a branch of Pleistocene stratigraphy than of physical sedimentology.

Thermokarst sedimentology raises at least three research problems. First, what facies, facies associations and sedimentary structures are associated with thermokarst? Second, what processes occur either during or as a result of thermokarst? Third, are there any features diagnostic of thermokarst? To address these problems this thesis has five objectives.

1.3 Objectives

1. To describe thermokarst facies, facies associations and sedimentary structures.
2. To describe and infer sedimentary processes associated with thermokarst.
3. To produce thermokarst facies models.
4. To establish criteria for identification of thermokarst-modified sediments.

To achieve these objectives it is first necessary to develop a field-based terminology that describes frozen ground. Thus the fifth objective is to classify frozen ground according to its structures and facies.

1.4 Methods

The methodology used in this study includes (1) facies analysis, (2) field observations of processes and (3) isotopic analysis of ground ice.

Facies analysis involves "...the description and classification of any body of sediment followed by the interpretation of its processes and environments of deposition, usually in the form of a facies model." (Anderton, 1985). This is subdivided into three stages, the first being a field description. The present study, comprising 24 weeks of fieldwork during the summers of 1989-1991, is based on numerous measured stratigraphic cross-sections and on several large (≥several m^2) sections showing lateral and vertical facies architecture (cf. Allen, 1983; Miall, 1985). Facies analysis is applied to both the ice-rich precursors (cryofacies underlying primordial surfaces; Sections 3.2 and 3.3) and thermokarst sediments (Chapters 3-7). Second, facies are classified. Besides the features normally used to characterise facies (e.g. grain size, sedimentary structures and organic material), this study considers the nature and distribution of ground ice (i.e. cryostructures; Section 2.2). Third, facies are interpreted in terms of depositional processes, and facies relationships in terms of depositional environments. By combining observations of ancient and modern deposits, it is possible to construct an idealized facies model, that is "... a general summary of a given sedimentary system..." (Walker, 1992, p.6).

A number of sedimentary processes were observed at the base of steep icy bluffs (Chapter 4), in thaw slumps (Chapter 4) and in thermokarst lakes (Chapter 5). But as some processes, for example loadcasting, are impossible to observe, thermokarst facies were studied in their geomorphic or cryostratigraphic context - e.g. melt-out diamicton directly above ice-rich cryofacies (Chapter 3) and thermokarst lake sediments in drained basins (Chapter 5), so minimising the number of inferences about depositional processes and environments.

The third method is the analysis of oxygen isotopes in ground ice. This relies on the fact that the $\delta^{18}O$ value of water (or ice) is strongly influenced by the temperature at which precipitation condenses: the lower the temperature, the more negative (isotopically lighter) is the resulting $\delta^{18}O$ value of precipitation (e.g. Bradley, 1985, p. 124-134). Providing no major

isotopic changes occur (by mixing, evaporation or fractionation) between precipitation and freezing, $\delta^{18}O$ values of the ice will reflect the palaeoclimate at the time of precipitation (e.g. Michel and Fritz, 1982; Mackay, 1983). Oxygen isotopes may be used also to detect thaw unconformities (e.g. Mackay and Lavkulich, 1974; Burn et al., 1986; Section 3.3.2.2). $\delta^{18}O$ analyses were conducted in the Stable Isotope Laboratory at the University of Ottawa.

1.5 Field area

1.5.1 Introduction

The field area is in the Tuktoyaktuk Coastlands, NWT (Fig. 1.1; Rampton, 1988, map 1647A). Thickly underlain by Quaternary sediments (Mackay, 1963; Rampton, 1988), this low-lying (rarely ≥60m asl) region has an arctic, coastal climate with long, cold winters and brief, cool summers (Ritchie, 1984, p.13-15). It is in the zone of continuous permafrost, the permafrost thickness ranging from less than 100m to c.740+m (Judge, 1986, Fig. 16.1). Mean annual air temperatures are typically c.-10°C to -12°C (Mackay, 1979, Fig. 4), and mean annual ground temperatures c.-8°C to -10°C (Mackay, 1979, Fig. 5). The vegetation is that of the low-arctic tundra zone, comprising mainly sedge- and shrub-tundra; in the south, there is forest-tundra (Rampton, 1988, Fig. 8; Ritchie, 1984, p.48-65).

1.5.2 Superficial deposits and Quaternary history

Summarised below are the superficial deposits and Quaternary history of the area between Richards Island and Nicholson Point (Figs 1.1 and 1.2; see Rampton, 1988, map 1647A).

The oldest unit, Kendall sediments, comprises interbedded clay, silt and sand, and contains marine shells. It underlies Hooper Clay. Both units are marine deposits, probably of Middle Pleistocene age. Hooper Clay underlies the Kidluit Formation.

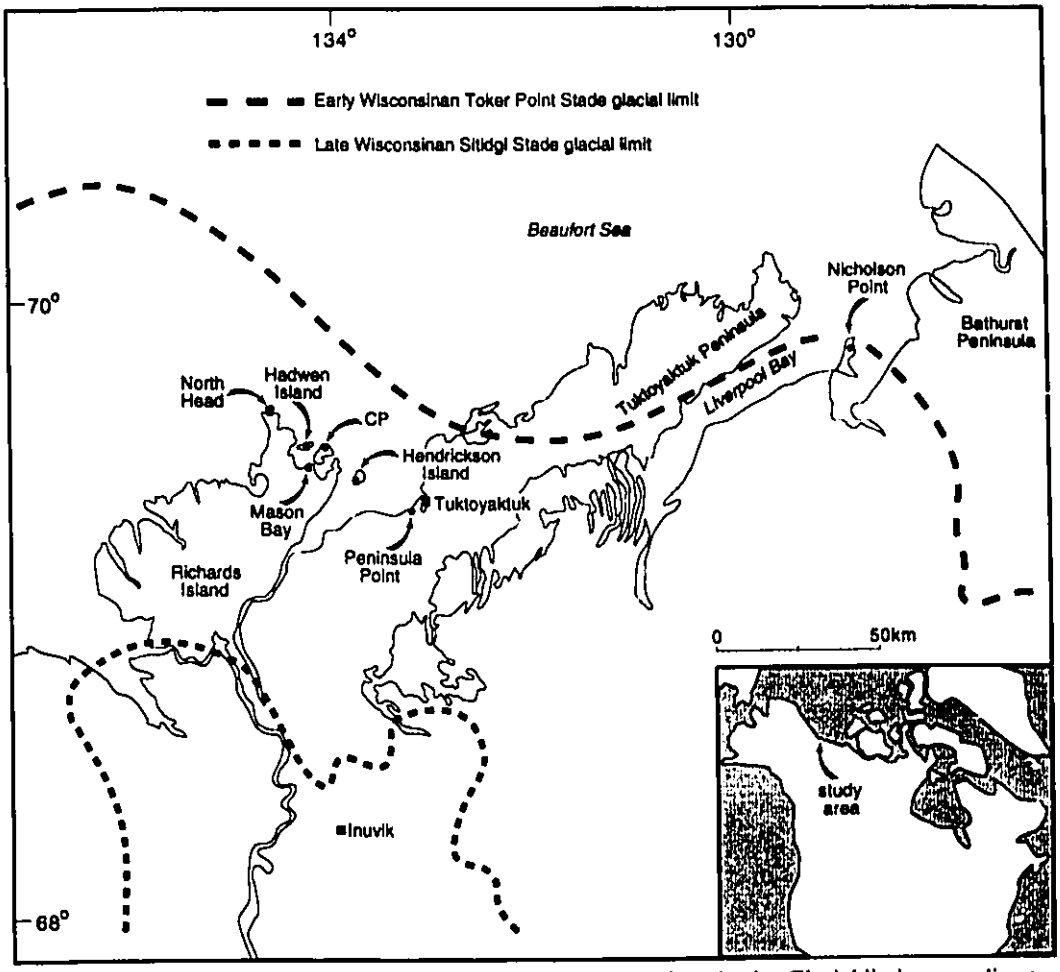

Fig. 1.1 Location map showing the field sites in the Tuktoyaktuk Coastlands. Glacial limits according to Rampton (1988). 'CP' denotes Crumbling Point.

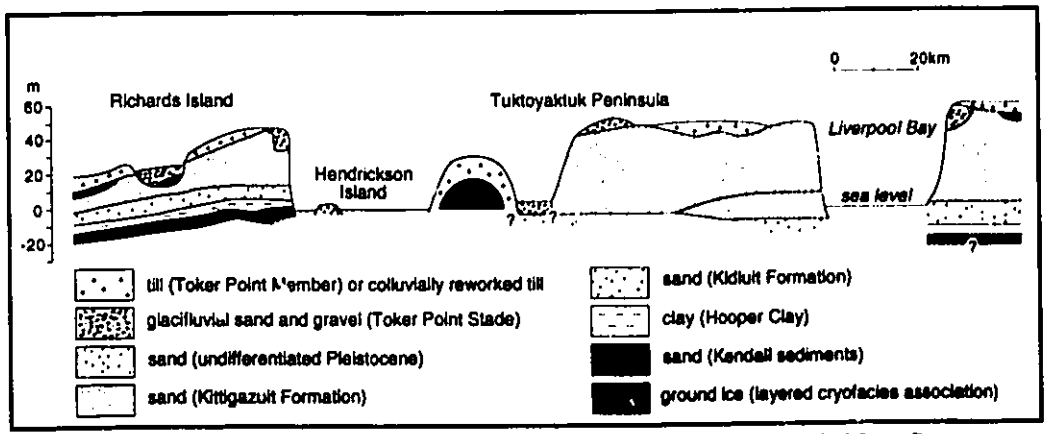

Fig. 1.2 Schematic Quaternary stratigraphy of the Tuktoyaktuk Coastlands (modified from Rampton, 1988, Fig. 53).

The Kidluit Formation comprises cross-bedded and organic-rich, grey sand that was likely deposited by braided rivers during an interglaciation. The Kidluit Formation underlies the Kittigazuit Formation.

The Kittigazuit Formation is an organic-poor, brown sand, commonly displaying large-scale, steeply dipping foresets, interpreted as both deltaic (Mackay,1963, p.18; Rampton,1988, p.39-42, 61-62) and aeolian in origin (Hopkins, 1982; Vincent, 1989, p.126; Vincent et al., 1989). Since the Kittigazuit Formation underlies Toker Point Stade deposits (see below), its age is likely Early Wisconsinan or older.

The Tuktoyaktuk Coastlands are widely mantled by sand, pebbly sand, gravel or pebbly, clayey diamicton (Rampton, 1988, map 1647A), many of which are assigned to the Toker Point Member. Sand, pebbly sand and gravel are interpreted as glacifluvial outwash, and undisturbed diamicton as till, all being deposited during a glaciation termed the Toker Point Stade (Rampton, 1988). At its maximum, Toker Point ice covered most the of the Tuktoyaktuk Coastlands (Fig. 1.1), deforming underlying sediments (e.g. Mackay, 1956a; Mathews and Mackay, 1960; Mackay et al., 1972; Rampton, 1982). During deglaciation, meltwater likely eroded tunnel valleys and deposited sand and gravel on outwash plains and valley trains. The Toker Point Stade is likely of Early Wisconsinan age, based on the fact that shell-bearing sediments in unglaciated terraces, or overlying Toker Point till, give radiocarbon dates of ≥35,000 BP (Vincent, 1989, p.128).

In the south Tuktoyaktuk Coastlands, much of the surface is covered by pebbly, clayey diamicton (Rampton, 1988, map 1647A) that is interpreted as till. This was deposited during the Sitidgi Stade, the last glaciation (maximum at c.13,000 BP; Fig. 1.2) to affect the Tuktoyaktuk Coastlands.

During the Holocene, peat has accumulated widely and aeolian, alluvial, colluvial, marine and thermokarst processes have been active locally (Rampton, 1988). With the

Holocene transgression (Mackay, 1963; Forbes, 1980; Hill et al., 1985), the mouths of river valleys have been drowned and ice-rich coasts have rapidly retreated (e.g. Mackay, 1986a).

Little is known about the Early and Middle Wisconsinan climate of the Tuktoyaktuk Coastlands. Allen et al. (1988) suggest that mean annual surface (ground) temperatures were c.-18°C and -8°C respectively. More is known about the Late Wisconsinan climate, which was colder and drier than present, perhaps analogous to modern, mid-arctic climates of N Banks and Victoria islands (Ritchie, 1984, p.118-121, 155).

The climate began to warm slowly at c.15,000 BP, and later, rapidly between 12,000-10,000 BP, with mean July temperatures at 10,000 BP likely exceeding those at present by 3-5°C (Ritchie, 1984, p. 154-156). At that time the Tuktoyaktuk Coastlands likely experienced greater continentality than at present (C.R. Burn, personal communication, January 1993), the contemporaneous shoreline lying further to the north. After this Late Wisconsinan-early Holocene warm interval (c.12,000-8,000 BP), the climate began to cool, and since c.4,500 BP, modern climatic conditions have prevailed (Ritchie, 1984, p. 154-156).

1.5.3 Ground ice

Ground ice includes all types of ice formed in freezing and frozen ground (Permafrost Subcommittee, ACGR, 1988). This definition is usually understood to exclude buried ice (e.g. Mackay, 1972a, Fig. 2; Harry, 1988), an exclusion that leads into a terminological cul-de-sac if the origin of the ice is unknown. It would be simpler if ground ice referred to all bodies of subsurface ice (cf. Shumskii, 1959, Fig. 57) and were prefixed by the genetic terms "glacial" or "periglacial" only if the genesis were known.

Ground ice is abundant beneath much of the Tuktoyaktuk Coastlands (e.g. Mackay, 1963; 1971; Rampton and Mackay, 1971; Pollard and French, 1980). On Richards Island (Fig. 1.1), periglacial ground ice comprises c. 50% by volume of the upper 10m of permafrost

(Lawrence and Proudfoot, 1977; Pollard and French, 1980). This ice is mainly pore and segregated ice (≥80%), with ice-wedge ice forming ≤20% of the total volumetric ice content (Pollard and French, 1980).

Segregated and intrusive ice commonly occur as massive ice and icy sediments (e.g. Mackay, 1966; 1971; 1989). Massive ice is defined as a large body of relatively pure ground ice whose gravimetric ice content is at least 250% (Permafrost Subcommittee, ACGR, 1988); thaw of 1m of massive ice releases 0.8+m of supernatant water (Mackay, 1971). Icy sediments contain excess ice, but their gravimetric ice content is less than 250% (Rampton and Mackay, 1971). Albeit laterally discontinuous (Section 1.6; Fig. 1.5), massive ice and icy sediments are common in the study area (Mackay, 1971; Rampton and Mackay, 1971, Figs. 2-4; French and Harry, 1990), massive ice typically occurring at depths of 6-25m, and icy sediments at all depths to at least 43m (Rampton and Mackay, 1971). In this area, massive ice generally overlies sand and gravel and underlies clay or pebbly clay (Mackay, 1973).

In terms of global permafrost the abundance of excess ice in the Tuktoyaktuk Coastlands appears to be unusual. Few other areas, for example the loessic regions of N Alaska (e.g. Carter, 1988) and NE Siberia (e.g. Tomirdiaro, 1982), the "Yedoma" complex of central Yakukia (e.g. Are, 1973; Soloviev, 1973) and areas of massive ice and icy sediments in NW Siberia (e.g. Kaplanskaya and Tarnogradskiy, 1986), are known to possess comparable amounts of excess ice.

1.5.4 Permafrost history

Beneath much of the the Tuktoyaktuk Coastlands, permafrost has existed since at least the Early Wisconsinan (Mackay, 1986b). This is indicated by three lines of evidence. (1) Near the inferred Toker Point glacial limit (Fig. 1.1), beds of ice and sediment are glacitectonically deformed (Mackay, 1971; Mackay et al., 1972). Since the deformation likely

occurred during the Early Wisconsinan Toker Point Stade (Rampton, 1988), the ice must predate this time (Mackay et al., 1972). (2) Kidluit Sand locally contains partially thawed ice wedges that likely predate the overlying Kittigazuit sand (Early Wisconsinan or older), because most slump structures (formed when the tops of the ice wedges melted) terminate at the Kidluit-Kittigazuit contact (Mackay and Matthews, 1983). (3) Heat-flow calculations suggest that the time required to grow 500-600m of permafrost probably exceeds 50,000 years (Mackay, 1979, p8).

Wisconsinan permafrost history is poorly known. During the Early Wisconsinan Toker Point Stade most of the Tuktoyaktuk Coastlands were glaciated (Fig. 1.1; Rampton, 1988). As glacier ice would have insulated the ground surface from the cold Wisconsinan climate (Judge, 1986), permafrost would have degraded from the bottom upward - by geothermal melting (cf. Mackay, 1972b), and, if the base of the glacier were at pressure-melting point, from the top downward - by pressure melting (French and Harry, 1990). But south of the Toker Point Stade glacial limit (Fig. 1.1), the extent to which permafrost degraded is unclear. Rampton (1974; 1988, p.67) suggests that permafrost degraded completely, French and Harry (1990) that it degraded partially.

As Toker Point Stade ice retreated and/or stagnated, basal glacier ice may have been buried by glacigenic sediments (e.g. Dallimore and Wolfe, 1988; French and Harry, 1990) and permafrost may have aggraded through saturated, coarse-grained materials (e.g. Mackay, 1971; Rampton, 1974; Mackay and Dallimore, 1992). In both cases, the water source could have been glacial meltwater (Rampton, 1974), and the resulting massive ice and icy sediments could be genetically segregated-intrusive ice (cf. Boulton, 1983; Mackay, 1989).

The Late Wisconsinan-early Holocene warm interval was an episode of regional thermokarst (cf. Rampton, 1974), when thermal contraction cracking likely ceased (Mackay, personal communication, February 1991). At that time the top of the permafrost thawed

regionally (Mackay, 1978; Section 3.3) and many retrogressive thaw slumps (Chapter 4) and thermokarst basins (Chapter 5) developed (Rampton, 1974).

Since c.4,500 BP, the beginning of the modern climatic regime (Ritchie, 1984, p.154-156), geocryological processes have probably been the same as those of today: gelifluction (Mackay, 1981), thermal contraction cracking (e.g. Mackay, 1992a) and local permafrost aggradation and pingo growth (e.g. Mackay, 1979; 1985). Modern thermokarst processes such as retrogressive thaw slumping (Mackay,1963, Fig. 21; 1966) occur only locally.

1.5.5 Rationale for selecting the Tuktoyaktuk Coastlands

The Tuktoyaktuk Coastlands were selected as the study area for five reasons: (1) the abundance of excess ice, (2) the regional distribution of thermokarst features (Rampton, 1988, map 1647A), (3) the juxtaposition of Late Wisconsinan-early Holocene and modern thermokarst features, (4) the opportunity to observe thermokarst-related sedimentary processes, and (5) the logistical support provided by the Inuvik Research Centre and the Polar Continental Shelf Project.

1.6 **Field sites**

Field sites were selected from reconnaissance and air photos according to three criteria:

1. Large natural sections through adjacent ice-rich uplands and thermokarst basins.
2. Variations in the amount, nature and distribution of ground ice and sediment beneath uplands; this is critical to assess the influence of substrate on thermokarst.
3. Minimal distance from Tuktoyaktuk, to reduce helicopter flying time.

The field sites comprise two geomorphological units: (1) a valley train and (2) an upland surface (typically 10-25m asl; Section 3.2) with deeply inset (≤20m) thermokarst basins.

1. North Head (69°43'N; 134°28'W)

North Head is a small island just to the north of Richards Island (Figs 1.1 and 1.3; see e.g. Kurfurst, 1987; Dallimore, 1991; Kurfurst and Dallimore, 1991). On the northwest margin of North Head the coastal bluffs form a 1,100m long section through a drained thermokarst basin and the adjacent upland surface (Fig. 1.3). The materials beneath North Head Upland (c.14-16m asl) are primarily sand, clay, diamicton and massive ice (Figs 4.1 and 5.12B). Northeast of the upland lies North Head Basin (0-5.5m asl), probably truncated near its centre. Work at North Head concentrated on resedimentation at the base of the steep icy bluff and on thermokarst-basin facies in North Head Lake and Basin.

2. Crumbling Point (69°36'N; 133°54'W)

Crumbling Point is the rapidly eroding headland of a small upland surface (Crumbling Point Upland; c.20-25m asl) on the northern tip of Summer Island, 38km northwest of Tuktoyaktuk (Fig. 1.4). This surface is variably underlain by massive ice, icy sediments, diamicton, ?Kidluit, ?Kittigazuit and aeolian sand (Section 3.3.2), and rimmed by several active and inactive retrogressive thaw slumps. By contrast, the upland surface to the southwest (c.12-13m asl) appears to be underlain only by (?Kittigazuit) sand. Between these upland surfaces lies the now-drained Crumbling Point Basin (3.5-4.5m asl; Fig. 1.4).

The following work was undertaken at Crumbling Point: (1) examination of sand v edges (Section 6.5) in the slump headwalls, and resedimentation processes and deposits (Sections 4.2 and 4.3) in the slump floors at Green Lake and Crumbling Point; (2) study of thermokarst-basin facies (Section 5.3) in Crumbling Point Basin; (3) observation of lacustrine processes around the margins of Crumbling Point Lake (Fig. 1.4), and lacustrine sediments in and adjacent to the lake.

Fig. 1.3 Stereo pair of **North Head**. Lying SW of North Head Basin (B), North Head Upland (U) is truncated along its NW margin, forming a steep icy bluff (arrow; section 4.1.1). To the SE of the upland is North Head Lake (L). Scale bar=1km. (August 1985; National Air Photo Library A26754-198+202)

Fig. 1.4 Stereo pair of **Crumbling Point**, Summer Island. The point itself (P) is on the N margin of Crumbling Point Upland (U), to the S of which lies Crumbling Point Lake (L), and to the W Crumbling Point Basin (B). On the S and E margins of the upland, there are stabilised slump scars (arrows), and active slumps occur at Crumbling Point and on the N margin of Green Lake (G). Scale bar=1km. (August 1985; N.A.P.L. A26750-212+216)

3. Mason Bay (69°33'N; 134°01'W)

The site at Mason Bay is on the SE margin of the bay (Fig. 1.1), where a drained thermokarst basin (5.5-10m asl) is truncated approximately through its centre (Fig. 1.5). East of the basin, an upland surface (c.26-27m asl) is underlain by massive ice, icy sediments, diamicton and aeolian sand. This is an area of extensive thaw slumping. A second upland (c.24m asl) to the west of the basin is capped by active dunes and underlain by the Kittigazuit Formation. Work at Mason Bay focussed on thermokarst-basin facies and on sand and composite wedges.

4. Hadwen Island (69°35'N; 134°06'W)

Hadwen Island lies 3km west of Summer Island, on the north side of Mason Bay (Fig. 1.1). The principal site, on the northern coast, is a partially drained thermokarst basin (4.5-6.5m asl; Fig. 1.5) truncated near its northern margin and flanked and underlain by Kittigazuit sand. The sand locally underlies massive ice, icy sediments, diamicton and aeolian sand. West of the basin, the west upland (c.21m asl) is capped by a dune complex. At Hadwen Island, the author studied thermokarst-basin facies and sand and composite wedges.

5. Hendrickson Island (69°29'N; 133°37'W)

Hendrickson Island, 9km southeast of Summer Island (Fig. 1.1), is a low-lying (generally ≤5m asl), sand-rich island, a remnant of an Early Wisconsinan valley train (Rampton, 1988, p.67). Here ice-wedge pseudomorphs were studied along the southern coastal bluff and thermokarst-basin facies in the ramparts of the collapsed pingo (see Porsild, 1938, Fig. 4).

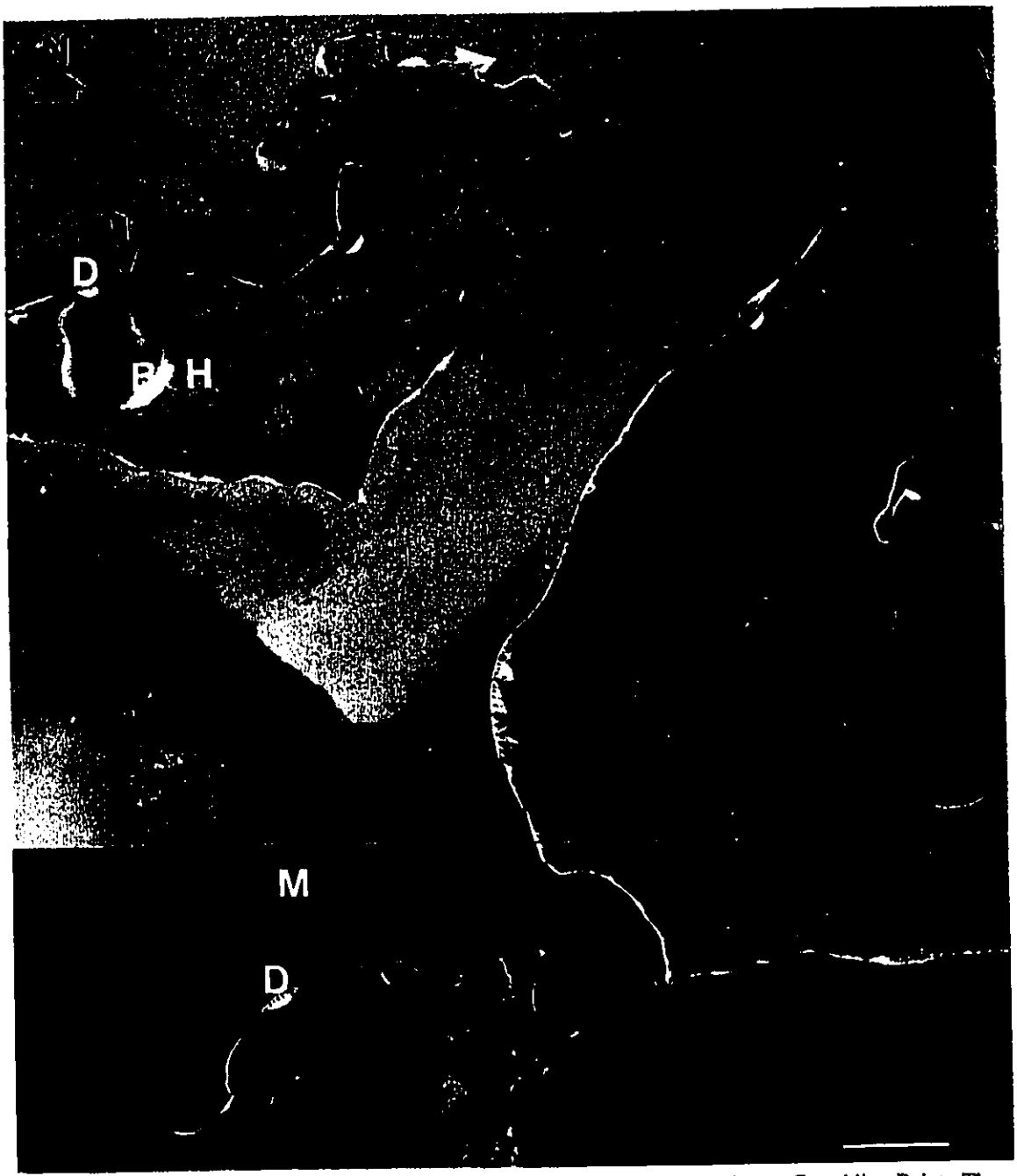

Fig. 1.5 Location of sites at **Mason Bay** (M) and **Hadwen Island** (H) in relation to Crumbling Point. The arrows mark thermokarst basins examined at both sites. Other features described here occur within 2km to the E and W of the basins. The landscape is that of a **primordial surface** (section 3.2) **pitted with deep thermokarst basins** (chapter 5 see Figs 1.3 and 1.4). Beneath it, massive ice and icy sediments are discontinuous, many areas being underlain instead by ice-poor sand, sand that has been locally reworked to form dune complexes (D), aeolian veneers (sections 3.3.2.1 and 5.3.8), sublacustrine benches (B; section 5.2.1), and also to infill thermal contraction cracks (sections 6.4 and 6.5). Scale bar=1km. (August 1985; N.A.P.L. A26750-216 + A26753-159)

6. Peninsula Point (69°25'N; 133°08'W)

Peninsula Point lies 5km southwest of Tuktoyaktuk (Fig. 1.1; see e.g. Mackay, 1963, Fig. 20; 1971, Figs. 2 and 3; Fujino et al., 1988). It comprises an upland surface (c.10m asl) that is underlain by diamicton and massive ice and that is rapidly retreating by thaw slumping. At this site, slump-floor deposits were examined.

7. Nicholson Point (69°56'N; 128°55'W)

Nicholson Point is an island in Liverpool Bay (Fig. 1.6). Its upland surface locally exceeds 90m, probably due to glacier ice-thrusting (Mackay, 1956a). Adjacent to the east coast, 2-4km south of Hepburn Spit, all that remains of the (much lower) upland surface are residuals rising a few m above a small thermokarst plain (c.7-8m asl). Beneath this plain, thermokarst-basin facies were studied.

These seven sites may be grouped in terms of the abundance of sand and mud, the main non-ice constituents in the thermokarst sedimentary system. At Crumbling Point, Mason Bay and Hadwen Island, massive ice and icy sediments are juxtaposed with, and penetrated by, ice-poor Pleistocene sand. Thus the thermokarst system is sand-rich (Fig. 1.5), as it is at Hendrickson Island, where massive ice and icy sediments are restricted to pingos. These sand-rich sites contrast with mud-rich ones at Peninsula Point and Nicholson Point. The site at North Head, with its abundance of both sand and mud is intermediate between these groups.

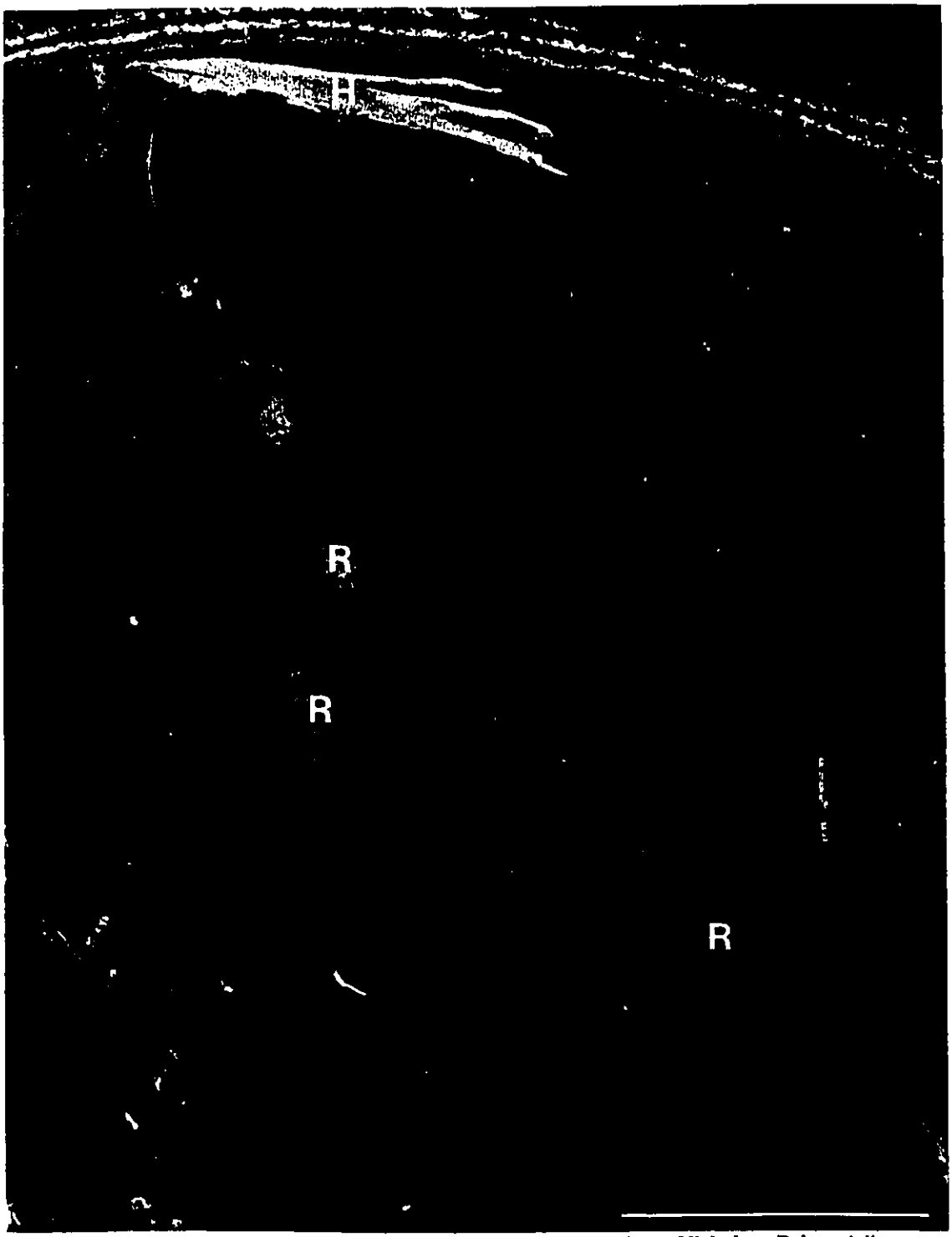

Fig. 1.6 Location of graphic logs (arrows; Fig. 5.7) in thermokarst basins at **Nicholson Point.** Adjacent to the E coastline, the landscape comprises coalescent thermokarst basins - a **thermokarst plain** - above which rise low residuals (R) of a primordial surface. (H) denotes Hepburn Spit. Scale bar=1km. (July 1984; N.A.P.L. A26551-202)

Chapter 2. CRYOSTRUCTURES AND CRYOFACIES

"The ice was here, the ice was there,
The ice was all around:"
(*The Ancient Mariner*, Coleridge)

2.1 Introduction

Ice within permafrost both imparts structures that are quite distinct from those formed in other sedimentary environments (see Allen, 1982; Collinson and Thompson, 1989) and adds to the list of features by which facies are distinguished. Therefore, to facilitate description of frozen ground, this chapter classifies the structures and facies of permafrost in the Tuktoyaktuk Coastlands. The classifications are applied in subsequent chapters.

2.2 Cryostructures

2.2.1 Introduction

The structural characteristics of frozen ground (i.e. the shape and distribution of ice and non-ice earth material with respect to each other) constitute its **cryostructure**. Cryostructures have commonly been confused with **cryotextures**. In petrology, **structure** denotes the megascopic features or a rock mass, whereas **texture** highlights the "... geometric aspects of, and the mutual relations among, its component particles or crystals;" - microscopic features that include grain size, shape and fabric (Bates and Jackson, 1987, p.681). Likewise, in pedology, soils are distinguished according to their texture (grain size) and structure (aggregate shape). In geocryology this distinction is blurred, largely because Russian workers use the term "texture" to describe what North Americans denote as "structure" (Jahn, 1975, p.XI). Thus

Kudriavtsev's (1978) classification of cryotextures (see comment under cryotexture in Permafrost Subcommittee, ACGR, 1988, p.24) is primarily one of cryostructures.

By analogy with petrology, cryotextures should be distinguished according to grain and/or crystal size, shape, the degree of crystallinity and the nature of the contacts between grains and crystals (cf. Whitten and Brooks, 1972, p. 446-447; cf. Shumskii, 1959, p.6). Cryotextures would also include cements, for example, contact, film and pore-filling types (e.g. Shumskii and Vyturin, 1966; Kudriavtsev, 1978, p.301-304). The only cryotextures in Kydriavtsev's (1978) classification would be (1) **massive porous**, a texture in which ice cement completely fills, but does not exceed, the pores of non-ice material and (2) **porphyry-like**, where large ice crystals occur in a groundmass of finely crystalline ice.

Cryostructures have also been confused because they have been applied restrictively. This restriction arose through a distinction between texture- and deposit-forming ice (see Kudriavtsev, 1978, p. 301-304), a distinction whereby cryostructures are assigned only to the former. No such distinction exists in either sedimentology or sedimentary petrology (e.g. . Collinson and Thompson, 1989; Blatt, 1992), for every sediment or sedimentary rock exhibits sedimentary structures, excluding those that are massive. Since the same rationale applies to frozen earth materials, regardless of their ice content, a cryostructural classification must apply to all bodies of frozen ground.

2.2.2 Existing classifications of cryostructures

Cryostructural classifications include those of Katasonov (1969, Tables 13-15; 1975, Fig. 1), Melnikov and Tolstikhin (1974, see Demek, 1978, Fig. 9.2), Kudriavtsev (1978, Table 26), Ivanov (1984, Fig. 36), and Popov et al. (1985b). Outside Russia the closest to a cryostructural classification is that of Linell and Kaplar (1966). For various reasons, all of these classifications are unsatisfactory.

First, some are complex and unwieldy. For example, Katasonov's (1969) classification comprises eighteen different cryostructures, and Popov et al.'s (1985b) fourteen, excluding those which are composite. This abundance reflects classification by size and number (i.e. whether cryostructures occur singly or collectively). For example, Popov et al. (1985b) recognize three size categories of reticulate cryostructure.

Second, the classifications apply foremost to permafrost containing little excess ice, detailing the distribution of ice in non-ice material, neglecting the opposite. For example, Kudriavtsev's (1978) classification contains seven cryostructural terms describing frozen ground whose ice content is approximately ≤50% by volume and only one term ("basal layered: ataxitic or breccia-like" e.g. Cheng, 1983; Shur, 1988) describing very ice-rich material. Yet ideally, a cryostructural classification should give equal importance to all types of frozen ground, irrespective of their ice content. To some extent this was done by Linell and Kaplar (1966); but their soil- (and engineering) based classification groups cryostructures uninformatively. While adequate to describe frozen soils and their engineering properties, it is too generalised for permafrost facies analysis.

2.2.3 A new classification of cryostructures

Following work in the Tuktoyaktuk Coastlands, cryostructures describing both the distribution of ice in non-ice material and vice-versa are proposed (Fig. 2.1). The guideline was adopted that cryostructures should be considered at the same scales as sedimentary structures (see e.g. Allen, 1982) - visible to the naked eye. Six cryostructures are distinguished.

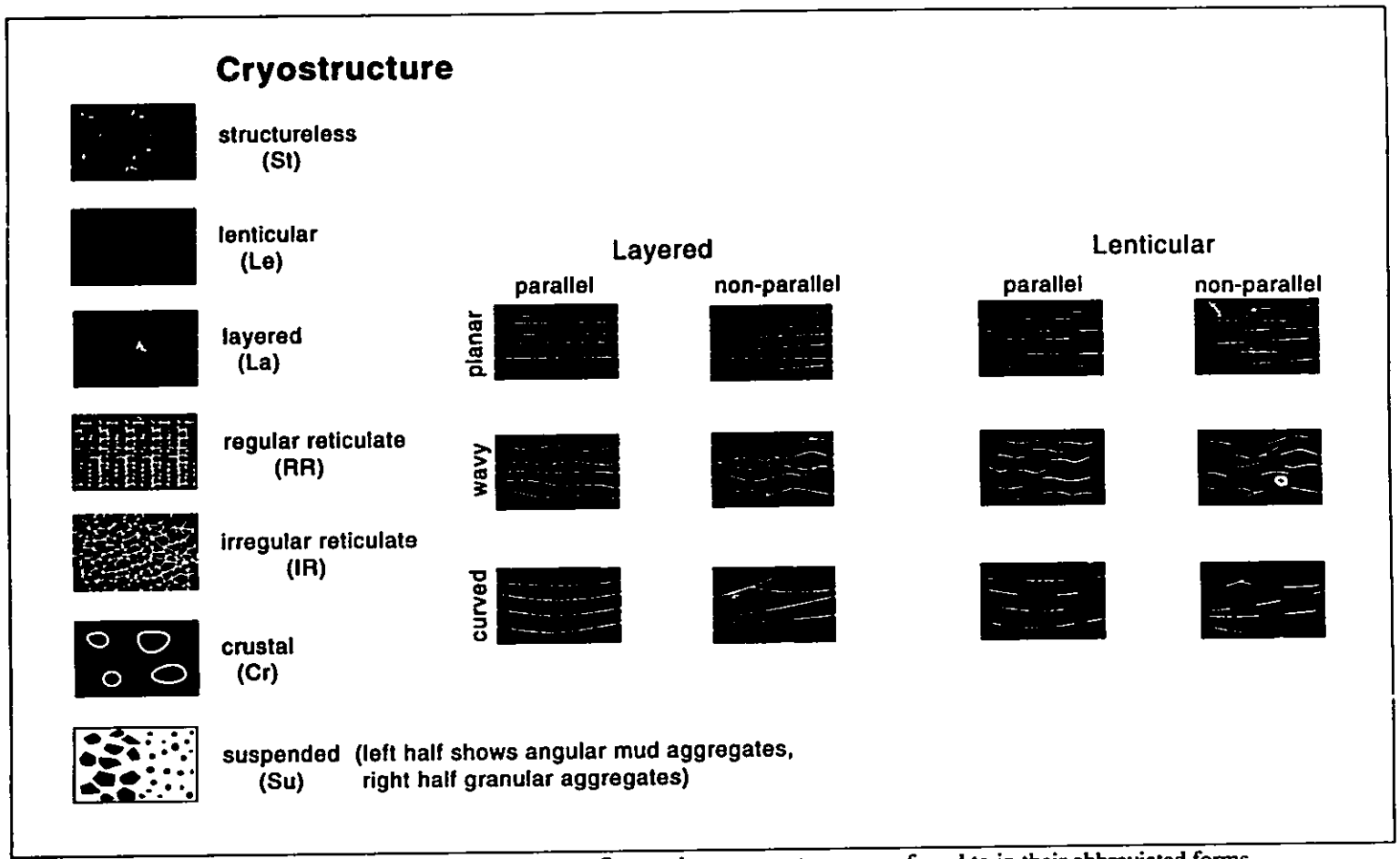

Fig. 2.1 A classification of cryostructures. In subsequent figures the cryostructures are referred to in their abbreviated forms. The terminology for layered and lenticular cryostructures is adopted from Collinson and Thompson, 1989, Fig. 2.6).

1. Frozen materials lacking structure are termed **structureless**. This is preferred to the term "massive" (see e.g. Kudriavtsev, 1978; Popov et al., 1985b), because it is more explicit and avoids confusion with "massive ice". Structureless cryostructures typify sands, gravels and some massive ice.

2. Lens-shaped bodies of ice in non-ice material (Fig. 2.2A; Permafrost Subcommittee, ACGR, 1988, Fig. 9b) or vice-versa (Fig. 2.2B) are described as **lenticular** (cf. "lenticular" in Kudriavtsev, 1978, Table 26; and in Popov et al., 1985b). No inclination is implied; lenses may vary from horizontal to vertical (Permafrost Subcommittee, ACGR, 1988, Fig. 9b). Lenses are described further by inclination, thickness, length, shape and relationship to each other; they may be planar, wavy or curved, and parallel or non-parallel (Fig. 2.1). Lenticular cryostructures are common in mud (Fig. 2.2A; Permafrost Subcommittee, ACGR, 1988, Fig. 9b), sand and ice (Fig. 2.2B).

3. Continuous bands of ice or sediment are referred to as **layered** (cf. "layered" in Kudriavtsev, 1978, Table 26; and in Popov et al., 1985b), individual layers being described in the same way as lenses (Fig. 2.1). Layered cryostructures are exhibited by massive ice, icy sediments and frost-fissure wedges (Chapter 6).

4. A three-dimensional net-like structure of ice veins is termed **reticulate**, of which there are two types, **regular** and **irregular**. Regular reticulate (cf. "lattice: cellular and blocky" in Kudriavtsev, 1978, Table 26; Permafrost Subcommittee, ACGR, 1988, Fig. 9c) is an oriented network of ice surrounding rectangular to rhombic, mud-rich blocks (Fig. 2.3A; Mackay, 1974, Figs 1, 3-5, 7-8). Reticulate ice veins vary in thickness from a few mm to c.10cm and the blocks vary in length from c.1-100cm (Mackay, 1974). Irregular reticulate (cf. "net form" in Kudriavtsev, 1978, Table 26) is an irregular network of ice veins surrounding irregular-shaped blocks of non-ice material (a few mm to c.25cm long; Fig. 2.3B).

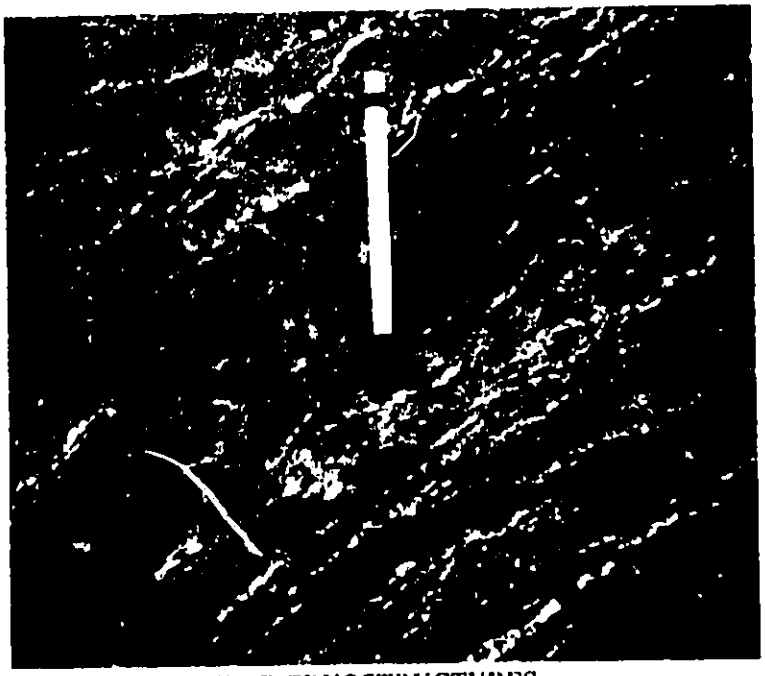

Fig. 2.2 **LENTICULAR CRYOSTRUCTURES**

(A) Thin, moderately dipping, wavy, non-parallel **ice lenses** (white) in icy diamicton (Table 2.1; section 5.3.6), North Head Basin. 14cm high pencil for scale. (August 13 1991)

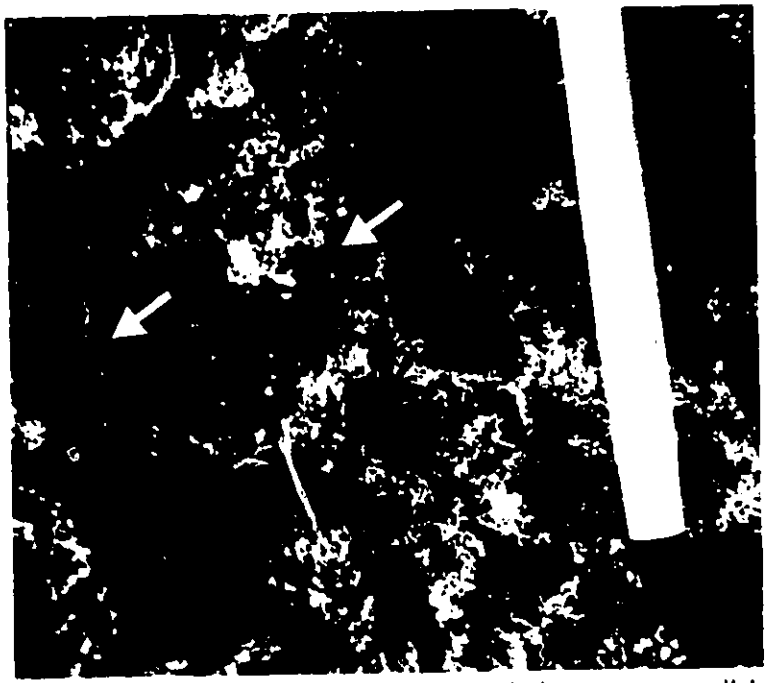

(B) Thin, very steeply dipping to vertical, wavy, non-parallel **sand lenses** (arrows) in sand-poor ice beside a sand wedge, Crumbling Point (section 3.3 .2.2). Pencil for scale. (June 1 1991)

Fig. 2.3 **RETICULATE CRYOSTRUCTURES**

(A) **Regular-reticulate** cryostructure in icy mud/muddy peat (section 5.3.5), North Head Basin. A dominantly vertical and horizontal network of ice veins (arrows) surrounds rectangular blocks of mud/muddy peat. 14cm high pencil for scale. (August 17 1991)

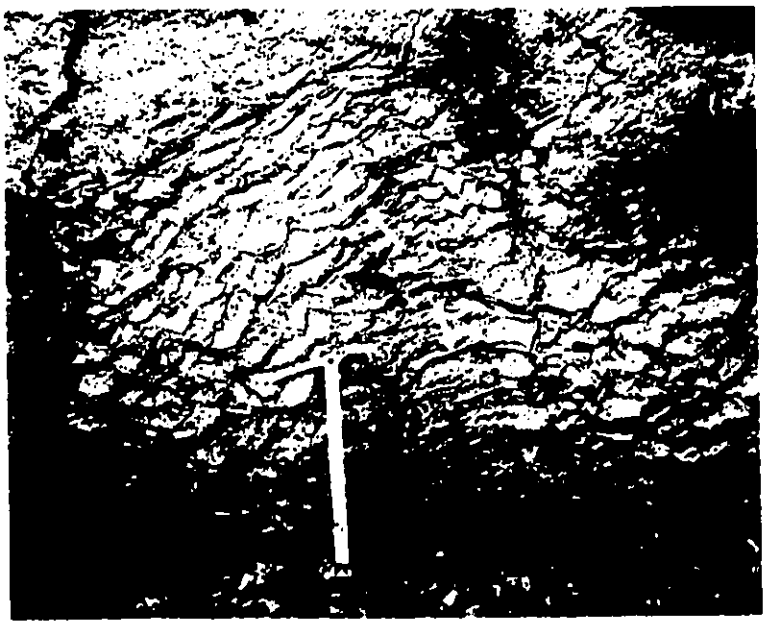

(B) **Irregular-reticulate** cryostructure in icy diamicton (section 5.3.6), North Head Basin. An irregular network of ice veins (arrows) surrounds blocks of diamicton. 50cm high ice axe for scale. (August 13 1991)

5. An ice crust or rim around a clast is described as **crustal** (cf. "crustal" in Kudriavtsev, 1978; and in Popov et al., 1985b). This is common just beneath the permafrost table, where ice crusts (≤ a few cm thick) may envelop pebbles and wood fragments.

6. Grains and aggregates suspended in ice are described as **suspended** (cf. "aggradational ice" in Mackay, 1972a, Fig. 2; "basal layered" in Kudriavtsev, 1978, Table 26; cf. "thick layered ground ice" of Cheng, 1983; cf. "ataxitic" of Shur, 1988, Figs 1 and 2). Individual grains vary from silt particles to boulders. Aggregates (e.g. of mud or sandy mud) range in diameter or length from ≤1mm to several cm+, and may be angular (Fig. 2.4A) to rounded (Fig. 2.4B), equant to elongate and variously inclined. Suspended cryostructure is common in massive ice (Fig. 2.4B) and also just beneath the permafrost table (Fig. 2.4A; e.g. Mackay, 1972a; Cheng, 1983; Burn, 1986; 1988; Shur, 1988).

For simplicity, this classification depicts cryostructures individually. In reality, many are transitional, composite and hierarchical. For example, transitional cryostructures can be partly suspended and partly irregular reticulate (Fig. 2.5A). Composite cryostructures include (a) structureless and crustal in a pebbly sand and (b) layered and lenticular along the sides of sand wedges (Fig. 2.5B). Hierarchical cryostructures may be organised fractally, for example where large irregular-shaped blocks separated by thick irregular reticulate ice veins are subdivided into smaller blocks and thinner veins. Also, different cryostructures may be organised hierarchically, for example where reticulate or suspended cryostructures are layered near the permafrost table (e.g. Shur, 1988, Fig. 2) or within massive ice and icy sediments. That cryostructures are commonly transitional, composite or hierarchical no more nullifies this classification than these properties nullify that of sedimentary structures (see e.g. Brookfield, 1977; Allen, 1983; Miall, 1985).

Fig. 2.4 **SUSPENDED CRYOSTRUCTURES**

(A) **Angular mud aggregates** in aggregate-poor ice (Table 2.1; section 2.3.2), McKinlay Lake, Bathurst Peninsula. (July 27 1990)

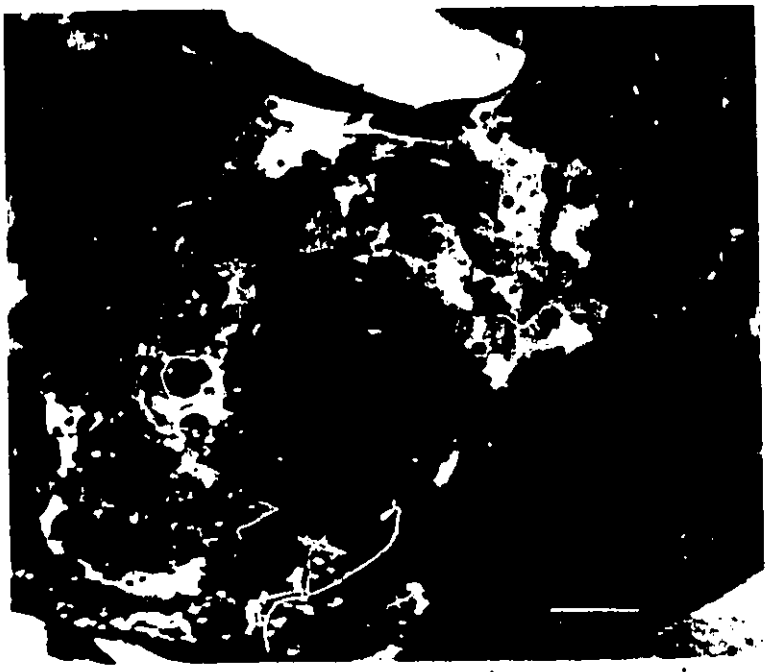

(B) **Granular mud aggregates** in aggregate-poor ice, layered cryofacies association (section 3.3.2.1), Crumbling Point. Scale bar = 1cm. (July 4 1990)

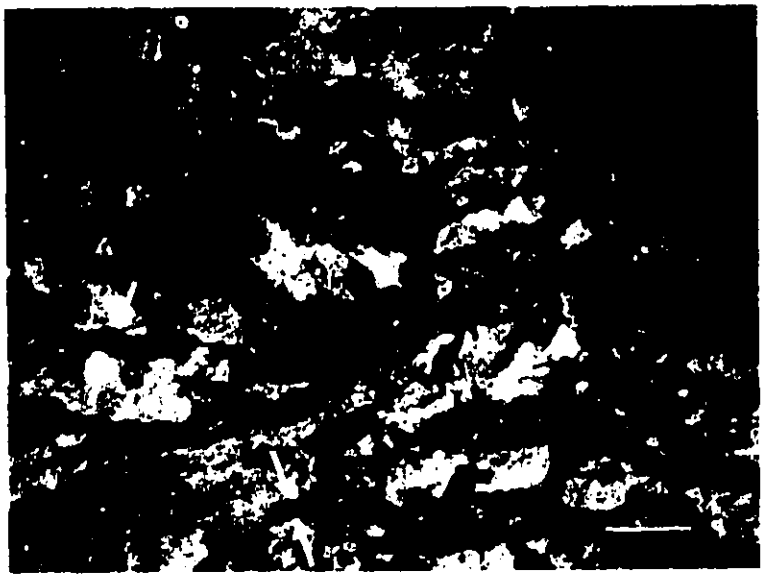

Fig. 2.5 **TRANSITIONAL CRYOSTRUCTURES**

(A) **Suspended/irregular-reticulate cryostructure** in icy diamicton, sand and diamicton cryofacies association (section 3.3 .2.3), Crumbling Point. Angular mud aggregates (pale grey) are surrounded by ice (dark grey). Some have 'matched' sides (arrows). Scale bar =1cm. (June 15 1991)

(B) **Lenticular /layered cryostructure** in sand-rich ice beside a sand wedge, Crumbling Point (cf. Fig. 3.4). Lenses and layers of sand (buff) are surrounded by ice (dark grey). Scale bar =1cm . (June 8 1991)

2.3 Cryofacies

2.3.1 Introduction

Frozen surface materials in the Tuktoyaktuk Coastlands have been described either in stratigraphical (e.g. Rampton and Mackay, 1971; Rampton, 1988) or soil (and engineering) terms (e.g. Linell and Kaplar, 1966). But these descriptions are of limited use to thermokarst sedimentology. For example, the terms "massive ice" and "icy sediments" (Section 1.5.3), akin to facies associations, are too comprehensive to serve at the small scale. What is needed instead is a classification that distinguishes individual facies. Although this was partially achieved in Linell and Kaplar's classification (see Linell and Kaplar, 1966, Fig. 2), theirs is limited to segregated ice and has only three major groups, groups distinguished by the size and visibility of ice bodies and subdivided cryostructurally. More useful to thermokarst sedimentology would be groups defined by the volumetric ice content and the grain size.

2.3.2 A classification of cryofacies

Just as sedimentologists define bio- or lithofacies, emphasising biological or lithological features (Reading, 1986, p.4), so cryolithologists define "permafrost facies" (see Katasonov, 1969; 1975; 1978), emphasising geocryological ones. The latter can be simply termed **cryofacies.**

Five categories of cryofacies are distinguished according to volumetric ice content (Table 2.1): (1) pure ice, (2) sediment-poor ice (≥90% volumetric ice content), (3) sediment-rich ice (50-<90% ice), (4) icy sediment (excess ice-<50% ice) and (5) ice-poor sediment (no excess ice). The first four, representing ice-rich permafrost, are thaw-sensitive (Permafrost Subcommittee, ACGR, 1988), prone to thermokarst; the fifth, representing ice-poor permafrost, is thaw-stable. These categories are subdivided into sandy and muddy (including

Table 2.1 Cryofacies in the Tuktoyaktuk Coastlands

Cryofacies	**Description**
pure ice	structureless and layered cryostructures (csts)
sand-poor ice	≥90% ice lenticular, layered and suspended csts.
aggregate-poor ice	≥90% ice mud aggregates lenticular, layered and suspended csts.
sand-rich ice	50-<90% ice lenticular, layered and suspended csts.
aggregate-rich ice	50-<90% ice mud aggregates lenticular, layered and suspended csts.
icy sand	excess ice-<50% ice structureless, lenticular, layered and suspended csts.
icy mud/diamicton	excess ice-<50% ice lenticular, layered, regular and irregular reticulate, crustal and suspended csts.
ice-poor material	no excess ice sand, gravel, mud, diamicton; pure peat structureless and irregular reticulate csts. various sedimentary structures.

diamicton) cryofacies, in accordance with the the predominantly sandy or muddy nature of non-ice materials in the Tuktoyaktuk Coastlands and with the need to evaluate substrate control on thermokarst. Cryofacies may be further divided cryostructurally (Fig. 2.1).

Cryofacies commonly contain mud in the form of angular or granular **mud aggregates**. Angular mud aggregates comprise angular to subangular, equant to elongate blocks (≤1mm to several dm+ in diameter or length). Many are "matched" across ice bodies (Fig. 2.5A; cf. Mackay, 1989, Fig. 3e). In aggregate-poor ice, common just beneath the permafrost table, mud aggregates possess a suspended cryostructure (Fig. 2.4A); in aggregate-rich ice, their cryostructure is transitional between reticulate and suspended (Fig. 2.5A); and in icy mud/diamicton, it is regular (Fig. 2.3A) or irregular (Fig. 2.3B) reticulate.

Granular mud aggregates, so named because of their similarity with granular aggregates in soils, are typically equant. Their diameter ranges from ≤0.5mm to 20+mm, but is commonly less than 10mm (Fig. 2.4B). In aggregate-poor- (Fig. 2.4B) and aggregate-rich ice, their cryostructure is suspended; in icy mud/diamicton and ice-poor material, it is irregular reticulate.

Cryofacies occur singly or collectively. A group of two or more genetically related cryofacies is termed a **cryofacies association** (cf. Reading, 1986, p5), and a group whose genetic relationship is unclear a **cryofacies assemblage**. Examples of cryofacies and cryofacies associations are given in Section 3.3.2 and in Chapters 4 and 5.

Chapter 3 **UPLANDS**

"The crown o' the earth doth melt"

(*Antony and Cleopatra*, Shakespeare)

3.1 **Introduction**

During regional thermokarst, new levels - the floors of thermokarst basins, valleys and plains - form by degradation of ice-rich surfaces. The relief between these surfaces (<1m to 30+m; e.g. Hussey and Michelson, 1966; Tomirdiaro, 1982) allows distinction between ice-rich **uplands** (this chapter) and thermokarst **lowlands** (Chapter 5), the two being separated by thermokarst slopes (Chapter 4). Uplands constitute the pre-thermokarst landscape, one susceptible to two kinds of thermokarst, downwearing and backwearing.

This chapter describes the nature and origin of upland surfaces and thaw contacts, and discusses the sedimentology of a thaw layer created by regional downwearing thermokarst.

3.2 **Upland surfaces and deposits**

Upland surfaces are of two types, **primordial** and **polycyclic**. Primordial surfaces form where (1) glaciers develop; (2) glacier ice is buried (e.g. by glacigenic or aeolian deposits; see e.g. Dort, 1967; Grosval'd et al., 1986; Astakhov and Isayeva, 1988; French and Harry, 1988; 1990; Brodzikowski and Van Loon, 1991, p.187-189); (3) permafrost aggrades syngenetically through fine-grained sediments such as loess (e.g. Tomirdiaro, 1982; Carter, 1988); and (4) permafrost aggrades epigenetically through saturated, coarse-grained sediments (e.g. Mackay, 1971). Their respective deposits are (1) glacier ice; (2) buried glacier ice; (3) pore, segregated and syngenetic ice-wedge ice; and (4) massive segregated-intrusive ice and icy sediments (i.e. intrasedimental ice; Mackay and Dallimore, 1992). These surfaces and deposits

are primordial with respect to thermokarst, experiencing a major episode of thermokarst but once (cf. "non-reversible" thermokarst of Tomirdiaro and Ryabchun, 1978).

Primordial surfaces are underlain by abundant excess ice, in the extreme form by valley glaciers and ice-sheets, and show a broadly constant relationship between depth and volumetric ice content (e.g. Williams and Yeend, 1979; Lawson, 1983, Fig. 3d and g). During Pleistocene glacial episodes these surfaces were extensive, for example in Siberia and the western Arctic (see e.g. Soloviev, 1973; Tomirdiaro, 1982; Vincent, 1983, Figs 78-79; Astakhov and Isayeva, 1988; Carter, 1988; Danilov et al., 1989) and, of course, in glaciated regions (e.g. Flint, 1971). However, with regional thermokarst during the Late Wisconsinan-early Holocene warm interval, many surfaces degraded, leaving only fragments in some areas of permafrost. It is these fragments that now comprise hillocks ("yedoma"; Tomirdiaro, 1982) and residual plateaus between thermokarst basins, valleys and plains (Figs 1.3-1.6).

Polycyclic surfaces form by repetitive thermokarst and permafrost aggradation (e.g. Britton, 1967; Soloviev, 1973; Tomirdiaro and Ryabchun, 1978; cf. Harry et al., 1988) i.e. they experience alternating episodes of ice loss and gain. Consequently, their upland-lowland relief seldom exceeds a few m (e.g. Sellmann et al., 1975), and their sediments are mainly thermokarst-basin facies (cf. Section 5.3) and pore, segregated and epigenetic ice-wedge ice (e.g. Soloviev, 1973; French et al., 1982; Harry, 1982).

Polycyclic surfaces contain relatively small total amounts of excess ice and their volumetric ice contents decrease rapidly with depth (e.g. Sellmann et al., 1975, Fig. 7). Forming numerous levels at slightly varying elevations (e.g. Hussey and Michelson, 1966), these surfaces abound near oriented thermokarst lakes on NE Tuktoyaktuk and N Bathurst peninsulas (Mackay, 1956b), SW Banks Island (Harry and French, 1983) and the Alaskan Arctic Coastal Plain (e.g. Carson and Hussey, 1962; Sellmann et al., 1975). Polycyclic surfaces occur also in thermokarst lowlands throughout Siberia (e.g. Soloviev, 1973).

3.3 Areal thermokarst

3.3.1 Introduction

Where ice (+/- non-ice material) partially thaws or where partially thawed (or eroded) surface ice is buried, the thawing front (or erosion surface) is marked by a **thaw (or erosional) contact.** Examples of this include the frost table, the base of active and residual thaw layers and the contact between supraglacial melt-out till and underlying glacier ice. Such contacts occur at all scales, from partially thawed ice wedges (Chapter 6) to regional thaw (or erosional) contacts. But they are preserved in only three situations: (1) where snow, sediment or organic material is deposited on surface ice (e.g. in the accumulation zones of glaciers; Paterson, 1981, p.5-9; or on lake and river ice); (2) where debris melts out of, and insulates, underlying glacier ice (e.g. Eyles, 1979; Astakhov and Isayeva, 1988); and (3) where the thaw layer above partially thawed ground ice refreezes (e.g. Mackay, 1975a; 1978). The first situation generates **primary thaw (or erosional) contacts**, the second and third **secondary thaw (or erosional) contacts** (cf. Mackay, 1989). Primary thaw (or erosional) contacts indicate that thawing (or erosion) proceeded subaerially, before surface ice (or exhumed ground ice) was buried; secondary thaw contacts that it proceeded subterraneanly, melting either buried surface or periglacial ground ice. Regional thaw contacts, such as the Late Wisconsinan-early Holocene (secondary) thaw contact of the western Arctic (e.g. Mackay, 1992b), form by **areal thermokarst.**

Areal thermokarst is here defined as a type of regional thermokarst in which downwearing occurs uniformly beneath upland surfaces and is poorly, if at all, expressed in the surface relief (Fig. 4.2). Where areal thermokarst affects materials containing excess ice, it forms (in permafrost areas) regional thaw contacts beneath melt-out deposits. Little studied except by glacial sedimentologists (e.g. Shaw, 1979, Fig. 2; 1982; 1985, p.38-45; Haldorsen and Shaw, 1982; Paul and Eyles, 1990), and then usually long after the glacier ice has melted

(see Lawson, 1979 for an exception), these deposits are probably widespread in areas of past and present glacial (see e.g. Gravenor and Kupsch, 1959; Shaw, 1982; Kaplanskaya and Tarnogradskiy, 1986; Astakhov and Isayeva, 1988) and periglacial (see e.g. Tomirdiaro, 1982) ground ice.

3.3.2 Crumbling Point Upland

3.3.2.1 Cryostratigraphy

Crumbling Point is an ideal location at which to study areal thermokarst because of the textural contrast between superficial sand and muddy diamicton, and the preservation, near to the ground surface, of a layered cryofacies association (Fig. 3.1A). At least 15m thick, this association underlies the primordial surface of Crumbling Point Upland (Fig. 4.2) and comprises mainly aggregate-poor and aggregate-rich ice, icy diamicton and ice-poor diamicton and sand. Mud aggregates are granular, and the volumetric ice content locally exceeds 95%. Layers (c.0.01-0.4m thick and c.2-60+m long) are horizontal to moderately inclined and parallel to subparallel. Some are deformed into recumbent isoclinal and chevron folds (Fig. 3.1A). Above this association is one of sand and diamicton cryofacies.

The sand and diamicton cryofacies association comprises icy and ice-poor diamicton locally overlain by a veneer of ice-poor sand. The veneer (≤c.1.5m thick) is structureless and discontinuous, merging locally with the tops of sand wedges (see Murton and French, 1993). This association (1.0-2.5m thick) occurs only between the sand wedges (Fig. 3.1A).

Separating the two associations at an average depth of 2.3m ($n=37$; $\sigma=0.3$m) is a sharp, planar to gently undulating contact (Fig. 3.1). This is absent within the sand wedges.

In the context of areal thermokarst these observations raise questions about the age and origin of the contact and of the sand and diamicton cryofacies association.

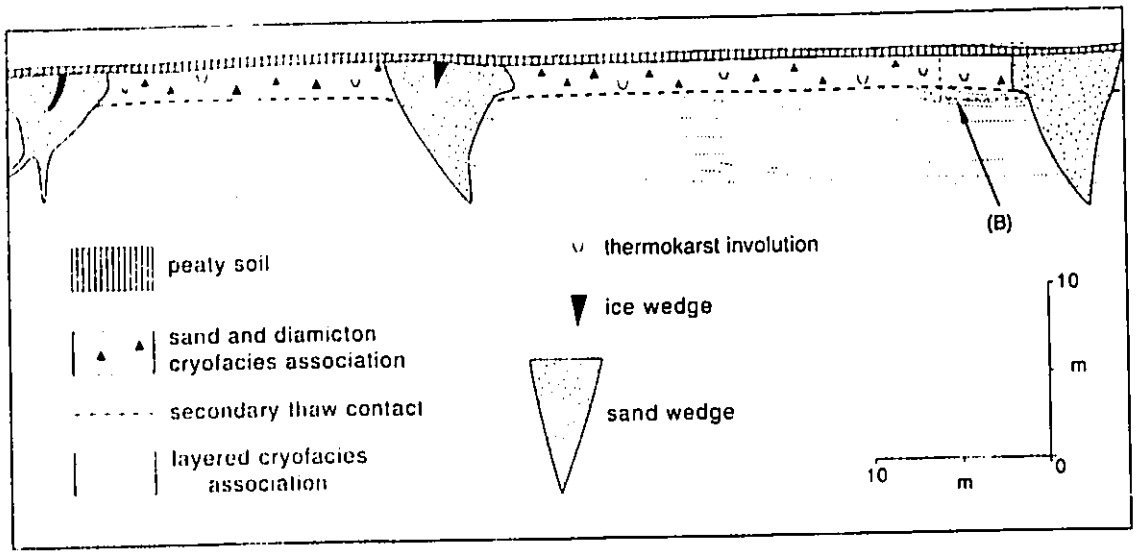

Fig. 3.1 **CRYOSTRATIGRAPHY OF CRUMBLING POINT**

(A) Sand wedges penetrating the **layered** and the **sand and diamicton cryofacies associations**. Between the associations, there is a sharp contact - here, an angular unconformity (B) - representing the **(ate Wisconsinan-early Holocene secondary thaw contact**. The overlying sand and diamicton association - here, primarily melt-out diamicton - contains thermokarst involutions (section 7.2) and represents the **refrozen thaw layer** (sections 3.3.2.3 and 3.3.2.4). (June 15 1991)

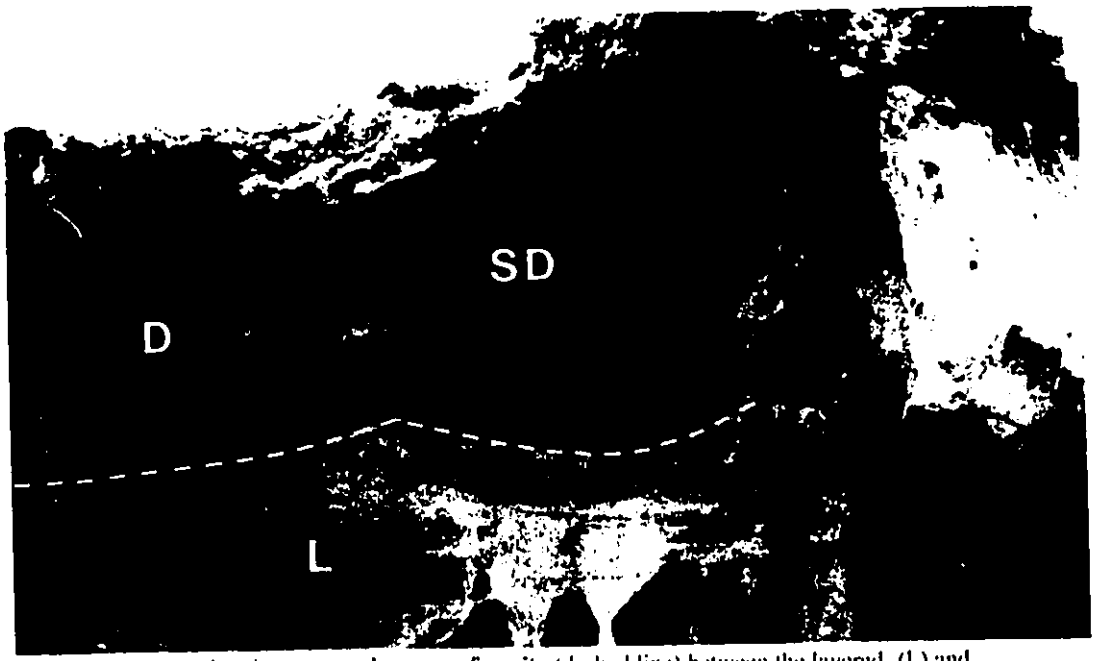

(B) Close-up showing an **angular unconformity** (dashed line) between the layered (L) and the sand and diamicton (SD) cryofacies associations. Sand ball-and-pillow structures within the icy to ice-poor diamicton (D) are thermokarst involutions (cf. Figs 7.1-7.4). See (A) for scale. (June 15 1991)

3.3.2.2 The contact between the cryofacies associations

The contact is a regional secondary thaw contact. This is indicated where it coincides with an angular unconformity, cryostructural and isotopic discontinuities, and the abrupt upward termination of ice along the sides of sand wedges.

(1) Layers in the layered association are locally truncated, delimiting an angular unconformity (Fig. 3.1).

(2) At the contact there is commonly a cryostructural discontinuity. For example, Fig. 3.2 shows a sharp, planar discontinuity between a suspended cryostructure and one that is transitional between suspended and irregular reticulate. Here the volumetric ice content abruptly decreases from c.90-95% in aggregate-poor ice below the contact to c.10-20% in icy diamicton above it. These changes likely reflect different conditions of freezing, the overlying icy diamicton freezing when less water was supplied to the freezing front.

(3) The average $\delta^{18}O$ value of ground ice above the contact is -24.7‰ SMOW (n=4; σ=1.6‰), that below it -30.2‰ (n=8; σ=0.8‰), indicating that the contact coincides with an isotopic discontinuity (Fig. 3.3). If this were a thaw contact, one would expect it to be marked thus (e.g. Burn et al., 1986), since the ground ice above it would likely have incorporated both meltwater that was isotopically identical to the parent (underlying) ground ice and atmospheric water that was isotopically heavier (reflecting the warmer climate during thaw). Consequently, ground ice above the contact should be isotopically heavier than that below it, as indeed found (Fig. 3.3).

(4) Along the sides of many sand wedges occurs a layer of sand-poor ice, sand-rich ice and icy sand (Fig. 3.4). Isotopically much lighter (the average $\delta^{18}O$ value =-29.0‰; n=5; σ=0.5‰) than local Holocene ground ice (see e.g. Mackay, 1983; Michel, 1990), and in particular, lighter than ice above the contact (average $\delta^{18}O$ value =-24.73‰; n=4; σ=1.6‰) and below the active layer, this sand-wedge related ice is likely of pre-Holocene age.

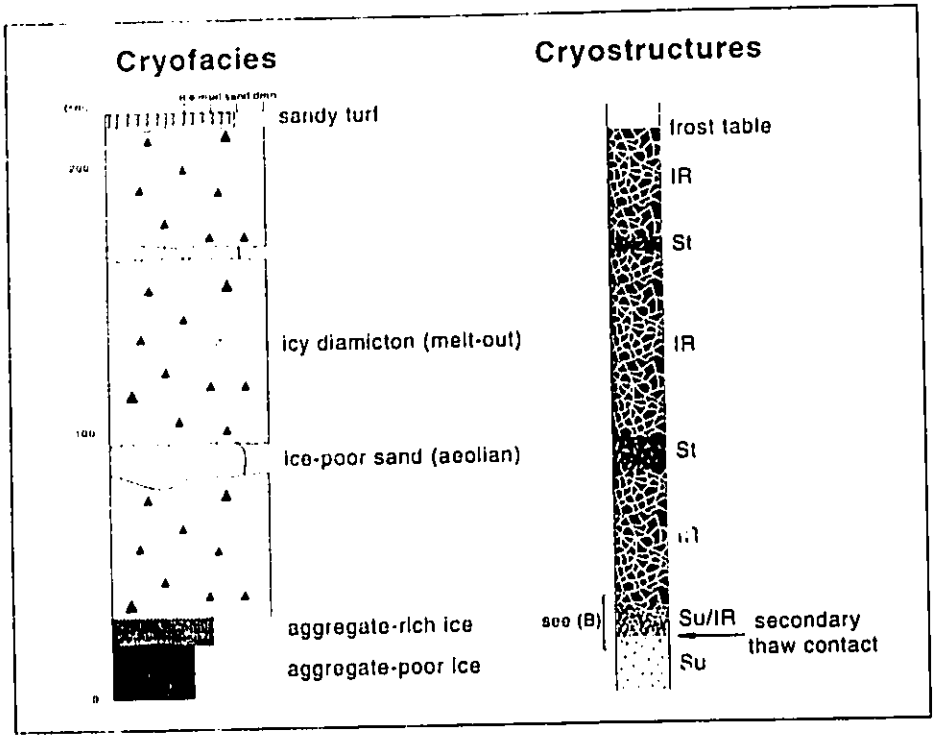

Fig. 3.2 **CRYOSTRUCTURAL DISCONTINUITY**

(A) Cryofacies and cryostructure logs across the contact between the layered and the sand and diamicton associations, Crumbling Point. At the contact, there is a cryostructural discontinuity (B) that is underlain by aggregate-poor ice with a **suspended cryostructure** and overlain by aggregate-rich ice whose cryostructure is **transitional between suspended and irregular reticulate.**

(B) Close-up of cryostructural discontinuity (at base of pencil). (June 6 1991)

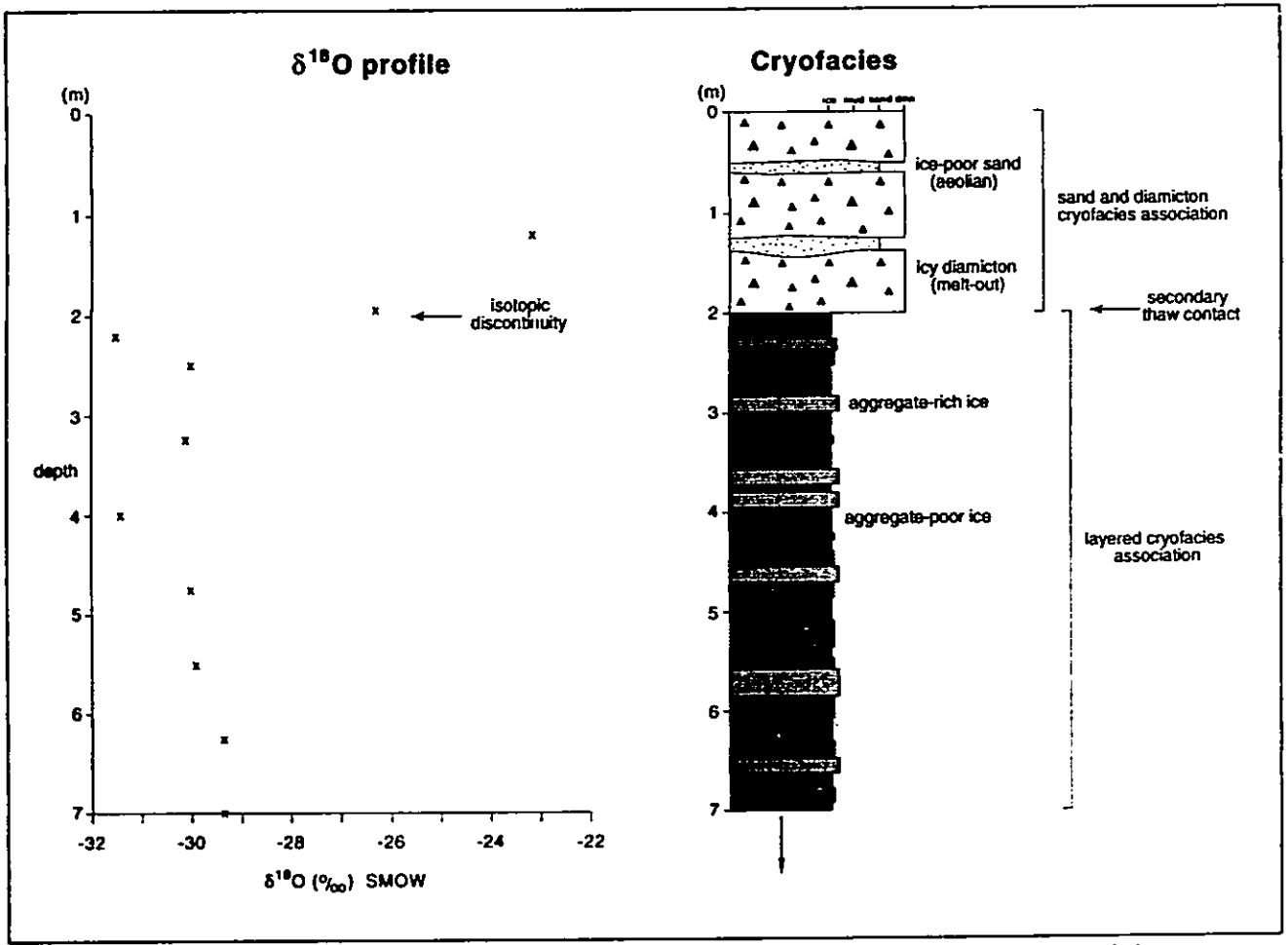

Fig. 3.3 $\delta^{18}O$ profile through the layered and the sand and diamicton cryofacies associations, Crumbling Point. At their contact, there is an isotopic discontinuity; the average $\delta^{18}O$ value of ground ice above the contact is -24.7‰, that below it -30.2‰. With increasing height above the contact, the $\delta^{18}O$ values become isotopically heavier. A schematic cryofacies log is shown on the right.

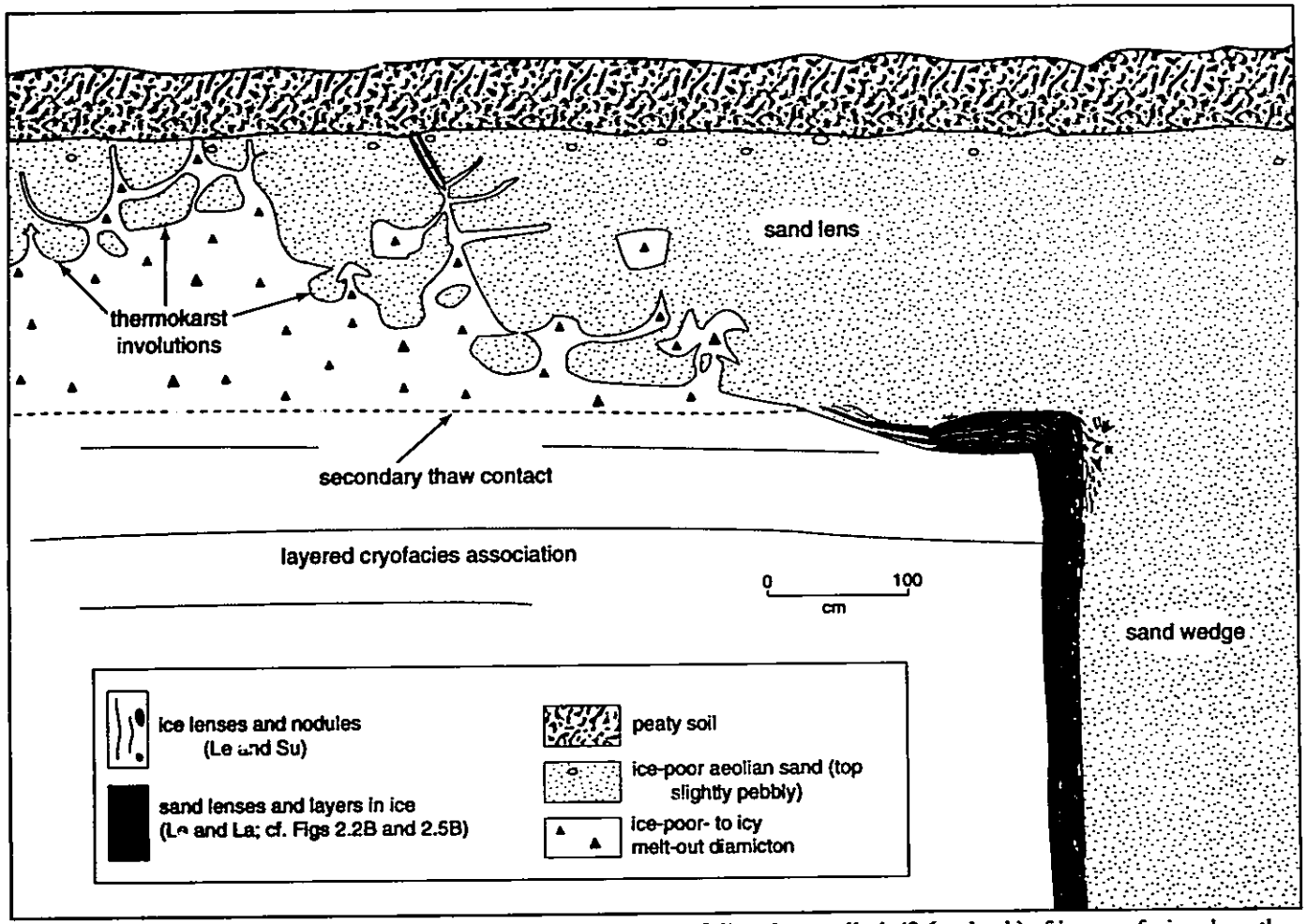

Fig. 3.4 Lower limit (2.5m depth) of thermokarst involutions (section 7.2) and upper limit (2.6m depth) of icy cryofacies along the base of a sand lens and the side of a sand wedge, Crumbling Point. The depth of this antithetic relationship coincides with the secondary thaw contact. (June 12 1991)

Assuming that it predates the contact and originally extended to the permafrost table, one would now expect this icy layer to terminate at the contact (i.e. at an average depth of 2.3m). This hypothesis can be test in large sand lenses whose base traverses the average depth of the contact. At one location the ice tapers out at a depth of 2.6m (Fig. 3.4), supporting the hypothesis.

The evidence above indicates that the contact is a thaw contact; and because it is younger and lower than the tops of the sand wedges (Murton and French, 1993; Fig. 5.11), the thaw contact must be secondary, one representing the base of an ancient thaw layer.

3.3.2.3 The sand and diamicton cryofacies association

The sand and diamicton cryofacies association formed by melt-out and soft-sediment deformation. This is indicated by four lines of evidence: (1) the underlying secondary thaw contact (see above); (2) the similarity between the sand and diamicton and the underlying cryofacies; (3) soft-sediment deformation structures and sand wedges with deformed tops; and (4) the relationships between the thickness of the diamicton and both the texture and the volumetric ice content of underlying cryofacies.

Both cryofacies in this association resemble underlying ones. The icy to ice-poor diamicton differs only in features relating to volumetric ice content (generally several % to c.40%). Thus, compared to underlying cryofacies, its clast density is higher and suspended cryostructures are rarer, features best explained by melting of the uppermost layered association (cf. Lawson, 1981, Fig.3 unit a). Likewise, the ice-poor sand resembles the underlying sand-wedge sand in terms of texture and grain-surface features (Murton and French, 1993). The sand is aeolian, deposited on the ground surface as a discontinuous veneer, and in thermal contraction cracks to form sand wedges (Section 6.5).

The sand and diamicton association contains abundant soft-sediment deformation structures and sand wedges with deformed tops. Suffice it here to say that these features must have formed when the association was unfrozen and that they occur only where the top of the layered association has melted (see Section 7.2). Melting is indicated where deformation structures overlie truncated bands in the layered association (Fig. 3.1) and where they abruptly cease at a certain depth, relating antithetically with ice along the sides of sand wedges (Fig. 3.4). In the last example deformation structures extend no deeper than 2.5m, whereas ice extends no higher than 2.6m (Fig. 3.4).

Finally, the diamicton is thickest where thawing progressed mainly through the layered association and thinnest where it progressed mainly through aeolian sand. For example, Fig. 3.5 shows a 1-3cm thick unit of diamicton beneath a 1.5m thick unit of sand. Conversely, in the absence of sand, the diamicton attains thicknesses of 2-2.5m (Fig. 3.1). The thickness of diamicton also varies inversely with the volumetric ice content of underlying cryofacies, being thickest (≤2.5m) above cryofacies which are ice-poor (Fig. 3.1) and thinnest above those which are ice-rich (Fig. 7.4B). For example, the average thickness of the diamicton in Fig. 6.4B is c.30cm, and the average excess ice content of the underlying cryofacies c.70%. Therefore approximately 1m of this cryofacies would have thawed to produce 30cm of melt-out diamicton.

The evidence above indicates that the sand and diamicton association is a partially refrozen thaw layer, either a deep active layer or a residual thaw layer.

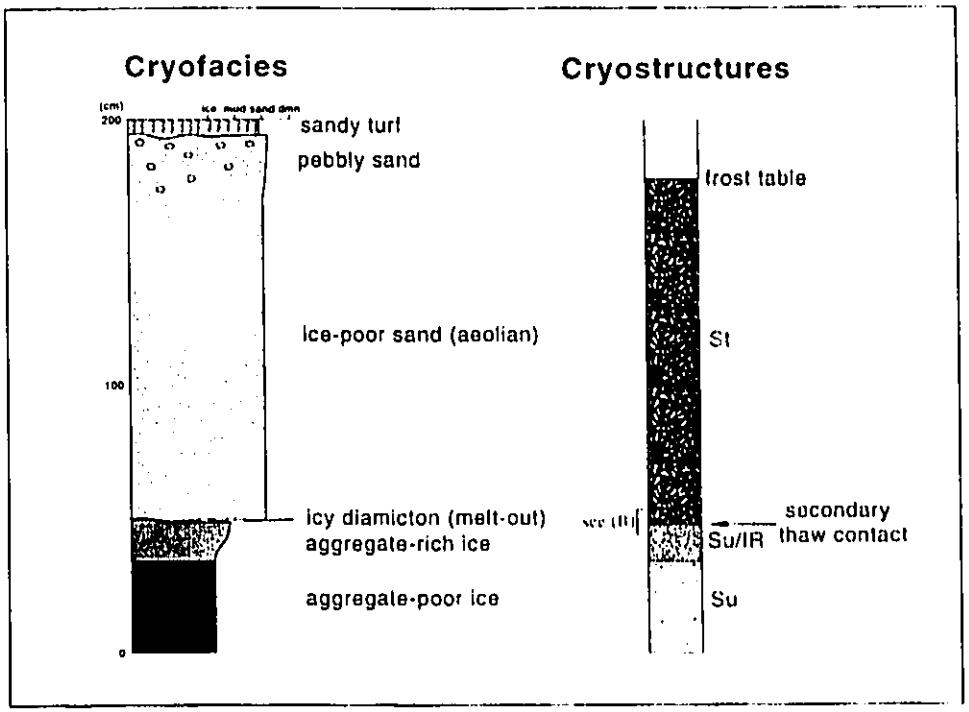

Fig. 3.5 **MELT-OUT DIAMICTON**

(A) Cryofacies and cryostructure logs through a 1.5m thick sand lens, Crumbling Point. Between the base of the lens and the top of the underlying aggregate-rich ice - part of the layered association, 2-3cm of melt-out diamicton overlies the secondary thaw contact (B).

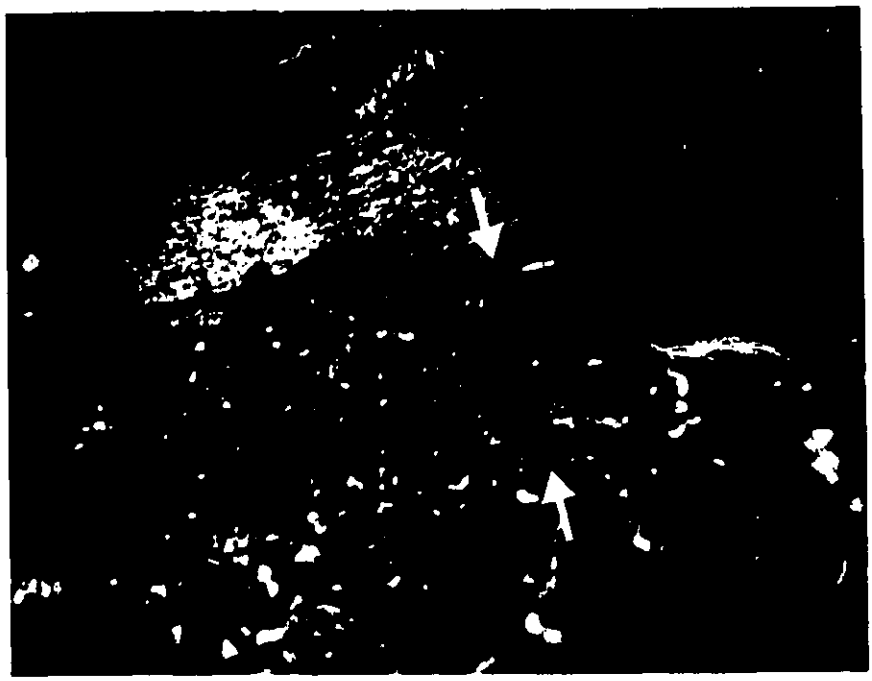

(B) Close-up of thin (3cm) unit of melt-out diamicton (between arrows). (May 31 1991)

3.3.2.4 The date of thawing

The thaw layer, melt-out diamicton and underlying secondary thaw contact likely formed during the Late Wisconsinan-early Holocene warm interval. This is suggested by two ^{14}C dates of 9,480 +/- 100 years BP (Beta-46224) and 8,860 +/-180 years BP (Beta-46223) from wood fragments above the contact. The first was from the bottom of a 40cm thick layer of fibric peat overlying a 1-1.5m thick sand lens that is separated from the underlying secondary thaw contact by 2-3cm of melt-out diamicton. The second was from a root suspended in slump-floor deposits above a slump-floor secondary thaw contact (Section 4.5; Fig. 4.10). The simplest interpretation of these dates is that the wood grew during the warm interval that formed both the underlying thaw contact and melt-out diamicton and that triggered the thaw slumping. The warm interval was likely that during the Late Wisconsinan-early Holocene, a time when the western Arctic experienced regional thermokarst (e.g. Mackay, 1978; French et al., 1983; Burn et al., 1986; Rampton, 1982, p.33; 1988, Fig. 66; Harry et al., 1988; Mackay, 1992b).

3.4 Conclusions

3.4.1 Substrate control on areal thermokarst

The sedimentological effects of areal thermokarst depend strongly on substrate, particularly on grain-size and volumetric ice content. Grain-size determines the texture of melt-out deposits, and volumetric ice content the potential thaw-settlement and the availability of meltwater for soft-sediment deformation. Beneath ice-rich parts of the upland surface at Crumbling Point, Mason Bay and Hadwen Island, a distinctive sand and diamicton cryofacies association overlies a secondary thaw contact. These features formed by partial melting of the underlying cryofacies, melting which had several consequences: (1) the formation of a secondary thaw contact; (2) the generation of meltwater and melt-out deposits in the overlying

thaw layer; (3) the deformation of the sand veneer, melt-out diamicton and the tops of sand wedges; and (4) the subsidence of the primordial surface. By contrast, where the upland surface overlies ice-poor cryofacies (e.g. ice-poor sand), areal thermokarst has not occurred. Thus primary sedimentary structures (e.g. vertical sand laminae in sand wedges) are well preserved (see Section 6.5.1; Fig. 6.10), and melt-out deposits closely resemble their underlying cryofacies. In such areas, only where the secondary thaw contact truncates ice and composite ice-sand wedges (Fig. 6.8) is it clear that the overlying sediment has thawed.

3.4.2 A criterion for identifying areal thermokarst: **thermokarst involutions**

There do not appear to be any ubiquitous sedimentological features diagnostic of areal thermokarst. While secondary thaw contacts are always present, without detailed geochemical sampling (see e.g. Péwé and Sellmann, 1973), they may be impossible to recognise in ice-poor cryofacies. Under special circumstances, however, one feature does appear to indicate areal thermokarst, namely the widespread occurrence of soft-sediment deformation structures in a particular cryostratigraphic horizon. These structures are termed **thermokarst involutions** (their discussion is deferred to Chapter 7). In the Summer Island area (Fig. 1.5), thermokarst involutions characterise the sand and diamicton cryofacies association. Here the special circumstances are (1) texturally distinct sediments and (2) a reverse-density gradient during areal thermokarst (Section 7.2). To apply the criterion, one must exclude deformation structures that are distributed only locally (e.g. ice-wedge casts and partially thawed ice wedges; Section 6.3) and those which are unrelated to areal thermokarst (e.g. structures in slump and thermokarst-basin facies; Chapters 4 and 5). In short, areal thermokarst may be inferred only where numerous thermokarst involutions occur within the same horizon at several well-spaced sites.

Chapter 4 SLOPES

"It is ... of the utmost importance that the [periglacial mass-movement] facies be studied in greater detail, particularly because its presence may be taken as a clue for establishing the boundary line between glacigenic and non-glacigenic environments."

(Brodzikowski and Van Loon, 1991, p.491)

4.1 Introduction

Icy slopes bordering upland surfaces retreat by backwearing thermokarst (Czudek and Demek, 1970; Lewkowicz, 1987; cf. "backwasting" of Eyles, 1979). Although studied intensively in terms of geomorphology (see e.g. French, 1976, p.119-125; Washburn, 1980a, p.195-198; Lewkowicz, 1988, p.348-353), backwearing thermokarst has been studied little in terms of sedimentology, except in glacigenic environments (Brodzikowski and Van Loon, 1991, p.346-349; 490-498; see e.g. Boulton, 1968; Eyles, 1979; Lawson, 1979; 1981; 1982; 1988; Brodzikowski and Van Loon, 1991, p.138-148).

This chapter describes the sedimentology of backwearing thermokarst in a permafrost environment, detailing the landforms, sedimentary processes and facies of **thermokarst slopes**. These slopes comprise steep icy bluffs and retrogressive thaw slumps.

4.1.1 Steep icy bluffs

Steep ($\geq 25^{o}$ to vertical) slopes containing small amounts of excess ice ($\leq$c.30-40%) are termed **steep icy bluffs** (Fig. 4.1). Observations at North Head indicate that they retreat by thermokarst and coastal erosion and suggest that they develop where the percentage of excess ice in upland materials is less than c.30-40%. The cryofacies beneath the northwesternmost

Fig. 4.1 **Steep icy bluff**, North Head. The cryofacies comprise ice-poor sand and sandy ice. Prior to digging, the ice was covered by slumped sand. Figure for scale. (June 15 1990)

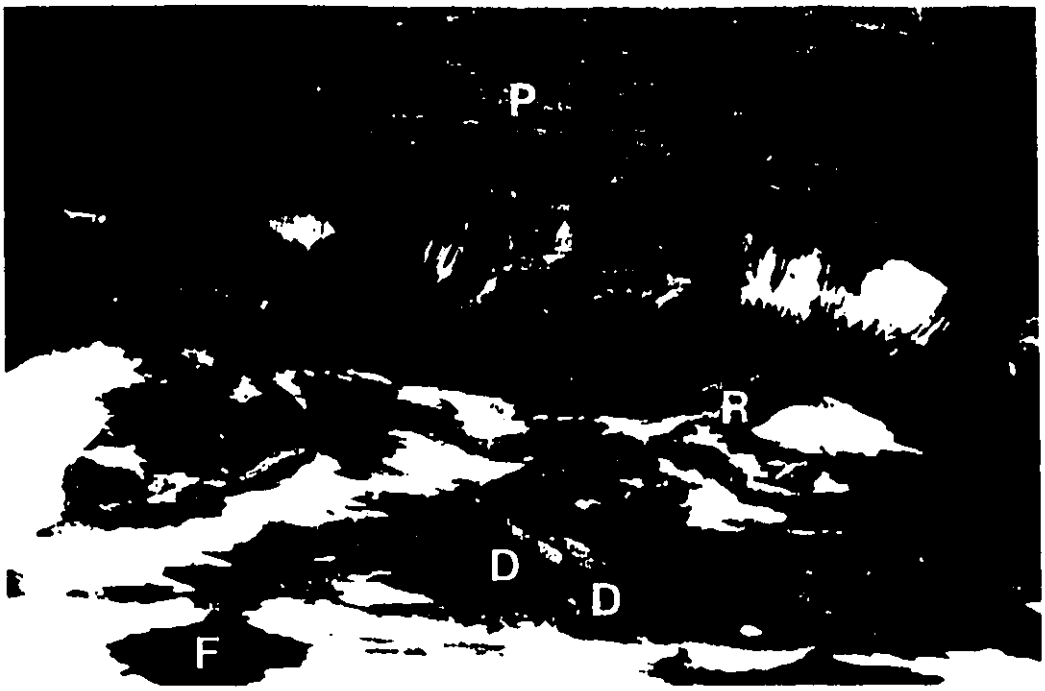

Fig. 4.2 **Retrogressive thaw slump**, Crumbling Point. Icy rills lead down from the headwall (16-18m high) to the slump floor, which comprises debris flows (D; section 4.2.1), braided systems (e.g. sand fans - F; section 4.2.2), and residuals (R) of old slump-floor deposits. The small, high-level slump in the centre has been temporarily stabilised by an apron of structureless sand (sections 4.2.5 and 4.3.4). The primordial (upland) surface (P), today retreating through backwearing thermokarst, experienced areal thermokarst (section 3.3) during the late Wisconsinan-early Holocene warm interval. (May 30 1991)

100m of the steep icy bluff here comprise pure ice, aggregate-poor ice, sand-poor ice and ice-poor sand (Fig. 4.1) and those beneath the northeasternmost 200m an ice-breccia cryofacies association (Fig. 5.12B). The number of steep icy bluffs in the Tuktoyaktuk Coastlands is unknown, because ground-ice exposures are ephemeral, but given the abundance of excess ice here, they may be common.

4.1.2 Retrogressive thaw slumps

Landforms with a gentle ($\leq 15^{o}$) footslope fronting a steep ($15\text{-}80^{o}$), extremely ice-rich headwall that is capped by non-ice material are called **retrogressive thaw slumps** (Fig. 4.2; e.g. Lewkowicz, 1988, p.348-353). The most active features of permafrost terrain (Burn and Lewkowicz, 1990), thaw slumps are common in areas of ice-rich permafrost (e.g. French, 1976, p. 119-122), around the margins of debris-mantled glaciers and in areas of stagnant glacier ice (e.g. Lawson, 1979; 1982, Figs. 3 and 4; Drewry, 1986, p. 134-137). In the Tuktoyaktuk Coastlands most slumps are triggered by coastal (or lacustrine or fluvial) erosion (see Mackay, 1963, Fig. 21). Observations at North Head suggest that they develop where the percentage of excess ice in upland materials exceeds c.30-40%.

4.2 Thermokarst-slope processes and landforms

The processes and landforms in slump floors and fronting steep icy bluffs are shown in Table 4.1.

Table 4.1 Thermokarst-slope processes, landforms and facies

Processes	Landforms	Facies
debris flow:		
large	debris flows	organic-rich diamicton
		sandy diamicton
small	fans	poorly stratified sand
sheetfloods	fans	well-stratified facies
channel floods	fans	well-stratified facies
	braided channels	well-stratified facies
	braidplains	well-stratified facies
suspension settling	mudflats	? muddy rhythmite
colluvial processes	diamicton aprons	organic-rich diamicton
(slide, flow, fall)	mixed aprons	sandy diamicton
	sand aprons	structureless sand

4.2.1 Debris flows

In the study area, debris flows may be subdivided into large and small flows. Large flows of muddy diamicton (+/- sand) are common in the floors of retrogressive thaw slumps. The flows are typically a few m to c.30m wide, several m to several da m long and 10cm to 2m high (Fig. 4.2). Extending downslump from the base of headwalls, they commonly override older flows and may terminate anywhere on slump floors, some even extending offshore, where they are eroded by waves.

Small debris flows in the form of sand flows are best developed on, and at the base of, the steep icy bluff at North Head. Here two end-members of sand flow are distinguished, lobate and sheet-like. Lobate sand flows are typically 0.5cm-10cm wide, 0.5-3cm thick and several cm to several m long (Fig. 4.3A). Most begin on the steep icy bluff, just below exposed or recently covered bodies of ground ice. After crossing the basal break-of-slope they decelerate and freeze as water infiltrates the underlying sand (cf. Bull, 1964) and as shear stresses decrease with the abrupt decline in slope angle. Most freeze within a few m of the basal break-of-slope, forming small, steep (12-24^{o}) fans (Fig. 4.3A).

Sheet-like flows also fringe the steep icy bluff at North Head. Generally a few mm to c.2cm thick, a few cm to c.3m wide and ≤several m long (Fig. 4.3B), they too are sand-rich, but contain more meltwater than lobate flows. Sheet-like flows commonly head from the incised lobes of lobate flows on the mid to upper parts of fans. At North Head, sheetflows form relatively large (≤c.10+m radius), moderately sloping (c.8-12^{o}) fans (Fig. 4.3B).

4.2.2 Sheetfloods

During warm, sunny summer afternoons, when slump headwalls ablate most rapidly (cf. Dylik, 1969; Lewkowicz, 1986), sheetfloods head from the mouths of headwall meltwater rills (Fig. 4.12) and from slump-floor gullies. With flow depths seldom exceeding 1cm the

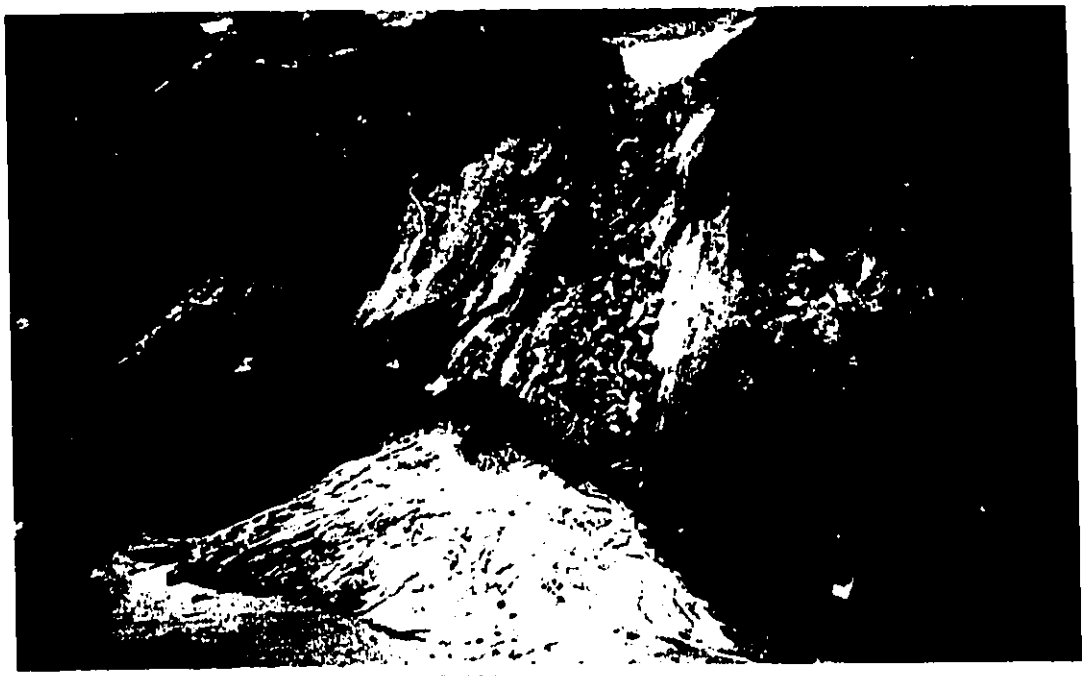

Fig. 4.3 **SAND FLOWS AND SAND FANS**

(A) Small **lobate sand flows** extend down from exposed ground ice (white) to a small fan at the base of a steep icy bluff, North Head. This fan formed within a few days of a storm eroding the bluff. 50cm high ice axe for scale. (August 8 1991)

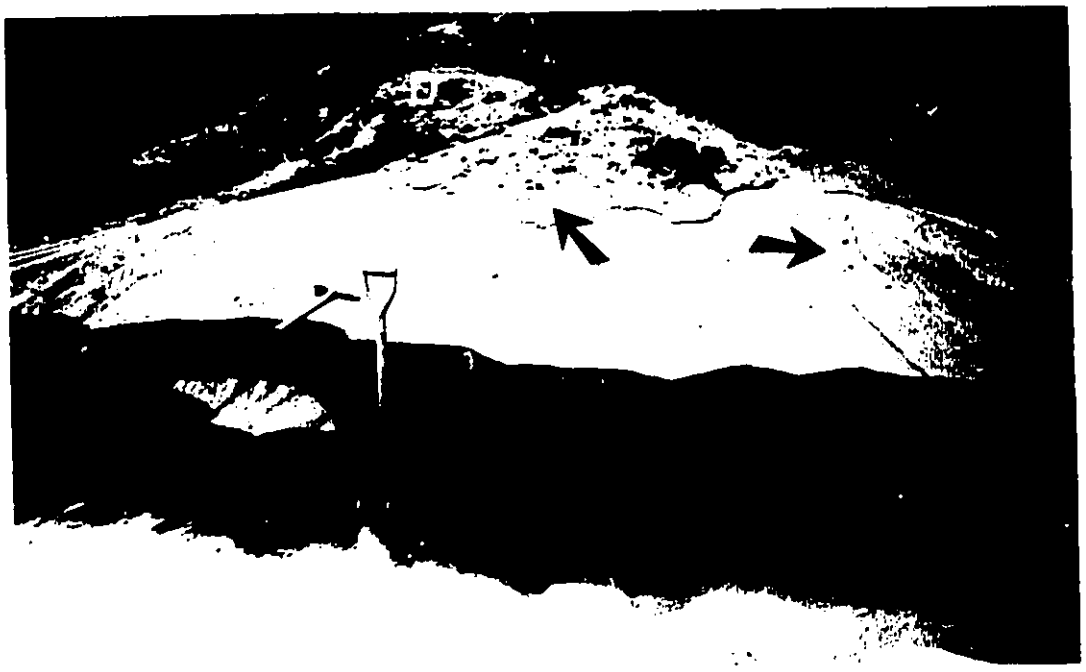

(B) Wave-truncated sand fan at the base of a steep icy bluff, North Head. The fan was built mainly by **sheet-like sand flows** (arrows) and **sheetfloods.** Blocks of moist sand and organic material occur on the fan surface and *well-stratified* **facies** (section 4.3.3) beneath it. The apex of the fan is covered by a large, sandy debris flow (D). 1m high shovel for scale. (August 5 1991)

floods transport sand, mud, organic debris, granular mud aggregates (cf. Rust and Nanson, 1989) and small pebbles, forming braided systems (fans, braided channels and braidplains) on slump floors (Fig. 4.4A).

Large (≤15+m radius) and gently sloping (≤8°) fans commonly develop beneath sand wedges (Fig. 4.4A) and at the mouths of meltwater gullies. The gullies themselves are commonly flat-floored and braided, adjacent gullies supplying sediment to braidplains. All of these landforms are characterised by longitudinal bars and shallow, low-sinuousity channels (Fig. 4.4). Small bars (typically a few to several cm wide and several cm to a few dm long; Fig. 4.4B) of mud aggregates (and/or sand) develop where particularly large (≤10mm diameter) aggregates are deposited, for example in reaches of flow divergence. As additional aggregates come to rest upstream of these blockages, bars form within as little as a few minutes. The small bars are commonly superimposed on large bars (≤several dm wide and ≤ a few m long), which are active only during the largest sheetfloods, namely during the hottest weather.

4.2.3 Channel floods

Sheetfloods usually coincide with channel floods elsewhere in slump floors. Channel floods, however, are more common and longer lasting, occurring whenever air temperatures exceed 0°C. These floods form straight to meandering channels up to c.2m wide and deep, with cross-profiles varying from box- to V-shaped. The channel floors are locally covered by a lag deposit of granules to cobbles, sometimes upstream-imbricated.

4.2.4 Suspension settling

When muddy slump floods flood, turbid meltwater may pond upslump of large debris flows. As floods abate, mud within ponds settles from suspension, forming mudflats:

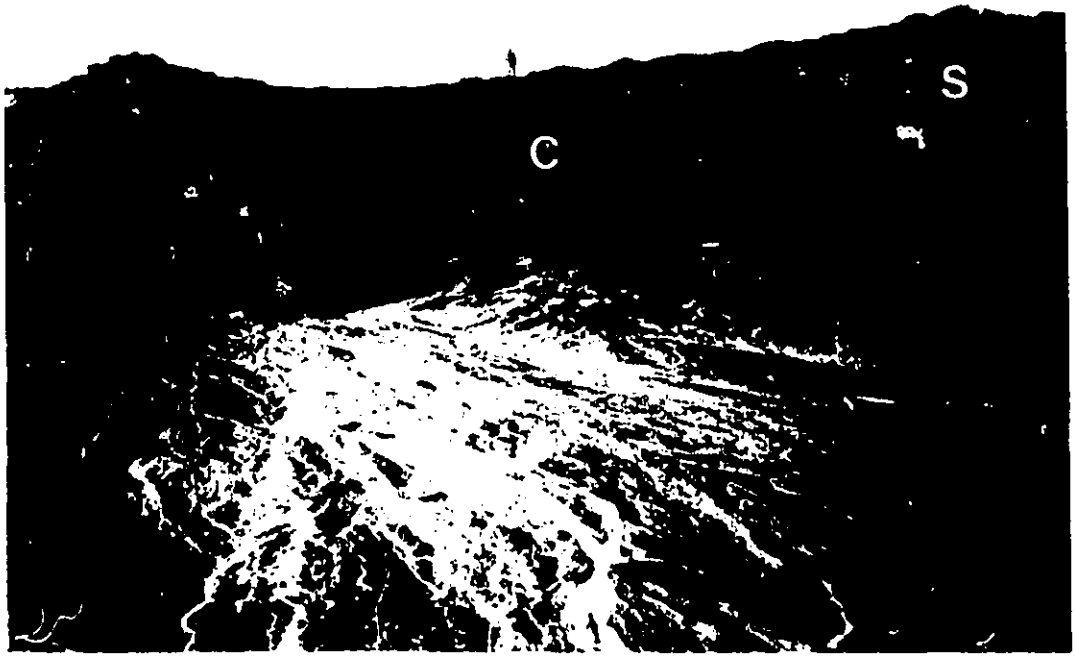

Fig. 4.4 **BRAIDED SYSTEMS**

(A) Large, coalescent **braided fans** (of sand, mud and granular mud aggregates) in a slump floor, Crumbling Point. The headwall exposes sand (S) and composite (C) wedges (sections 6·4-6.5). Figure for scale. (July 10 1990)

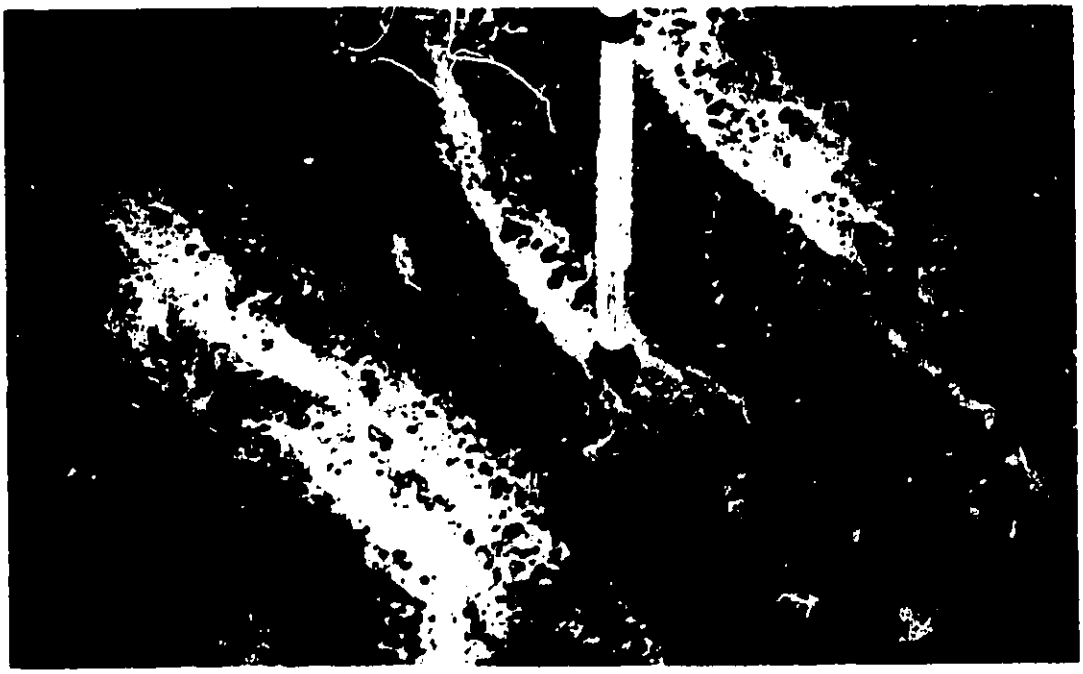

(B) **Longitudinal bars of granular mud aggregates** on the surface of a sand fan that is similar to (A), Crumbling Point. Melting-out from aggregate-rich cryofacies in the slump headwall (Fig. 2.4B), the aggregates are transported downslump by sheetfloods. As the sheetfloods wane, they deposit mud drapes (≤1.5mm thick; D) over both the bars and the intervening channels. 14cm high pencil for scale. (September 2 1991)

featureless, almost horizontal surfaces incised by meandering channels and interspersed with blocks of peat and sod. Mudflats are well developed in the slump floors at Peninsula Point.

4.2.5 Colluvial processes

On slump headwalls and steep icy bluffs, material is deposited by colluvial processes (fall, slide and flow). For example, blocks of peat and sod fall from most upland surfaces, and sand-bed slides and sandflows occur on the steep icy bluff at North Head and on many degrading sand wedges. Such processes and their deposits form **colluvial aprons**.

Colluvial aprons (cf. "ice-slope colluvium" of Lawson, 1981; 1987) are subdivided according to their dominant composition (e.g. diamicton, mud, sand, peat and mixed aprons), the most common being diamicton, sand and mixed aprons. Found in most slumps, diamicton aprons typically form beneath free faces (≤c.4m high) in dried slump-floor diamicton (e.g. flanking residuals in Fig. 4.2). Sand aprons are common at North Head and Crumbling Point (Fig. 4.5A). At the latter they form by destruction of sand wedges, developing best where the height of the headwall is less than the depth of the wedges (≤10m; Fig. 4.5A). Mixed aprons occur at Crumbling Point, Mason Bay and Hadwen Island (Fig. 4.5B), where some retreating slopes contain both sand and diamicton.

4.2.6 General comments

The spatial relationships between slump-floor processes and landforms are complex and dynamic. During the thaw season, meltwater discharge and sediment supply - the prime controls on slump-floor sedimentation - continuously change according to erosion, weather, time of day, amount of snowpack remaining at the base of thermokarst slopes, and variable exposures of cryofacies. For example, slump-floor processes tend to be most active during

Fig. 4.5 **COLLUVIAL APRONS**

(A) **Sand apron** (S) of structureless sand (section 4.3.4) beneath an eroded sand wedge (W). Crumbling Point. 10m high headwall. (August 27 1991)

(B) **Mixed organic and diamicton apron** rimming the floor of a slump, Hadwen Island. The slump is littered with chunks of peat and sod. Sand buttresses (B; sand wedges) are flanked by small sand aprons. Figure (arrow) for scale. (July 6 1991)

mid-afternoon, when air temperatures are typically highest. This variability in meltwater discharge and sediment supply changes the location of slump-floor processes and landforms, individual forms migrating across slump floors, burying, eroding or deforming adjacent ones. For example, large debris flows commonly override fans, mudflats and braidplains, buckling sediments in front of them. At the shoreline, slump-floor and marine (or lacustrine) processes interact (e.g. fan progradation and wave erosion).

Some thermokarst-slope processes form a continuum. This is best illustrated between the highly viscous, lobate sand flows and highly fluid sheetfloods (cf. Bull, 1964; 1977), the former tending to occur on the mid to upper parts of fans, the latter on the lower parts. This continuum is strongly controlled by the moisture content (cf. Lawson, 1979).

4.3 **Thermokarst-slope facies**

At the base of steep icy bluffs and in slump floors, five facies are distinguished (Table 4.1). Because they are deposited on footslopes formed by backwearing thermokarst, the resedimentation deposits are termed **thermokarst-slope facies**.

4.3.1 Organic-rich diamicton

Debris flows, colluvial processes and the slow downslump movement of slump-floor debris all deposit **organic-rich diamicton**. This is commonly structureless and has a variable matrix of sand and mud. Clasts (typically subrounded to rounded pebbles and cobbles) are matrix-supported and randomly dispersed, elongate ones showing a very weak preferred orientation (Fig. 4.6). Organic material comprises fragments of charcoal and plants as well as blocks of peat and sod; the blocks are generally a few cm to a few dm in length or diameter and variously inclined. Plants rooted in sod blocks include *Salix* spp., *Dryas* spp., *Cassiope* spp., *Senecio congestus* and grasses. Diamicton may be vertically fractured, and

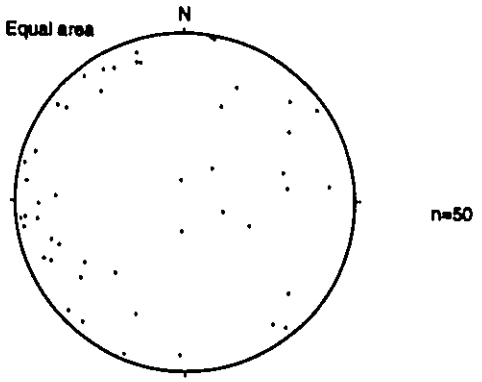

Fig. 4.6 Scatter plot on a stereonet showing the angle and direction of dip of elongate clasts in sandy diamicton, Crumbling Point. The eigenvalue is 0.48 (very weak preferred orientation).

Fig. 4.7 Sandy diamicton with steeply dipping to vertical sand lenses (arrows), Crumbling Point. Some lenses contain organic material (black). 12cm high trowel handle for scale. (August 30 1991)

some is crudely parallel-bedded, bed thickness being a few to several dm (Mackay,1963, Fig. 20); such beds likely represent individual debris flows. This facies commonly overlies gently curved secondary thaw contacts, and where the thickness of diamicton exceeds several dm, permafrost may aggrade upwards into its base, forming irregular reticulate and (inclined) lenticular cryostructures (Table 2.1; Fig. 6.12A).

Organic-rich diamicton has a sandy subfacies, **sandy diamicton** (Fig. 6.12A). Abundant on headwalls and in slump floors at Crumbling Point and Mason Bay, this characterises areas where ice-rich cryofacies abut aeolian sand.

Sandy diamicton comprises either a mixture of structureless, fine-grained sand and organic-rich diamicton or irregular masses and lenses of sand within the diamicton. The lenses are of two kinds: (1) steep ($\geq 40^{o}$) to vertical and (2) horizontal to moderately inclined. The first ($\leq$1mm to several cm thick and a few cm to several dm+ long) are parallel to subparallel, steeply inclined lenses dipping upslump (Fig. 4.7) and possessing sharp, curved to wavy sides. Some lenses contain elongate clasts and blocks of organic material that parallel their sides. On adjacent ground surfaces occur abundant desiccation cracks. It would seem likely, therefore, that the lenses are sand-filled cracks, the sand having been washed or blown into them.

Horizontal to moderately inclined ($\leq$c.40^{o}) sand lenses (a few mm to several dm thick and a few cm to several m long) commonly parallel to subparallel the ground surface (Fig. 6.12). Some bifurcate, and the thickest may contain blocks of diamicton and peat as well as vague, plane parallel laminated muddy sand and sandy mud. These lenses likely form as sand masses that were streaked out by slump-floor sediments moving downslump. This is suggested by (1) the overturning and streaking of sand wedges (Section 6.5.3; Fig. 6.12), (2) the fact that most lenses are parallel/subparallel to the ground surface and (3) their morphological similarity to glacitectonic lamination (see Hart et al., 1990, Fig. 4).

Sandy diamicton forms in two locations: (1) in mixed colluvial aprons (Fig. 6.12A) and (2) in slump floors. In the latter it is probably deposited by both debris flow and the slow downslump movement (probably some form of creep) of slump-floor deposits above secondary thaw contacts. Because there are numerous ice lenses immediately above these contacts, promoting frost creep, and since the contacts themselves are smooth, gently sloping downslump (Fig. 6.12), slow downslump movement may, like cohesive debris flows, also involve plug-like movement (cf. Mackay, 1981).

4.3.2 Poorly stratified sand

As examined by sectioning fans at North Head, lobate sand flows deposit **poorly stratified sand**. This facies comprises gently dipping (c.10-20^{o}), parallel-subparallel, highly lenticular laminae or beds of fine to slightly muddy sand (Fig. 4.8). The strata (a few mm to several cm thick and commonly ≤several dm wide and long) are internally structureless, probably due to the lack of sorting within sand flows. Upper and lower contacts of strata are usually slightly curved to gently undulating, similar to the fan surface (Fig. 4.8). The lower contact of poorly stratified sand tends to be sharp and non-erosive, its geometry depending on that of the underlying surface (Fig. 4.8).

4.3.3 Well-stratified facies

It was observed at North Head, Peninsula Point and Crumbling Point that sheetfloods and highly fluid sheet-like sand flows deposit **well-stratified facies.** This comprises discontinuous, planar parallel to slightly curved, subparallel, very gently dipping beds (0.5mm to 5cm thick) of sand and/or mud (Figs 4.3B and 4.9). Very thin beds (0.5-1.5mm) of mud or sandy mud tend to be more extensive and their upper and lower contacts more parallel than the more lens-like sand beds (a few mm to 5cm thick), which are deposited by sheetfloods and

Fig. 4.8 **Poorly stratified facies** (P) in a fan built by sand flows, North Head. Note the indistinct stratification and the sharp, planar contact (marked by the pencil) between the fan and the underlying beach sand. On the far ...face, there are lobate sand flows (arrows) and fallen chunks of sod. (August 2 1991)

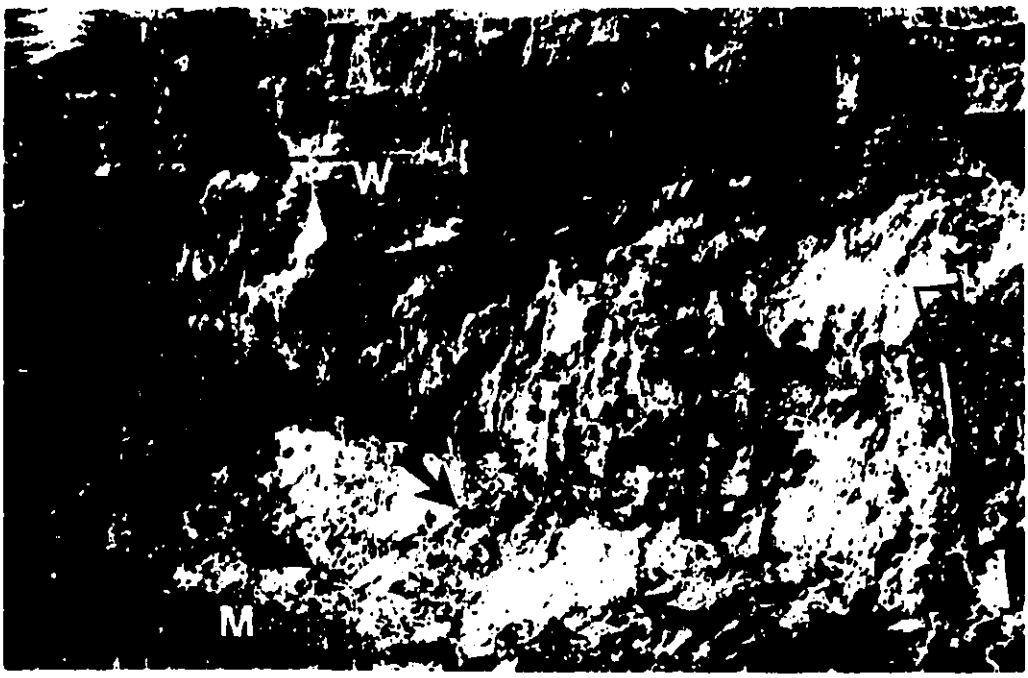

Fig. 4.9 **Well-stratified facies** (W) capping **structureless sand** (S) and **melt-out diamicton** (M), Crumbling Point. The diamicton overlies a slump-floor secondary thaw contact (not visible) and is contiguous with diapirs (arrows) in the overlying sand. 1m high shovel for scale. (July 29 1989)

highly fluid flows intermediate between sand flows and sheetfloods. Locally, there are graded beds with mud aggregate-rich sand bases and silty sand tops, these beds likely being deposited by waning sheetfloods or highly fluid, partially turbulent sand flows. Channel fills (≤c.5cm deep and ≤c.20cm wide) are common. Small lenses (≤a few mm thick and ≤10cm wide) of fine sand rich in granular mud aggregates may represent sections through small longitudinal bars. Tabular, poorly consolidated, subangular to subrounded mud aggregates (typically 1-2mm thick, a few to 15mm long, and a few to several mm wide) whose long axes parallel bedding are likely rip-up clasts formed in braided channels. Lower contacts of well-stratified facies, sharp and planar to irregular (Fig. 4.9), represent the buried surfaces of beaches and slump floors. Upper contacts were not observed.

From this description it would seem that well-stratified facies resembles some "rhythmically stratified sands" described from Pleistocene sediments in central and NW Europe, sediments believed to have been deposited by "sheetwash" on periglacial slopes (see e.g. Dylik, 1969, 383-384; 394-396; Pécsi, 1969, 25-26; Brodzikowski and Van Loon, 1991, 385-391).

4.3.4 Structureless sand

The bases of the steep icy bluff at North head and of many slump headwalls at Crumbling Point, Mason Bay and Hadwen Island are covered by sand aprons whose deposits comprise structureless sand (Fig. 4.5A). This is fine-grained and forms irregular sheets (≤several dm thick and ≤100m+ long). At Crumbling Point most sheets are inclined (≤50^{0}), overlying secondary thaw contacts (Fig. 4.5A).

4.3.5 Diamicton and/or muddy sand

Above slump-floor secondary thaw contacts at Crumbling Point, there is commonly a layer (≤c.25cm thick) of diamicton and/or muddy sand (Figs 4.9-4.11). The diamicton is readily distinguished from organic-rich diamicton by the absence of organic material and by numerous soft-sediment deformation structures (flame structures and irregular masses and streaks; Section 7.2) that penetrate overlying facies (Figs 4.9-4.10). Many of these structures are steeply inclined (upslump) to vertical, and some bifurcate upwards and merge downwards into a layer of structureless diamicton above a secondary thaw contact (Fig.4.10). The sand is also structureless and contains little (usually no more than several percent) mud. The layer of diamicton and/or muddy sand is commonly frozen, possessing an irregular reticulate or (inclined) lenticular cryostructure.

Diamicton and/or muddy sand are melt-out deposits formed by subslump melting. This is indicated in Fig. 4.11, where diamicton and peat-rich structureless sand deposited by a mixed apron overlies a 5cm thick layer of icy muddy sand, the latter overlying an angular unconformity (secondary thaw contact) above the layered cryofacies association. The muddy sand, distinct from the sand above it (Section 4.3.4), is identical to that a few cm below the thaw contact, except that its cryostructure is (inclined) lenticular rather than structureless. Clearly, it melted out from such a unit, before refreezing and developing a lenticular cryostructure. Deformation structures in melt-out deposits form by fluidisation (see Section 7.3), loading and buoyancy (cf. Section 7.2). The upslump dip of flames and streaks probably reflects downslump movement of slump-floor deposits.

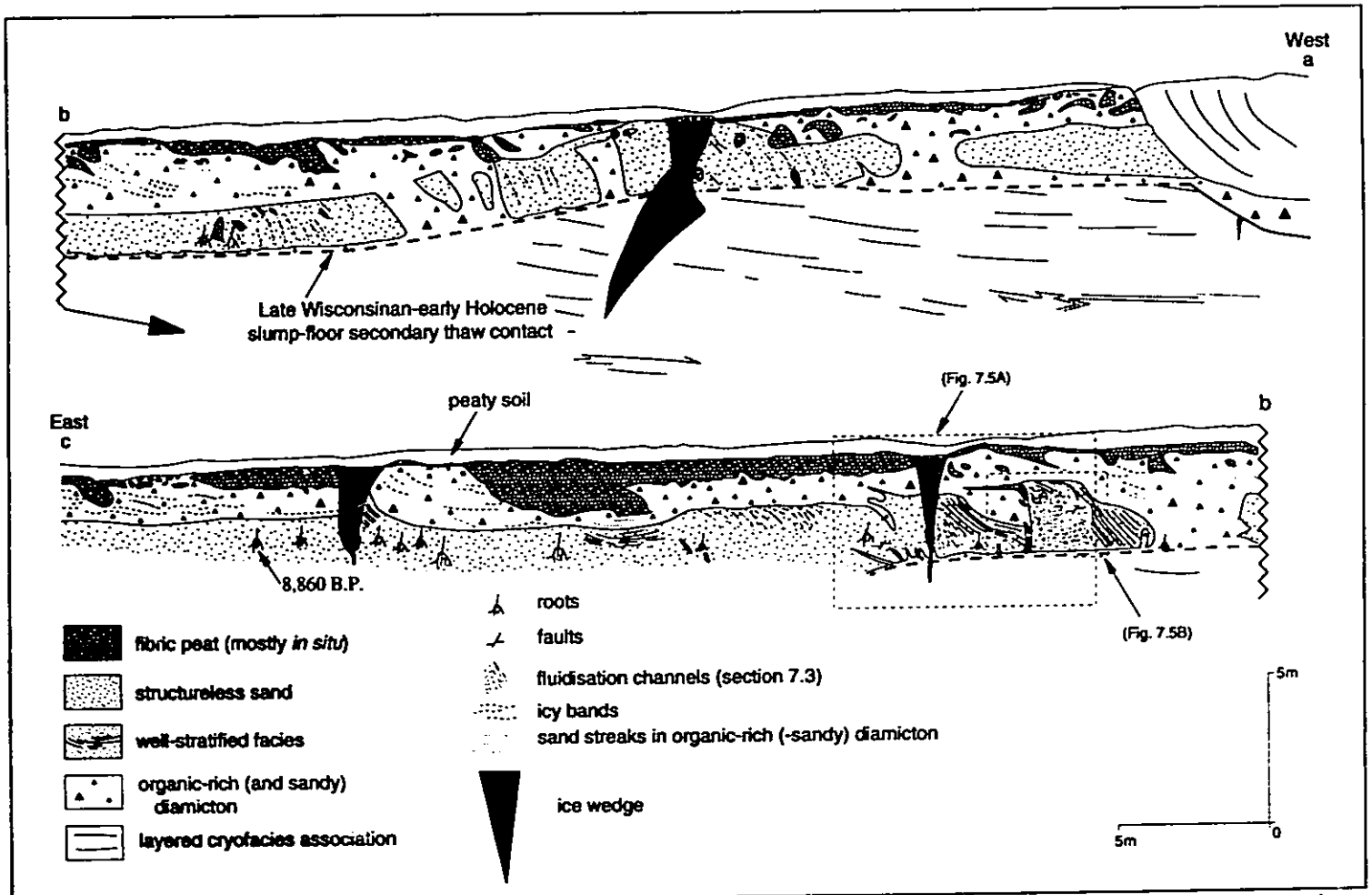

Fig. 4.10 Late Wisconsinan-early Holocene slump-floor facies beneath Slump Basin, Crumbling Point. The facies overlie a secondary thaw contact that dips gently east towards the basin centre. Above the contact a root (arrow) was radiocarbon dated to 8,860 +/- 180 BP (Beta-46233). Note the abrupt lateral facies changes between diamicton and sand (cf. Fig. 4.12). The curved secondary thaw contact that truncates an ice wedge near 'a' underlies a stabilised, modern slump. (September 3 1991)

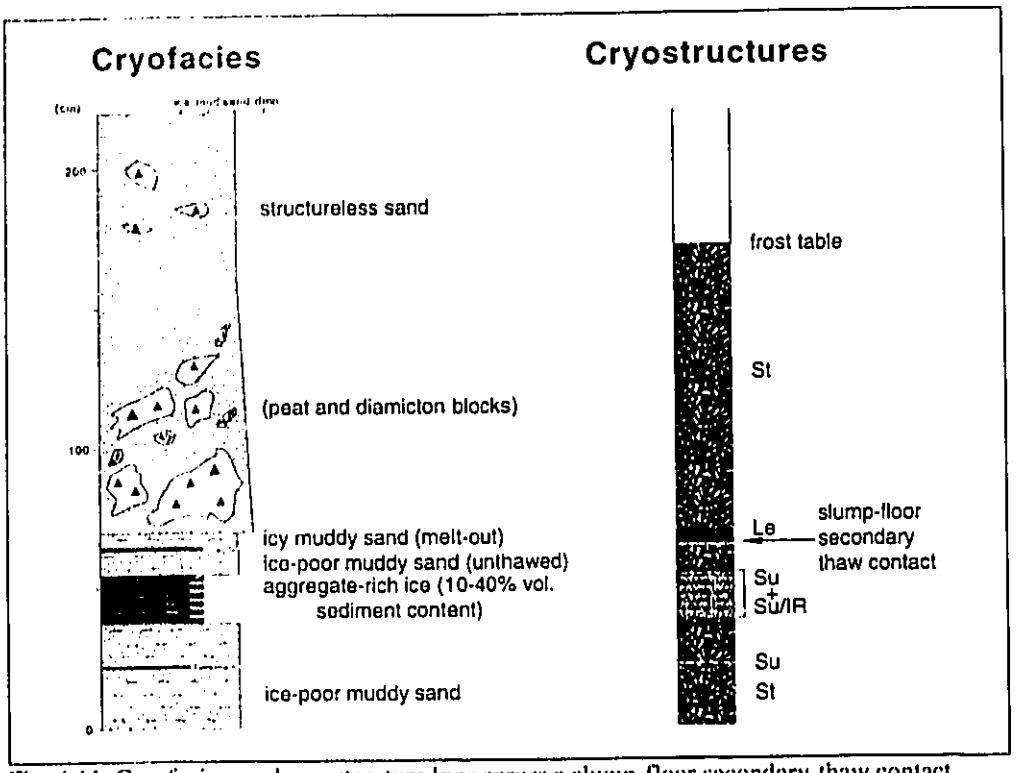

Fig. 4.11 Cryofacies- and cryostructure logs across a slump-floor secondary thaw contact, Crumbling Point. The contact underlies 5cm of icy muddy sand (lenticular cryostructure) that melted out from the underlying ice-poor muddy sand (structureless cryostructure). Above the **melt-out sand** is a unit of structureless sand containing blocks of peat and diamicton, a unit deposited by a mixed apron. (July 1 1990)

Fig. 4.12 **Abrupt lateral facies change** between structureless sand (S) and sandy diamicton (D), Crumbling Point. These facies overlie a slump-floor secondary thaw contact (arrows) beneath a small, stabilised, high-level slump. In the centre of the photo a sand wedge supplies sand to a basal fan, part of which is submerged by a **sheetflood**. The headwall is c.8m high. (July 28 1989)

4.3.6 Organic material

Thermokarst-slope facies contain abundant organic material (peat, sod, plant fragments and charcoal), most of which is supplied from vegetation on the upland surface and from peat beneath it. During backwearing thermokarst this material is redeposited on slump floors and at the base of steep icy bluffs, where it may be buried or transported downslope. Consequently, slump floors, for example, are littered with organic bodies of diverse size, shape and inclination (Fig. 4.5B), bodies transported downslump by sheetfloods, debris flows or slow movement (?creep) of slump-floor materials.

4.4 **Facies models**

Sedimentation accompanying backwearing thermokarst in the Tuktoyaktuk Coastlands is depicted in two facies models: (1) a steep icy bluff (Fig. 4.13) and (2) a retrogressive thaw slump (Fig. 4.14). Each is divided into mud- and sand-rich parts.

4.4.1 Steep icy bluff

The steep icy bluff model (Fig. 4.13) is based on modern sedimentation at the base of North Head Upland. In mud-rich sections (Fig. 4.13A), large, muddy debris flows extend down onto the beach, depositing organic-rich (and sandy) diamicton; in sand-rich sections (Fig.4.13B), fans prograde over the marine (or lacustrine) beach. Fan progradation and degradation are strongly controlled by storm-wave action. Waves erode fan deposits and undercut the steep icy bluff, exposing ground ice and, when air temperatures exceed 0°C, triggering lobate sand flows on the steep icy bluff (Fig. 4.3B). Crossing the basal break-of-slope, these flows rapidly build small, steep fans of poorly stratified sand. As fans prograde, fewer highly viscous flows reach their distal portions. Such flows quickly dewater and freeze just beyond the basal break-of-slope; only the more fluid, sheet-like flows reach their distal

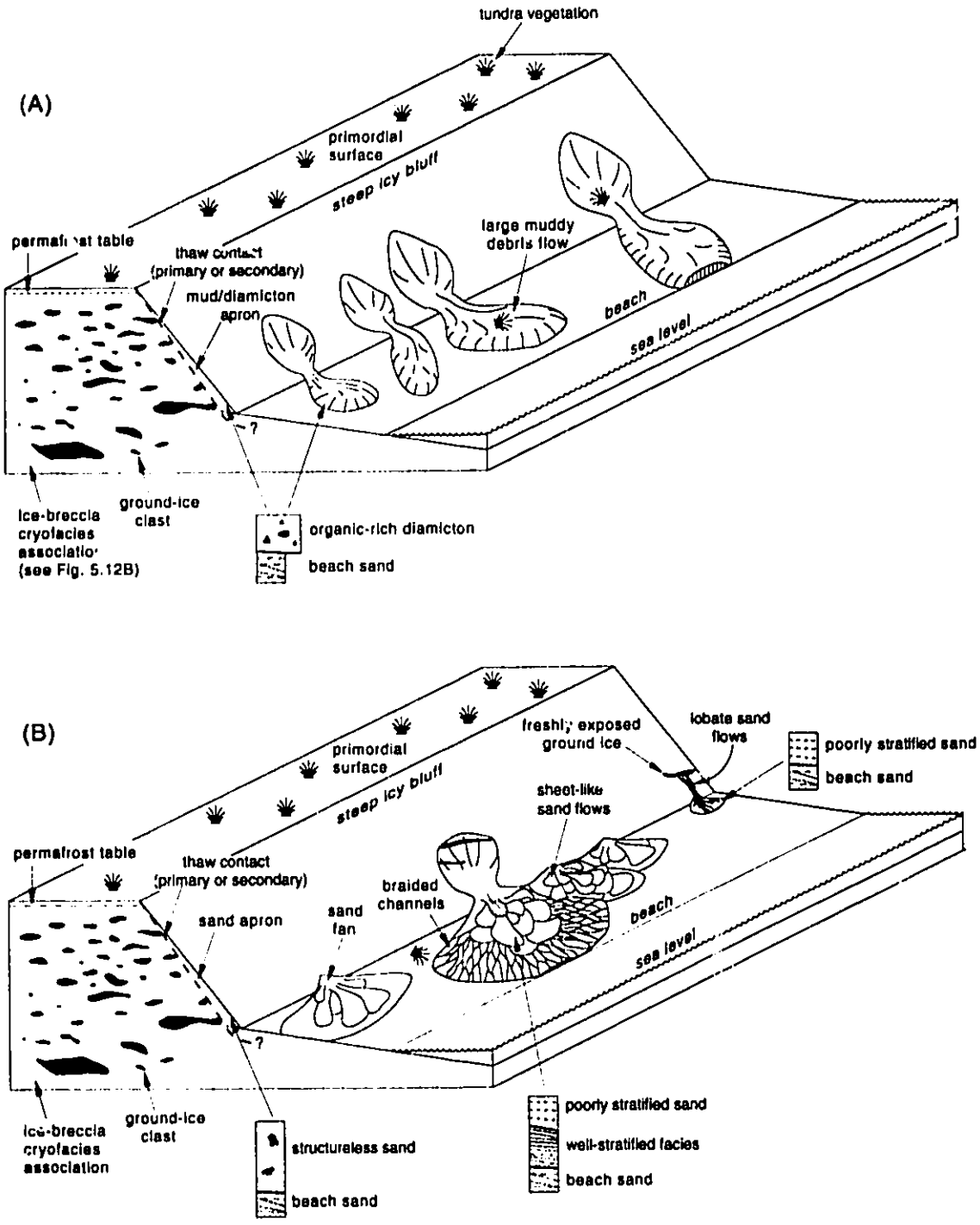

Fig. 4.13 **Facies model of steep icy bluff**: (A) mud-rich part; (B) sand-rich part.

parts. Prograding fans flatten basinwards, and sheetflood processes become increasingly important, depositing well-stratified facies. Thus the areal distribution of sedimentation style gradually changes with fan progradation.

4.4.2 Retrogressive thaw slump

The mud-rich part of the thaw-slump facies model (Fig. 4.14A) is based on slumps at North Head and Peninsula Point. Here large, muddy debris flows fringe the base of the headwall, depositing a blanket of organic-rich diamicton (≤c.4m thick) above the slump-floor secondary thaw contact. Successive flows form crudely bedded diamicton. Many flows are sooner or later traversed by braided channels that deposit well-stratified facies or by V-shaped, non-braided channels that deposit discontinuous gravel lags. At channel mouths, sheetfloods may build fans that prograde over older debris flows and pass distally into mudflats. In front of steep slopes where little or no ground ice is exposed, colluvial processes build small peaty diamicton aprons.

The sand-rich part of the thaw-slump model (Fig. 4.14B) is based on slumps at Crumbling Point, Green Lake, Hadwen Island and Mason Bay, slumps where backwearing thermokarst supplies large amounts of sand to slump floors. If sand supply exceeds basal resedimentation, sand aprons deposit structureless sand. Long (≤100m) aprons form where the headwall parallels the axial planes of sand wedges (Fig. 4.5A), and short ones where it intersects them at high angles (Fig. 4.5B). (In the latter case the wedges may protrude into the slump floor as buttresses flanked by sand aprons (Fig. 4.5B).) But if sand supply is less than basal resedimentation, sand fans deposit well-stratified facies.

At the base of headwalls, beneath sand-wedge toes that funnel sand-laden meltwater, sheetfloods may build sand fans (Fig. 4.12). On either side of the wedges, smaller fans grow at the mouths of other headwall rills, adjacent fans commonly coalescing and passing

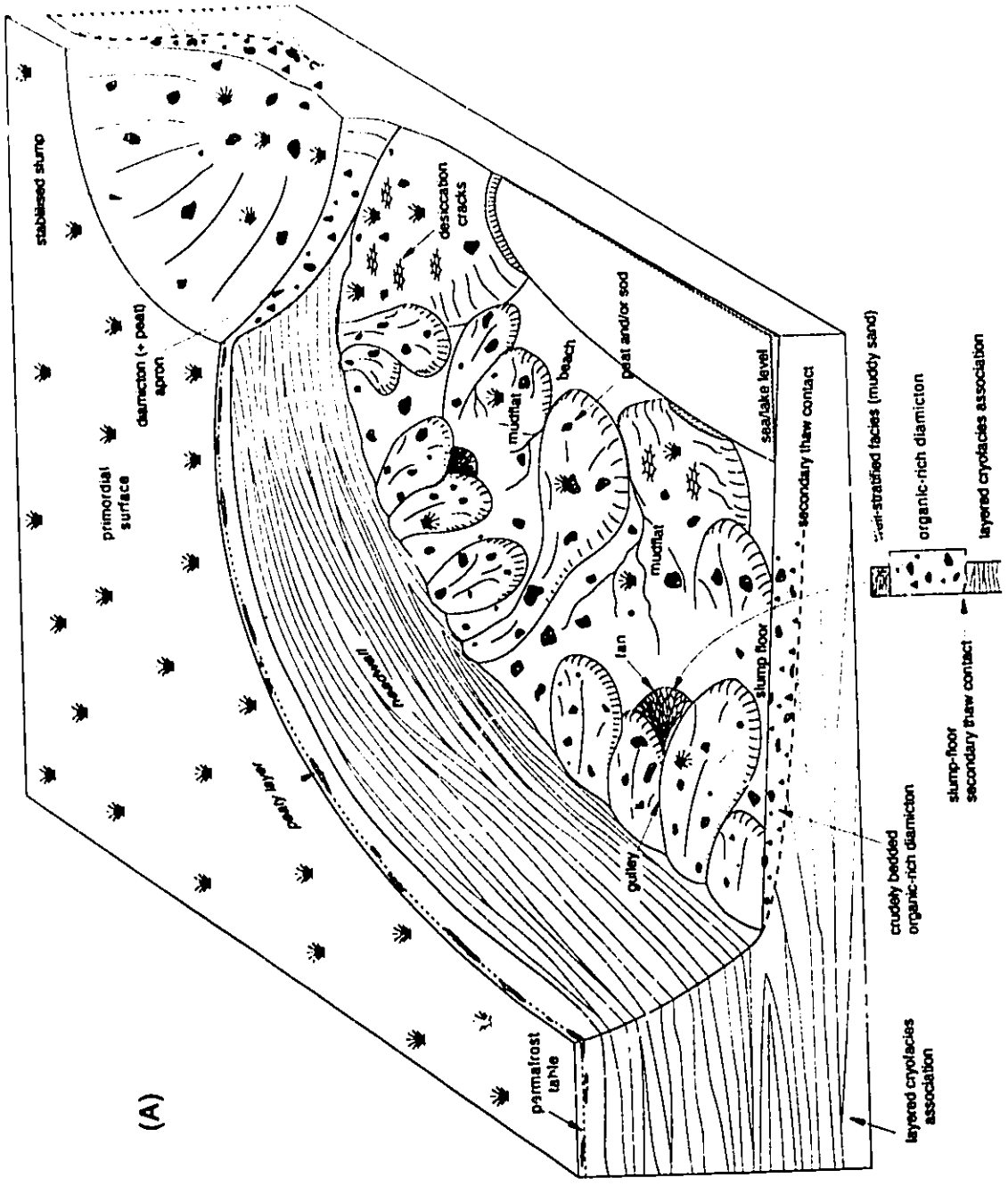

Fig. 4.14 Facies model of retrogressive thaw slump: (A) mud-rich part.

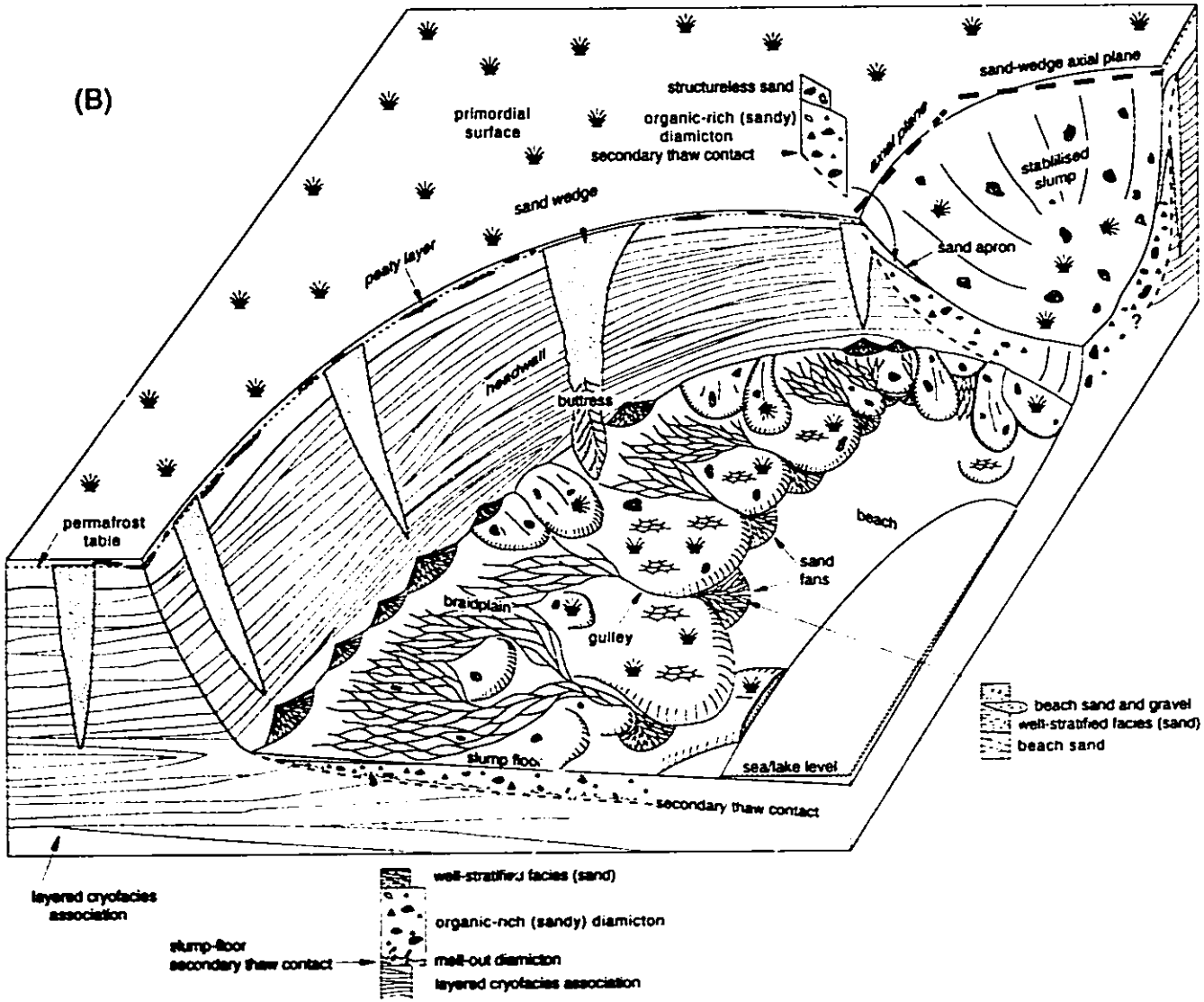

(B) sand-rich part.

distally into braidplains. With yet other fans prograding from the mouths of slump-floor channels, deposition of well-stratified facies is widespread (Fig. 4.14B).

Where sand-rich cryofacies are locally absent (e.g. between sand wedges) or where the sand supply is small, large, muddy debris flows form at or near to the base of the headwall. In the mid to distal slump floor, older, stabilised flows are colonised by plants (e.g. Burn and Friele, 1989) and criss-crossed by desiccation and tension cracks into which sand (and organic material) is be washed and/or blown, forming steep to vertical sand lenses in sandy diamicton (Fig. 4.7). Conversely, sandy diamicton with horizontal to moderately inclined sand lenses forms where downslump movement shears out bodies of sand such that they are aligned roughly parallel to the ground surface (Fig. 6.12). These sand bodies may be incorporated into organic-rich diamicton in at least three ways: (1) cohesive blocks of (moist) sand may fall into muddy debris flows or mixed colluvial aprons; (2) the tops of sand wedges extending above secondary thaw contacts may be folded and sheared downslope (Fig. 6.12); and (3) saturated sandy facies may be buckled up in front of debris flows, later to be incorporated into them as the flows advance (this may explain the rare occurrence of poorly preserved well-stratified facies in thick sand lenses).

The variety of cryofacies and resedimentation processes in sand-rich slumps generates a complex facies pattern of proximal and distal slump facies. Proximal slump facies display abrupt vertical or lateral facies changes (marked by sharp, irregular contacts; Figs 4.12 and 6.13B) between structureless sand and organic-rich (and sandy) diamicton, changes reflecting the distribution of sand bodies. For example, because sand wedges form a polygonal network, headwall retreat episodically exposes different wedges. As each wedge melts, sand is redeposited on the lower headwall and adjacent slump floor, commonly forming aprons of structureless sand upslump of, or above, organic-rich (and sandy) diamicton (Fig. 4.5A). Where the aprons themselves are eroded (e.g. by colluvial and aeolian processes), fresh

sections of the layered cryofacies association are exposed. Consequently, diamicton aprons and/or large debris flows may start to form on or at the base of such headwalls, depositing organic-rich diamicton above, or upslump of, structureless sand (Figs. 4.12 and 6.13B). Through time, therefore, headwall retreat is marked by a proximal slump facies association comprising discontinuous bodies of structureless sand (typically a few dm to 1.5m thick and a few m to several da m wide or long) interspersing organic-rich (and sandy) diamicton.

Distal slump facies are also characterised by abrupt facies changes, but mainly those between well-stratified facies, diamicton and organic-rich (and sandy) diamicton, a pattern reflecting resedimentation and, to a lesser extent, melt-out. During warm summer days, the activity, size and location of large debris flows, channels and braided systems is always changing. For example, debris flows commonly stabilise in mid to lower-slump floors, later to be buried by braided systems. In this way organic-rich (and sandy) diamicton is capped with well-stratified facies (Fig. 4.9). These deposits may later be deformed and buried by renewed debris-flow activity. Coevally with surfaces processes, sediments melt out from the underlying cryofacies, veneering subslump secondary thaw contacts with diamicton (and/or muddy sand). These deposits commonly deform (Figs. 4.9 and 4.10) as a result of loading, buoyancy, water-escape (Fig. 7.5; Section 7.3) and the downslump movement of overlying sediments. Finally, in the distal part of slumps, resedimentation processes interact with marine (or lacustrine) processes, forming, for example, interbedded sequences of well-stratified facies, driftwood and beach sands and gravels.

In both models the major controls on sedimentation are the supply of meltwater and sediment, controls which themselves depend on the snowcover, volumetric ice content and grain size of cryofacies, prevailing atmospheric conditions (e.g. Lewkowicz, 1986) and resedimentation processes. Besides determining the potential amount of ground-ice derived meltwater, volumetric ice content also influences the nature of backwearing thermokarst: if the

excess ice content of upland materials is less than c.30-40%, the slopes bordering upland surfaces are steep icy bluffs, whereas if it exceeds 30-40%, they are slump headwalls. Grain size control is summarised thus: (1) where mud-rich cryofacies outcrop, sedimentation is dominated by large, muddy debris flows; (2) where sand-rich cryofacies outcrop, it is dominated by small sand flows and alluvial processes; and (3) where both mud and sand-rich cryofacies outcrop, it is affected equally by debris-flow and alluvial processes. Finally, atmospheric conditions govern the intensity and types of processes, for example promoting sheetflooding during the hottest days.

4.5 Conclusions

Thermokarst-slope facies are poorly preserved because of basal erosion and resedimentation. They may be preserved, however, if basal erosion is absent (cf. Dylik, 1963b; 1969), as occurs in "dry" thermokarst basins - those lacking thermokarst lakes (see Chapter 5). One example is Slump Basin at Crumbling Point, where slump-floor facies overlie a gently curved secondary thaw contact (Figs 4.10 and 7.5). Radiocarbon dated at 8,860 +/- 180 years BP (Beta-46223), these deposits (and the underlying contact) likely formed during the Late Wisconsinan-early Holocene warm interval. Another (?Late Wisconsinan-early Holocene) example occurs at Peninsula Point. At both sites thermokarst-basin facies (Chapter 5) are absent and slump-floor facies locally underlie thick (≤1.5m), woody fibric peat, features suggesting that thermokarst lakes never formed (cf. Rampton, 1982, p.33).

4.5.1 Criteria for identifying thermokarst-slope facies:

(1) **organic-rich diamicton**

(2) **granular mud aggregates in stratified facies**

(1) Organic-rich (and sandy) diamicton is easily recognised by the presence of roots, fragments of wood and charcoal and/or suspended blocks of peat in structureless diamicton. In sandy areas the diamicton may contain sand lenses (Figs 4.7 and 6.12A).

(2) Throughout the Tuktoyaktuk Coastlands granular mud aggregates abound in aggregate-rich cryofacies (Fig. 2.4B). During backwearing thermokarst the aggregates melt-out and are redeposited near the base of thermokarst slopes (Fig. 4.4B), where they are commonly preserved as subrounded to rounded, 1-6mm diameter mudballs in well- and poorly stratified facies. Although (sand-sized) mud aggregates also occur in some ancient fluvial sandstones and in bedload rivers of modern, seasonally hot-dry environments (Rust and Nanson, 1989), those in the Tuktoyaktuk Coastlands are significantly larger.

Chapter 5 BASINS

"... Thaw lake sediment sequences are widespread in subarctic and low-arctic regions but are commonly misinterpreted or go unrecognized..." (Hopkins and Kidd, 1988)

5.1 Introduction

Ice-rich upland surfaces commonly degrade both vertically and laterally, becoming inset with thermokarst basins. These closed depressions vary from tiny ponds above ice wedges (e.g. French, 1976, p.117) to large basins (≤40m deep and ≤10-15km in diameter) in upland and polycyclic surfaces (see Czudek and Demek, 1970, Fig. 14; Rampton, 1974, Fig. 7; French, 1976, p.111-116, 122-125; Ashley, 1988, Table 1 and Fig. 1; Section 3.2). Abundant in ice-rich areas, large thermokarst basins are important depositional environments.

Although the depositional processes and facies within glacial thermokarst basins have been described in some detail (see e.g. Eyles et al., 1987; Shaw, 1988), those within thermokarst basins in permafrost areas have been described little (Section 5.2). This is because the research concerning permafrost lakes has focussed on other aspects, namely lake orientation (e.g. Mackay, 1956; Carson and Hussey, 1962; Harry and French, 1983), dating of lacustrine strandlines (Carson, 1968), chronology of thermokarst lakes (e.g. Rampton, 1988; Burn and Smith, 1990), the distribution of ground ice (e.g. Lawson, 1983; French and Harry, 1983) and regional descriptions (e.g. Wallace, 1948; Hopkins, 1949; Czudek and Demek, 1970; Dredge and Nixon, 1979; Klassen, 1979; Sellmann et al., 1975; Williams and Yeend, 1979; Rampton, 1982; 1988). While the sedimentology of periglacial thermokarst basins has recently begun to be investigated (see Sher et al., 1979, p.57-58; 88-93; Ivanov, 1984, 94-96; Hopkins and Kidd, 1988), until it is more fully scrutinised, basin sequences will likely continue to be misinterpreted or go unrecognised.

This chapter summarises the literature about the processes and sediments of thermokarst basins in permafrost areas, details the facies and facies associations of deep basins in the Tuktoyaktuk Coastlands and proposes a local facies model.

5.2 Thermokarst basins

Thermokarst basins are of two types: lacustrine and drained or non-lacustrine. Lacustrine basins contain thermokarst lakes. Because they are prone to drainage (e.g. by basin coalescence or thermal erosion along ice wedges; see e.g. Harry and French, 1983; Mackay, 1988), many lacustrine basins are partially or wholly drained, a state after which deposition within them is the same as that within non-lacustrine (i.e. never lake-filled) basins.

Thermokarst basins may also be subdivided into deep and shallow basins, the former inset into primordial surfaces by depths of typically 10-30m (e.g. Tomirdiaro, 1982; Carter, 1988), the latter inset into polycyclic surfaces by those of only several dm to a few m (e.g. Sellmann et al., 1975). Deep basins are commonly non-oriented, whereas shallow basins are commonly oriented (e.g. Mackay, 1956b). But exceptions do occur, for example on Richards Island and NE Tuktoyaktuk Peninsula (Fig. 1.1), where some deep basins respectively show pronounced NE-SW and N-S orientations (Mackay, 1956b; Burn, 1992).

5.2.1 Lacustrine basins

Lacustrine basins may be subdivided into shallow- and deep-water zones. The shallow-water zone lies between storm-wave base and high-water mark, the deep-water zone below storm-wave base (generally at a depth of 0.2-1m; cf. Carson and Hussey, 1962). In sandy lakes the shallow-water zone is commonly separated from the deep by a riser fronting a sublacustrine bench (B in Fig. 1.5; e.g. Hopkins and Kidd, 1988). But not all thermokarst lakes possess both zones (see e.g. Dredge and Nixon, 1979).

5.2.2 Lacustrine facies

Based on the literature and the author's observations of thermokarst lakes, thermokarst lake facies are classified in Table 5.1.

Table 5.1 Thermokarst-lake facies

SHALLOW-WATER			
inorganics	gravel sand and gravel sand	} beaches/sublacustrine bench	
biogenics	organics	allochthonous	-detrital peat bars/sheets -peat and sod blocks/slabs
		autochthonous	-sunken vegetation/peat mat -log layers
	inorganics	shell lags	
DEEP-WATER	organic-rich silt and clay		

Inorganic shallow-water facies range from silt (Dredge and Nixon, 1979; Hopkins and Kidd, 1988) to openwork gravel. In the Tuktoyaktuk Coastlands, openwork gravel, comprising rounded to well-rounded pebbles and cobbles, is common in water shallower than c.20cm, because sand and silt are winnowed out during storms. Here the presence or absence of gravel reflects clast supply: where abundant clasts are supplied (by bank collapse or debris flows), the shallow-water zone comprises sheets of openwork gravel; where both clasts and sand are supplied, it comprises patches of sandy gravel and sand; and where few clasts are supplied, it is sandy and commonly covered by wave (Fig. 5.1) and current ripples (cf.

Carson and Hussey, 1962; Hopkins and Kidd, 1988) and scours. On a sandy sublacustrine bench on Hadwen Island (B in Fig. 1.5) the author observed wave ripples and asymmetric scours in water as deep as 40cm. The scours probably formed by erosion from storm-generated longshore currents, because their axis of bilateral symmetry was parallel to wave ripples and their upcurrent sides were consistently east of their downcurrent sides, eastward being one of the two directions of local storm winds.

Biogenic shallow-water facies are divided into organic (i.e. humus and decayed parts of plants and animals) and inorganic (e.g. mollusc shells) fractions (cf. West, 1977, p.53-70). The organic fraction may be allochthonous or autochthonous. Allochthonous organic material is mostly detrital peat, a structureless mass of fine plant stems and fibres derived from sunken tundra mats and from bank and aquatic vegetation (e.g. Carson and Hussey, 1962; Dredge and Nixon, 1979). Detrital peat may also contain short and blunt sticks and twigs, commonly aligned (Hopkins and Kidd, 1988). The size and shape of peaty deposits varies greatly. On the smallest scale, plant stems frequently collect in ripple troughs (Fig. 5.1). But where detrital organic material is more abundant it forms large sheets (commonly 5-50+m^2 in area and ≤c. 20cm thick). At the largest scale, detrital peat forms beaches and sublacustrine bars and sheets (≤15+m wide, ≤800m long, and ≤5m thick; Fig. 5.10; e.g. Carson and Hussey, 1960; 1962; Tedrow, 1969, plate 3; Dredge and Nixon, 1979; Hopkins and Kidd, 1988). Such deposits are highly erodible. For example, in Crumbling Point Lake (Fig. 1.4), detrital-peat bars are reworked during each storm. The distribution of detrital peat is affected by lake depth: in shallow lakes, detrital peat may cover the entire lake floor (e.g. Dredge and Nixon, 1979), whereas in deeper lakes, capable of generating higher velocity waves, detrital peat is typically concentrated on beaches (Carson and Hussey, 1962).

Fig. 5.1 **Wave ripples** near the shore of a sandy sublacustrine bench, thermokarst lake, Hadwen Island. Plant stems are concentrated along ripple troughs. 14cm high pencil for scale. (July 15 1991)

Fig. 5.2 **Pebbly** sand lenses (arrows) interbedded with fine sand (F) and detrital peat (P), E margin of Crumbling Point Basin. 20cm high trowel for scale. (August 21 1991)

Detrital peat, sand and gravel are commonly juxtaposed vertically and laterally (e.g. Carson and Hussey, 1962). For example, in the Summer Island area, mats of detrital peat locally veneer sandy sublacustrine benches.

The shallow-water zone commonly contains blocks and slabs of peat or sod derived from bank collapse or subsidence of the tundra mat (Tedrow, 1969; Hopkins and Kidd, 1988). If buoyant, this organic material may be transported by wave and current action (Carson and Hussey, 1960), accumulating in sheltered areas (Hopkins and Kidd, 1988); if not, it accumulates *in situ*.

Autochthonous organic material in tundra thermokarst lakes comprises sunken mats of tundra vegetation or peat that form when organic material submerges into expanding lakes (e.g. Wallace, 1948; Carson and Hussey, 1960; 1962; Carson, 1968). The vegetation includes *Salix* spp. (willows), *Betula* spp. (birches), *Eriophorum* spp. (cottongrasses), *Carex* spp. (sedges), graminae (grasses) and mosses; and peat varieties include sedge, woody sedge, brown moss and Sphagnum peat (NWWG, 1988, p. 29-53). In the boreal forest, trees tilt and fall into thermokarst lakes, forming log layers (e.g. Wallace, 1948; McCulloch and Hopkins, 1966; Burn and Smith, 1990).

Inorganic biogenic material in thermokarst lakes includes ostracod valves (e.g. Brigham, 1985), *Chara* encrustations (e.g. Michel et al., 1989) and mollusc shells (e.g. Burn and Smith, 1990). In the field area, mollusc shells include lymnaeids, valvatids, sphaeriids and planorbids (identified by A. Martell, October 1991).

The deep-water zone of thermokarst lakes is dominated by horizontal, thinly bedded silt, clay and organic material (Harry, 1982, p.126-130; Hopkins and Kidd, 1988) that settles from suspension. The coarser particles settle after summer storms, the finer during winter, beneath lake ice. Deep-water deposits are rich in detrital peat. Hopkins and Kidd (1988)

suggest that "turbidity currents generated on the steep marginal sublacustrine slopes, though as yet undetected, may dominate sediment deposition processes in the central basin."

5.2.3 Vertical sequences

Vertical sequences (≤c.11m thick; e.g. Williams and Yeend, 1979; Nelson, 1982, p.21; Rampton, 1982; 1988; Hopkins and Kidd, 1988) in thermokarst basins are of three types: (1) fining-upward, (2) coarsening-upward and (3) peat-capped.

There are two types of fining-upward sequence. The first comprises a sandy unit above ice-wedge pseudomorphs and below fine-grained deposits (Hopkins and Kidd, 1988, Fig.3; cf. Carson, 1968; cf. Nelson, 1982, Fig. 4; p.21). The sandy unit is "well [stratified] fine sand, silt, organic silt, and detrital peat interspersed with flattened masses of peat in which woody shrubs may be rooted" (Hopkins and Kidd, 1988). This unit represents the progradation of shallow-water deposits across the floors of expanding thermokarst lakes. In sandy terrain, sublacustrine benches comprise foreset-bedded sand with organic laminae. The overlying, fine-grained unit (thin, horizontally stratified silt or organic silt) is a deep-water deposit.

The second type of fining-upward sequence comprises diamicton and/or bedded deposits beneath lacustrine sediments (e.g. Müller, 1962, Fig. 4; Rampton and Bouchard, 1975; Rampton, 1982, p.33; Harry et al., 1988, Fig. 3). The diamicton and bedded deposits probably form respectively by debris flow and slope wash.

On SW Banks Island a coarsening-upward sequence of laminated, organic silt beneath ripple cross-laminated silty sand was interpreted as deep-water lacustrine sediments beneath material deposited during or after lake drainage (Harry, 1982, p.126-130).

Finally, where lacustrine sediments are absent, diamicton may be capped by peat (Rampton, 1982, p.33). This suggests that lakes or ponds did not form in these thermokarst basins; instead, peat accumulated directly above debris-flow deposits.

5.2.4 The Tuktoyaktuk Coastlands

In the Tuktoyaktuk Coastlands, primordial and polycyclic surfaces are pitted by large thermokarst basins. Typically 0.1-2.5km in diameter and 1-15+m in depth (Figs 1.3-1.5), the basins may be oriented (e.g. Mackay, 1956b; 1963, p.46-55) or non-oriented. Many formed during the Late Wisconsinan-early Holocene warm interval (Rampton, 1974), where the thaw layer intercepted massive ice or icy sediments (Rampton, 1988, Fig. 65) or where ponding or thermal erosion thawed ice wedges (cf. Kachurin, 1962; Soloviev, 1973). Once small depressions had formed, they grew rapidly, subsiding by melting of underlying ice and widening by thaw slumping. But as the climate cooled after c.4,500 years BP (Ritchie, 1984, p.154-156), thermokarst activity lessened (Rampton, 1974). Today basin expansion is minimal, and many basins have drained (see Mackay, 1988; 1992b).

5.3 **Deep thermokarst-basin facies**

Based on sections at North Head, Crumbling Point, Hadwen Island, Mason Bay and Nicholson Point (Fig. 1.1), the author distinguishes eight facies of deep non-oriented thermokarst basins (Table 5.2). For logistical reasons - distance from Tuktoyaktuk, the facies of shallow oriented basins are not considered.

Table 5.2 Thermokarst-basin facies

LACUSTRINE FACIES:	NON-LACUSTRINE FACIES:
shallow-water	-root-rich fine sand
-pebbly sand/sandy gravel	*-in situ* peat
-fine sand	
-detrital peat	
-impure sand	
deep-water	
-mud/muddy peat	
-diamicton (lacustrine and non-lacustrine)	

5.3.1 Pebbly sand/sandy gravel

Pebbly sand/sandy gravel (Fig.5.2) is structureless, its clasts (granules to large cobbles) commonly rounded and imbricated. In pebbly sand, clasts are matrix-supported; in sandy gravel, they are either matrix or clast supported. The matrix is fine to coarse sand. Cryostructures are structureless and crustal, and there is no excess ice. Pebbly sand forms lenses or sheets (≤c.1.8+m thick and ≤50+m long), and sandy gravel forms lenses (2-60+cm thick and 0.2-5+m long), commonly bifurcating. Upper and lower contacts are generally sharp and planar to gently undulating, but gradational contacts occur where pebbly sand grades into fine sand or where sandy gravel grades into pebbly sand. The lower contact of sandy gravel is commonly an angular unconformity. The facies occurs at or near basin margins.

Pebbly sand/sandy gravel is interpreted as a beach to shallow-water facies because of (1) its basin-margin location; (2) its sharp (erosional) lower contacts; (3) its thin, lens-shaped

geometry and (4) the absence of mud. Clasts are reworked from material deposited in thermokarst lakes by debris flows and bank collapse.

5.3.2 Fine sand

Fine sand is well sorted and may be structureless, laminated or thinly bedded (Fig. 5.3). Three types of laminae occur: (1) silty, (2) lens-shaped and (3) low angle. Silty laminae (0.5-7mm thick and a 3-80+cm long) are horizontal to gently dipping, occasionally covering small, rounded, symmetrical ripple forms. More commonly they comprise planar to irregular wavy laminae (Fig. 5.3A). Lens-shaped laminae (3-7mm thick and commonly 20-30cm long), some with broad, concave-upward bases, consist of medium to fine sand surrounded by fine sand. Low-angle laminae (1-4mm) are horizontal to gently dipping (≤ several °), planar, and parallel to subparallel (i.e. very low angle cross-cutting). Thinly (1-8cm thick) bedded fine sand comprises horizontal to gently dipping (≤ several °), low-angle cross-beds (Fig.5.3B), occurring beneath small sandy risers on the floors of drained basins. Beds generally dip in the same direction as the risers, towards basin centres. Fine sand generally has sharp and planar to gently undulating contacts, except where it grades into pebbly sand. This facies forms lenses or sheets (typically 0.05-1m thick) that extend several m to several da m basinward from basin margins.

Fine sand is interpreted as a beach to shallow-water facies. First, the rounded, symmetrical ripple forms are probably wave ripples (Fig. 5.1), and the silty laminae fairweather drapes. Second, the horizontal to low-angle, planar parallel-subparallel laminae represent swash cross-stratification (see Harms et al., 1975), which forms in the foreshore zone of sandy beaches (e.g. Reinson, 1984). Third, the abundance of fine sand rimming drained basins corresponds with fine sandy sublacustrine benches (Figs 1.5 and 5.1).

Fig. 5.3 **FINE SAND**

(A) **Silty laminae** (arrows) in fine sand (F), Hadwen Basin. The sand overlies detrital peat (black) and underlies interbedded fine sand and detrital peat. The section is capped by root-rich sand (R; section 5.3.8). The recumbent, isoclinal fold is the snout of a buried gelifluction lobe. 21cm high notebook for scale. (July 17 1991)

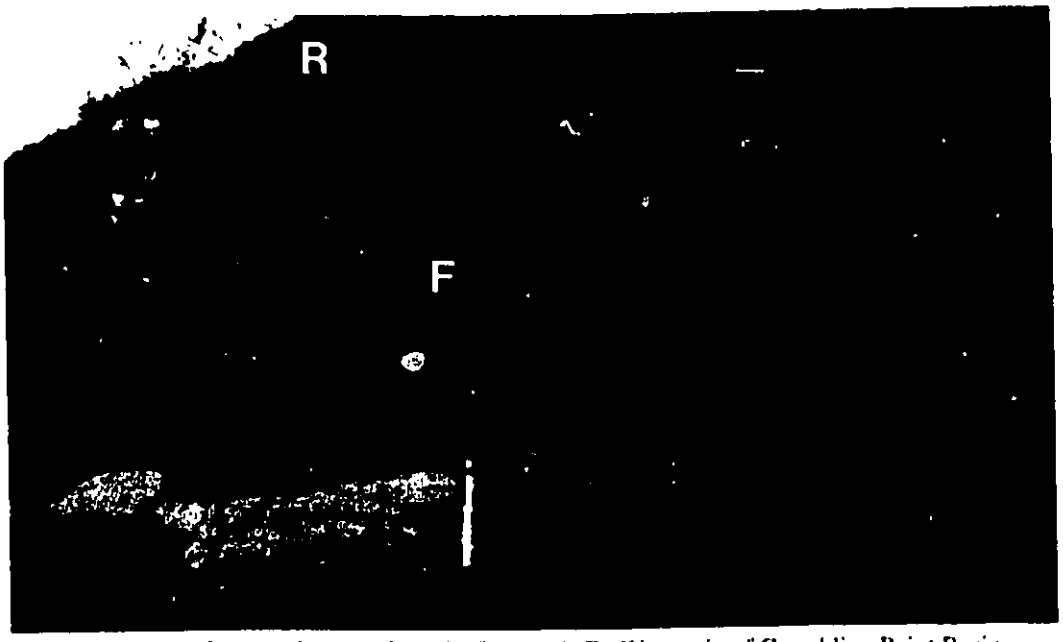

(B) **Thin, low-angle cross-beds** in fine sand (F), W margin of Crumbling Point Basin. Near the bottom, the sand is interlaminated with detrital peat (black). Like (A), the section is capped with root-rich sand (R). 14cm high pencil for scale. (August 28 1991)

5.3.3 Detrital peat

Detrital peat varies from humic to fibric and may be either bedded (Figs 5.2 and 5.3B) or structureless. The bedded variety attains thicknesses of several dm and the structureless one of c.2m (Fig. 5.3). Beds (commonly 0.5-8cm thick) range from horizontal to gently dipping (≤ c.15°), planar parallel to gently undulating and subparallel. They are internally structureless. Detrital peat is commonly sandy and may contain abundant freshwater mollusc shells, many disarticulated and broken, and also horizontally aligned plant stems and wood fragments. Its cryostructure is usually structureless, but where the facies is slightly muddy, it is lenticular. Low-angle truncation surfaces are sometimes common. The upper and lower contacts of detrital peat are typically sharp, planar to undulating, the lower one commonly being erosional. Detrital peat is most abundant near the margins of drained basins (Figs 5.2 and 5.3B) and beneath small risers. It also occurs beneath drained residual ponds.

Detrital peat is interpreted as a beach to shallow-water facies. This is because its variable thickness and abrupt terminations are best explained by the variable thickness and discontinuous nature of peat bars or mats rimming thermokarst lakes. That the peat is detrital is indicated by disarticulated and broken freshwater bivalve shells, the worn appearance of wood fragments and typically by the absence of roots extending down from it.

5.3.4 Impure sand

Impure (fine) sand contains variable amounts of peat, mud, pebbles, cobbles and wood or charcoal fragments (Figs 5.4 and 5.5). Peat and mud occur as streaks, irregular masses or beds, the peat being mesic to fibric and commonly containing wood fragments (Fig. 5.5). Impure sand may be structureless (Fig. 5.5) or bedded (Fig. 5.4). Beds (0.3-25cm thick), some structureless, some grading upwards from fine to silty sand, gently to moderately dip (≤c.20°). Foresets (0.3-4+m long) commonly flatten into topsets (Fig. 5.4B) and comprise all

Fig. 5.4 **IMPURE SAND**, North Head Basin

Both (A) and (B) are part of the same cross-bed (1-3+m thick and 120m long), whose foresets mainly comprise fine sand (grey-buff) and muddy detrital peat (black).

(A) **Reactivation surfaces** (arrows) and small **high-angle faults**. Figure for scale. (August 14 1991)

(B) Foresets leading up into well-developed **topsets.** Interbedded within the impure sand is a **wedge-shaped body of diamicton** (D; see Fig. 5.10). Figure for scale. (August 14 1991)

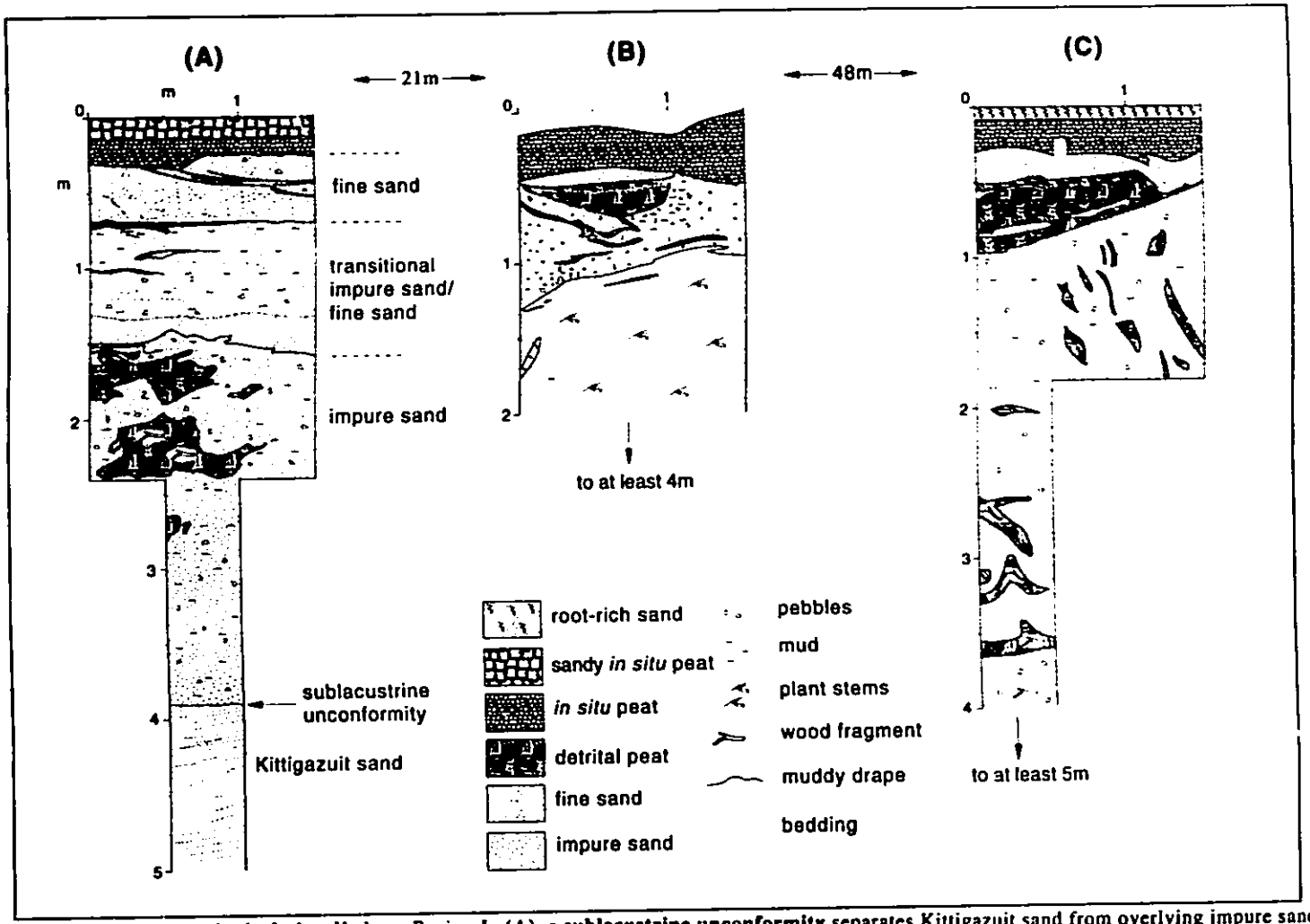

Fig. 5.5 Thermokarst-basin facies, Hadwen Basin. In (A), a **sublacustrine unconformity** separates Kittigazuit sand from overlying impure sand. The impure sand contains (1) blocks of detrital peat derived from peat and vegetation on the primordial surface and (2) mud and pebbles likely supplied to the thermokarst lake by debris flows. All three sections show an **upward facies change** from impure sand to fine sand, indicating that the degree of lacustrine sorting increased through time,probably as the influx of diamicton decreased. After the lake partially drained (see Fig. 1.5), the fine sand was colonised by peat-forming vegetation. The resulting *in situ* peat was then locally capped by root-rich sand. (July 12-13 1991)

gradations between fine sand, mud and detrital peat. Those which are sandy tend to thicken downdip or form lenses (≤25cm thick and 1+m long), whereas peaty foresets commonly taper out downdip, rarely exceeding 5cm in thickness (Fig. 5.4A), and may contain leaves, plant stems, aligned wood fragments and freshwater mollusc shells. Where foresets are well developed, there are numerous reactivation surfaces (Fig. 5.4A) and some stringers of pebbly sand. This facies also contains many small (≤20cm throws; typically a few cm), high-angle (≥35°) faults (Fig. 5.4A), most of which are reverse and syndepositional. Cryostructures are mainly structureless, although in muddy units, small (1-3mm thick) ice lenses form a lenticular cryostructure. Upper and lower contacts of impure sand are generally sharp and undulating to irregular, except where it grades into pebbly sand/sandy gravel. Impure sand generally occurs stratigraphically low in basin-margin sections, as shown in Hadwen Basin, where it overlies a sublacustrine unconformity (Fig. 5.5).

Impure sand is interpreted as a shallow-water facies deposited rapidly during the early stages of lake growth (cf. Hopkins and Kidd, 1988). That it was deposited in shallow water is suggested by (1) its dominantly sandy nature, (2) clasts that were likely reworked from underlying diamicton and concentrated above unconformities (Fig. 5.12A) and (3) irregular masses of woody fibric peat (Fig. 5.5) that were probably derived locally from undercut banks (cf. Hopkins and Kidd, 1988); such peat or turf blocks are common in the shallows of nearby lakes. Deposition in young lakes is suggested by (a) the occurrence of impure sand stratigraphically low in basin fills, locally above sublacustrine unconformities (Fig. 5.5A); (b) syndepositional faults, which probably formed as a result of lake-bottom subsidence (e.g. Are, 1973, p.7) when underlying ground ice melted (cf. McDonald and Shilts, 1975; Rust and Romanelli,1975; Shaw, 1982; Eyles et al., 1987) and (c) the impure nature of this facies, which probably reflects mixing of upland materials. Finally, rapid deposition would deny

sufficient time for thorough sorting and may account for the presence of structureless units, perhaps deposited by sediment gravity flows.

5.3.5 Mud/muddy peat

Mud/muddy peat (Figs 5.6 and 5.7) is distinguished from detrital peat by the abundance of mud and by its greater volumetric ice content, this facies being the most ice-rich basin facies (≤c.50% volumetric ice content; generally ≤c.15%) and having the greatest diversity of cryostructures (lenticular, irregular and regular reticulate). Lenticular cryostructures comprise ice lenses and veins (commonly 1-7mm thick and a 0.03-0.5m long). The lenses tend to parallel bedding, the thickest (≤1cm) typically in muddy peat or along contacts with sandy facies. Irregular reticulate cryostructure, the most abundant, comprises equant to slightly elongate angular (to subangular) mud aggregates (0.2-5cm) between an ice network. Its volumetric ice content is highly variable (0-c.50%). Regular reticulate cryostructure was observed only in North Head Basin (Fig. 2.3A), where block size increased with depth from 1-2cm long axis near the top of the unit to ≤12cm long axis 2m below.

Mud/muddy peat may contain peat blocks, wood fragments, freshwater mollusc shells, occasional clasts and a small amount of sand. It may be structureless or bedded. Beds (0.5-100+cm thick; typically 1-30cm) are horizontal to gently dipping (≤15°), planar to gently curved and parallel (Fig. 5.7; cf. Ivanov, 1984, p.94). Many are laterally continuous for 10-30+m, commonly dipping towards basin centres. Upper and lower contacts may be sharp or gradational, and planar, curved or undulating. Mud/muddy peat is thickest (≤c.8m at Nicholson Point; Fig. 5.7A) beneath basin centres.

Mud/muddy peat is interpreted as a deep-water facies. Such fine and/or light material would have settled from suspension beneath storm-wave base, thus accounting for thick sequences of this facies in basin centres.

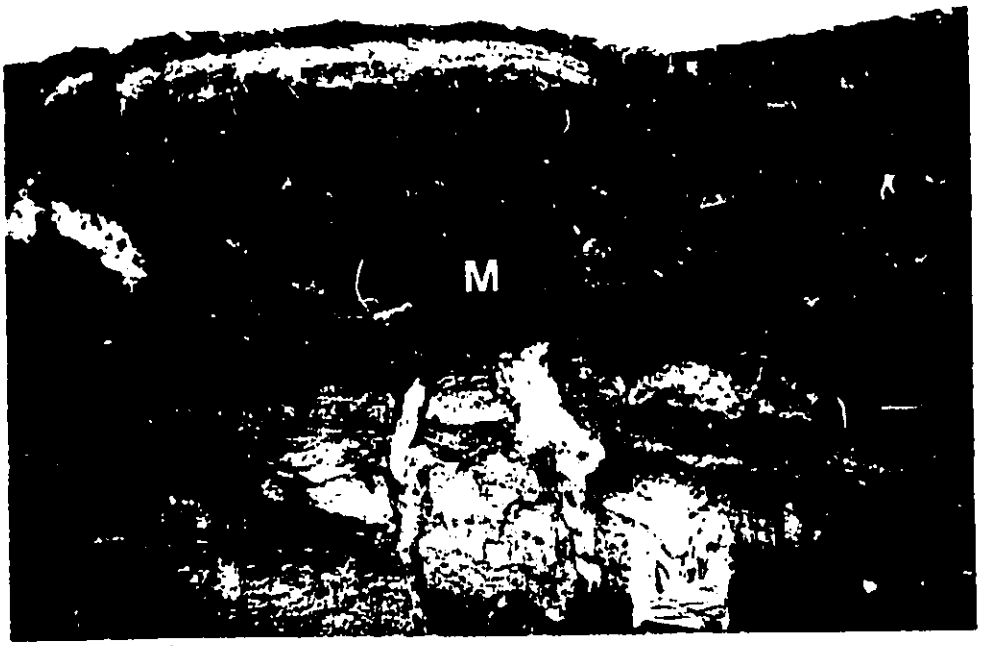

Fig. 5.6 **MUD/MUDDY PEAT**

(A) Thin horizontal beds of mud-muddy peat (M) overlie impure sand (I) and underlie fine sand (F), North Head Basin. The section is capped by *in situ* peat (black) and penetrated by ice wedges (white) that have grown since the lake drained. Figure for scale. (August 14 1991)

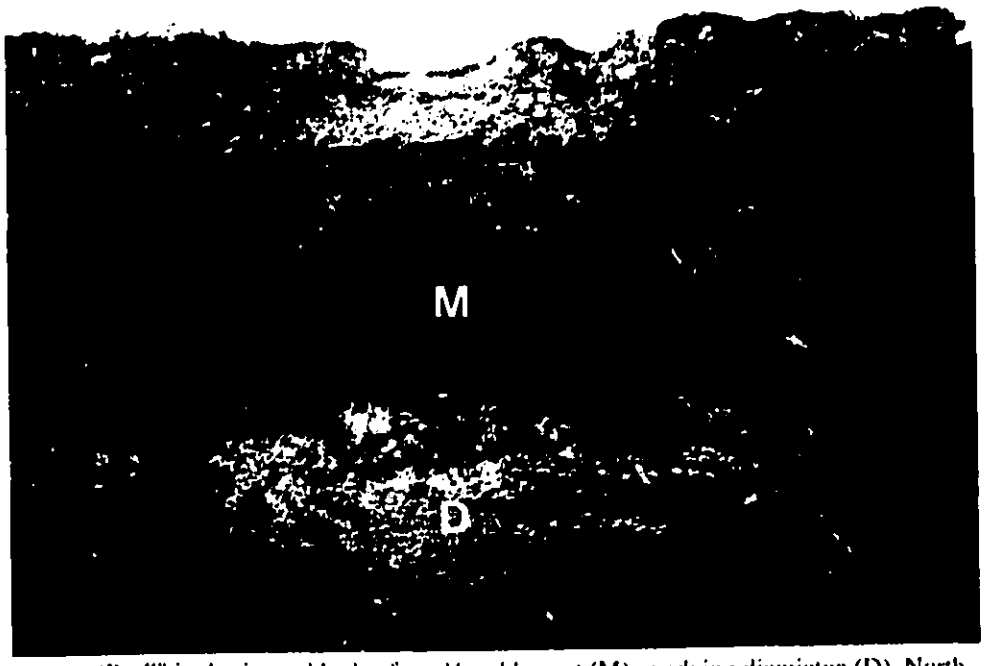

(B) Thin, horizontal beds of mud/muddy peat (M) overlying diamicton (D), North Head Basin. Between (A) and (B; 150m apart), there is a **lateral facies change** in the basal unit (diamicton and impure-sand facies association; section 5.4.2; see also Fig. 5.10). Section is 3.5m high. (August 14 1991)

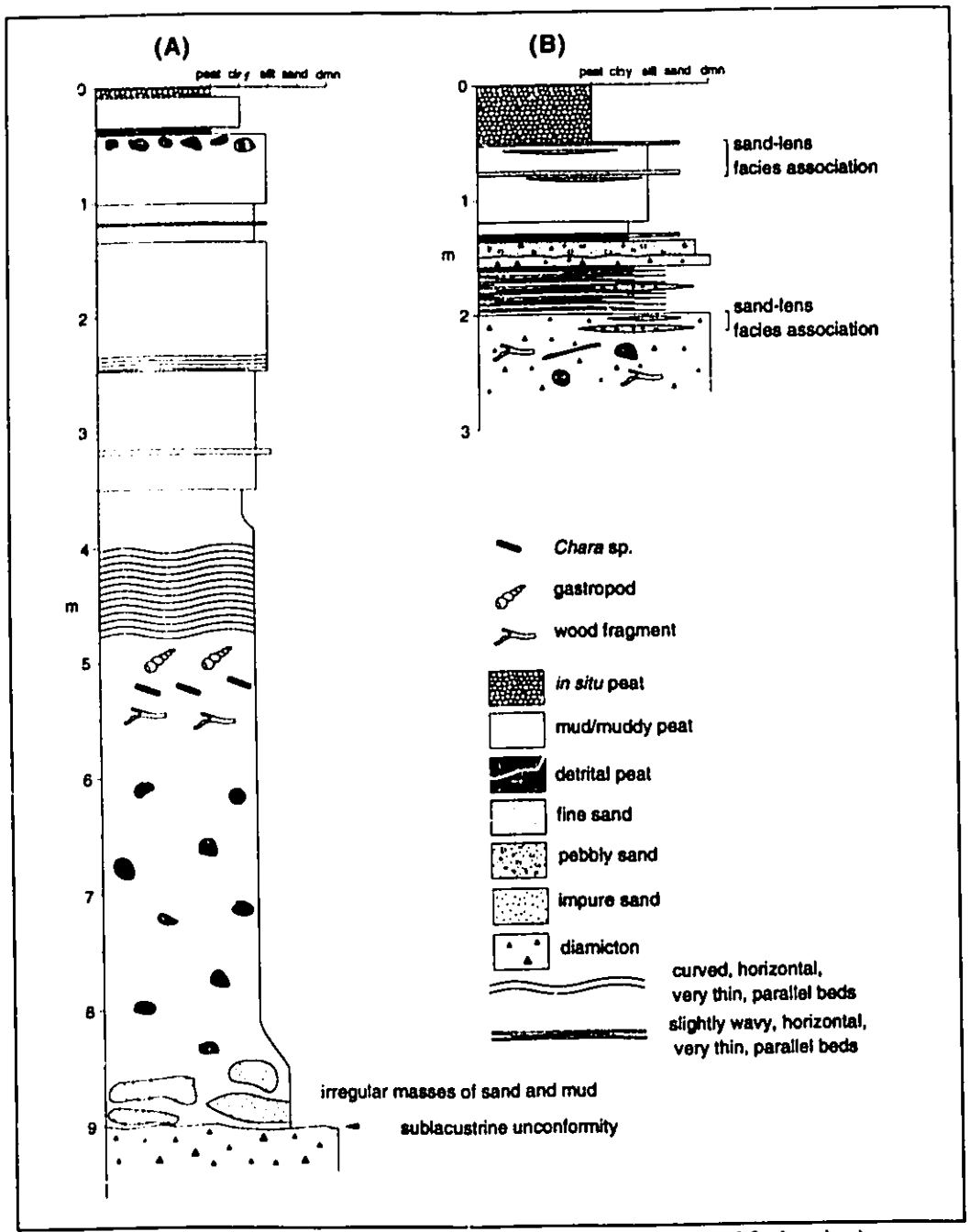

Fig. 5.7 Graphic logs through thermokarst basins, Nicholson Point. (See Fig. 1.6 for location.)
(A) **Basin-centre** sequence. Structureless, organic-free diamicton (? *in situ* or redeposited till) underlies a sequence dominated by mud/muddy peat. (August 23 1990)
(B) **Basin-margin** sequence. Unlike (A), this has no dominant facies, instead comprising both diamicton and mud/muddy peat, each with interbedded fine and pebbly sand (sand-lens facies association). The diamicton contains abundant organic material. (August 24 1990)

5.3.6 Diamicton

The diamicton facies is a structureless pebbly (to cobbly) mud (Figs 5.4B, 5.6B, and 5.7). Clasts are randomly dispersed and matrix ranges from mud to sandy mud. Diamicton deposits commonly contain wood fragments and peat, and sometimes, charcoal fragments, freshwater mollusc shells, high-angle faults, sand bodies and lenses of pebbly sand. The sand bodies vary from gently dipping (10-15°) beds (≤15cm thick and ≤2m long) of fine or impure sand to irregular streaks and diapirs. Cryostructures include structureless, irregular and regular reticulate (Fig. 2.3B), and excess ice contents seldom exceed several percent. Upper and lower contacts are generally sharp and conformable. Diamicton forms bodies of variable size and shape (e.g. diapirs, lenses, amorphous masses and flame structures). Areal distribution and abundance of diamicton varies. For example, it may underlie lacustrine deposits (Fig. 5.12A) or occur within them (Figs. 5.4B and 5.7B), and at two or more levels. In addition, it commonly occurs in gelifluction sheets on basin sides.

Diamicton is interpreted as a sediment-gravity-flow deposit. Being structureless and with randomly dispersed clasts, it is most likely deposited by cohesive debris flows (cf. Nemec and Steel, 1984). Its variable geometry and occurrence is probably due to episodic flows generated in the floors of retrogressive thaw slumps. In lacustrine basins, some of these flows probably continue underwater, accounting for the presence of freshwater mollusc shells, occasional crude bedding and interbedding with impure sand (Fig. 5.4B; cf. Brodzikowski and Van Loon, 1991, Fig. 280). Lenses of pebbly sand/sandy gravel in diamicton (Fig. 5.7B) suggest that some flows experienced wave reworking; modern examples of this occur in front of thaw slumps at North Head and Crumbling Point, where debris flows commonly straddle the lake- or seashore. Around basin margins, diamicton interbedded with non-lacustrine facies is likely deposited by gelifluction.

5.3.7 *In situ* peat

In situ peat is structureless and mesic to fibric, with roots extending down into underlying facies. It commonly contains variable amounts of fine sand (Fig. 5.5A). The facies is generally 5-30cm thick, but beneath high-centre polygons it may attain thicknesses of a few m (≤3.5m at Nicholson Point; cf. Zoltai and Tarnocai, 1975). Where *in situ* peat forms the surface horizon it may support living mosses, *Carex* spp., *Eriophorum* spp., grasses and *Salix* spp. Basal contacts are typically sharp and planar to undulating (Fig. 5.6A). Upper contacts are normally gradational and planar to undulating.

In situ peat forms in wet floors of drained and partially drained basins (cf. Ivanov, 1984, p.96). For example, in a basin on Hadwen Island, 20-30cm of *in situ* peat has formed since the lake partially drained (Fig. 5.5). The sandy nature of this facies reflects aeolian deposition and/or peat colonisation of sandy sublacustrine benches. Because the relative rates of aeolian deposition and peat accumulation can vary, there is probably a continuum between pure *in situ* peat and pure root-rich sand.

5.3.8 Root-rich sand

Root-rich sand is well sorted, commonly containing horizontal, root-rich horizons (0.5-15+cm thick; Fig. 5.8). The roots are typically those of graminae, *Dryas* spp. and *Salix* spp. Although the sand itself is commonly structureless, it locally contains horizontal/subhorizontal, wavy beds (1-5cm thick) of fine and silty sand. At Mason Bay and Hadwen Island, root-rich sand merges into active dunes on the upland surface (D in Fig. 1.5).

Root-rich sand is an aeolian deposit of drained and non-lacustrine basins (see e.g. Harry, 1982, p.126-130), forming where the sand is trapped by vegetation (cf. Pissart et al., 1977). Wherever this facies occurs, Kittigazuit or Kidluit sand (Rampton, 1988) outcrops nearby, suggesting that some of the sand is derived locally. In addition, some is likely derived

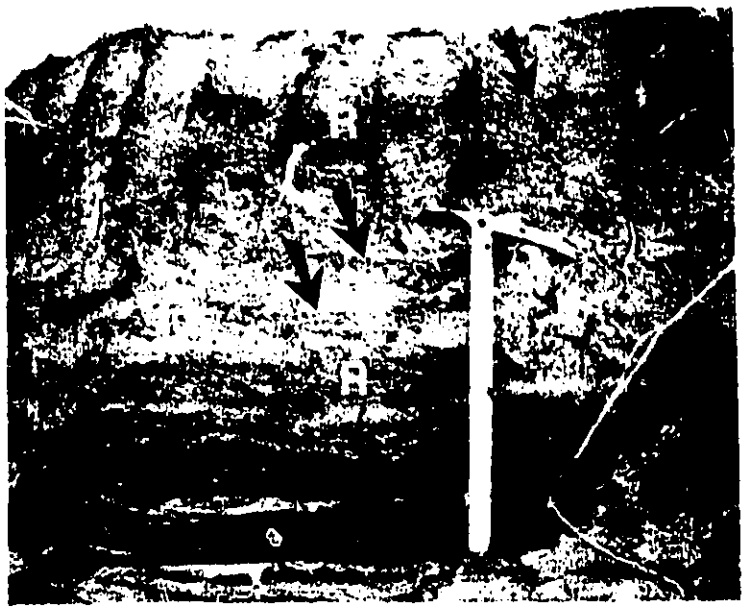

Fig. 5.8 **Root-rich sand**, Mason Bay Basin. This unit contains root-rich (R) and root-poor (P) horizons; arrows mark their contacts. Internally, these units are structureless. The facies overlies interbedded fine sand and detrital peat 50cm high ice axe for scale. (Photo courtesy of Andy Green; July 2 1991)

Fig. 5.9 **Fine-sand and detrital-peat facies association**, Mason Bay Basin. The association comprises two units: the upper is planar, parallel bedded, the lower highly deformed. Deformation structures in the latter suggest that it liquefied - probably due to cyclic, wave-induced stresses. As the unit resedimented, escaping pore water locally breached the base of the upper unit, forming small **fluidisation channels** (type B pillars (arrow)). The association is capped by root-rich sand (R) and underlain by detrital peat (black). Section is 1m high. (July 1 1991)

from newly emergent sublacustrine benches (cf. Mackay, 1974b). Aeolian sand has probably been deposited in thermokarst basins throughout their history, but where deposited in lakes it is reworked by lacustrine processes. Therefore, only in drained or non-lacustrine basins does it form a distinct facies.

5.4 Facies associations

Three facies associations can be identified in thermokarst basins.

5.4.1 Fine-sand and detrital-peat association

Comprising interbedded fine sand and detrital peat (Figs 5.3B, 5.8 and 5.9), the fine-sand and detrital-peat association varies considerably in terms of (1) the proportions of sand and peat, (2) stratification, (3) bed thicknesses and (4) bed numbers. It may be dominated by either facies. Beds may be lenticular; horizontal, planar (Fig. 5.9) to wavy parallel or low-angle cross beds (Fig. 5.3B). Beds tend to be structureless, except for those, of sand, thicker than c.5cm, which may be laminated (Section 5.3.2). Bed thicknesses range from c.0.2-60+cm, individual beds commonly varying over lateral distances of a few metres. For example, on the eastern margin of Crumbling Point Basin, detrital peat thins upslope (over a distance of several m) from c.30cm to c.2cm. Bed numbers range from a few to thirty or more in a 1m high section. Upper and lower contacts tend to be sharp and planar to undulating.

This association occurs beneath the margins of drained basins, behind risers and in basin centres. For example, in Crumbling Point Basin (Fig. 1.4) it underlies the eastern (Fig.5.2), western (Fig. 5.3B) and southeastern margins. At Mason Bay it underlies most of the basin, but is particularly well developed beneath a drained residual pond in the basin centre. Here the association is thickest (≤1.5m) beneath the marginal riser, where beds dip several degrees toward the basin centre, oriented approximately parallel to the front of the riser and

containing many truncation surfaces. Beneath the depression centre the association is thinner (several dm), its beds horizontal, planar and parallel.

The fine-sand and detrital-peat association forms on beaches (e.g. Carson and Hussey, 1962) and in shallow water (cf. Ivanov, 1984, p.95). Modern examples were observed in plan on the beaches and in the shallows of thermokarst lakes in the Summer Island area (Section 5.2.2). Truncation surfaces form by erosion during summer storms, storms whose wave-induced cyclic stresses locally trigger liquefaction and fluidisation, forming water-escape structures (e.g. type B pillar in Fig. 5.9; see Lowe, 1975, p.173).

5.4.2 Diamicton and impure-sand association

The diamicton and impure-sand association is well developed at Crumbling Point (Fig. 5.10A), North Head (Figs 5.4 and 5.10B) and Mason Bay (Fig. 5.11). At North Head it forms a basal unit 1-3+m thick and at least 220m long. From NE to SW, diamicton comprises the first 40m of the measured section. Thereafter, a few SW-dipping sandy foresets appear, gradually becoming more prominent to the SW. Between 70m and 90m, two large (10m and 13m long and ≤ 0.75m thick) lenses of diamicton are surrounded by impure sand (Fig. 5.10B). Between 100m and 120m, the association changes into foreset-bedded impure sand (Figs 5.4 and 5.10B), foresets consistently dipping (c.10° and 25°) to the SW. Between them diamicton is locally interbedded. At the SW margin of the basin the foresets flatten and onlap over a basal unconformity (Fig. 5.12A). At Crumbling Point, diamicton forms large tongues or diapirs in impure sand (Fig. 5.10A). At Mason Bay, impure sand (or pebbly sand) commonly occurs as diapirs or irregular masses in diamicton (Fig. 5.11).

The diamicton and impure-sand association has several distinctive features: (1) there are numerous diapirs (Figs 5.10-5.11), load casts and small, high-angle faults (Fig. 5.4A) ; (2) contacts tend to be sharp and irregular; (3) the size, shape and abundance of diamicton and

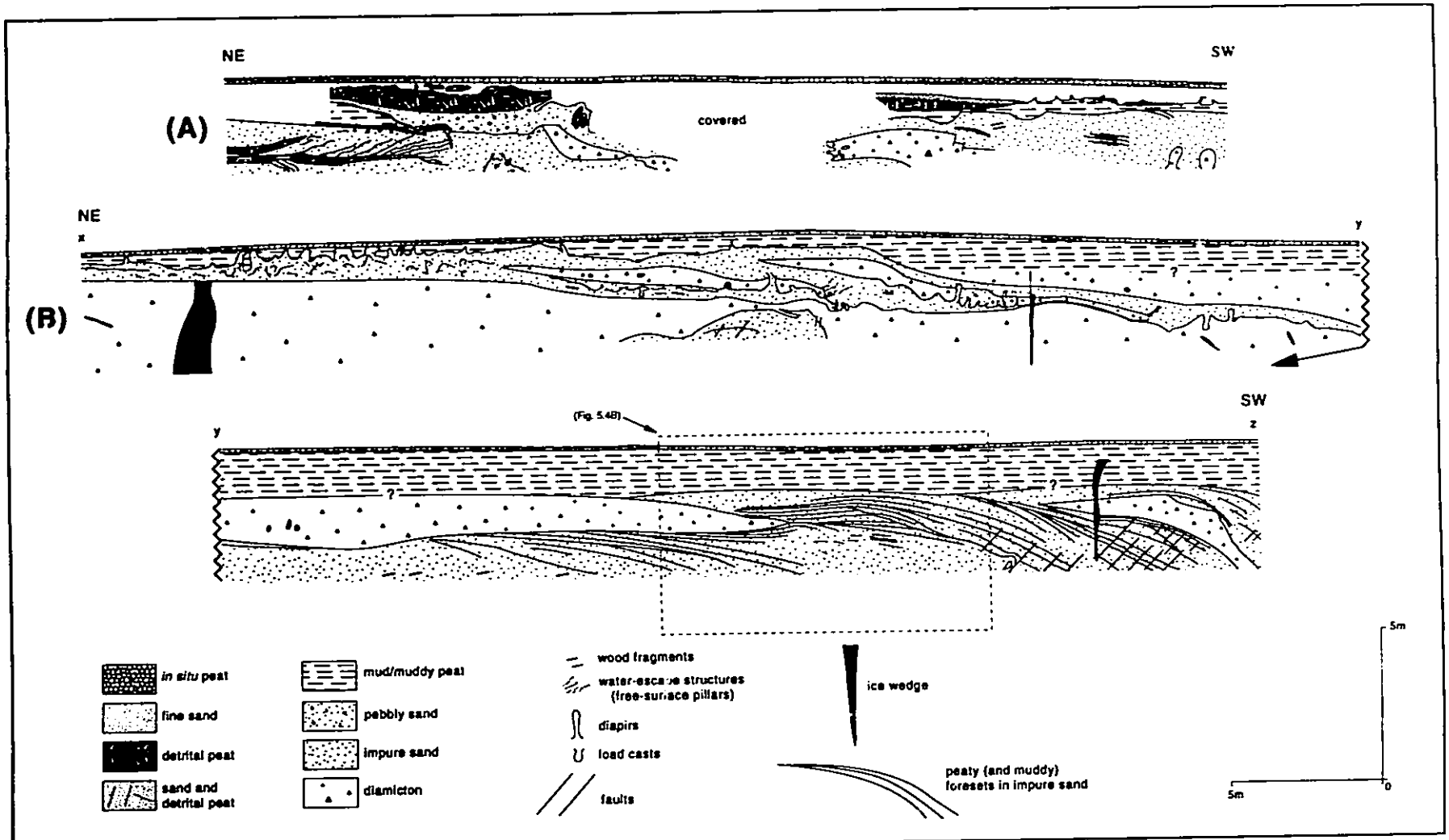

Fig. 5.10 **Architecture of thermokarst-basin facies:** (A) Crumbling Point; (B) North Head. At both sites, the lowest exposed unit is the **diamicton and impure-sand facies association**; note the irregular size and shape of diamicton bodies within it. In (B), from NE to SW, the association changes from diamicton (Fig. 5.6B) to impure sand (Figs 5.4 and 5.6A) with diamicton interbeds (subaqueous debris flows), **a facies change representing the progradation** of a sublacustrine bench. The upper unit comprises mud/muddy peat, fine sand, and detrital peat. It contains abundant soft-sediment deformation structures - diapirs and load casts. Deformation was likely triggered by cyclic, wave-induced stresses (cf. Fig. 5.9). In (A), the large lens of detrital peat was deposited in shallow water near the margin of the former lake. (A - August 28 1991; B - August 14 1991)

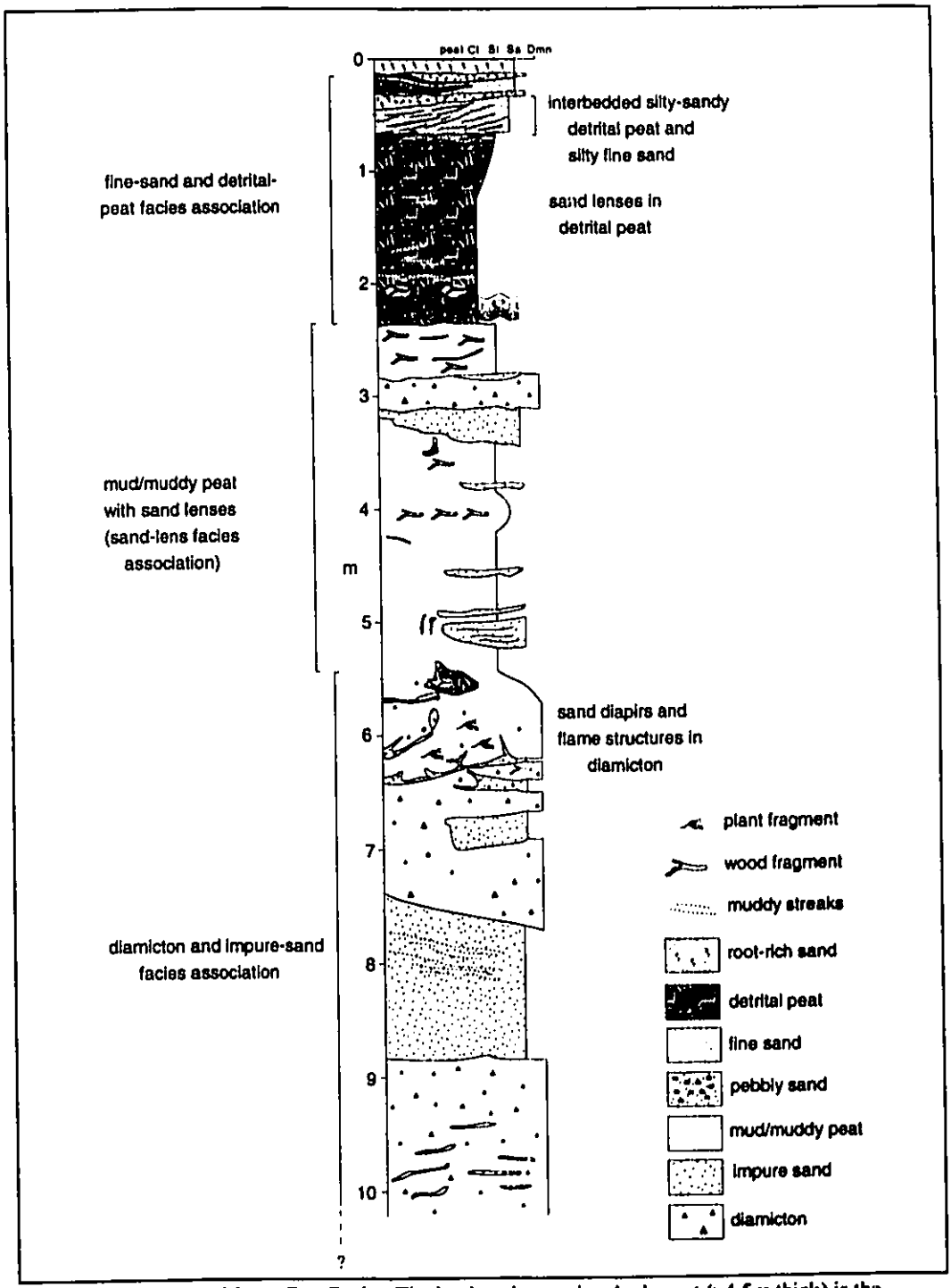

Fig. 5.11 Graphic log, Mason Bay Basin. The log has three units: the lowest (>4.5m thick) is the diamicton and impure-sand facies association; the middle unit is dominated by mud/muddy peat; and the upper unit is the fine-sand and detrital-peat association. Note the **upward increase in peat.** (June 29 1991)

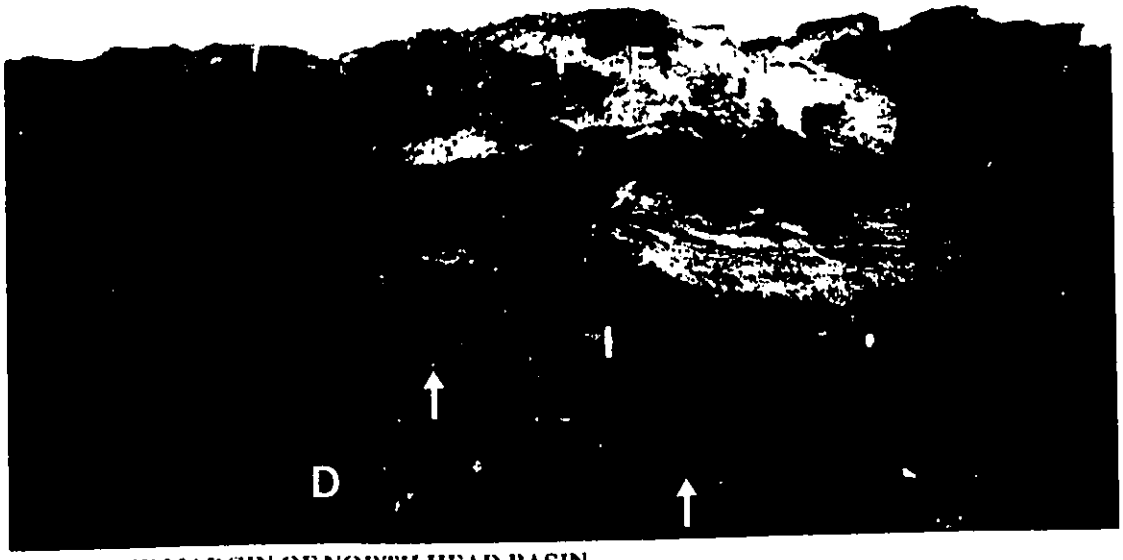

Fig. 5.12 **SW MARGIN OF NORTH HEAD BASIN**

(A) Marginal lacustrine sediments comprise impure sand (I) and detrital peat (black) capped by fine sand (F) and pebbly sand (P). These form a large lens (10m wide and 4m thick; SW half in B) whose foresets - in impure sand and detrital peat - flatten and onlap over a **basal unconformity** (white arrows) veneered by sandy gravel that was reworked from underlying diamicton (D). The flattening records the SW termination of bench progradation and the deposition of **beach deposits** in shallow water at the margin of the former lake. In the centre of the photo, a pseudomorph overlies a partially-thawed ice wedge (black arrow; see Fig. 6.1; section 6.2.1). Section is 4.5m high. (August 14 1991)

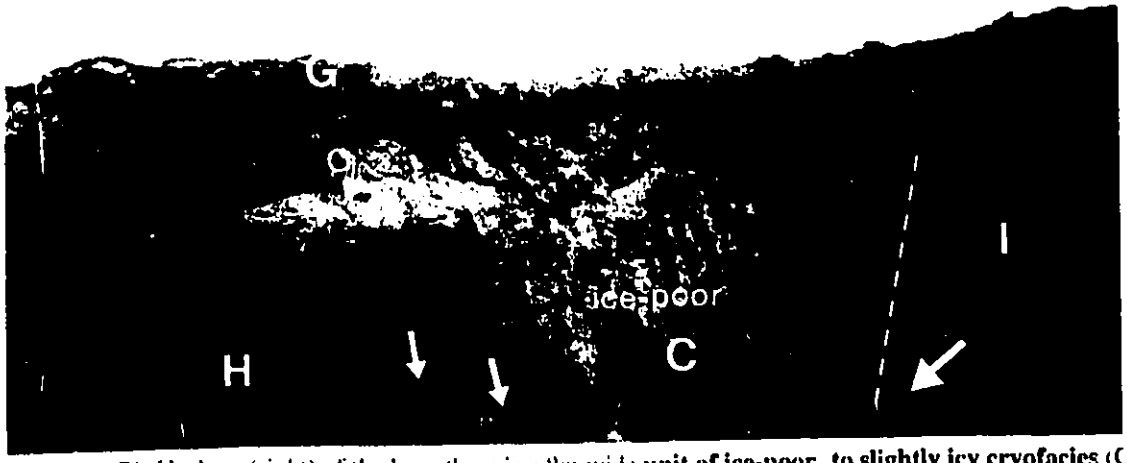

(B) Upslope (right) of the lens, there is a 8m wide **unit of ice-poor to slightly icy cryofacies** (C). Containing small sand lenses (small arrows) that characterise the ice-breccia association (I), this ice-poor unit is identical to the latter, except for the absence of ice clasts, an absence due to thawing within the **former lake talik**. The outer edge of the talik, marked by a **secondary thaw contact** (dashed line), must be just to the left (basinward) of the most NE ice clast (large arrow) in the ice-breccia association. Approximately 4m to the right of the tape, the ice-poor unit merges laterally into a **homogenised facies** (H) - note the changing colour from medium to dark grey, a change likely indicating resedimentation of the ice-poor unit, probably by debris flows. The large sand lens is partially covered by a **gelifluction sheet** (G) whose snout coincides with the tape. Moving downslope, this sheet has **overturned the bedding** (O) in the underlying sand. Stakes are 2m apart. (August 12 1991)

sand bodies is highly variable (Figs 5.4B and 5.10) and (4) the association forms relatively thick (≤3+m) units that are stratigraphically low in basin fills (Fig. 5.11). The association is widespread in marginal areas. But it is unclear if it also underlies basin centres.

This association is likely deposited in young, rapidly expanding thermokarst lakes (see Sections 5.3.4 and 5.3.6) by prograding sublacustrine benches. The bench deposits at North Head show that the inner part of the bench comprised diamicton, and the outer impure sand (Fig. 5.10B). Bench progradation was initially dominated by debris-flow diamictons, but through time the front of the bench became increasingly sandy. This change suggests that either the sediment source changed, as more sand-rich cryofacies were exposed around the basin, or, more likely, as the bench prograded and as backwearing thermokarst consumed the source upland, that fewer debris flows reached the front of the bench, those which did being increasingly wave-reworked. Such reworking may explain the scattered clasts and pebble stringers in impure sand, the fines being winnowed away and deposited in basin deeps. Large lenses of diamicton (Fig. 5.10B) and diamicton interbeds (Fig. 5.4B) are probably individual debris flows. At North Head the transition from diamicton to impure sand was marked first by the appearance of occasional SW-dipping sand beds and later by foresets in impure sand (Fig. 5.4). These foresets indicate that the bench was fronted by a riser dipping 10-25° SW, its crest broadly convex. Numerous reactivation surfaces (Fig. 5.4A) show that the riser was episodically eroded. Progradation and erosion of the riser was likely in part controlled by bimodal, wave-induced currents during summer storms. The cyclic loading generated by storm waves may have formed some of the diapirs and load casts in this association. During fairweather the riser would have been partially covered by detrital peat and/or mud. The bench prograded right to the SW shore (Fig. 5.12).

This association was deposited in thermokarst basins receiving large influxes of sand and diamicton that was generated by backwearing thermokarst. At Crumbling Point the

evidence for this is not only the association itself but also the abundant sand and diamicton-rich slump-floor deposits on the northern margin of Crumbling Point Upland (Fig. 4.10) and the old slump scars on the southern and eastern margins (Fig. 1.4). Such large-scale slumping is now uncommon in the Tuktoyaktuk Coastlands, being confined mainly to exposed coasts like Crumbling Point. However, in such situations, debris transported to the sea is likely reworked more thoroughly (cf. Aigner, 1985; Swift et al., 1985) than it would be in thermokarst lakes. Thus there are few, if any, modern analogues of this association, the closest which the author observed being at Green Lake (Fig. 1.4), where slumping transports small quantities of sand and diamicton onto a sandy sublacustrine bench.

5.4.3 Sand-lens association

The sand-lens association typically comprises lenses of fine sand (or pebbly sand) in diamicton or mud/muddy peat (Fig. 5.7B). The lenses are commonly 0.2-10+cm thick and 5-50+cm long. Thin lenses appear to be structureless, while those thicker than a few cm may contain slightly wavy, muddy laminae. Upper and lower contacts are typically sharp and planar to curved. This association was observed both beneath basin margins (Fig. 5.7B) and centres. In North Head Basin it underlies a drained residual pond.

Where lenses of pebbly sand occur in diamicton, for example near the margin of a basin at Nicholson Point (Fig. 5.7B), they likely formed by wave and/or current reworking of sandy debris flows. Reworking may also occur in residual ponds, such as the now-drained one in the centre of North Head Basin. But in this example the source of fine sand is uncertain. Possibly, the sand was deflated from the freshly exposed lake floor after the lake had partially drained. The origin of fine sand lenses in thick mud/muddy peat is unknown but may relate to sediment-gravity flows (cf. Hopkins and Kidd, 1988).

5.5 The margins of thermokarst basins

At the margins of thermokarst basins there is both a secondary thaw contact and a change between basin and upland cryofacies. The facies change may be shown by cryofacies that are deformed and/or homogenised. Deformed basin cryofacies, which occur at North Head, Crumbling Point, Mason Bay and Hadwen Island, typically comprise folded and thrusted fine sand and detrital peat (Figs 5.12B and 5.13). The folds are generally isoclinal and recumbent to gently dipping. They may occur singly or collectively, their axial planes oriented parallel or subparallel to the ground surface. Where folds are abundant they are commonly stacked and separated by low-angle thrusts (Fig. 5.13). Invariably underlying gelifluction sheets (Figs 5.12B and 5.13), these structures must have been formed by compressive flow (cf. Shaw, 1977, Fig. 1) as the sheets moved downslope, shearing underlying materials.

Homogenised cryofacies occur at the SW margin of North Head Basin. Here the upland cryofacies comprise irregular bodies of ice-poor sand (?glacitectonic lamination; cf. Hart et al., 1990, Fig. 4) and mud interspersed with clasts of pure to sediment-rich ice. Together these cryofacies form a (glacitectonic) ice-breccia association (Fig. 5.12B). At the basin margin, beneath the SW end of a lens of beach deposits (Fig. 5.12A), the ice-poor continuation of this association (see below) merges into diamicton deposited within the basin, a change marked by the appearance of peat, clasts and charcoal, and by the disappearance of lens-shaped sand bodies, which characterise the ice-breccia association. Thus the cryofacies become homogenised (Fig. 5.12B), probably as a result of redeposition by debris flows.

Approximately 8m upslope of this facies change the disappearance of ice clasts in the ice-breccia association marks a secondary thaw contact (Fig. 5.12B). This explains why the non-ice components of the association (the sand lenses in Fig. 5.12B) continue for c.8m downslope of the last ice clast. In other words, the association continues basinward of the

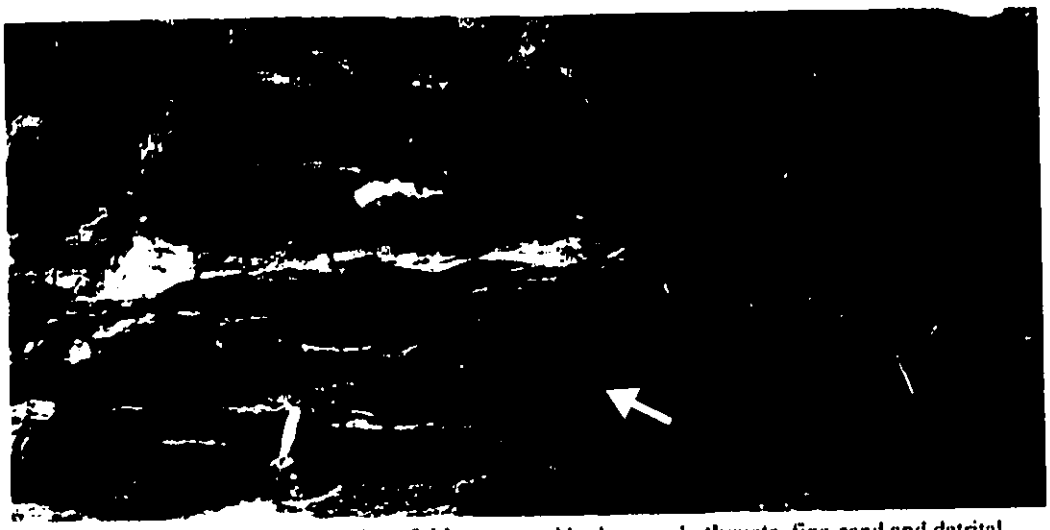

Fig. 5.13 Stacked, isoclinal, recumbent **folds** separated by low-angle **thrusts**, fine-sand and detrital-peat association, E margin of Crumbling Point Basin. These structures **underlie a gelifluction sheet** (moving to right). Note the infilled burrow (arrow) of *Spermophilous undulatus* (arctic ground squirrel). Vertical lines are 1m apart. (August 21 1991)

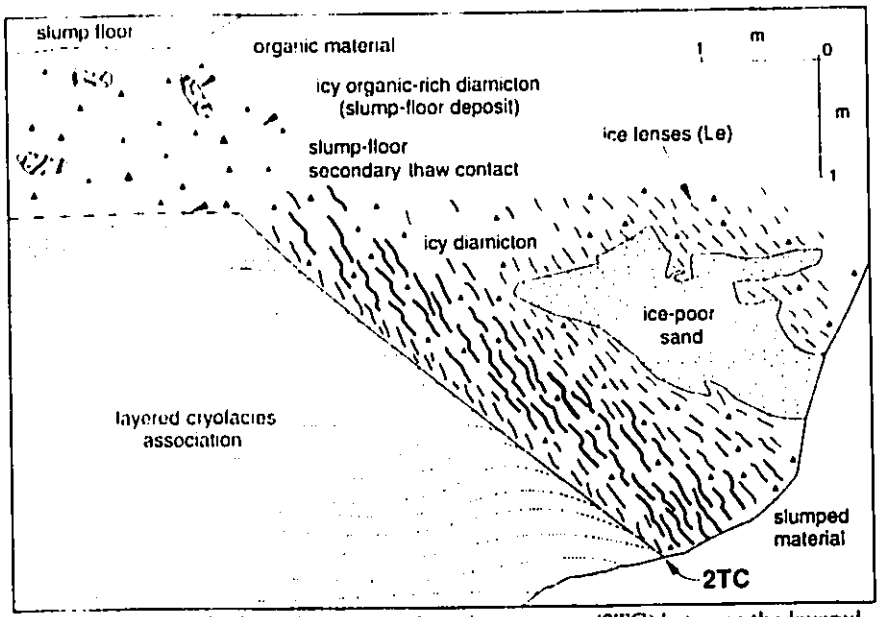

Fig. 5.14 Steeply dipping, planar secondary thaw contact (2TC) between the layered cryofacies association and (?melt-out) diamicton, E margin of Mason Bay Basin (the basin is to the right). The contact is interpreted as the **E edge of the former lake talik**. Note that the ice lenses in the icy diamicton run parallel-subparallel to the contact, an orientation that would have been orthogonal to the direction of **inward freezing** of the talik after the lake had drained. (June 26 1991)

thaw contact, but in ice-poor form. Likewise, on the eastern margin of Mason Bay Basin the layered cryofacies association terminates laterally at a sharp, planar contact that steeply dips (c.45°) towards the basin (Fig. 5.14). Truncating bands in this association, the contact underlies muddy (?melt-out) diamicton whose ice lenses (lenticular cryostructure) are oriented parallel/subparallel to the contact (Fig. 5.14). These secondary thaw contacts at Mason Bay and North Head likely mark the sides of former sub-lake taliks. After the lakes drained, the sediments basinward of the contacts refroze, the orientation of the freezing plane being strongly influenced by that of the contact. Hence the ice lenses at Mason Bay also dip steeply towards the basin (cf. Demek, 1978, Fig. 9.2).

5.6 Facies model

A three-stage facies model is proposed for deep thermokarst basins in the Tuktoyaktuk Coastlands (Fig. 5.15).

During the first stage, basins (typically lacustrine) form and grow by rapid lake-bottom subsidence and backwearing thermokarst (Fig. 5.15A). Backwearing thermokarst rapidly transports abundant upland materials into thermokarst lakes (cf. Rampton, 1974; Eyles, 1979), initiating sublacustrine benches. Three benches are shown in Fig. 5.15A. The middle one, narrow and formed of diamicton, was deposited by subaqueous debris flows close to the retreating upland. The left-hand bench comprises both diamicton and impure sand, diamicton forming the proximal part, impure sand the distal. The impure sand was deposited further from the retreating upland, allowing more time for reworking. As the bench prograded, fewer debris flows reached the riser - hence the offshore transition from diamicton to impure sand. The third type of bench, on the right-hand side of Fig. 5.15A, comprises impure sand (Fig. 5.5). It forms in front of retreating sand-rich uplands.

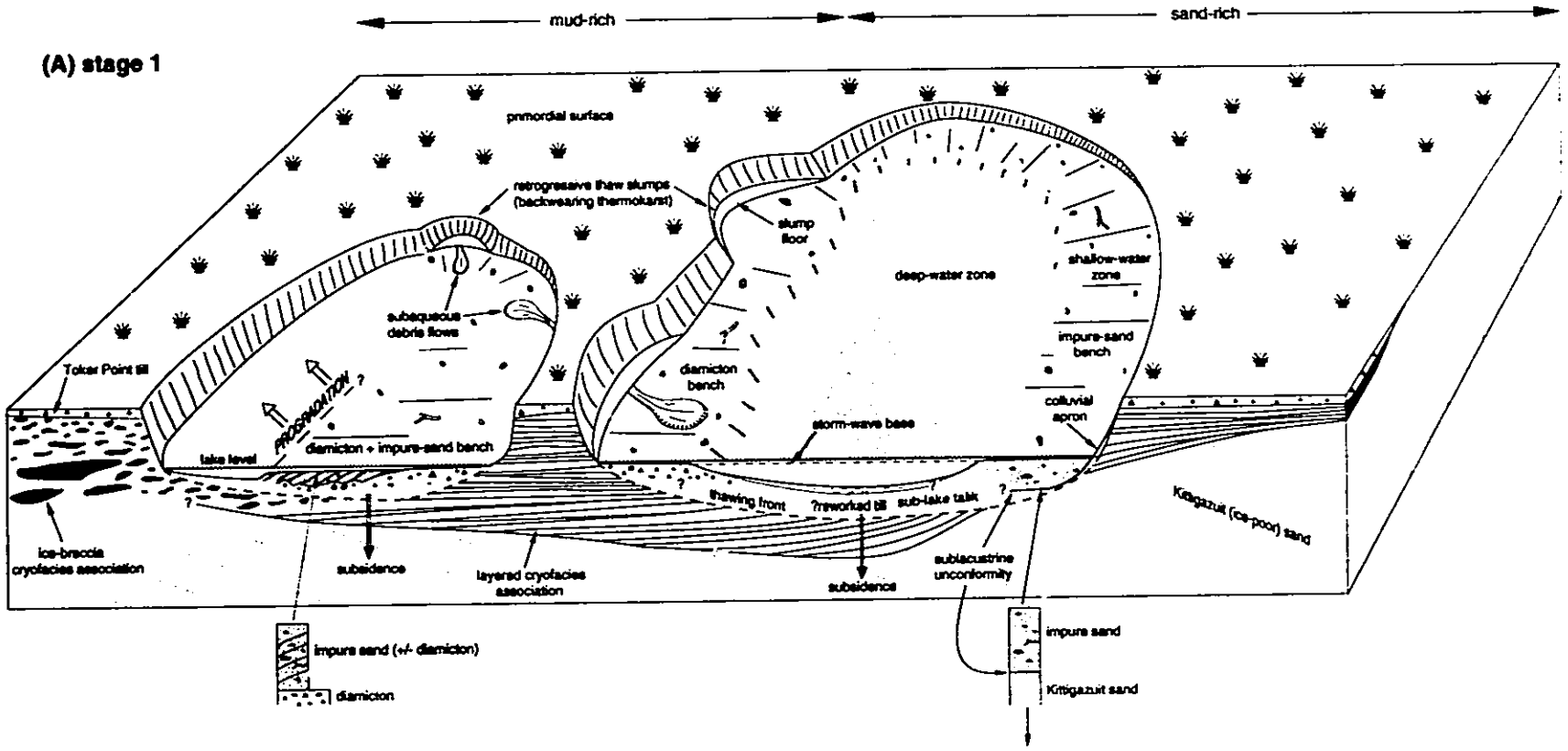

Fig. 5.15A Facies model of deep thermokarst basin comprising mud- and sand-rich parts and showing basin evolution in three stages (A-C).
Stage 1: Sub-lake and backwearing thermokarst operate most rapidly, backwearing thermokarst transporting large amounts of upland materials into basins. The materials are redeposited as diamicton and/or impure sand, and form sublacustrine benches. Coevally, mud/muddy peat accumulates in the deep-water zone, and a shallow sub-lake talik develops beneath each basin.

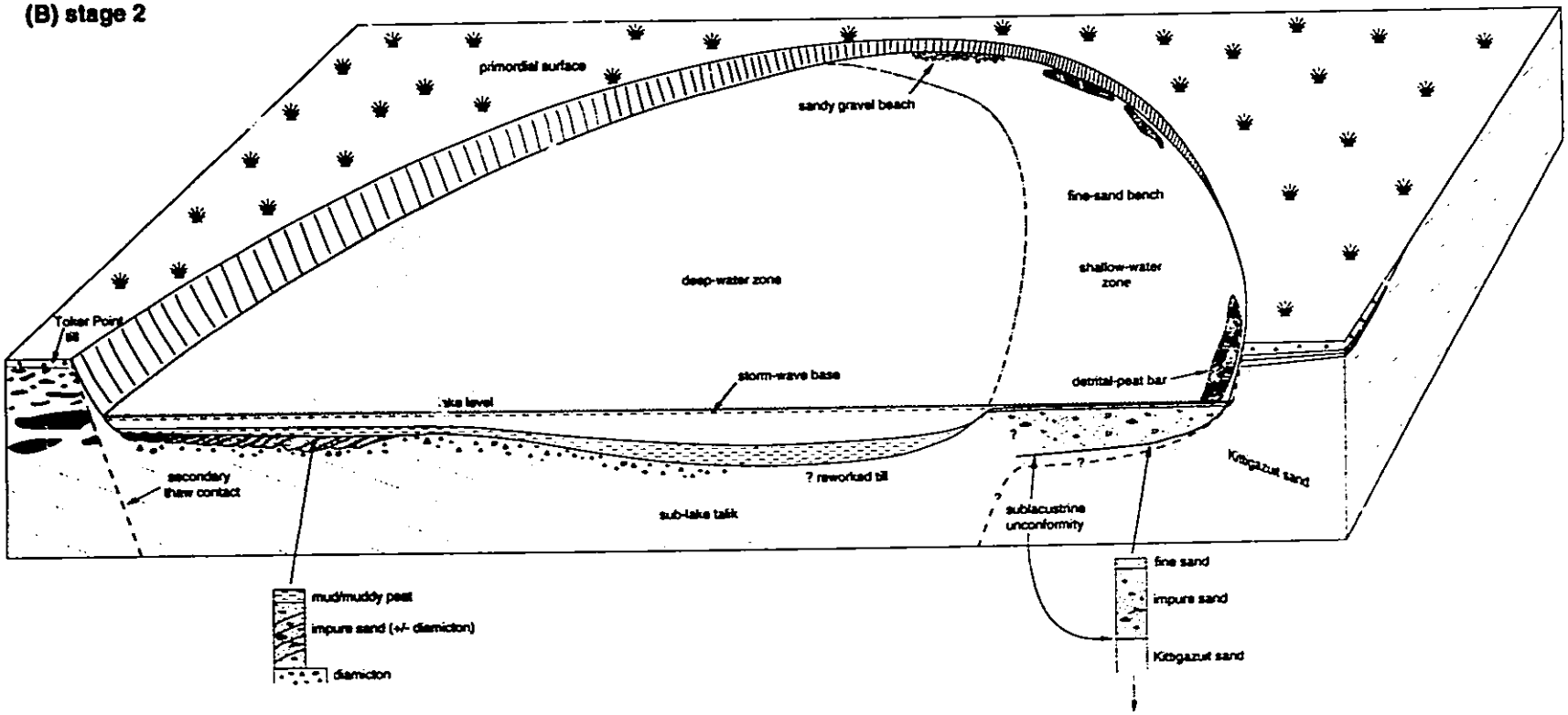

Fig. 5.15B Stage 2: Sub-lake and backwearing thermokarst cease or greatly diminish, reducing the influx of upland materials, and thereby changing the dominant basin infilling to mud/muddy peat. Over large areas of the shallow-water zone, detrital peat, fine sand and pebbly sand/sandy gravel accumulate, the last two facies forming by wave and current reworking of diamicton and impure sand (note that fine sand caps impure sand). Meanwhile, the sub-lake talik attains its maximum size.

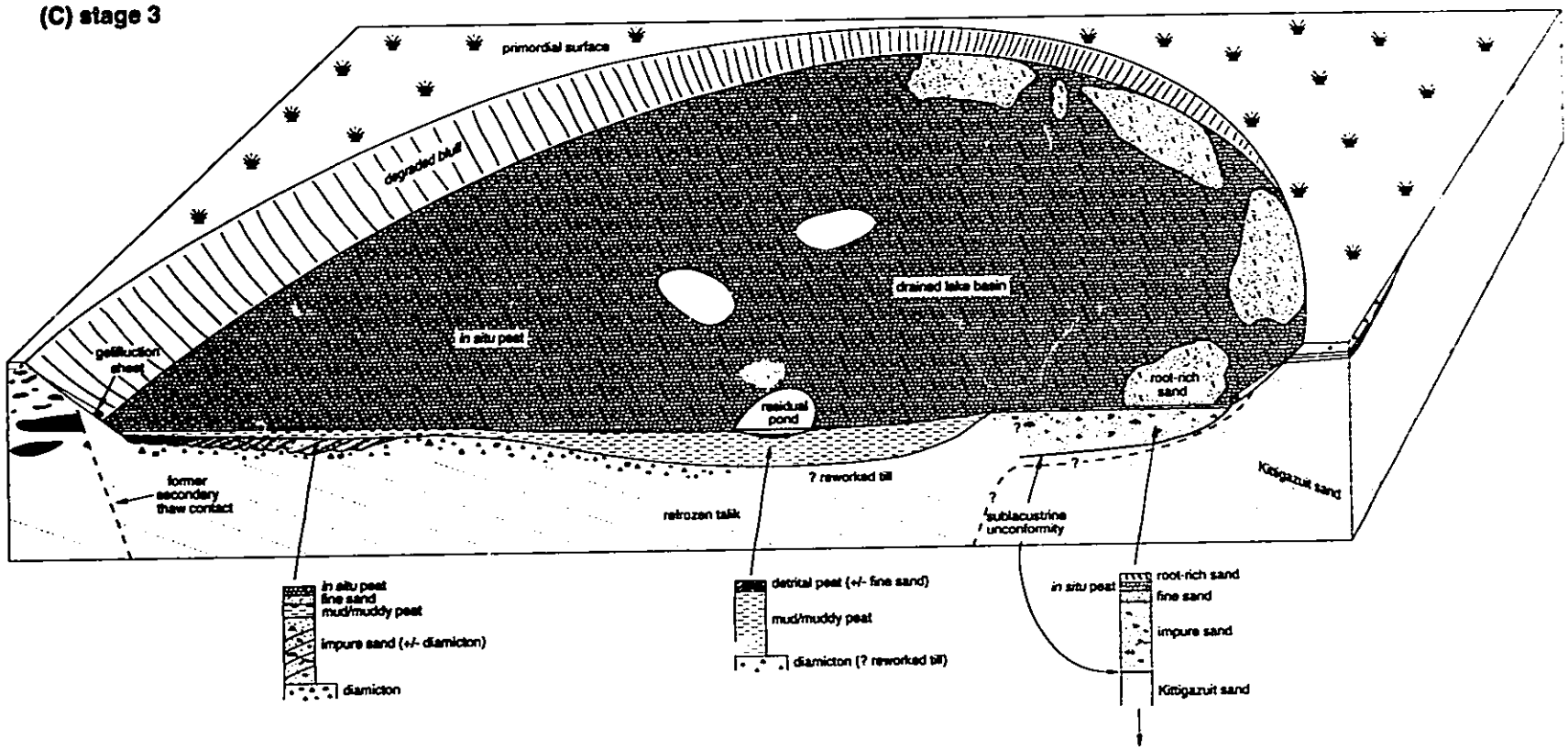

Fig. 5.15C Stage 3: The basin drains and begins to infill with *in situ* peat, root-rich sand and, around the basin margins, with material redeposited by gelifluction. Detrital peat (+/- fine sand) accumulates in residual ponds. Basin margin slopes decline by gelifluction and, in sandy areas, by deflation. As the sub-lake talik refreezes, a secondary thaw contact is preserved around the basin margins. (See Fig. 5.5 for legend.)

Sediment supplied to thermokarst lakes may or may not be reworked by waves and currents. Reworking depends on the nature of the sediment and on the balance between sediment supply, erosion and subsidence. For example, sand and disaggregated organic material are readily eroded and redistributed, whereas muddy debris flows and large blocks of sod and peat are less erodible, accounting for the occurrence of diamicton beds (Fig. 5.4B) and organic blocks within impure sand (Fig. 5.5).

The sediments of young sublacustrine benches are distinct from those of mature benches (fine sand; stage two), the former being (1) poorly sorted, (2) organic-rich (wood fragments and large blocks of peat and sod; Fig. 5.5), (3) faulted (Fig. 5.4A) and (4) overlying sublacustrine unconformities (Fig. 5.5A). These features respectively reflect (1) rapid sedimentation, (2) the destruction of vegetated and peaty upland surfaces, (3) melt-out of underlying ground ice and (4) the early time of deposition.

The second stage begins when lakes approach their maximum size and depth (Fig. 5.15B). By then lake-bottom subsidence and backwearing thermokarst have ceased or greatly slowed. Lake-bottom subsidence ceases when sub-bottom excess ice has melted out, as indicated by horizontal beds of mud/muddy peat overlying ice-wedge pseudomorphs, and by the absence of faults in the upper units of mud/muddy peat and of the fine-sand and detrital-peat association. Also during this stage, sub-lake taliks stabilise, forming lateral secondary thaw contacts with upland cryofacies (Fig. 5.15B). The rate of backwearing thermokarst may decline if the climate cools or if much of the ground ice adjacent to basins has melted. As the rate declines, so does the influx of upland materials to lakes, a decline reflected by both the development of fine sand veneers on sublacustrine benches and a change in the dominant lacustrine facies to mud/muddy peat.

Around basin margins in sandy terrain, the tops of sublacustrine benches are reworked by waves and currents. Mud and detrital peat are winnowed from underlying impure sand,

leaving a veneer of well sorted and rippled fine sand (Figs 1.3; 5.5; 5.10a; 5.15B). On inner parts of benches, detrital peat accumulates locally, commonly interbedded with fine sand to form the fine-sand and detrital-peat association. Between storms or during winter, small amounts of mud settle on benches, producing silty drapes (Fig. 5.3A). In areas that are particularly turbulent and/or that have received large influxes of pebbles and cobbles, clasts may be reworked, forming lenses of pebbly sand/sandy gravel (Fig. 5.2). In basin centres the finest material settles from suspension, forming thick units of mud/muddy peat.

The third stage begins when a lake partially or completely drains (Fig. 5.15C). In the former case, fine sand may accumulate in turbulent shallow water, and detrital peat and/or mud/muddy peat (+/- fine sand) in residual ponds. Where lacustrine sediments are exposed, they are quickly colonised by vegetation (e.g. Mackay, 1986c), *in situ* peat forming where the water table is near to the ground surface. In sandy areas aeolian sand is deposited as a veneer of root-rich sand. On the marginal slopes of drained (or non-lacustrine) basins, superficial sediments are deformed and redistributed by gelifluction (Fig. 5.13).

This facies model is to some extent idealised. First, the stages are diachronous (cf. Hopkins and Kidd, 1988). For example, the occurrence of mud/muddy peat within ice-wedge pseudomorphs indicates that deposition of this facies locally begins during stage one. (This also indicates that the diamicton and impure-sand association is not necessarily deposited across the whole basin floor.) Second, not all basins in the Tuktoyaktuk Coastlands experience each stage, many prematurely coalescing and draining. Third, because thermokarst-lake facies are absent in non-lacustrine basins, thermokarst-slope facies may directly underlie *in situ* peat (Fig. 4.10; cf. Rampton, 1982, p.33).

In some respects this facies model resembles those proposed for other periglacial (see Hopkins and Kidd, 1988) and glacial thermokarst basins (see Shaw, 1988, Fig. 1). For example, impure sand (stage one) resembles Hopkins and Kidd's basal sandy unit, and

mud/muddy peat (stage two) their upper, fine-grained, organic-rich unit. But in other respects the model differs. For example, in the Tuktoyaktuk Coastlands, diamicton is abundant, highlighting the importance of sediment gravity flows during the early stages of lake growth (cf. Eyles et al., 1987; Shaw, 1988). Furthermore, vertical sequences vary considerably between basin margins and centres. Marginal sequences are commonly dominated by a basal unit of diamicton and/or impure sand and an upper unit of fine sand (+/- diamicton, detrital peat, mud/muddy peat and pebbly sand/sandy gravel; Fig. 5.7B), whereas central sequences tend to be dominated by a thick (≤8m) unit of mud/muddy peat. This variation suggests that sediment gravity flows and wave or current reworking are more common around basin margins, whereas suspension settling dominates basin centres and the later stages of basin evolution (cf. Shaw, 1988, Fig. 1). However, the model differs from Shaw's in two main respects: (1) the abundance of organic material and (2) the apparent absence of varves and of current-laminated sand facies within mud/muddy peat, differences presumably reflecting smaller influxes of meltwater and clastic sediment into periglacial thermokarst basins than into glacial ones.

5.7 Conclusions

The intensity of thermokarst in deep thermokarst basins is broadly reflected in basin sequences. Basal sediments texturally resemble adjacent upland cryofacies (cf. Rampton, 1982, p.32-33; 1988, p.54; Hopkins and Kidd, 1988). For example, in sandy areas like Hadwen Island, the basal sediments are mainly impure sand; in muddy areas like Nicholson Point, they are mainly diamicton; and in areas where both sand and mud are abundant (e.g. North Head), they coexist as the diamicton and impure-sand association. This textural similarity is due to resedimentation of upland materials during early and rapid basin expansion (stage one), when thermokarst is widespread and intense. But as backwearing thermokarst decreases, so does the input of clastic sediment, with the result that the infill becomes organic-rich, finer grained (stage two; cf. Hopkins and Kidd, 1988) and more uniform - an infill but indirectly related to thermokarst; one simply accumulating in lakes. Consequently, the distinguishing features of thermokarst-basin sequences in the Tuktoyaktuk Coastlands are not their upper deposits but their basal ones.

5.7.1 A criterion for identifying thermokarst-basin facies: **Impure sand +/- diamicton**

The impure-sand facies appears to be unique to thermokarst lakes. It is readily identified by the presence of some of the following features: interbedded sand and peaty foresets (Fig. 5.4); irregular blocks of peat in sand (Fig. 5.5); small high-angle faults (Fig. 5.4A); variable amounts of mud, clasts and organic debris; and associated diamicton.

Chapter 6 FROST-FISSURE PSEUDOMORPHS

"These processes [thaw modification of frost-fissure wedges] are still poorly understood, and warrant further attention within the contemporary permafrost environment."
(Harry and Gozdzik, 1988)

6.1 Introduction

Permafrost environments contain abundant frost-fissure wedges (see reviews by Jahn, 1975, p.31-84; French, 1976, p.21-27, 84-93, 236-245; Washburn, 1980a, p.102-117; Popov et al., 1985, p.185-208). The recent literature on these wedges typically focusses on three aspects: (1) the controls over thermal contraction cracking (Romanovskii, 1985; Mackay, 1984; 1986; 1992a), (2) veins and wedges of primary infilling (e.g. Jahn, 1983; Harry et al., 1985; Jetchick and Allard, 1990; Mackay, 1990), and (3) the occurrence of frost-fissure pseudomorphs and their palaeoenvironmental significance (e.g. Vandenberghe, 1983a; 1983b; French and Gozdzik, 1988).

Review of the literature indicates that the modification of frost-fissure wedges during thaw is poorly documented. This chapter therefore describe the pseudomorphs which overlie ice, sand and composite wedges that have partially thawed, inferring from them specific thaw-modification processes.

6.2 Thaw modification

The thaw of ice wedges and (sometimes) their secondary infilling is termed 'thaw transformation' (Harry and Gozdzik, 1988). This is but one aspect of thaw modification, defined here as the general process whereby frost-fissure wedges are modified during thaw and by which frost-fissure pseudomorphs sometimes develop. Thaw modification includes not

only the melting of seasonal ice veins in both the active layer and in seasonally frozen ground but also, and more importantly, that of wedges in permafrost. Though much has been inferred about thaw modification from frost-fissure pseudomorphs in non-permafrost areas (e.g. Jahn, 1975, p.51-84; French, 1976, p. 236-245; Washburn, 1980a, p.102-117; Vandenberghe, 1983a), observations from modern permafrost environments are remarkably few (Dylik, 1966; see e.g. Katasonov and Ivanov, 1973, Fig. 11; Nekrasov and Gordeyev, 1973, Fig. 11; Mackay, 1976; Mackay and Matthews, 1983; Gray and Seppälä, 1991). Yet it is in these environments, where pseudomorphs can be related unequivocally to partially thawed wedges, that thaw modification should be scrutinised.

Since many inferences about Pleistocene permafrost and stadial palaeoclimates rely heavily on supposed frost-fissure pseudomorphs (e.g. Kolstrup, 1985; Rose et al., 1985a; Worsley, 1987; Johnson, 1990; Ballantyne and Harris, in press), it is critical to distinguish *bona fide* pseudomorphs from fissures, veins or wedges that are unrelated to thermal contraction cracking (e.g. Johnsson, 1959; Thorson et al., 1986; Burbidge et al., 1988). To do this requires an understanding of thaw modification.

6.3 Ice wedges

6.3.1 Slow subsidence

On the SW margin of North Head Basin, a pseudomorph overlies an inactive, partially thawed ice wedge (Figs 5.12A and 6.1). The wedge (130cm long) penetrates impure sand and tapers downward from 10cm (true width) at the top to a few mm at the base, where it divides into several ice veins. Its sides are slightly curved and its top (160cm below the ground surface) is convex-up. Above the ice wedge is a deformed, U-shaped pseudomorph (60-70cm deep and ≤20cm wide). This gradually tapers downward, its sides sharp and irregular, with a relief of a few cm (Fig. 6.1). The basal 20cm of the pseudomorph is offset 10cm upslope of

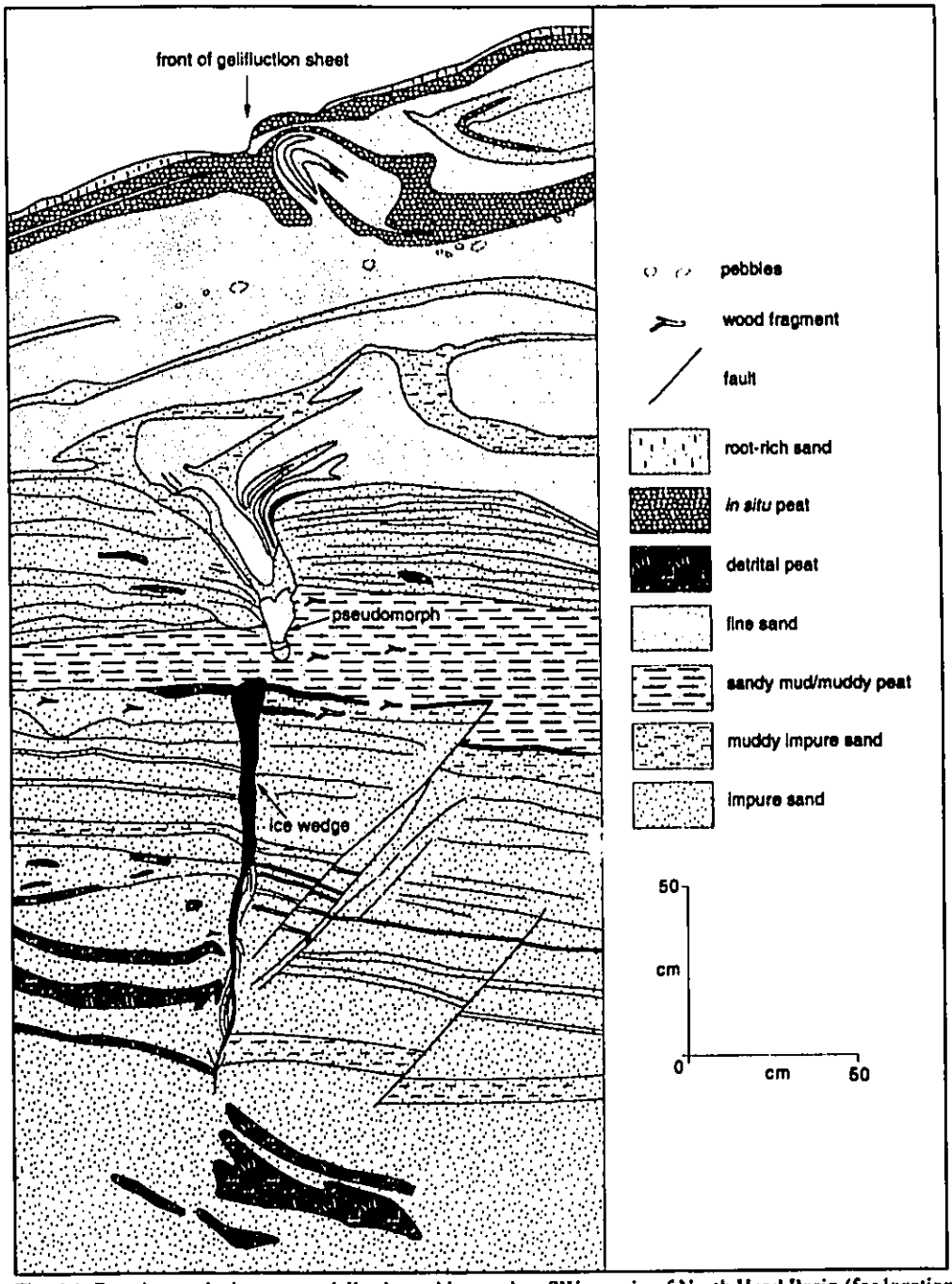

Fig. 6.1 Pseudomorph above a partially-thawed ice wedge, SW margin of North Head Basin (for location see Fig. 5.12A). The top of the ice wedge is **convex-up**. The faults adjacent to the wedge formed when underlying ice melted out during the deposition of the impure sand (cf. Fig. 5.4A). The peat associated with the gelifluction sheet has moved a short distance downslope. (June 20 1990)

the top of the wedge and the upper 40-50cm steeply dips upslope. The pseudomorph comprises fine sand and a small amount of slightly muddy sand. Thin beds of muddy sand immediately above and upslope of it are abruptly oriented downward into the pseudomorph and parallel its sides.

This pseudomorph likely formed by gradual subsidence as the top of the ice wedge melted slowly. Slow melting is indicated by the convex-up top of the wedge. Although convex-up tops form by both thaw and diapiric uplift (e.g. Mackay, 1976; 1990). In this example, however, thaw is the more likely as this wedge is of Holocene age and has probably been thaw-truncated only recently (cf. Katasonov and Ivanov, 1973, Fig. 11; Nekrasov and Gordeyev, 1973, Fig. 11). Convex-up thaw tops form because, other things being equal, thawing is faster in ice-poor materials than in those which are ice-rich. Slow subsidence coeval with thawing of the wedge is suggested by (1) the relatively unhomogenised material within the pseudomorph (contrast with Figs 6.2-6.4) and (2) the absence of a tunnel (or tunnel infill) above the wedge. The lack of faults in the downturned beds adjacent to the pseudomorph is more compatible with gradual subsidence than with rapid collapse into a void. This pseudomorph has been folded downslope by the overriding gelifluction sheet (cf. Gozdzik, 1967).

6.3.2 Thermal erosion

Pseudomorphs may also form when ice wedges are thermally eroded (e.g. Péwé et al., 1969). Three examples of pseudomorphs relating to thermal erosion are shown in Figs 6.2-6.4. All underlie ice-wedge troughs. The first is on Hendrickson Island (Figs 1.1 and 6.2), where many ice wedges penetrate fine sand (Toker Point glacifluvial outwash; Rampton, 1988, Fig. 56) and underlie fibric peat. At the S coastal bluff an ice wedge has melted completely, leaving a pseudomorph (Fig. 6.2A). But 3m inland the top of the wedge lies only 45cm beneath the trough floor; thus the thawed top of the wedge slopes seaward. The pseudomorph

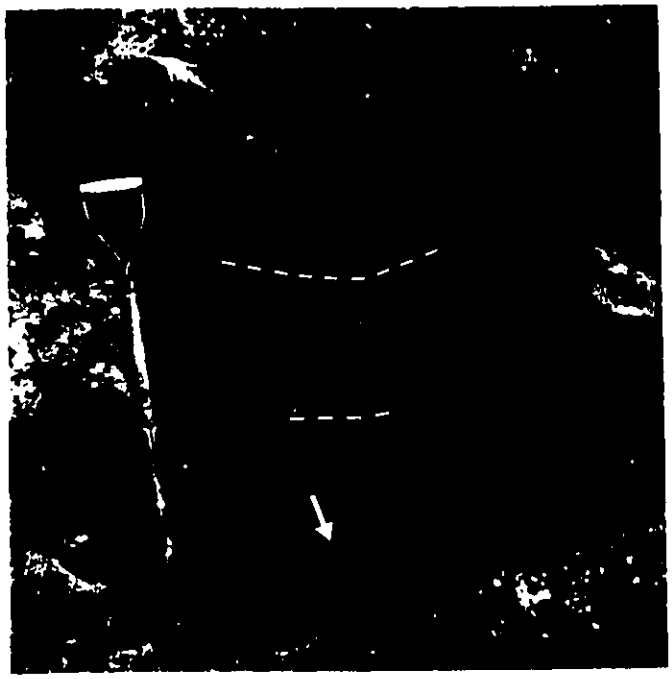

Fig. 6.2 **ICE-WEDGE PSEUDOMORPH**

(A) Ice-wedge pseudomorph in sand, Hendrickson Island. The pseudomorph has three parts: the lower comprises bedded and structureless peaty sand (see B), the middle is a **tunnel** (between dashed lines), and the upper comprises peat and vegetation. The sides of the pseudomorph are irregular - note the small, folded sand tongue (arrow). Shovel for scale.

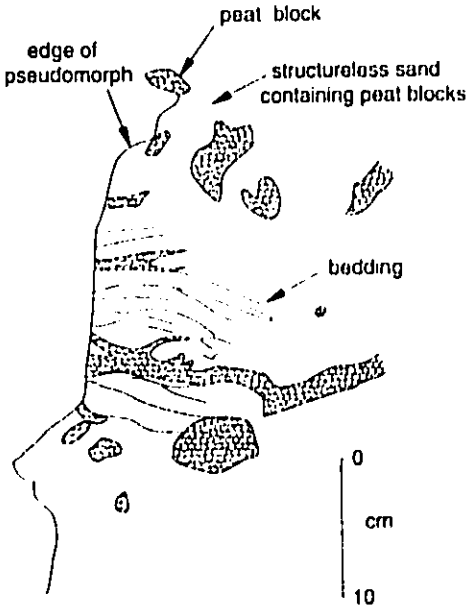

(B) Close-up of basal unit. This comprises **bedded** and **structureless sand** containing **peat blocks**. (Both August 4 1989)

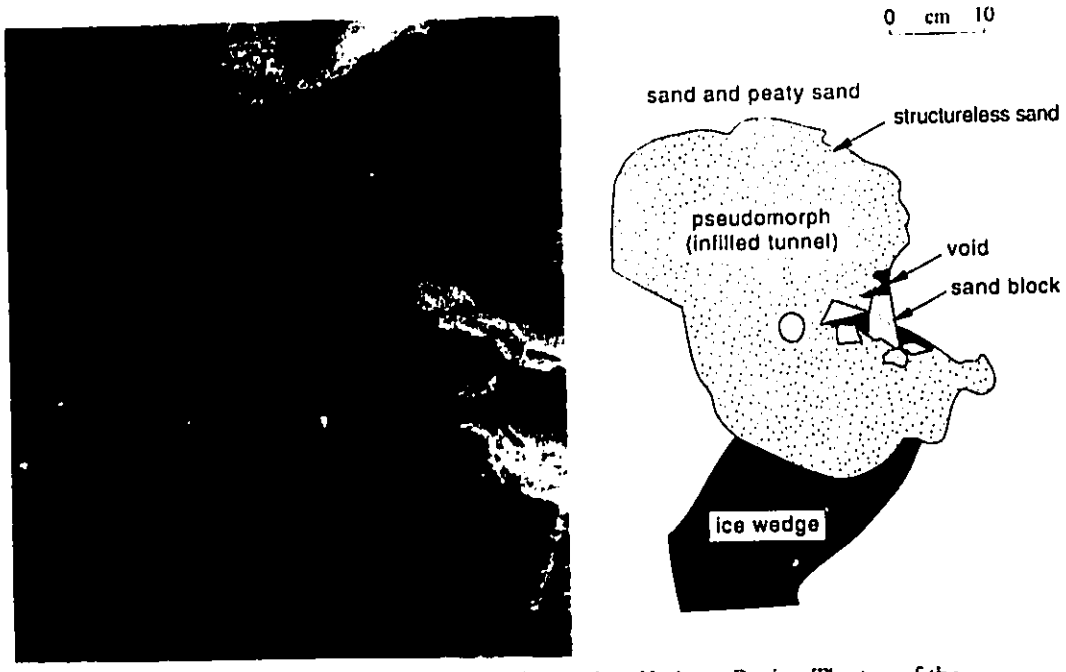

Fig. 6.3 Pseudomorph above a partially-thawed ice wedge, Hadwen Basin. The top of the wedge is **concave-up**. Above it a pseudomorph has formed by the infilling of a **tunnel**, of which all that remains are small **voids**. Some of these abut on locally derived **sand blocks**. (July 17 1991)

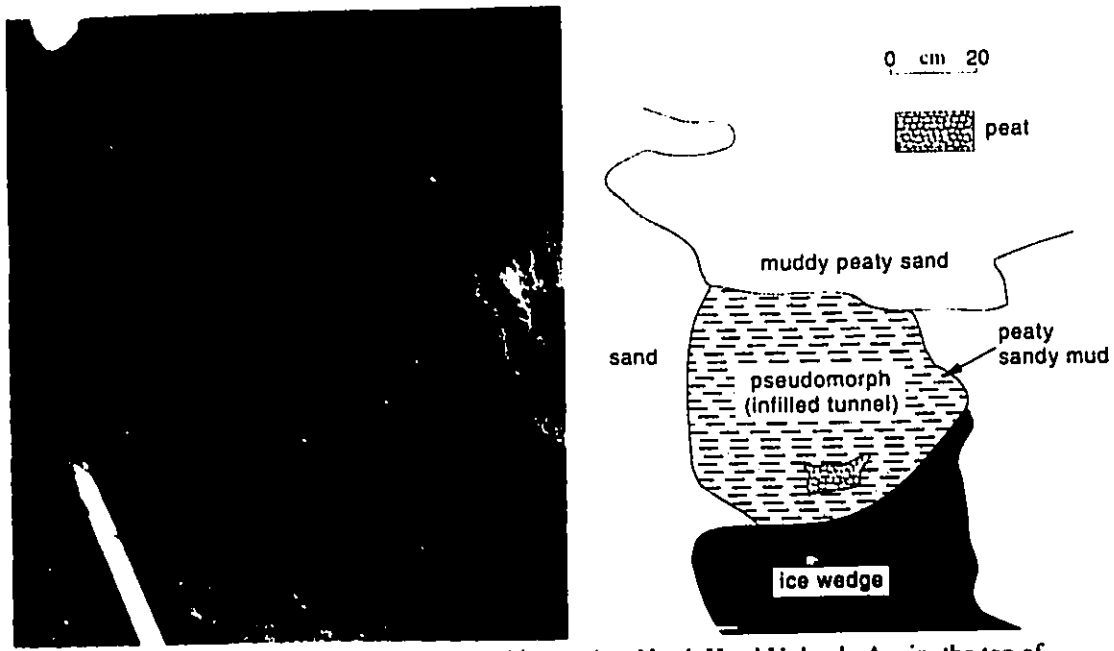

Fig. 6.4 Pseudomorph above a partially-thawed ice wedge, North Head Upland. Again, the top of the wedge is **concave-up**, and the overlying pseudomorph likely formed by the infilling of a **tunnel**. A single block of peat occurs near the base of the pseudomorph. (July 3 1989)

(c.120cm deep) is wedge-shaped, tapering downward from c.80-90cm to an acuminate, two-pronged toe (Fig. 6.2). Its sides are sharp and irregular. Internally it has three units. The lower (c.40-50cm thick) comprises structureless fine sand with dispersed peat blocks and includes a 15-20cm thick subunit of bedded peat and fine sand (Fig. 6.2B). The beds are horizontal/subhorizontal and parallel/subparallel, the sand beds (0.3-4cm thick) generally thicker than peat beds (2mm to c.2cm), which commonly bifurcate and curve (Fig. 6.2B). This bedded subunit also contains randomly dispersed peat blocks (1-7cm in maximum dimension; Fig. 6.2B). The middle part of the pseudomorph is a tunnel (40cm high and 40cm wide; Fig. 6.2A) extending inland for at least 50cm. The upper part comprises structureless fibric peat, sod and living *Betula nana* (Fig. 6.2A), all contiguous with the superficial organic layer. Left of the pseudomorph, bedding in the host sand is abruptly oriented downward (this is not clear in Fig. 6.2A).

The second example, in Hadwen Basin, shows an ice wedge, penetrating sand and peat, whose top is 25cm wide and gently concave-up (Fig. 6.3). The overlying pseudomorph is c.40cm deep and 19-33cm wide, its contacts sharp and curved to slightly irregular. It has a two-part filling. The lower infill comprises both interstitial sand and angular to subrounded blocks of peaty sand, some blocks buried, others forming an openwork breccia within a small cavity (Fig. 6.3). The upper infill comprises structureless, fine humic sand.

In the third example, from the steep icy bluff at North Head, an ice wedge penetrates fine sand and underlies a small pseudomorph. The wedge is 2.5m deep, tapering downward from c.60cm to bifurcate in two acuminate basal points (not shown). The top of the wedge is concave-up, underlying a pseudomorph of structureless peaty sandy mud which is 50-60cm deep and 50-60cm wide, its sides sharp and curved. Near the bottom of the pseudomorph is a single chunk of fibric peat (Fig. 6.4).

In all three examples the ice wedges were thermally eroded and the pseudomorphs formed by mass movement (fall and ?sand flows) and/or fluvial processes. Thermal erosion is indicated by the concave-up tops of the wedges. Two lines of evidence suggest that deposition occurred by fall. First, both the Hendrickson and Hadwen pseudomorphs contain voids (Figs 6.2 and 6.3). Representing tunnels, or collapsed tunnels, the voids formed as the wedges were thermally eroded underground (cf. Shumskii, 1959, p.45-46; Mackay, 1974b, Fig. 2; 1988). In the Hendrickson example the tunnel is well preserved due to (1) the binding effect of the overlying, root-laced fibric peat and (2) the shear strength of moist wall sand (cf. McKee and Bigarella, 1972). But in the Hadwen example the tunnel has been almost completely infilled, leaving only a small void and the faint outline of the former tunnel (Fig. 6.3). Although not even a small void remains at North Head, the cylindrical lower part of the pseudomorph likely represents a tunnel fill (Fig. 6.4). Second, near the base of all three pseudomorphs occur blocks of sand or peat (Figs 6.2-6.4) that must have fallen from the tunnel walls or roof, or that have been transported along the tunnel.

The only fully developed pseudomorph, that on Hendrickson Island, likely formed by a combination of fall, fluvial and/or debris-flow processes. Probably, during a warm summer (?1988 or 1989), water ponding above the ice wedge began to flow along the top of the wedge towards the coastal bluff, thermally eroding the wedge and forming a tunnel. The base of the tunnel was then infilled by sand and peat falling or being washed into it. Meanwhile, thaw of adjacent host sand triggered the collapse of small tongues of wall sand (Fig. 6.2A); hence the base of the pseudomorph does not match the shape of the ice-wedge toe. As thermal erosion progressed inland, meltwater and/or small sand flows deposited thin beds of sand (Fig. 6.2B). The irregular nature of the beds may reflect deposition by small sand (debris) flows (cf. Fig. 4.3A), individual flows later being veneered with peat falling from the tunnel roof or being washed along the tunnel; possibly, the beds record a (?diurnal) periodicity of melting. Then at

some stage, fluvial and/or sand-flow deposition at this section ended, perhaps because melt-water percolated into locally thawed sand or because the tunnel partially collapsed, covering the bedded unit with peat blocks and structureless sand (Fig. 6.2B). When the pseudomorph was examined the superficial organic layer was subsiding into the tunnel.

Neither of the other involutions developed into full pseudomorphs, because thermal erosion of the ice wedges ceased (cf. Soloviev, 1973, p.21). Subsequently, the tunnels were infilled with material falling from their walls and/or transported downtunnel, most likely by sediment gravity flows. This infilling is clearly shown by the Hadwen tunnel fill (Fig. 6.3), whose structureless upper part resembles the smaller and more rounded infilled burrows of *Spermophilous undulatus* (arctic ground squirrel; Fig. 5.13).

Sometimes it is difficult to interpret how thaw modification proceeds. For example at Crumbling Point, two large (≤80cm wide and ≥3.5m deep) ice wedges penetrating fine sand are thaw truncated 80-95cm below the ground surface, their tops planar to slightly convex-up (Fig. 6.5). The left-hand pseudomorph extends 50-60cm below the lower contact of the adjacent peaty soil (Fig. 6.5B), widening slightly (from 70cm to 90cm) towards the ground surface. Its sides are sharp and irregular, with a relief of several cm. The pseudomorph comprises structureless peaty diamicton above a basal peat-rich layer (10cm thick) similar to that at the base of the adjacent soil. At the bottom right of the pseudomorph is a tongue of structureless fine sand (Fig. 6.5B).

The origin of this pseudomorph is unclear. Although its peaty base must have been once contiguous with the basal peaty horizon of the soil (Fig. 6.5B), it is unclear if the pseudomorph formed by tunnel collapse, gradual subsidence or by a combination of both. However, it did form by linear thawing of an ice wedge, because the top of the wedge is below adjacent ground ice (not shown). The basal sand tongue (Fig. 6.5B) may represent wall sand that collapsed into a tunnel; equally, the planar to slightly convex-up top of the wedge may

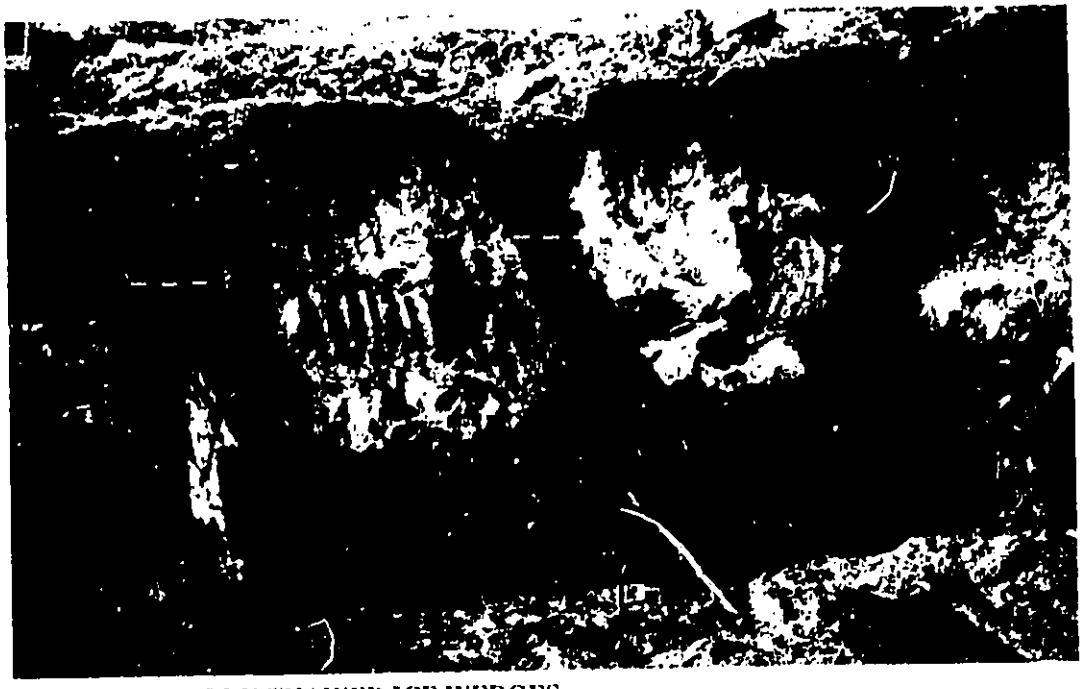

Fig. 6.5 **PARTIALLY THAWED ICE WEDGES**

(A) Two ice wedges in sand, Crumbling Point. The tops of both are **planar to slightly convex-up** (dashed lines; see B) and underlie pseudomorphs of peaty diamicton. Figure for scale.

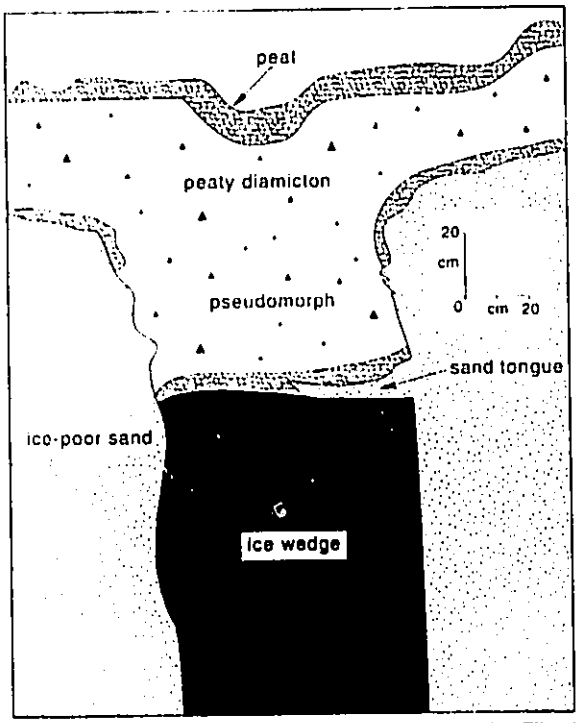

(B) Close-up of left hand wedge and overlying pseudomorph. The latter has irregular sides, a basal peaty layer, and a basal sand tongue. (Both June 29 1990)

have formed by meltwater seeping (as opposed to rapidly flowing along a tunnel) downslope through the basal part of the ice-wedge trough. If so, the overlying peat may have subsided as the ice wedge melted. In short, both mechanisms may have occurred.

6.3.3 Refreezing

Thaw modification of ice wedges may cease at any time due to water freezing in voids within or above ice wedges, forming thermokarst cave or pool ice (Shumskii, 1959, p.45-46; Harry, 1982, Figs 3.5 and 3.6; Mackay, 1988). An example from North Head shows the concave-up top of a large ice wedge (apparent width ≥2.25m) overlain by 2-35cm of icy muddy peat, above which occurs a large (0.34m thick and 2.8m long) ice lens (Fig. 6.6). The ice, mostly clear or bubble-rich, is yellow-brown in the centre.

This lens is pool ice formed above a thermally eroded ice wedge. Thermal erosion is indicated by the concave-up top of the wedge. The veneer of (icy) muddy peat was deposited on the floor of a tunnel by water flowing along the top of the wedge and/or from material falling from the tunnel roof. Just before refreezing, the tunnel was filled with water - a thermokarst pool. As the pool froze inwards and impurities were expelled ahead of the freezing plane, the centre of the pool ice became discoloured.

6.4 **Composite wedges**

Composite wedges of primary infilling contain both ice and non-ice material (cf. Berg and Black, 1966, p.75; Romanovskii, 1973, p. 266-269; Jahn, 1975, p.74-78). Two examples were examined on Hadwen Island. The first is associated with a two-part composite wedge that penetrates the layered cryofacies association (Fig. 6.7). The eastern half of the wedge is a sandy ice wedge, the western half an icy sand (to sand) wedge. The sandy ice wedge is 50-60cm thick, a typical section across it containing c.70 sand laminae. These are

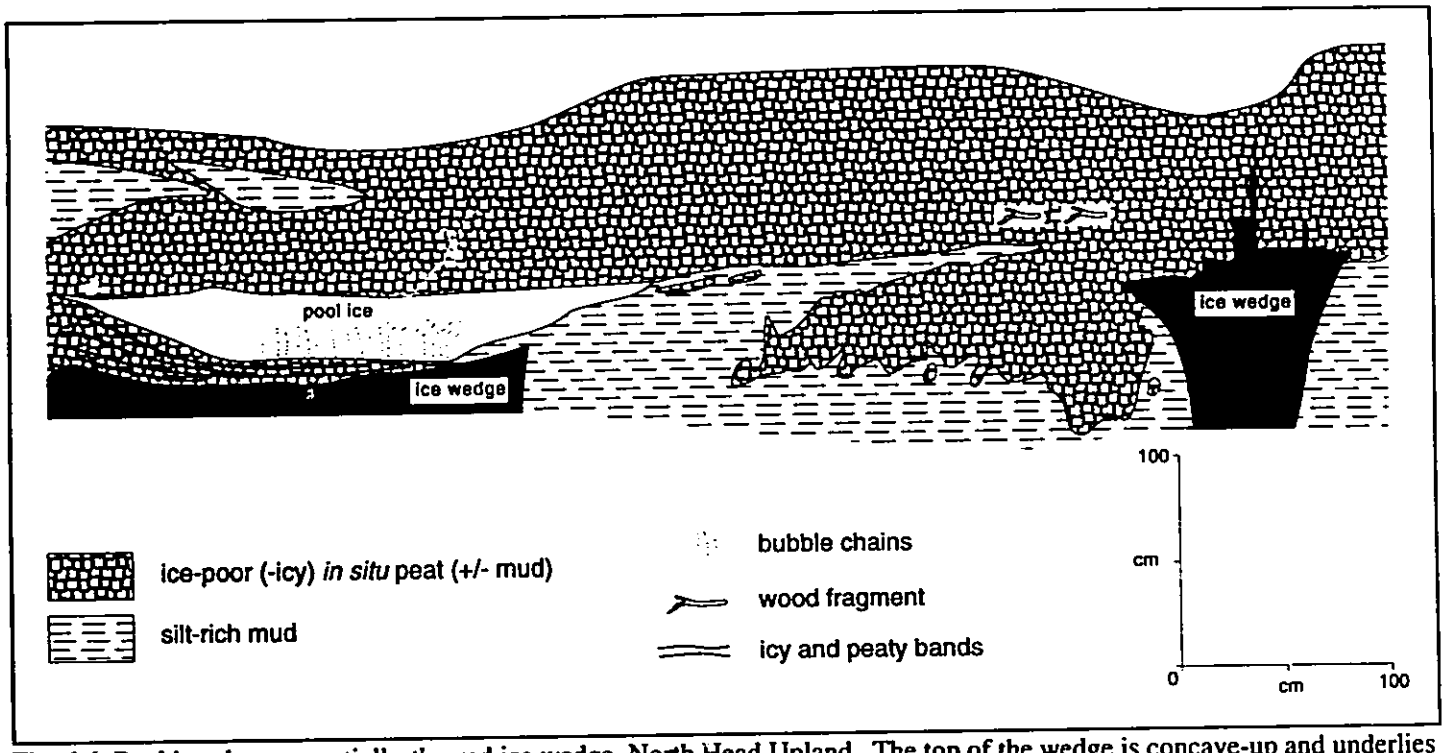

Fig. 6.6 Pool ice above a partially-thawed ice wedge, North Head Upland. The top of the wedge is concave-up and underlies icy muddy peat. The overlying ice lens (pool ice) contains bubble chains and has a yellow-brown central streak. Both the peat and the pool ice have infilled a tunnel that formed when the ice wedge was thermally eroded. Prior to freezing, the tunnel was filled with water - a thermokarst pool, at the bottom of which accumulated muddy peat. The pool later froze inwards, discolouring the centre of the resulting pool ice. (August 5 1991)

Fig. 6.7 **PARTIALLY THAWED COMPOSITE WEDGE**

(A) Above the ice-rich portion of composite wedge 1, Hadwen Island, **streaks of silty sand** (arrows) penetrate **structureless fine sand**. Conversely, above the sand-rich portion (on the right), faint, steeply dipping sand laminae (L) are preserved. The *pencil* marks the contact between the ice-rich and ice-poor portions of the wedge.

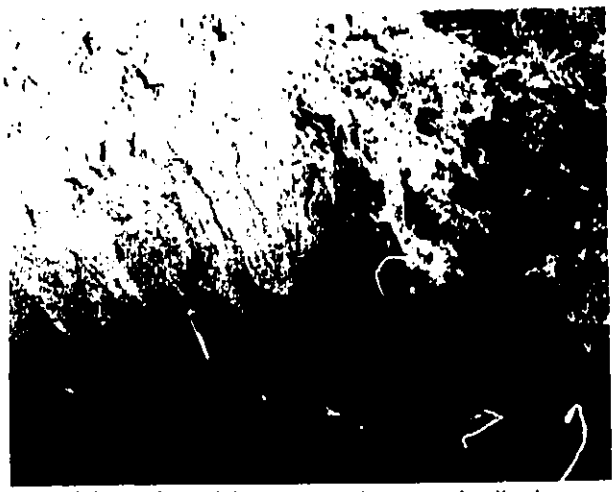

(B) Above the sand-rich portion of the same wedge, steeply dipping to vertical **sand laminae are well preserved**. The contact between the ice-rich and ice-poor portions forms a step in the bottom right. In both (A) and (B), the pencil marks the secondary thaw contact at the top (excavated) of the unthawed wedge. (Both July 17 1991)

0.5-20mm thick (generally ≤4mm) and 0.05-1+m long (generally 0.1-0.4m), many pinching, swelling and bifurcating. They comprise slightly silty fine sand, and some contain occasional small pebbles whose long axes parallel the laminae. Within the intervening ice laminae are numerous suspended sand grains. The overall volumetric sand content of the sandy ice wedge is c.10-15%. The western half of the wedge is almost the inverse of the left, with ice laminae in sand. But the ice laminae are few (at most 16 in any one section) and their number varies significantly over a lateral distance of a few m, such that the northern part is strictly a sand wedge (Fig. 6.7B). At a depth of c.1m the composite wedge is truncated by a planar secondary thaw contact (Fig. 6.7). Above this, on the sandy side of the wedge, steeply dipping to vertical sand laminae are poorly (Fig. 6.7A) to well preserved (Fig. 6.7B). But above the icy half they have been destroyed, leaving a pseudomorph comprising irregular streaks of silty fine sand within structureless fine sand (Fig. 6.7A).

The second example, penetrating Kittigazuit sand, also has distinct sand- and ice-rich parts (Figs 6.8 and 6.9). Its top is thaw truncated 3.7m below the ground surface. As before, vertical sand laminae are preserved only above the sand-rich part of the wedge. Above the ice-rich part, structureless sand contains vertical streaks of pebbly muddy sand (Fig. 6.8).

The degree of thaw modification of these composite wedges depends on their iciness (cf. Romanovskii, 1973, p.269). Above ice-poor parts, primary sedimentary structures (sand laminae) are poorly to well preserved (Figs 6.7B and 6.8); above the ice-rich parts they have been destroyed, leaving structureless sand containing irregular streaks of silty fine sand (Figs 6.7A) or vertical tongues of pebbly muddy sand (Fig. 6.8). While the silty sand obviously melted out of the sandy ice wedge, how exactly the streaks formed is unclear; possibly, they relate to water-escape. The vertical tongues of pebbly muddy sand likely formed by subsidence, as the underlying sandy ice wedge melted.

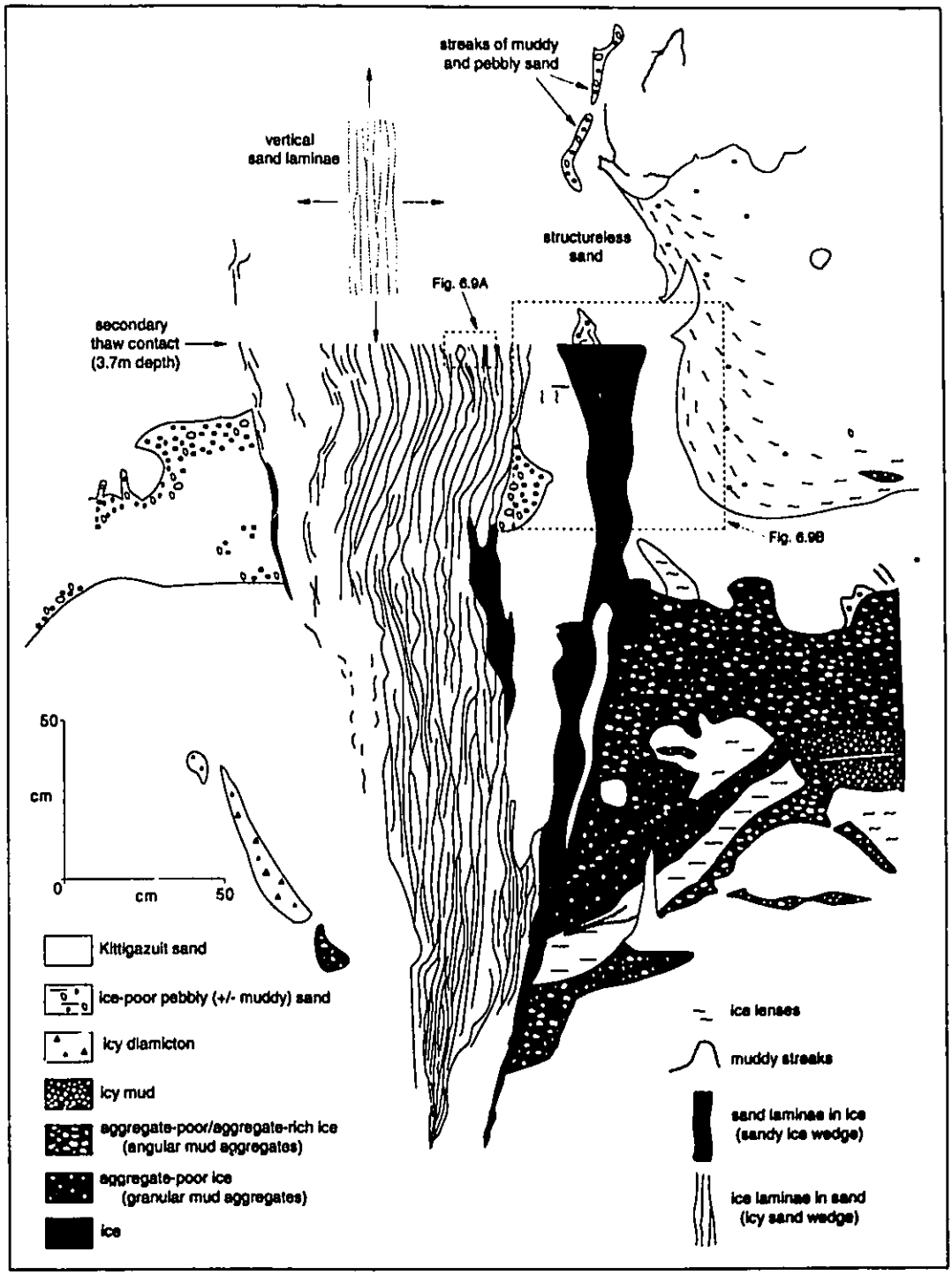

Fig. 6.8 Partially thawed composite wedge 2, in (ice-poor) Kittigazuit sand, Hadwen Island. It comprises an **icy sand wedge** (left) and a **sandy ice wedge** (right). At a depth of 3.7m, ice laminae are truncated along a **planar horizontal contact** (Late Wisconsinan-early Holocene secondary thaw contact; see Fig. 6.9A). Where this contact truncates the icy sand wedge, vertical sand laminae are preserved above it; but where it truncates the sandy ice wedge, they are not preserved. Instead, the overlying sand is structureless, containing streaks of muddy and pebbly sand. (July 9 1991)

Fig. 6.9 **PARTIALLY THAWED COMPOSITE WEDGE**

(A) Close-up of the **secondary thaw contact** (arrows) above the icy sand-wedge portion of composite wedge 2 (see Fig. 6.8 for location), Hadwen Island. The **contact truncates ice laminae** (dark grey; thermal contraction cracks infilled with ice). But steeply dipping to vertical **sand laminae are preserved above it** (they are not clear in the photo because the sand is moist and the section was scraped to the frost table). 3cm pencil tip for scale.

(B) Sandy ice-wedge portion of composite wedge 2 (see Fig. 6.8). The sand above the secondary thaw contact (at bottom of pencil) is **structureless**. (Both July 9 1991)

6.5 Sand wedges

A priori, thaw modification of sand wedges would seem slight (e.g. Gozdzik, 1973; Jahn, 1975, p. 60-63). While this may indeed be true in areas of ice-poor permafrost, in the ice-rich Tuktoyaktuk Coastlands this generalisation applies only locally. Here the degree of thaw modification depends on the nature of host sediment and slope angle. Three types of thaw modification may be distinguished.

6.5.1 Preservation

In certain flat areas, sand wedges penetrating ice-poor sand are well preserved. One example, beneath a drained thermokarst basin on N Hadwen Island, contains numerous vertical/subvertical sand laminae (Fig. 6.10). The beds adjacent to the wedge are upturned. Although there is no obvious secondary thaw contact, the top of the wedge must have thawed, since it is truncated by a sublacustrine unconformity and overlain by lacustrine sediments (impure sand; Section 5.3.4). Thus the top of the wedge must once have been within a sublacustrine talik or active layer. However, because of the host material is ice-poor, thaw modification has been negligible.

6.5.2 Loading, buoyancy and spreading

In flat areas where sand wedges penetrate the (ice-rich) layered cryofacies association, wedges whose sides extend above the Late Wisconsinan-early Holocene secondary thaw contact are locally deformed (Fig. 6.11). The style of deformation (load, flame and diapiric structures) resembles that which characterises the sand and diamicton cryofacies association (Sections 3.3.2.3 and 7.2). But in addition the tops of some wedges appear to have sagged and laterally spread. Deformation likely coincided with the formation of thermokarst involutions (Chapter 7), occurring by loading, buoyancy (Section 7.2) and the lateral spreading

PARTIALLY THAWED SAND WEDGES

Fig. 6.10 Sand wedge in ice-poor Kittigazuit sand, Hadwen Island. Its **sand laminae are perfectly preserved.** The top of the wedge is truncated by a sublacustrine unconformity (arrows) and overlain by lacustrine sediments (peat-rich impure sand; section S 3.4). Figure for scale. (July 18 1991)

Fig. 6.11 Sand wedge penetrating both the layered (L) and the sand and diamicton (D) cryofacies associations, Crumbling Point. Above the late Wisconsinan-early Holocene secondary thaw contact (dashed line), the wedge has **deformed sides** (arrows). But within it, vertical **sand laminae are well preserved.** Figure for scale. (June 7 1991)

of sand in saturated melt-out diamicton. Subsequently, the deformed tops of wedges have partially refrozen.

6.5.3 Folding, shearing and mass movement

Sand wedges which cross inclined secondary thaw contacts are commonly folded, sheared and/or truncated. For example, at Mason Bay the upper 10-15cm of an acuminate sand-wedge toe (60cm high) curves downslope immediately above a secondary thaw contact (Fig. 6.12A), vertical/subvertical sand laminae within the wedge doing likewise. Downslope of the toe the secondary thaw contact is paralleled by elongate sand lenses in the overlying sandy diamicton (Section 4.3.1). In another example, from Green Lake, the folded toe continues for at least 4m downslope of the *in situ* toe (Fig. 6.12B), forming a large, subhorizontal sand lens that is distally streaked. Within the lens, sand laminae run parallel to its upper and lower contacts.

The sand lenses and folded sand-wedge toes at Mason Bay and Green Lake formed by folding and shearing of thawed sand-wedge sand as overlying material moved downslope. Elongate sand lenses close to the secondary thaw contacts indicate that this movement involved basal shearing - a plug-like movement (cf. Mackay, 1981). Assuming that the orientation of ice lenses above the secondary thaw contact partially reflects stresses within the moving layer, then their upward flattening (until they parallel the underlying thaw contact; Fig. 6.12A) suggests that the zone of most intense shearing overlies the contact by at least 15cm. Where shearing is accompanied by subslump melting, a process that replenishes the supply of sand-wedge sand to the moving layer, sheared sand-wedge toes may remain connected with their parent *in situ* toes (Fig. 6.12B). But in the absence of subslump melting, shearing may completely truncate the toes (see left-hand toe in Fig. 6.13A).

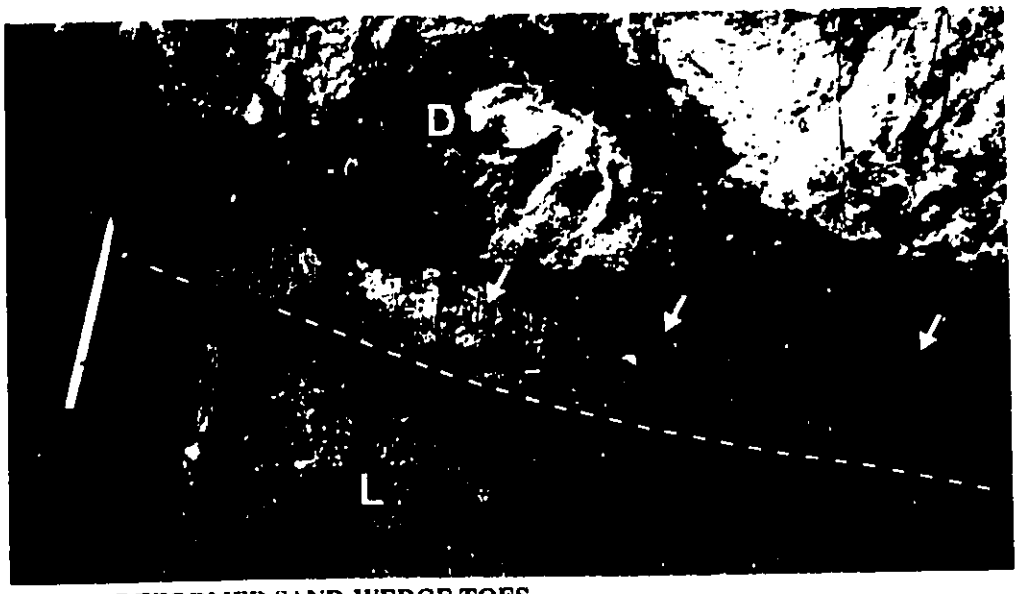

Fig. 6.12 **DEFORMED SAND-WEDGE TOES**

(A) **Folded sand-wedge toe** in the layered cryofacies association (L) , Mason Bay. Only that part of the toe above the secondary thaw contact (dashed line) is folded (downslump). Just above the contact, a **lenticular cryostructure** comprises steeply dipping ice lenses that flatten upwards until they parallel both the contact and the **sand lenses** (arrows) in the overlying sandy diamicton (D). The lenses formed by shearing of sand-wedge sand (section 4.3.1). 50cm high ice axe for scale. (June 25 1991)

(B) **Folded and sheared sand-wedge toe.** Green Lake, Summer Island. Downslope (to right) of the *in situ* toe and just above the secondary thaw contact (dashed line), there is a layer of diamicton (arrow) that thickens downslope and is devoid of organic material. This layer formed by **subslump melt-out** after the wedge had begun to be folded and sheared. Figure for scale. (August 24 1991)

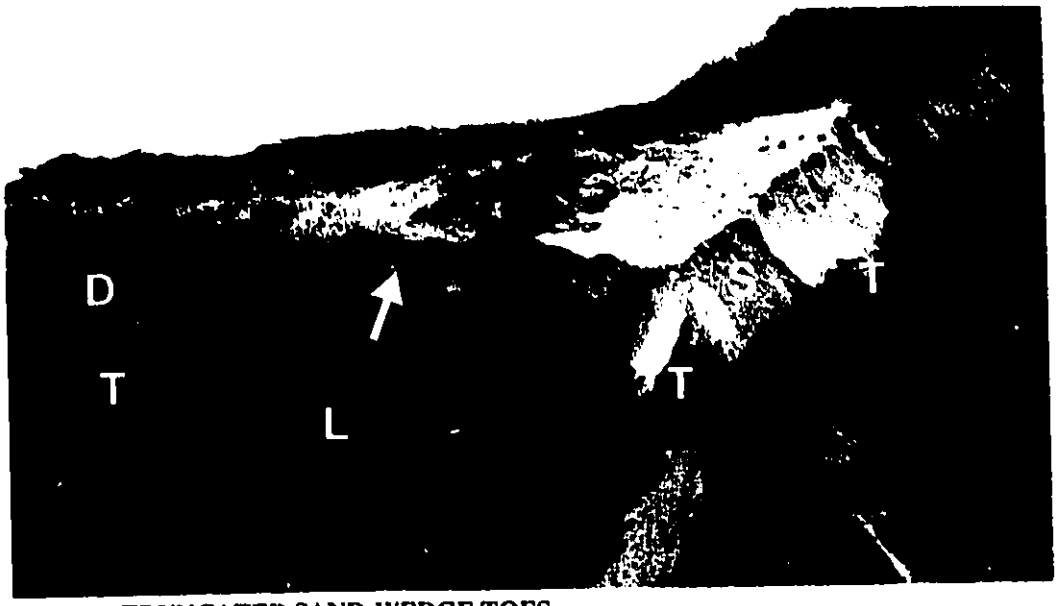

Fig. 6.13 **TRUNCATED SAND-WEDGE TOES**

(A) Three truncated sand-wedge toes (T) in the layered cryofacies association (L), Crumbling Point. The left-hand toe underlies organic-rich diamicton (D), indicating that the top of this wedge was eroded and transported downslump. The toes in the middle and on the right underlie structureless sand (S) eroded from another wedge upslump. Headwall on left is 3m high. (July 10 1990)

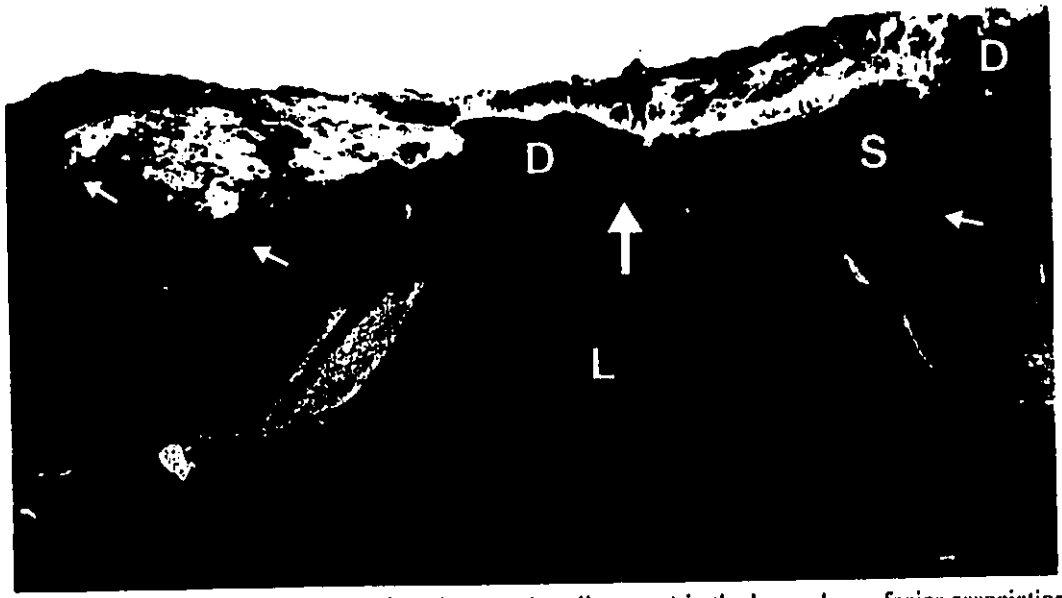

(B) Three truncated sand-wedge toes (small arrows) in the layered cryofacies association (L), Crumbling Point. Structureless sand (S) derived from the wedge in the upper left forms a sand apron above the two lower toes. In both (A)and (B), **abrupt lateral (+/- vertical) facies changes** (large arrows) occur between structureless sand and organic-rich (-sandy) diamicton (D). Figure for scale. (September 2 1991)

Sand-wedge toes are also commonly truncated. At Crumbling Point such truncation is obvious where they sharply underlie organic-rich diamicton (Fig. 6.13A). But where they underlie fine sand (Fig. 6.13) the only difference between the sand within the *in situ* toe and that above it is that the latter is structureless, sometimes containing blocks of peat and sod. Truncation and burial occur by mass movement associated with retrogressive thaw slumping. For example, sand derived upslope from thawing sand wedges falls, flows and/or slides downslope to bury (beneath aprons of structureless sand) sand-wedge toes truncated by mass movement in slump floors. This is illustrated by the upper left-hand wedge in Fig. 6.13B. The same process occurred in the two lower toes, only to a greater extent, leaving small truncated toes that have been buried by sand derived both from the eroded upper part of these wedges and from the wedge upslope (again, the upper left-hand wedge in Fig. 6.13B).

6.6 Conclusions

From these partially thawed wedges and their associated pseudomorphs several conclusions are drawn. First, the direction of thaw varies: many wedges thaw downwards, those on exposed bluffs also thaw inwards (Fig. 6.2) and thermally eroded ice wedges may thaw radially outwards, forming tunnels (Fig.6.2; cf. Mackay, 1974b, Fig.2; also, personal communication, July 1991). Second, as ice-rich wedges melt, resedimentation within them may involve both vertical and lateral sediment movements, the latter being important in the infilling of tunnels (Fig. 6.2). Third, tunnels may be infilled with ice (Fig. 6.6), peat (Fig. 6.2A) and/or clastic sediment (Fig. 6.2A). Fourth, thaw modification is commonly partial and/or incremental.

Thaw modification of frost-fissure wedges is strongly controlled by slope angle and substrate. Pseudomorphs overlying dipping secondary thaw contacts are deformed or truncated by mass movement. Substrate control reflects both the grain size of non-ice material

and the volumetric ice content of material within and adjacent to wedges. Wherever the volumetric ice content of wedges and their host materials contrasts significantly the wedges can be thaw-modified substantially. While modification is unusual with thawing sand wedges, occurring only where they penetrate ice-rich material (Fig. 6.11), it is inevitable with thawing ice wedges. However, ice-wedge pseudomorphs (e.g. Vandenberghe, 1983a; French and Gozdzik, 1988) develop only where the ice content of the host is low, a fact doubtless explaining why the author observed them only in ice-poor sand. But in the Tuktoyaktuk Coastlands, as in many other areas of permafrost, such pseudomorphs are unrepresentative of most ice wedges, these wedges tending to be larger and more common in muddy sediments than in sand or gravel (cf. Romanovskii, 1985). Because the author studied thermokarst sedimentology in both mud- and sand-rich areas, the apparent preservational bias towards ice-wedge pseudomorphs in sand is believed to be a real one (cf. Black, 1976; Harry and Gozdzik, 1988), a bias reflecting greater thaw modification of ice wedges in muddy sediments. Typically more ice-rich than sand and gravel, fine-grained sediments (loess excluded; Jahn, 1975, p.72) deform more upon thawing, and so are less likely to preserve pseudomorphs.

Chapter 7 THERMOKARST INVOLUTIONS

"Unfortunately we have hardly any information on the kind of [sedimentological] disturbances that are the result of the thaw of permafrost (thermokarst)." (Maarleveld. 1981)

7.1 Introduction

In mid-latitudes which experienced Pleistocene periglaciation, unconsolidated sediments are commonly deformed. The deformation structures are termed in the European literature 'Brodelboden' or 'cryoturbations' (e.g. Edelmann et al., 1936; Troll, 1944), and in the American 'involutions' (e.g. Denny, 1936; Sharp, 1942). The structures are commonly interpreted in terms of Pleistocene frost action, soft-sediment deformation or a combination of both (e.g. Jahn, 1975, p.132-140; French, 1976, p.42, 227-229; Washburn, 1980a, p.96-102, 170-173; Vandenberghe, 1988). However, their precise origin is difficult to establish, because many of the structures appear to be azonal and polygenetic (e.g. Mills, 1983). Furthermore, while there are relatively few descriptions of such deformation structures from modern permafrost environments (e.g. French, 1986), it is to these areas that the Pleistocene structures are frequently referred.

This chapter offers potential analogues for some Pleistocene deformation structures. Specifically, it has three objectives: (1) to describe and interpret soft-sediment deformation structures here termed **thermokarst involutions**; 2) to infer their formative conditions and (3) to consider their Pleistocene significance.

7.1.1 The nature of thermokarst involutions

The descriptive term "involution" encompasses a wide variety of generally small deformation structures in earth materials. Many involutions could equally be called soft-

sedimentary deformation structures (see e.g. Allen, 1982, p.343-393; Mills, 1983; Van Loon and Brodzikowski, 1987). Involutions which develop by freezing-related processes have been termed **periglacial involutions** (French, 1976, p.42). To distinguish them from involutions formed as a direct consequence of thermokarst, the latter are here termed **thermokarst involutions.** These are soft-sediment deformation structures that form primarily by either loading and buoyancy or by water-escape during thermokarst (French, 1979; Vandenberghe and Broek, 1982; Vandenberghe, 1988).

Two categories of thermokarst involutions are distinguished: (1) loading and buoyancy structures and (2) water-escape structures.

7.2 Loading and buoyancy structures

Loading and buoyancy structures are common above secondary thaw contacts relating to areal thermokarst, thaw slumping and melting ice wedges. Most occur in the sand and diamicton cryofacies association at Crumbling Point, Mason Bay and Hadwen Island (Section 3.3.2.3). They comprise load casts, pseudo-nodules, ball-and-pillow structures and diapirs.

Load casts occur where the sand veneer caps melt-out diamicton (Figs 3.4 and 7.1). Comprising fine sand, they vary from a few cm to c.90cm in width and from a few cm to a few dm in depth. Their bottoms are flat to broadly concave-up. Pseudo-nodules and ball-and-pillow structures of sand are suspended in melt-out diamicton (Figs 7.2-7.3). They vary in height and width from a few cm to several dm. Pseudo-nodules are rarer, comprising rounded and slightly elongate sand masses with flat to concave-up bottoms which form laterally extensive rows (Fig. 7.2). Ball-and-pillow structures are much more variable in shape (Figs 3.1 and 7.3); some form pipe-like necks to underlying sand masses (Fig. 7.3B). Their bottoms may be flat, concave-up, acuminate or irregular. Diapirs of melt-out diamicton vary from vertical and symmetrical structures (Fig. 7.4B) to moderately inclined and asymmetrical

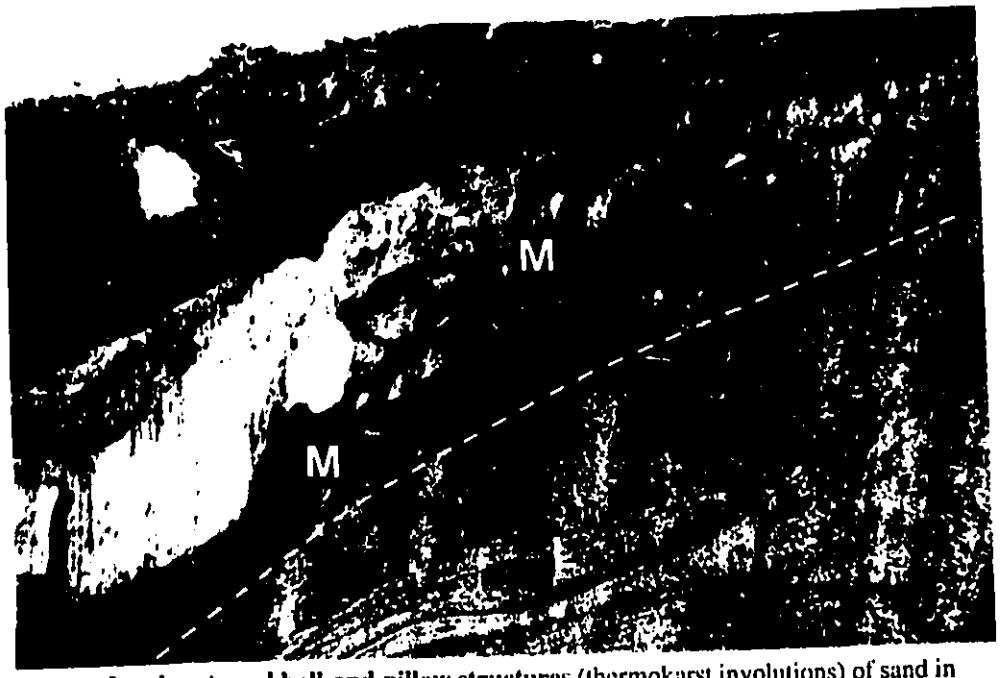

Fig. 7.1 **Load casts and ball-and-pillow structures** (thermokarst involutions) of sand in melt-out diamicton (M), Crumbling Point. The bottoms of the involutions are flat to concave-up, and none coincide with the Late Wisconsinan-early Holocene secondary thaw contact (dashed line). At this location the thaw contact rises, probably due to local thinning of the overburden and consequent arching of the layered cryofacies association (L; cf. Mackay, 1989, Fig. 5). Section is 3m high. (June 12 1991)

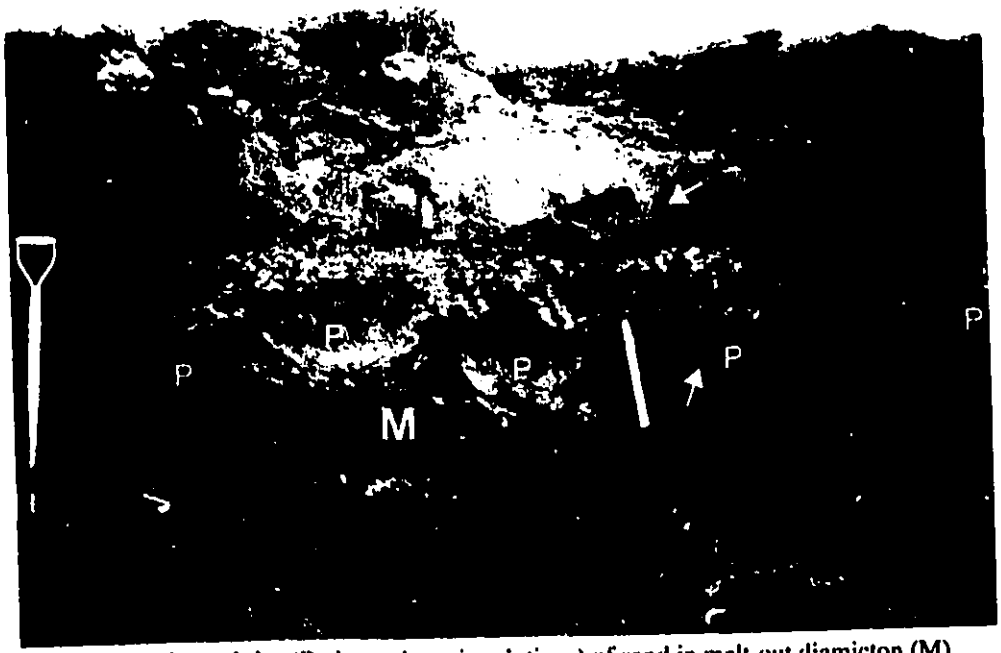

Fig. 7.2 **Pseudo-nodules** (P; thermokarst involutions) of sand in melt-out diamicton (M), Crumbling Point. The diamicton underlies the aeolian sand veneer (V). Flame structures (arrows) penetrate the veneer as well as some pseudo-nodules. 50cm high ice axe for scale. (September 5 1991)

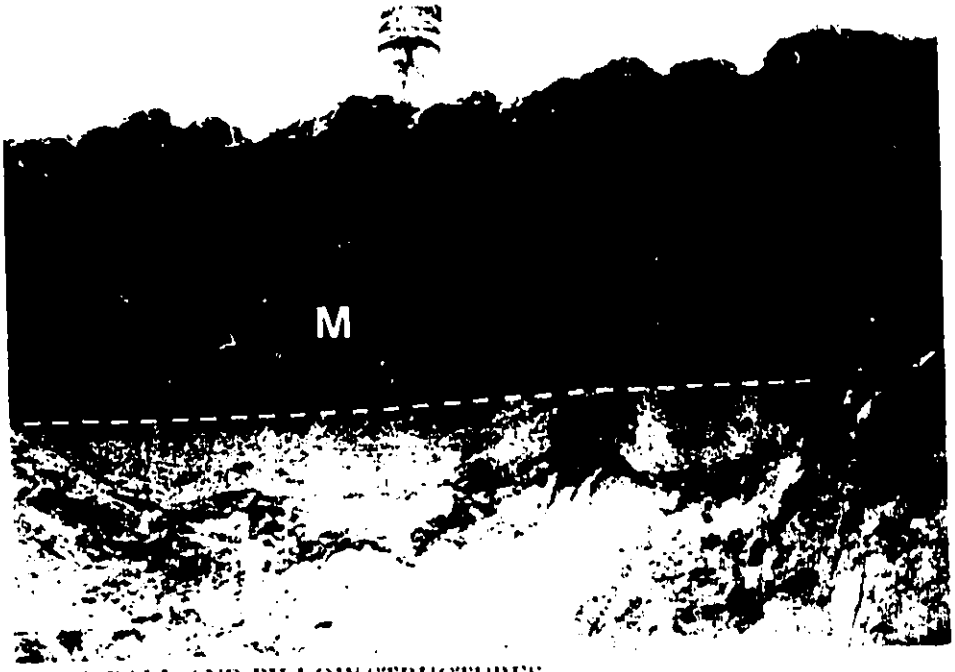

Fig. 7.3 **BALL-AND-PILLOW STRUCTURES**

(A) Sand ball-and-pillow structures (thermokarst involutions) in melt out diamicton (M) above the layered cryofacies association (L), Crumbling Point. These structures are of **variable size, shape, depth and spacing.** None of their bottoms coincide with the underlying late Wisconsinan-early Holocene secondary thaw contact (dashed line). Figure for scale.

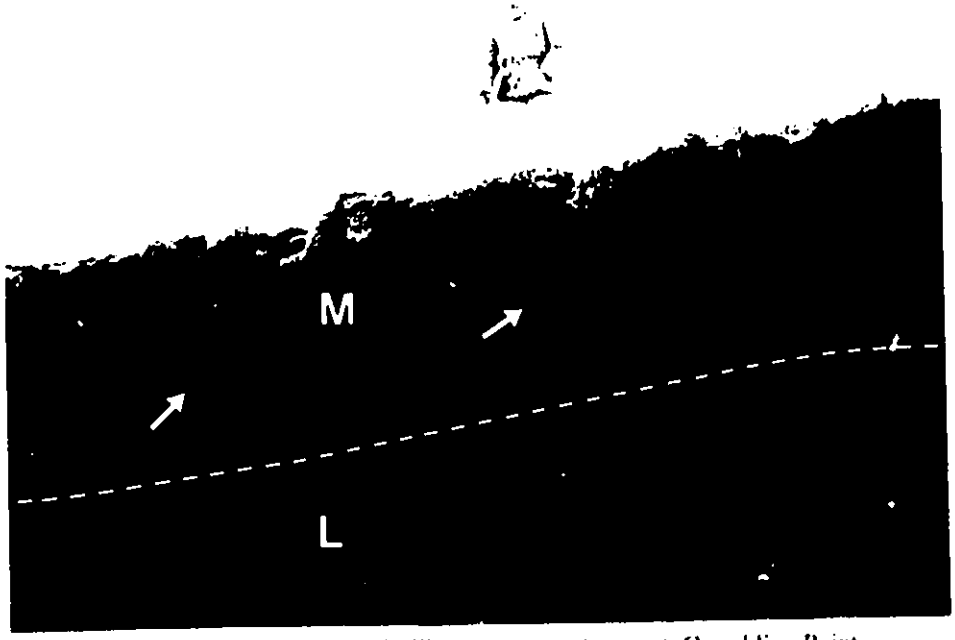

(B) **Pipe-like** sand ball-and-pillow structures (arrows), Crumbling Point. Melt-out diamicton (M) overlies the layered cryofacies association (L), the two being separated by the late Wisconsinan-early Holocene secondary thaw contact (dashed line). Figure for scale. (Both June 15 1991)

Fig. 7.4 **DIAPIRS**
Diapirs (thermokarst involutions) of melt-out diamicton in sand, Crumbling Point.
(A) Bifurcating **flame structure**. Figure for scale. (June 1 1991)

(B) **Round-topped diapirs** (R; thermokarst involutions), some of which are contiguous with underlying melt-out diamicton (M) above the secondary thaw contact (dashed line). L denotes the layered cryofacies association. 2m high section. (June 4 1991)

ones that bifurcate (Fig. 7.4A). Their tops may be rounded or acuminate (i.e. flame structures). Diapirs range in height from a few cm to c.1.4m and in width from a few mm to c.70cm. Some are contiguous with underlying melt-out diamicton; others are isolated in sand.

Some general characteristics typify these involutions. First, the bottoms of very few, if any, terminate at the secondary thaw contact, most ending 0.1-1m above it (Figs 7.1-7.4). Second, the bottoms of most adjacent involutions are at dissimilar stratigraphic depths (Fig. 7.2). Third, the size, spacing and number of adjacent involutions varies considerably over lateral distances of a few da m. Fourth, the local thickness (≤c.2.5m) of the sand and diamicton unit always exceeds the maximum height (≤c.1.4m) of the involutions within it. Fifth, involutions are absent where the thickness of sand above the layered cryofacies association exceeds c.2.5m (Fig. 3.4).

The involutions likely formed as underlying ice melted within a deepening thaw layer (cf. French, 1979). Melting is indicated by the underlying secondary thaw contact (Section 3.3.2.2) and by the flow-like nature of the involutions and the high yield strengths of the now-frozen base of the sand and diamicton horizon, features which indicate that deformation occurred when these facies were unfrozen. The water source was probably dominated by meltwater from the underlying icy materials. The meltwater mixed with Late Wisconsinan-early Holocene atmospheric water, as indicated by an average $\delta^{18}O$ value of -24.73‰ SMOW (n=4; σ=1.55‰) for ground ice from between the thaw contact and the base of the modern active layer. Assuming a $\delta^{18}O$ value of c.-14.0‰ to -16.0‰ for Late Wisconsinan-early Holocene atmospheric water (cf. Michel and Fritz, 1982; F.A.Michel, personal communication, May 1992), the above value of -24.73‰ is much closer to that of the underlying layered association (-29.95‰) than to Late Wisconsinan-early Holocene water. Furthermore, the degree of meltwater domination increased with depth, as indicated by $\delta^{18}O$ values of -26.27‰ and -26.30‰ from ice immediately overlying the secondary thaw contact

(Fig. 2.8; cf. "aggradational ice" of Mackay, 1983). This is to be expected since the basal ice is closer to the meltwater source.

The involutions formed by loading and buoyancy in a gravitationally unstable system. Sand with a higher bulk density sank into muddy diamicton of lower density, forming load casts, pseudo-nodules and ball-and-pillow structures (cf. Kelling and Walton, 1957; Kuenen, 1958; Butrym et al., 1964; Anketell, et al., 1970; Allen, 1982, p.354-364), and diamicton ascended into sand, forming diapirs (cf. Anketell, et al., 1970; Allen, 1982, p.355-357). Although the bulk densities at the time of deformation are unknown, modern field measurements indicate that the sand bulk density exceeds that of the diamicton by c.5%. This would generate deformation by loading and buoyancy, providing the underlying muddy diamicton were liquidized (cf. Allen, 1982, p.357, 363). Liquidization was probably caused by increasing pore-water pressure (e.g. Allen, 1985, p.185-186), as meltwater was generated faster than it could drain (cf. Morgenstern and Nixon, 1971). Poor drainage is indicated by the abundance of fine-grained melt-out diamicton and the almost flat secondary thaw contact. The pipe-like nature of some thermokarst involutions indicates that some of the overlying sand liquefied during deformation (Fig. 7.3B; see Anketell, et al., 1970).

Buoyancy structures also occur in slump-floor deposits (Figs 4.9; Section 4.3.5), but differ from the above examples in that many flame structures dip upslump, because of shearing as material moves downslump (cf. Fig. 7.5; Section 6.5.3; cf. Anketell et al., 1970). Finally, load structures are also associated with partially thawed ice wedges (Section 6.3).

7.3 Water-escape structures

Above a slump-floor secondary thaw contact at Crumbling Point, Late Wisconsinan-early Holocene slump-floor deposits contain water-escape structures (Figs 4.10 and 7.5). The structures comprise alternating streaks of fine sand and muddy sand to sandy mud (Fig. 7.5). The streaks are vertical to subvertical, varying in width from a few mm to c.10+cm and in length from several cm to c.1.2+m. Most gradually taper upward to points, although one with a rounded top underlies the core of a small anticline (Fig. 7.5B). The muddy streaks are contiguous with a basal (melt-out) diamicton above the thaw contact. The sand streaks occur locally, where structureless or well-stratified sand is interspersed with diamicton. In well-stratified sand, the sand streaks truncate bedding.

Several lines of evidence suggest that many of the streaks are fluidisation channels formed by upward water-escape. First, the colour contrast between the (yellow to pale grey) sand streaks and the (olive grey) well-stratified sand is explained most simply by elutriation of mud from sand (e.g. Lowe, 1975). Second, the upward-tapering muddy streaks likely formed by longitudinal vortices in rapidly ascending water. Third, vertically to subvertically oriented streaks would be expected during fluidisation of superficial sediments, because such sediments would dilate most easily upwards; hence the streaks may be free-surface pillars (see Lowe, 1975, Figs 4c and 9). Fourth, the localised distribution of streaks probably reflects the heterogeneous nature of the slump-floor sediments: cohesive masses of muddy peat and diamicton would have precluded fluidisation of the underlying sand, accounting for the absence of streaks beneath diamicton units. Fluidisation would have been restricted to areas of non-cohesive or poorly cohesive sand (e.g. Lowe, 1975; Allen, 1982, p.344). Likewise, where streaks are common, only some reach the surface of the bed, probably reflecting small-scale variations in cohesiveness or permeability. For example, the small anticline above the round-

Fig. 7.5 **FLUIDISATION CHANNELS**

Fluidisation channels (thermokarst involutions) in slump-floor deposits, Slump Basin, Crumbling Point (see Fig. 4.10 for location).

(A) Above the layered cryofacies association (L) a slump-floor secondary thaw contact (dashed line) gently dips towards the basin centre (to left). Above the contact is a thin (≤c.30cm) unit of melt-out diamicton (M) underlying a sand-rich unit (c.2m thick) that comprises well-stratified facies (W) interspersed with diamicton (D) and peat bodies (P). To the right of the ice wedge, steeply dipping to vertical **streaks** (arrows) **occur locally**. Figure for scale.

(B) Close-up of streaks (for location see (A) and Fig. 4.10). Upward-tapering, dark grey, muddy streaks (arrows) are contiguous with a layer of melt-out diamicton (M) above the thaw contact (dashed line). They alternate with yellow to pale grey streaks of fine sand. One round-topped sand streak (S) underlies the core of a small anticline (C). **Beneath diamicton bodies** (D), **bedding in the well-stratified facies is preserved** (P); but **wherever streaks occur, it is absent**. The streaks are interpreted as fluidisation channels (free-surface pillars). The folds near the top were formed (after fluidisation) by drag from the downslump movement of overlying icy diamicton. Shovel handle for scale. (Both September 3 1991)

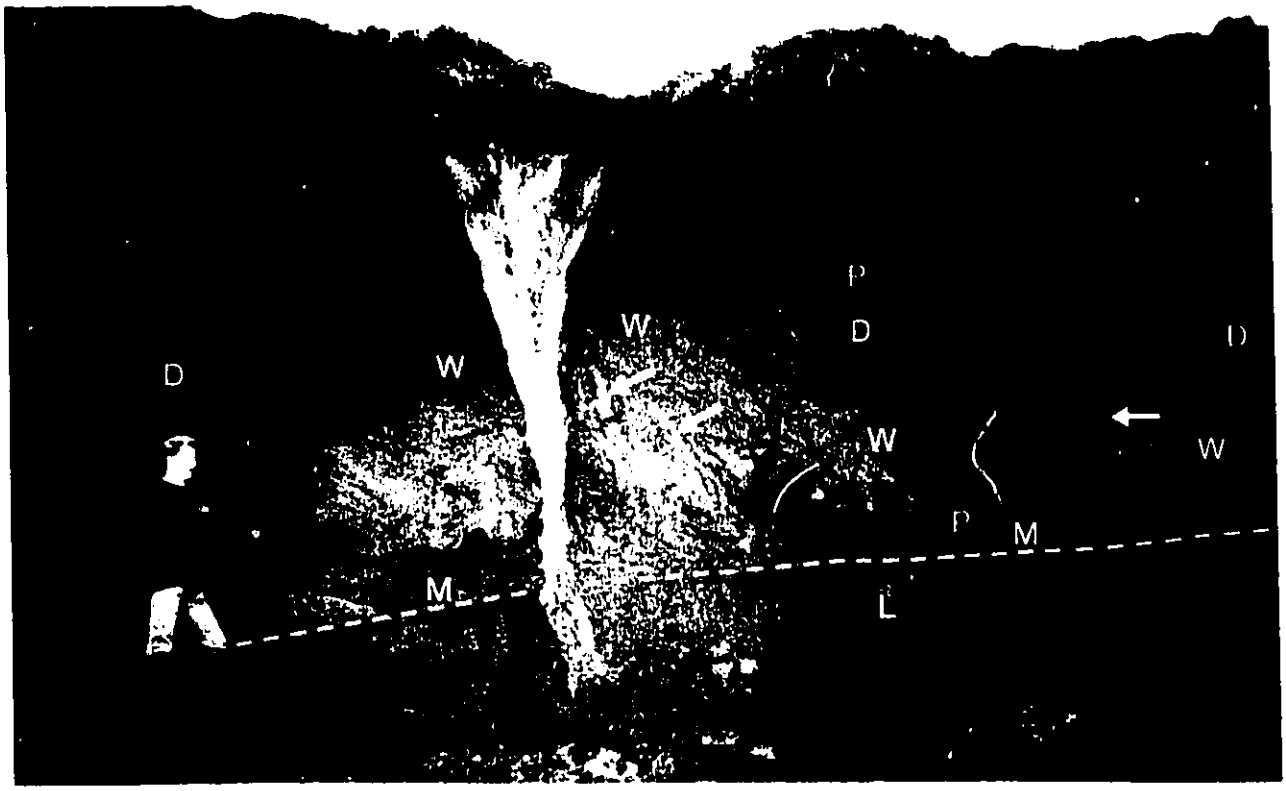
D
W
W
P
D
D
W
W
P
M
M
L

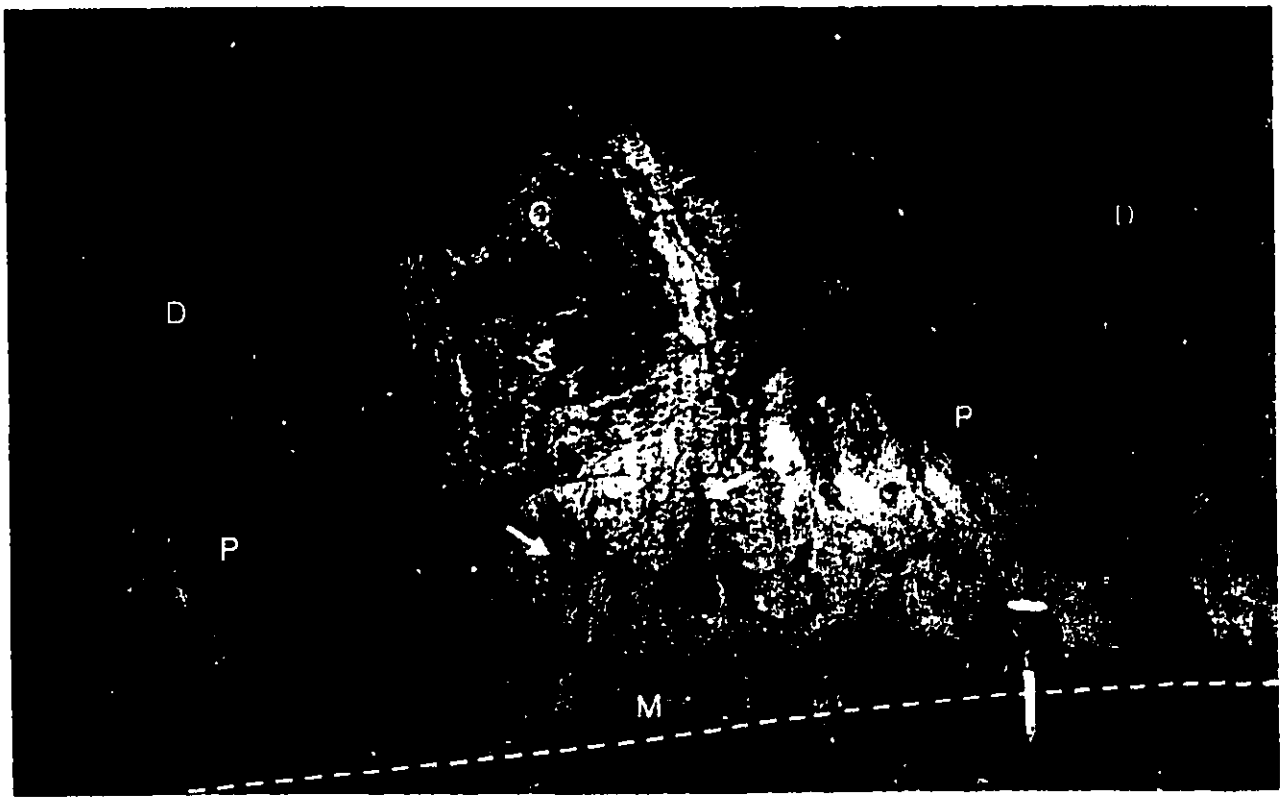
C
D
D
P
P
M

topped streak in Fig. 7.5B deformed hydroplastically, presumably because thin muddy beds within the well-stratified sand locally precluded fluidisation.

The open system required for fluidisation was probably generated by the slump morphology, the underlying secondary thaw contact and the slump-floor deposits (Fig. 4.10). The steaks underlie a basin (c.250m across) shaped like a truncated saucer. Beneath the basin a secondary thaw contact parallels the basin surface and underlies a thin (generally 5-25cm thick) layer of melt-out diamicton. Above the thaw contact is a discontinuous sand-rich unit (≤2m thick) of structureless and well-stratified sand. During the Late Wisconsinan-early Holocene thermokarst interval, water percolating through the sandy unit towards the basin centre would have created the open system necessary for fluidisation. At times, water would have been supplied to the basin centre faster than it could drain, drainage being impeded by the underlying thaw contact and by diamicton masses and muddy laminae within the slump-floor deposits. Thus groundwater pressure was at times likely artesian. Fluidisation probably occurred during mid to late summer, when the slump-floor deposits were unfrozen (and hence free to dilate upwards) and when both melt- and rainwater were abundant (cf. French, 1976, p.43 and Fig. 3.12; Shilts, 1978; Mackay, 1980). Fluidisation may have been triggered by summer rainstorms or increasing pore-water pressures.

7.4 Formative Conditions

From the preceding observations, conditions favouring the development of thermokarst involutions are suggested. First, ice-rich permafrost must thaw. The thickness need only be small; at Crumbling Point it is estimated that between a few dm and c.2-3m of the layered cryofacies association thawed, according to volumetric ice content. Furthermore, given the evidence for soft-sediment deformation within icy-bottomed active layers (e.g. Shilts, 1978; Mackay, 1980; Zoltai and Tarnocai, 1981; French, 1988, p.168-173), thawing of the thin (few

m) ice-rich layer beneath the permafrost table (e.g. Büdel, 1982, p. 82-83; Cheng, 1983; Burn, 1988) would likely supply enough water for pervasive soft-sediment deformation.

Second, thermokarst involutions are most likely to form in areas of poor drainage. This favours flat landscapes, where the impermeable base of the active or residual thaw layer (i.e. secondary thaw contact) parallels the ground surface. Where increasing pore-water pressure induces liquidization, there must be an additional, higher permeability barrier such as saturated muds with low hydraulic conductivities or sandy, silty sediments which dry to form poorly permeable carapaces (e.g. Shilts, 1978; Egginton and Dyke, 1982). A less likely possibility is an upper seasonally frozen layer in frost-stable materials (i.e. sand or gravel; e.g. Gullentops and Paulissen, 1978); however, without significant throughflow or pore-water expulsion, it is difficult to envisage how large quantities of meltwater would accrue at freezeback. With permeability barriers above and below thawed sediments, meltwater may accumulate within thaw layers, sometimes raising pore-water pressure above hydrostatic. Thermokarst involutions formed by water-escape (Section 7.3) are most likely to form in depressions where throughflow generates artesian pressures.

Third, the sediments involved must vary to some degree in texture or composition (e.g. Kolstrup, 1987). They should also be susceptible to fluidisation, liquefaction (e.g. fine sand and coarse silt; Allen, 1985, p.181) or hydroplastic deformation (e.g. argillaceous materials).

Thermokarst involutions formed by loading and buoyancy necessitate a reverse density gradient. This may be depositional or post-depositional in origin, the former arising where sediment of a higher bulk density overlies that of a lower density, the latter where unconfined and uncohesive sediment dilates when pore-water pressure exceeds hydrostatic (e.g. Vandenberghe and Broek, 1982; Allen, 1985, p.185-186). For deformation to ensue, the sediments must have a very low yield strength. Thermokarst involutions formed by

fluidisation necessitate open-system groundwater conditions that are capable of generating artesian pressures.

7.5 Pleistocene significance

These field observations are the first to describe from a modern permafrost environment involutions that are unequivocally related to thermokarst. They permit comment on the disparity in size, morphology and abundance between involutions described from areas of former permafrost and those from modern active layers (e.g. Jahn, 1975, p.134; French, 1976, p.227-229; for the latter see also Shilts, 1978; Mackay, 1980; Zoltai and Tarnocai, 1981; Hallet and Prestrud, 1986; French, 1988; Washburn, 1989; Van Vliet-Lanoe, 1991). In the active layer, loading and buoyancy structures tend to be smaller and rarer (e.g. French, 1986, Figs 4 and 5) than the structures described from superficial sediments in areas of former permafrost (e.g. Eissmann, 1981; Vandenberghe and Broek, 1982; Strunk, 1983). Judging by the thermokarst involutions observed at Crumbling Point, this disparity probably reflects the massive scale of soft-sediment deformation that accompanies regional thermokarst.

The field observations also permit evaluation of some inferences about thermokarst-related deformation in areas of former permafrost. Several inferences are supported. First, at Crumbling Point, deepening of the thaw layer engendered widespread soft-sediment deformation by loading and buoyancy while some of the sediments were in a liquidized condition. Similar conditions have been inferred from Pleistocene involutions in Europe (e.g. Butrym et al., 1964; Gozdzik, 1973; Vandenberghe and Broek, 1982; Vandenberghe, 1988). Second, thermokarst involutions in the Summer Island area occupy a relatively thick (1-2.5m) cryostratigraphic horizon representing the deepened Late Wisconsinan-early Holocene active layer or residual thaw layer. This supports the hypothesis that many involutions in areas of former Pleistocene permafrost occur in layers significantly thicker (≤3m; Williams, 1975) than

many active layers associated with stable permafrost conditions (e.g. French, 1979; Maarleveld, 1981). Third, thermokarst involutions within the same cryostratigraphic horizon have been observed at sites several km apart (Crumbling Point, Mason Bay and Hadwen Island; Fig. 1.5), supporting the view that thermokarst involutions commonly form over large areas (cf. Van der Hammen et al., 1967; Vandenberghe, 1988, p.194). Thus the abundance of loading and buoyancy structures within certain Weichselian stratigraphic horizons in Europe (e.g. Gozdzik, 1973; Vandenberghe, 1983b, Fig. 4) may be unrelated to frost action, relating instead to regional thermokarst.

One may also question the validity of several inferences about Pleistocene thermokarst involutions. First, the size and shape of many involutions at Crumbling Point are incompatible with Vandenberghe's (1988) morphological classification (Vandenberghe, 1988, Fig. 8.1). The shapes of some are difficult to reconcile with Vandenberghe's Types 2 and 4 involutions, because irregular and asymmetrical involutions are as common as those which are regular and symmetrical (Figs 7.3 and 7.4). Furthermore, there is only local evidence for the regular spacing of Vandenberghe's Type 2 involutions (Vandenberghe, 1988, Fig. 8.1). Finally, there is no evidence for Vandenberghe's size distinction between Type 2 involutions (generally 0.6-2m), attributed to thermokarst, and Type 3 involutions (a few cm to c.0.5m), attributed to a non-thermokarst origin. Because many involutions at Crumbling Point are much smaller than 0.6m, this distinction is unwarranted.

Second, if the implication that (a) flat-bottomed involutions and (b) horizons of involutions whose bottoms occur at a similar depth coincide with, or lie a small distance above, the permafrost table (Vandenberghe, 1983a; 1983b; 1988) were correct, one would expect to find at least some involutions immediately above secondary thaw contacts. However, at Crumbling Point exceedingly few lie within 10cm of the contact (Figs 7.1-7.3). The

possibility that some involutions formed when the thaw contact was at a shallower depth does not explain why many do not coincide with the present contact.

Third, it is questionable whether the thickness of a thaw layer can be accurately inferred from the size of involutions within it (see Vandenberghe, 1983a; 1983b). This is because (1) many of the involutions at Crumbling Point are small; (2) the local thickness of the sand and diamicton horizon (≤c.2.5m) always exceeds the maximum size (≤c.1.4m) of involutions within it; and (3) very few, if any, of the involutions coincide with the secondary thaw contact. Furthermore, since thermokarst involutions probably form diachronously as a thaw layer thickens, there is no reason why the involutions within a single stratigraphic horizon should all necessarily relate to any one thickness of a Pleistocene thaw layer. In short, thermokarst involutions indicate only the minimum thickness of a thaw layer.

Fourth, because thermokarst involutions develop in thaw layers which are deeper than the pre-thermokarst active layer (cf. French, 1979; Maarleveld, 1981; Vandenberghe and Broek, 1982; Vandenberghe, 1983a; 1983b; 1988), it is erroneous to infer from them active layer depths and, from these, periglacial palaeoclimates (see e.g. Williams, 1975; Maarleveld, 1976). With isolated involutions it may be impossible to know if thawing occurred locally during stable permafrost conditions or regionally during climatic warming. But where numerous involutions occur in a single, widespread stratigraphic horizon (e.g. Vandenberghe, 1983b), they are more likely to have formed during the latter. Nonetheless, it remains to be demonstrated whether involutions can be used to reconstruct mean annual or summer temperatures during transitional periods of warming. More generally, because the depth of thaw is controlled not only by climate but also by microclimatic properties like aspect, vegetation and moisture content, all palaeoclimatic reconstructions using thermokarst involutions should be treated with extreme caution.

7.6 Conclusions

Thermokarst involutions are most likely to occur in fine-grained sediments of low relief that have experienced permafrost growth and degradation. This view is supported by the numerous loading and buoyancy structures described from the lowlands of central and western Europe which hosted Pleistocene permafrost (e.g. Eissmann, 1981; Vandenberghe and Broek, 1982; Kolstrup, 1987). Indeed, as French (1979) has already suggested concerning areas such as lowland Europe, thermokarst involutions are probably for more common than has been generally recognised.

Although the involutions described here are not unique to areas of thermokarst, they are, nonetheless, particularly abundant in this environment. This is because wherever the top of ice-rich permafrost degrades regionally, saturated soil conditions may develop above an impermeable secondary thaw contact, making soft-sediment deformation almost inevitable.

Finally, thermokarst involutions should not be confused with cryoturbations. In its original sense, cryoturbation refers to "all sediment movements affected by cold" (Edelmann, et al., 1936). This loose term has been subsequently used to describe both a variety of freeze-thaw-related processes (typically in the seasonally frozen layer) as well as the resulting deformation structures (ACGR, 1988, p.25, 33). Yet only if the process of cryoturbation is taken to include that of thermokarst can thermokarst involutions be termed cryoturbations, an inclusion that seems illogical inasmuch as thermokarst relates not to cold conditions (freezing) by rather to warm ones (thawing).

Chapter 8 CONCLUSIONS

"O, that this too too solid flesh would melt,
Thaw, and resolve itself into a dew;"
(*Hamlet* Shakespeare)

8.1 Facies model

Figure 8.1 shows the thermokarst sedimentary system of the Tuktoyaktuk Coastlands synthesised as a local facies model (Fig. 8.1). Several points about this model are emphasised. First, it illustrates the effects of regional thermokarst. Beneath the ice-rich primordial surface areal thermokarst forms a thick thaw layer containing melt-out deposits. Coevally, new lowland surfaces develop by retreat of steep icy bluffs and expansion of retrogressive thaw slumps and thermokarst basins. Thus in ice-rich terrain, thermokarst deposits completely mantle upland and lowland surfaces. Second, the proportions of the landscape consumed by down- and backwearing thermokarst changes through time, as the latter progressively destroys the primordial surface. Third, the discontinuous nature of the (ice-rich) layered and ice-breccia cryofacies associations limits the distribution of thermokarst sediments and implies that the ultimate thermokarst landscape will have an irregular topography. Fourth, thermokarst sediments are prone to reworking. For example, thaw-layer deposits may be reworked by thermokarst-slope processes, and thermokarst-slope facies by thermokarst-lake processes.

The thermokarst system is dominated by the processes of melt-out, resedimentation and soft-sediment deformation. While in this environment melt-out is ubiquitous, it is recorded directly by thaw-layer deposits alone and, more typically, is inferred from its consequences, soft-sediment deformation and resedimentation. It is these processes which best characterise

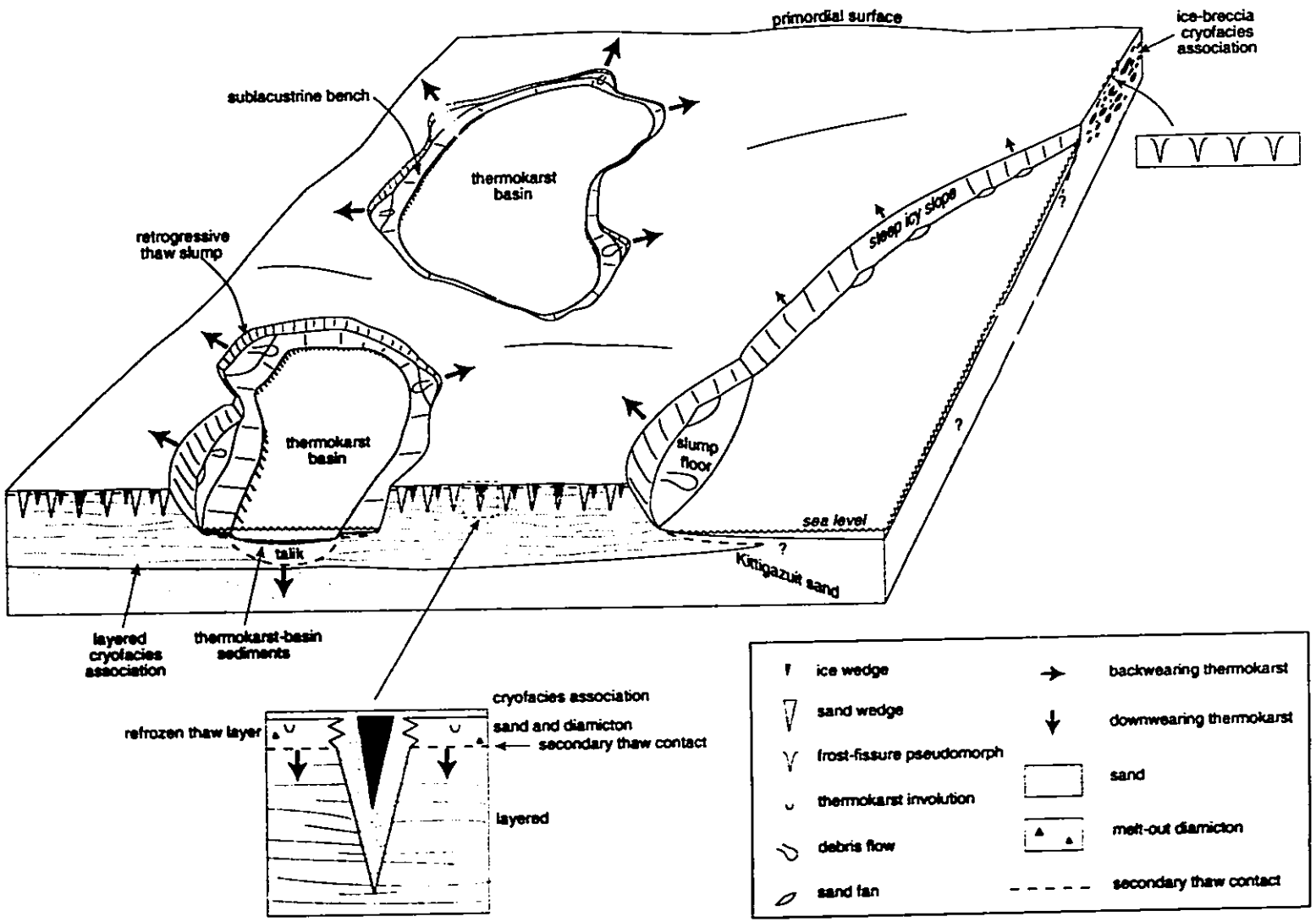

Fig. 8.1 Facies model of the thermokarst sedimentary system in the Tuktoyaktuk Coastlands

the thermokarst system. Soft-sediment deformation by loading, buoyancy and water-escape is common above secondary thaw contacts but obvious only where sediments contrast texturally. Resedimentation of upland materials by alluvial, colluvial and lacustrine processes is effected by backwearing thermokarst associated with thermokarst slopes and basins. Resedimentation is the initial depositional process in the development of thermokarst lowlands and the principal sedimentological consequence of thermokarst in the Tuktoyaktuk Coastlands.

The preservation potential of thermokarst sediments varies with depositional environment. Thermokarst-basin sediments are the most likely to be preserved, since they underlie relatively ice-poor lowland surfaces; only locally are basin sediments reworked (e.g. by marine processes). Thaw-layer deposits are less likely to be preserved, because in areas with thick bodies of excess ice (c.10+m), the primordial surface may be consumed by back-wearing thermokarst before the excess ice within it has completely melted out by downwearing thermokarst. Thermokarst-slope facies have the lowest preservation potential; they cover but a small area of the landscape and are commonly reworked by lacustrine processes.

Thermokarst sediments in the Tuktoyaktuk Coastlands may be distinguished by applying the five proposed criteria. The criteria most readily identified are organic-rich (and sandy) diamicton, impure sand (+/- diamicton) and frost-fissure pseudomorphs. The diamicton and sand are distinctive facies, commonly forming thick, laterally extensive units. Frost-fissure pseudomorphs are usually distinctive by virtue of their size, shape and polygonal pattern. Granular mud aggregates in stratified facies are small-scale features that are observed only with detailed examination. Finally, apart from those overlying frost-fissure pseudo-morphs, thermokarst involutions can be identified with confidence only where they occupy a single, widespread stratigraphic horizon. These involutions are, however, particularly informative, inasmuch as where they are widespread, they indicate regional thermokarst. The other criteria, by contrast, do not discriminate between thermokarst that is local or regional.

8.2 Summary

Thermokarst sedimentology is the study of the sediments and processes associated with thaw of ice-rich terrain. This thesis has examined the thermokarst sedimentology of the Tuktoyaktuk Coastlands, NWT, using facies analysis, field observations of processes and oxygen-isotopic analysis of ground ice. Its major findings are summarised thus:

(1) **The thermokarst sedimentary system** of the Tuktoyaktuk Coastlands comprises three subenvironments (**uplands, slopes** and **basins**) and two groups of sedimentary structures (**frost-fissure pseudomorphs** and **thermokarst involutions**; Fig. 8.1). Its sedimentary processes are those of melt-out, resedimentation (by fluvial, colluvial and lacustrine processes) and soft-sediment deformation (by loading, buoyancy and water-escape).

(2) To facilitate description of frozen ground, classifications of **cryostructures** (Fig. 2.1) and **cryofacies** (Table 2.1) are proposed.

(3) Ice-rich upland surfaces may experience **areal thermokarst**. This is a type of regional thermokarst in which downwearing occurs uniformly beneath upland surfaces and is poorly, if at all, expressed in the surface relief (Section 3.3; Fig. 4.2). At Crumbling Point, areal thermokarst during the Late Wisconsinan-early Holocene warm interval formed melt-out deposits within a deepening thaw layer. The base of the now-refrozen thaw layer is marked by a regional secondary thaw contact.

(4) As upland surfaces retreat by backwearing thermokarst, upland materials are redeposited at the base of **thermokarst slopes**: steep icy bluffs and retrogressive thaw slumps (Chapter 4). The **resedimentation processes and facies** of these slopes (Table 4.1) are summarised in **two facies models** (Figs 4.13 and 4.14).

(5) Upland surfaces also degrade by a combination of back- and downwearing thermokarst that forms **thermokarst basins** (Chapter 5). Eight **thermokarst-basin facies**

(Table 5.2) and three **facies associations** are synthesised in a **facies model** of a deep thermokarst basin (Fig. 5.15). Three stages of basin infilling are identified: (1) resedimentation of upland materials and initiation of sublacustrine benches; (2) suspension settling of fine materials and reworking of the tops of benches; and (3) non-lacustrine infilling by gelifluction, peat accumulation and aeolian deposition.

(6) **Frost-fissure pseudomorphs** develop by **thaw modification** of frost-fissure wedges (Chapter 6). Thaw-modification processes, inferred from partially thawed ice, composite and sand wedges, include slow subsidence, thermal erosion, refreezing, loading, buoyancy, spreading, folding, shearing and mass movement.

(7) **Thermokarst involutions** are soft-sediment deformation structures that form during thermokarst, primarily by water-escape or by loading and buoyancy (Chapter 7). Both types of involutions form beneath slump floors; those generated by loading and buoyancy also develop within thick thaw layers. Involutions within a Late Wisconsinan-early Holocene thaw layer at Crumbling Point probably reflect the massive scale of soft-sediment deformation that accompanies regional thermokarst, and they provide a potential analogue for some Pleistocene involutions in the mid-latitudes.

(8) Five **criteria** are proposed to identify **thermokarst-modified sediments**:

1. Organic-rich (and sandy) diamicton
2. Impure sand (+/- diamicton)
3. Granular mud aggregates in stratified facies
4. Frost-fissure pseudomorphs
5. Thermokarst involutions

8.3 Limitations

Although sections through permafrost are common around shorelines and in the headwalls of thaw slumps throughout the Tuktoyaktuk Coastlands, there are few large, pristine sections across thermokarst basins. Usually formed during summer and autumn storms, these sections degrade rapidly and should be examined within several days of their formation. But in three visits to North Head and four to Crumbling Point, large sections were observed only once at each site. Consequently, most sections through thermokarst basins had to be hand-dug and were small (usually ≤2m wide and ≤4m deep). While small sections serve for distinguishing individual facies, they do not reveal facies architecture (cf. Allen, 1983; Miall, 1985).

The treatment of thermokarst facies is selective. Two categories of thermokarst basins are omitted, namely, collapsed pingos containing lakes and shallow (oriented) basins in polycyclic surfaces. The former, uncommon and rarely truncated, likely possess facies similar to those in residual ponds (detrital peat, mud/muddy peat and fine sand), and the latter, although common, were eschewed for logistical reasons.

8.4 Future work

This study of thermokarst sedimentology suggests at least six avenues for future research.

First, a systematic study is required of the sedimentary processes and facies in **modern thermokarst lakes**. Critical areas include (1) study of storm and fairweather processes and deposits, (2) sediment movement and deposition on the flats and risers of sandy sublacustrine benches, and (3) coring of basin-centre deposits to map the distribution and interpret the origin of thin sand units in mud/muddy peat.

Second, more needs to be known about the sedimentology of **shallow thermokarst basins** and the development of oriented thaw lakes. In the field area there are sections across these on NE Tuktoyaktuk Peninsula and N Bathurst Peninsula.

Third, a detailed study is required of the **basal unit of deep thermokarst basins**, the diamicton and impure-sand facies association. This study might address issues such as the asymmetric infilling of basins (Figs 5.12A and 5.15A), sediment transport within young basins and the origin of reactivation surfaces in, and risers to, sublacustrine benches. The simplest hypothesis which may explain some of these features is that sedimentation was strongly controlled by unequal and bimodal wave-induced currents during summer storms. However, the details are presently unclear.

Fourth, certain aspects of thermokarst sedimentology lend themselves to experimental study. For example, thaw modification of ice wedges could be artificially induced in the field by thermal erosion or by microclimatic alteration (e.g. removal of vegetation), and thermokarst involutions could be simulated in the laboratory by thaw of ice-rich sediments. More valuable still, in view of the importance of basin evolution to sedimentology, would be a large-scale field experiment involving the artificial formation of a thermokarst basin. The advantage of conducting this experiment in a thermokarst environment over one that is ice-free is that basin subsidence due to melt-out of underlying ground ice would simulate subsidence in much larger, ice-free sedimentary basins. Monitoring of the rates, nature and controls of basin infilling would provide a means of field-testing concepts developed in sequence stratigraphy, concepts of profound significance for hydrocarbon exploration.

Fifth, the facies models for retrogressive thaw slumps and deep thermokarst basins imply that detailed facies analysis is essential to fully interpret the palaeoenvironmental and chronologic significance of organic material selected from slump and basin sediments for radiocarbon dating. These sediments comprise both allochthonous and autochthonous organic

material, the former derived from pre-existing upland surfaces, the latter produced within slump floors and thermokarst basins. For example, most (allochthonous) organic material deposited during the first stage of thermokarst-basin growth is likely to be older than that (autochthonous) deposited during the second, and the second older in turn than that during the third. This hypothesis should be tested in a study involving dating of numerous samples collected from a single basin.

Finally, the thermokarst sedimentology of the Tuktoyaktuk Coastlands should be compared with that of other active thermokarst areas and then applied to the geological record. Comparison is essential to evaluate the generality of the facies models proposed for the Tuktoyaktuk Coastlands. Application to the geological record is suggested by both the abundance of thermokarst sediments and structures in this area and by the repeated episodes of Quaternary (and pre-Quaternary) post-glacial warming. Assuming that in ice-rich areas such warming induced regional thermokarst, then thermokarst features are probably much more common than has been recognised in the Quaternary record of the mid- and high-latitudes, as well as in ancient sedimentary rocks traditionally interpreted in terms of continental glaciation.

Hopefully, this thesis will encourage others to pursue some of these avenues.

REFERENCES

Aigner, T. 1985. *Storm Depositional Systems*. Lecture Notes in Earth Sciences, Volume **3**, Springer-Verlag, Germany, 174p.

Allen, D.M., Michel, F.A. and Judge, A.S. 1988. The permafrost regime in the Mackenzie Delta, Beaufort Sea region, N.W.T. and its significance to the reconstruction of the palaeoclimatic history. *Journal of Quaternary Science*, **3**, 3-13.

Allen, J.R.L. 1982. *Sedimentary Structures: their Character and Physical Basis*. Developments in Sedimentology, **30B**, Elsevier, Amsterdam, 663p.

Allen, J.R.L. 1983. Studies in fluviatile sedimentation: bars, bar-complexes and sandstone sheets (low-sinuousity braided streams) in the Brownstones (L. Devonian), Welsh borders. *Sedimentary Geology*, **33**, 237-293.

Allen, J.R.L. 1985. *Principles of Physical Sedimentology*. Allen & Unwin, London, 272p.

Anderton, R. 1985. Clastic facies models and facies analysis. In: (eds P.J. Brenchley and B.R.J. Williams) *Sedimentology: Recent Developments and Applied Aspects* Blackwell, Oxford, p. 31-47.

Anketell, J.M., Cegla, J. and Dzulynski, S. 1970. On the deformational structures in systems with reversed density gradients. *Rocznik Polskiego Towarzystwa Geologicznego*, **40**, 3-30.

Are, F.E. 1973. *Development of thermokarst lakes in central Yakutia*. Guidebook, Permafrost: Second International Conference, Yakutsk, USSR Academy of Sciences Yakutsk, 29p.

Ashley, G.M. 1988. Classification of glaciolacustrine sediments. In: (eds R.P. Goldthwait and C.L. Matsch) *Genetic Classification of Glacigenic Deposits*, Balkema, Rotterdam, p.243-260.

Ashley, G.M., Shaw, J. and Smith, N.D. 1985. *Glacial Sedimentary Environments.* Society of Economic Paleontologists and Mineralogists Short Course **16**, SEPM, Tulsa, OK, 246p.

Astakhov, V.I. and Isayeva, L.L. 1988. The "Ice Hill"; an example of "retarded deglaciation" in Siberia. *Quaternary Science Reviews*, **7**, 29-40.

Ballantyne, C.K. and Harris, C. in press. *The Periglaciation of Great Britain.* Cambridge University Press, Cambridge.

Bates, R.L. and Jackson, J.A. 1987. *Glossary of Geology, Third Edition.* American Geological Institute, Alexandria, Virginia, 788p.

Berg, T.E. and Black, R.F. 1966. Preliminary measurements of growth of non-sorted polygons, Victoria Land, Antarctica. In: (ed. J.C.F. Tedrow) *Antarctic Soils and Soil-Forming Processes*, American Geophysical Union Antarctic Research Series, **8**, p.61-108.

Boardman, J. 1987 (ed.). *Periglacial Processes in Britain and Ireland.* Cambridge University Press, Cambridge, 296p.

Black, R.F. 1969. Thaw depressions and thaw lakes: a review. *Biuletyn Peryglacjalny*, **19**, 131-150.

Black, R.F. 1976. Periglacial features indicative of permafrost: ice and soil wedges. *Quaternary Research*, **6**, 3-26.

Blatt, H. 1992. *Sedimentary Petrology.* W.H. Freeman and Company, New York, 514p.

Boggs, S. 1987. *Principles of Sedimentology and Stratigraphy.* Merrill Publishing Company, Columbus, 784p.

Boulton, G.S. 1968. Flow tills and related deposits on some Vestspitzbergen glaciers. *Journal of Glaciology*, **7**, 391-412.

Boulton, G.S. 1983. Debris and isotopic sequences in basal layers of polar ice sheets. In: (ed. G. de Q. Robin) *The Climatic Record in Polar Ice-Sheets*, Cambridge University Press, Cambridge, p.83-89.

Boulton, G.S. and Paul, M.A. 1976. The influence of genetic processes on some geotechnical properties of glacial tills. *Quarterly Journal of Engineering Geology*, **9**, 159-193.

Bradley, R.S. 1985. *Quaternary Paleoclimatology: Methods of Paleoclimatic Reconstruction.* Allen & Unwin, Boston, 472p.

Brigham, J.K. 1985. *Marine stratigraphy and amino-acid geochronology of the Gubik formation, western Arctic coastal plain, Alaska.* United States Geological Survey Open File Report **85-381**, 218p.

Britton, M.E. 1967. Vegetation of the arctic tundra. In: (ed. H.P. Hansen) *Arctic Biology*, Oregon State University Press, Corvallis, p.67-130.

Brodzikowski, K. and Van Loon, A.J. 1991. *Glacigenic Sediments*. Developments in Sedimentology **49**, Elsevier, Amsterdam, 674p.

Brookfield, M.E. 1977. The origin of bounding surfaces in ancient eolian sandstones. *Sedimentology*, **24**, 303-332.

Brookfield, M.E. and Ahlbrandt T.S. (eds) 1983. *Eolian Sediments and Processes.* Developments in Sedimentology, **38**, Elsevier, Amsterdam, 660p.

Brown, R.J.E., 1970. *Permafrost in Canada - Its Influence on Northern Development*; University of Toronto Press, 234 p.

Brown, R.J.E. 1970. *Permafrost in Canada - Its Influence on Northern Development.* University of Toronto Press, 234 p.

Bryant, R.H. and Carpenter, C.P. 1987. Ramparted ground-ice depressions in Britain and Ireland. In: (ed. J. Boardman) *Periglacial Processes in Britain and Ireland.* Cambridge University Press, Cambridge, p.183-190.

Büdel, J. 1982. *Climatic Geomorphology*. Princeton University Press, Princeton, N.J. 443p.

Bull, W.B. 1964. Alluvial Fans and Near-Surface Subsidence in Western Fresno County, California. *United States Geological Survey Professional Paper* **437A**, 71p.

Bull, W.B. 1977. The alluvial-fan environment. *Progress in Physical Geography*, **1**, 222-270.

Burbidge, G.H. French, H.M. and Rust, B.R. 1988. Water escape fissures resembling ice wedge casts in Late-Quaternary subaqueous outwash near St. Lazare, Québec, Canada. *Boreas*, **17**, 33-40.

Burn, C.R. 1986. *On the origin of aggradational ice in permafrost.* Unpublished PhD Thesis, Carleton University, Ottawa, 222p.

Burn, C.R. 1988. The development of near-surface ground ice during the Holocene at sites near Mayo, Yukon Territory, Canada. *Journal of Quaternary Science*, **3**, 31-38.

Burn, C.R. 1992. Thermokarst lakes: Canadian landform examples - 24. *The Canadian Geographer*, **36**, 81-85.

Burn, C.R. and Friele, P.A. 1989. Geomorphology, vegetation succession, soil characteristics and permafrost in retrogressive thaw slumps near Mayo, Yukon Territory. *Arctic*, **42**, 31-40.

Burn, C.R. and Lewkowicz, A.G. 1990. Retrogressive thaw slumps. *The Canadian Geographer*, **34**, 273-76.

Burn, C.R., Michel, F.A. and Smith, M.W. 1986. Stratigraphic, isotopic and mineralogical evidence for an early Holocene thaw unconformity at Mayo, Yukon Territory. *Canadian Journal of Earth Sciences*, **23**, 794-803.

Burn, C.R. and Smith, M.W. 1990. Development of thermokarst lakes during the Holocene at sites near Mayo, Yukon Territory. *Permafrost and Periglacial Processes*, **1**, 161-176.

Burton, R.G.O. 1987. The role of thermokarst in landscape development in eastern England. In: (ed. J. Boardman) *Periglacial Processes in Britain and Ireland*, Cambridge University Press, Cambridge, p. 203-208.

Butrym, J., Cegła, J., Dzulynski, S. and Nakonieczny, S. 1964. New interpretation of "periglacial structures". *Folia Quaternaria*, **17**, 34p.

Carson, C.E. 1968. Radiocarbon dating of lacustrine strands in Arctic Alaska. *Arctic*, **21**, 12-26.

Carson, C.E. and Hussey, K.M. 1960. Hydrodynamics of three arctic lakes. *Journal of Geology*, **68**, 485-600.

Carson, C.E. and Hussey, K.M. 1962. The oriented lakes of Arctic Alaska. *Journal of Geology*, **70**, 417-439.

Carter, L.D. 1988. Loess and deep thermokarst basins in Arctic Alaska. In: *Permafrost, Fifth International Conference, Proceedings, vol. 1*, Tapir, Trondheim, p.706-711.

Cheng, G. 1983. The mechanism of repeated segregation for the formation of thick-layered ground ice. *Cold Regions Science and Technology*, **8**, 57-66.

Clark, M.J. (ed.) 1988. *Advances in Periglacial Geomorphology*. John Wiley & Sons, Chichester, 481p.

Clayton, L. 1964. Karst topography on stagnant glaciers. *Journal of Glaciology*, **5**, 107-112.

Collinson, J.D. and Thompson, D.B. 1989. *Sedimentary Structures*. London, Unwin Hyman, 207p.

Czudek, T. and Demek, J. 1970. Thermokarst in Siberia and its influence on the development of lowland relief. *Quaternary Research*, **1**, 103-120.

Dallimore, S.R. (ed.) 1991. *Geological, Geotechnical and Geophysical Studies along an Onshore-offshore Transect of the Beaufort Shelf*. Geological Survey of Canada, Open File **2408**, 264p.

Dallimore, S.A. and Wolfe, S. 1988. Massive ground ice associated with glaciofluvial sediments, Richards Islands, N.W.T. Canada. In: *Permafrost, Fifth International Conference, Proceedings, vol. 1*, Tapir, Trondheim, p. 132-137.

Daly, B. and Cooper, M.R. 1976. Clastic wedges and patterned ground in the Late Ordovician-Early Silurian tillites of South Africa. *Sedimentology*, **23**, 271-283.

Danilov, I.D., Parunin, O.B. and Polyakova, Ye.I. 1989. The origin and age of the "Icy Complex" in the north of West Siberia. *Polar Geography and Geology*, **13**, 297-304.

Danilova, N.S. 1978. Distribution and conditions of formation of the loess deposits of central Siberia. In: *Permafrost:USSR Contribution to the Second International Conference*, Yakutsk, U.S.S.R. National Academy of Sciences, Washington D.C. p.119-121.

Demek, J. 1978. Periglacial geomorphology. In: (eds C. Embleton, D. Brunsden and D.K.C. Jones) *Geomorphology: Present Problems and Future Prospects*, Oxford University Press, Oxford, p.139-155.

Denny, C.S. 1936. Periglacial phenomena in southern Connecticut. *American Journal of Science*, **32**, 322-342.

Deynoux, M. 1982. Periglacial polygonal structures and sand wedges in the late Precambrian glacial formation of the Taoudeni Basin in Adrar of Mauretania (West Africa). *Palaeogeography, Palaeoclimatology, Palaeoecology*, **39**, 55-70.

Dinter D.A., Carter, L.D. and Brigham-Grette, J. 1990. Late Cenozoic geologic evolution of the Alaskan North slope and adjacent continental shelves. In: (eds A. Grantz, L. Johnson and J.F. Sweeney) *The Arctic Ocean Region*, The Geology of North America, Vol. L, Geological Society of America, Boulder, Colorado, p.459-490.

Dixon, J.C. and Abrahams, A.D. (eds) 1992. *Periglacial Geomorphology*. The Binghamton Symposia in Geomorphology: International Series, No.**22**, Wiley, Chichester, 354p.

Dort, W. Jr. 1967. Internal structure of Sandy Glacier, Southern Victoria Land, Antarctica. *Journal of Glaciology*, **6**, 529-540.

Dredge, L.A. and Nixon, F.M. 1979. Thermal sensitivity and the development of tundra ponds and thermokarst lakes in the Manitoba portion of the Hudson Bay Lowland. In: *Current Research, Part C*, Geological Survey of Canada, Paper **79-1C**, p.23-26.

Dreimanis, A. 1989. Tills: their genetic terminology and classification. In: (eds R.P. Goldthwait and C.L. Matsch) *Genetic Classification of Glacigenic Deposits*. Balkema, Rotterdam, p.17-83.

Drewry, D. 1986. *Glacial Geologic Processes*. Arnold, London, 276p.

Dylik, J. 1963a. Traces of thermokarst in the Pleistocene sediments of Poland. *Bulletin de la Société des Sciences et des Lettres de Lodz*, **IV**, 2.

Dylik, J. 1963b. Periglacial sediments of the Sw. Malgorzata Hill in the Warsaw-Berlin Pradolina. *Bulletin de la Société des Sciences et des Lettres de Lodz*, **XIV**, 1

Dylik, J. 1964. Le thermokarst, phénomène négligé dans les études du Pléistocène. *Annales de Geographie*, **73**, 523-533.

Dylik, J. 1965. Right and wrong in sceptical views on the problem of periglacial phenomena revealed in Pleistocene deposits. *Bulletin de la Société des Sciences et des Lettres de Lodz*, **XVI**, 8.

Dylik, J. 1966. Problems of ice-wedge structures and frost-fissure polygons. *Biuletyn Peryglacjalny*, **15**, 241-291.

Dylik, J. 1968. Thermokarst. In: (ed. R.W. Fairbridge) *Encyclopedia of Geomorphology*, Reinhold Books Co. p.1149-1151.

Dylik, J. 1969. Slope development under periglacial conditions in the Lodz region. *Biuletyn Peryglacjalny*, **18**, 381-410.

Dylik, J. 1971. L'érosion thermique actuelle et ses traces figées dans le paysage de la Pologne Centrale. *Bulletin de L'Academie Polonaise des Sciences, Serie des Sciences de la Terre*, **XIX**, 55-61.

Edelmann, C.H., Florschutz, F. and Jeswiet, J. 1936. Ueber spätpleistozäne und frühozäne kryoturbate Ablagerungen in den ostlichen Niederlanden. *Verhand. Geolog. serie* **11**, 301-336.

Egginton, P.A. and Dyke, L.D. 1982. Density gradients and injection structures in mudboils in central district of Keewatin. In: *Current Research, Part B*, Geological Survey of Canada, Paper **82-1B**, p.173-176.

Eissmann, L. 1981. Periglaziäre Prozesse und Permafroststrukturen aus sechs Kaltzeiten des Quartärs. *Altenburger Naturwissenschaftliche Forschungen*, **1**, 3-171.

Eyles, N. 1979. Facies of supraglacial sedimentation on Icelandic and Alpine temperate glaciers. *Canadian Journal of Earth Sciences*, **16**, 1341-1361.

Eyles, N. and Clark, B.M. 1985. Gravity-induced soft-sediment deformation in glaciomarine sequences of the Upper Proterozoic Port Askaig Formation, Scotland. *Sedimentology*, **32**, 789-814.

Eyles, N., Clark, B.M. and Clague, J.J. 1987. Coarse-grained sediment gravity flow facies in a large supraglacial lake. *Sedimentology*, **34**, 193-216.

Eyles, N. and Eyles, C. H. 1992. Glacial depositional systems. In: (eds R.G. Walker and N.P. James) *Facies Models: Response to Sea Level Change*, Geological Association of Canada, p.73-100.

Eyles, N. and Rogerson, R.J. 1977. Artificially-induced thermokarst in active glacier ice. an example from northwest British Columbia, Canada. *Journal of Glaciology*, **18**, 437-444.

Ferrians, O.J. Kachadoorian, R. and Greene, G.W. 1969. *Permafrost and related engineering problems in Alaska*. United States Geological Survey, Professional Paper **678**, 37p.

Fleisher, P.J. 1986. Dead-ice sinks and moats: environments of stagnant ice deposition. *Geology*, **14**, 39-42.

Flint, R.F. 1971. *Glacial and Quaternary Geology*. Wiley, New York, 892p.

Forbes, D.L. 1980. Late Quaternary sea levels in the southern Beaufort Sea. In: *Current Research, Part B*, Geological Survey of Canada, Paper **80-1B**, p.75-87.

French, H.M. 1974. Active thermokarst processes, Eastern Banks Island, Western Canadian Arctic. *Canadian Journal of Earth Sciences*, **11**, 785-794.

French, H.M. 1975. Man-induced thermokarst Sachs Harbour airstrip. Banks Island, N.W.T. Canada. *Canadian Journal of Earth Sciences*, **12**, 132-144.

French, H.M. 1976. *The Periglacial Environment*. Longman, London, 309p.

French, H.M. 1979. Periglacial geomorphology. *Progress in Physical Geography*, **3**, 264-273.

French, H.M. 1986. Periglacial involutions and mass-displacement structures, Banks Island, Canada. *Geografiska Annaler*, **68A**, 167-174.

French, H.M. 1987. Permafrost and ground ice. In: (eds K.J. Gregory and D.E. Walling) *Man and Environmental Processes*, John Wiley & Sons, Chichester, p.237-269.

French, H.M. 1988. Active layer processes. In: (ed. M.J. Clark) *Advances in Periglacial Geomorphology*, John Wiley & Sons, Chichester, p.151-177.

French, H.M and Gozdzik, J.S. 1988. Pleistocene epigenetic and syngenetic frost fissures, Belchatow, Poland. *Canadian Journal of Earth Sciences*, **25**, 2017-2027.

French, H.M. and Harry, D.G. 1988. Nature and origin of ground ice, Sandhills Moraine, southwest Banks Island, Western Canadian Arctic. *Journal of Quaternary Science*, **3**, 19-30.

French, H.M. and Harry, D.G. 1990. Observations on buried glacier ice and massive segregated ice, western Arctic coast, Canada. *Permafrost and Periglacial Processes*, **1**, 31-43.

French, H.M. and Karte, J. 1988. A periglacial overview. In: (ed. M.J. Clark) *Advances in Periglacial Geomorphology*, John Wiley & Sons, Chichester, p.463-473.

French, H.M., Harry, D.G. and Clark, M.J. 1982. Ground ice stratigraphy and late-Quaternary events, southwest Banks Island, Canadian Arctic. In: (ed. H.M. French) *The R.J.E. Brown Memorial Volume, Proceedings of the Fourth Canadian Permafrost Conference*, National Research Council of Canada, Ottawa, p.81-90.

French, H.M., Pollard, W.H. and Burn, C.R. 1984. *Permafrost and Ground Ice Investigations, Mayo, Interior Yukon.* Contract Report **SU83-001158**, Earth Physics Branch, Energy, Mines and Resources, Canada, Ottawa, 78p.

Fujino, K., Sato, S., Matsuda, K., Sasa, G., Shimizu, O. and Kato, K. 1988. Characteristics of the massive ground ice body in the Western Canadian Arctic. In: *Permafrost, Fifth International Conference, Proceedings, vol. 1*, Tapir, Trondheim, p.143-147.

Gozdzik, J.S. 1967. Fauchage des fentes encoin du aux mouvements de masses sur des pentes douces. *Biuletyn Peryglacjalny*, **16**, 133-146.

Gozdzik, J.S. 1973. Geneza i pozycja stratygraficzna struktur peryglacjalnych w srodkowej Polsce (Origin and stratigraphical position of periglacial structures in middle Poland), (Polish with English summary). *Acta Geographica Lodziensia*, **31**, 119p.

Gravenor, C.P. and Kupsch, W.O. 1959. Ice-disintegration features in Western Canada. *Journal of Geology*, **67**, 48-64.

Gray, J.T. and Seppälä, M. 1991. Deeply dissected tundra polygons on a glacio-fluvial outwash plain, northern Ungava Peninsula, Québec. *Géographie physique et Quaternaire*, 45, 111-117.

Grosval'd, M.G., Vtyurin, B.I., Sukhodrovskiy, V.L. and Shishorina, Zh.G. 1986. Underground ice in western Siberia: origin and geological significance. *Polar Geography and Geology*, **10**, 173-183.

Gullentops, F. and Paulissen, E. 1978. The drop soil of the Eisden type. *Biuletyn Peryglacjalny*, **27**, 105-115.

Haldorsen, S. and Shaw, J. 1982. The problem of recognizing melt-out till. *Boreas*, **11**, 261-277.

Hallet, B. and Prestrud, S. 1986. Dynamics of periglacial sorted circles in Western Spitsbergen. *Quaternary Research*, **26**, 81-99.

Harms, J.C., Southard, J.B., Spearing, D.R. and Walker, R.G. 1975. *Depositional Environments as Interpreted from Primary Sedimentary Structures and Stratification Sequences*. Lecture notes: Society of Economic Paleontologists and Mineralogists Short Course **2**, Dallas, 161p.

Harris, S.A. 1986. *The Permafrost Environment*. Croom Helm, London, 276p.

Harry, D.G. 1982. *Aspects of the Permafrost Geomorphology of Southwest Banks Island, Western Canadian Arctic*. Unpublished PhD Thesis, University of Ottawa, Ottawa, 230p.

Harry, D.G. 1988. Ground ice and permafrost. In: (ed. M.J. Clark) *Advances in Periglacial Geomorphology*, John Wiley & Sons, Chichester, p.113-149.

Harry, D.G. and French, H.M. 1983. The orientation and evolution of thaw lakes, southwest Banks Island, Canadian Arctic. In: *Permafrost: Fourth International Conference, Proceedings*, Fairbanks, Alaska, U.S. National Academy Press, Washington, D.C. p.456-461.

Harry, D.G. and French, H.M. 1988. Cryostratigraphic studies of permafrost, Northwestern Canada. In: *Permafrost, Fifth International Conference, Proceedings, vol. 1*, Tapir, Trondheim, p.784-789.

Harry, D.G., French, H.M. and Pollard, W.H. 1985. Ice wedges and permafrost conditions near King Point, Beaufort Sea coast, Yukon Territory. In: *Current Research, Part A*, 111-116 Geological Survey of Canada, Paper **85-1A**.

Harry, D.G. and Gozdzik, J.S. 1988. Ice wedges: growth, thaw transformation, and palaeoenvironmental significance. *Journal of Quaternary Science*, **3**, 39-55.

Harry, D.G., French, H.M. and Pollard, W.H. 1988. Massive ground ice and ice-cored terrain near Sabine Point, Yukon Coastal Plain. *Canadian Journal of Earth Sciences*, **25**, 1846-1856.

Hart, J.K., Hindmarsh, R.C.A. and Boulton, G.S. 1990. Styles of subglacial glaciotectonic deformation within the context of the Anglian Ice-sheet. *Earth Surface Processes and Landforms*, **15**, 227-241.

Healy, T.R. 1975. Thermokarst - a mechanism of de-icing ice-cored moraines. *Boreas*, **4**, 19-23.

Hill, P.R., Mudie, P.J., Moran K. and Blasco, S.M. 1985. A sea-level curve for the Canadian Beaufort Shelf. *Canadian Journal of Earth Sciences*, **22**, 1383-1393.

Hopkins, D.M. 1982. Aspects of the paleogeography of Beringia during the late Pleistocene. In: (eds D.M. Hopkins, J.V. Matthews Jr., C.E. Schweger and S.B. Young) *Paleoecology of Beringia*, Academic Press, New York, p.3-28.

Hopkins, D.M. and Kidd, J.G. 1988. Thaw lake sediments and sedimentary environments In: *Permafrost, Fifth International Conference, Proceedings, vol. 1*, Tapir, Trondheim, p.790-795.

Hussey, K.M. and Michelson, R.W. 1966. Tundra relief features near Point Barrow, Alaska. *Arctic*, **19**, 162-184.

Ivanov, M. 1984. *Cryogenous Structure of Quaternary Deposits of the Lena-Aldan Depression*. Novosibirsk, Izdalielstova "Nauka", 124p. (In Russian)

Jahn, A. 1975. *Problems of the Periglacial Zone* (Zagadnienia strefy peryglacjalnef). Panstwowe wydawnictwo Naukowe, Warsaw, 223p.

Jahn, A. 1983. Soil wedges on Spitsbergen. In: *Proceedings, Fourth International Permafrost Conference*, Fairbanks, Alaska, 535-530 National Academy Press, Washington, D.C.

Jetchick, E. and Allard, M. 1990. Soil wedge polygons in northern Québec: description and paleoclimatic significance. *Boreas*, **19**, 353-367.

Johnson, P.G. 1992. Stagnant glacier ice, St. Elias Mountains, Yukon. *Geografiska Annaler*, **74A**, 13-19.

Johnson, W.H. 1990. Ice-wedge casts and relict patterned ground in central Illinois and their environmental significance. *Quaternary Research*, **33**, 51-72.

Johnsson, G. 1959. True and false ice-wedges in southern Sweden. *Geografiska Annaler*, **41**, 15-33.

Johnston, G. H. 1981. *Permafrost: Engineering Design and Construction*. John Wiley & sons, Toronto, 540p.

Judge, A. 1986. Permafrost distribution and the Quaternary history of the Mackenzie-Beaufort region: a geothermal perspective. In: (eds J.A. Heginbottom and J-S Vincent) *Correlation of Quaternary Deposits and Events Around the Margin of the Beaufort Sea*, Geological Survey of Canada Open File Report **1237**, p. 41-45.

Kachurin, S.P.1962. Thermokarst within the territory of the USSR. *Biuletyn Peryglacjalny*, **11**, 49-55.

Katasonov, E.M. 1969. Composition and cryogenic structure of permafrost. In: *Permafrost Investigations in the Field*, Technical Translation **1358**, National Research Council of Canada, Ottawa, p.25-36.

Katasonov, E.M. 1975. Frozen-ground and facial analysis of Pleistocene deposits and paleogeography of central Yakutia. *Biuletyn Peryglacjalny*, **24**, 33-40.

Katasonov, E.M. 1978. Permafrost-facies analysis as the main method of cryolithology. In: *Permafrost:USSR Contribution to the Second International Conference*, Yakutsk, U.S.S.R. National Academy of Sciences, Washington D.C. p.171-176.

Katasonov, E.M. and Ivanov, M.S. 1973. *Cryolithology of central Yakutia*. Guidebook, Permafrost: Second International Conference, Yakutsk, USSR Academy of Sciences Yakutsk, 38p.

Kaplanskaya, F.A. and Tarnogradskiy, V.D. 1986. Remnants of the Pleistocene ice sheets in the permafrost zone as an object for paleoglaciological research. *Polar Geography and Geology*, **10**, 257-266.

Kelling, G. and Walton, E.K. 1957. Load cast structures: their relationship to upper surface structures and their mode of formation. *Geological Magazine*, **94**, 481-490.

Klassen, R.W. 1979. Thermokarst terrain near Whitehorse, Yukon Territory. In: *Current Research, Part A*, Geological Survey of Canada, Paper **79-1A**, p.385-388.

Kolstrup, E. 1985. Late Pleistocene periglacial conditions in Blaksmark near Varde (Denmark). *Geologie en Mijnbouw*, **64**, 263-269.

Kolstrup, E. 1987. Tre eksempler på involutioner nær Varde (Three examples of involutions near Varde). *Dansk Geologisk Forening*, Årsskrift for 1986, 67-74.

Kudriavtsev, V.A. (ed) 1978. *Obshcheye Merslotovedeniya (Geokriologiya)*(General Permafrost Science) Izd.2, (edu 2) moskva (Moscow), Izdatel'stvo Moskovskogo Universiteta (Moscow University Editions), 404p. (In Russian)

Kuenen, Ph. H. 1958. Experiments in geology. *Transactions of the Geological Society of Glasgow*, **23**, 1-28.

Kurfurst, P.J. (ed) 1987. *Geotechnical Investigations of Northern Richards Island, N.W.T.*. Geological Survey of Canada, Open File **1707**, 146p.

Kurfurst, P.J. and Dallimore, S.R. 1991. Engineering geology of nearshore areas off Richards Island, N.W.T.: a comparison of stable and actively eroding coastlines. *Canadian Geotechnical Journal*, **28**, 179-188.

Lawrence, D.E. and Proudfoot, D.A. 1977. *Mackenzie Valley Geotechnical Data Bank.* Geological Survey of Canada, Open Files **421-425**, p.24.

Lawson, D.E. 1979. Sedimentological analysis of the western terminus region of the Matanuska Glacier, Alaska. *Cold Regions Research and Engineering Laboratory Report*, **79-9**.

Lawson, D.E. 1981. Distinguishing characteristics of diamictons at the margin of the Matanuska Glacier, Alaska. *Annals of Glaciology*, **2**, 78-84.

Lawson, D.E. 1982. Mobilization, movement and deposition of active subaerial sediment flows, Matanuska Glacier, Alaska. *Journal of Geology*, **90**, 279-300.

Lawson, D.E. 1983. Ground ice in perennially frozen sediments, Northern Alaska. In: *Permafrost: Fourth International Conference, Proceedings*, Fairbanks, Alaska, National Academy Press, Washington D.C. p. 695-700.

Lawson, D.E. 1986. Response of permafrost terrain to disturbance: a synthesis of observations from northern Alaska, U.S.A.. *Arctic and Alpine Research*, **18**, 1-17.

Lawson, D.E. 1988. Glacigenic resedimentation: classification concepts and application to mass-movement processes and deposits. In: (eds R.P. Goldthwait and C.L. Matsch) *Genetic Classification of Glacigenic Deposits*, Balkema, Rotterdam, p.147-169.

Leeder, M.R. 1982. *Sedimentology: Process and Product.* Allen & Unwin, London, 344p.

Lewkowicz, A.G. 1986. Rates of short-term ablation of exposed ground ice, Banks Island, Northwest Territories, Canada. *Journal of Glaciology*, **32**, 511-519.

Lewkowicz, A.G. 1987. Nature and importance of thermokarst processes, Sand Hills Moraine, Banks Island, Canada. *Geografiska Annaler*, **69A**, 321-327.

Lewkowicz, A.G. 1988. Slope processes. In: (ed. M.J. Clark) *Advances in Periglacial Geomorphology*, John Wiley & Sons, Chichester, p.325-368.

Linnell, K.A. and Kaplar, C.W. 1966. Description and classification of frozen soils. In: *Proceedings, Permafrost International Conference*, Lafayette, In: National Academy of Science-National Research Council Publication **1287**, p.481-487.

Lowe, D.R. 1975. Water escape structures in coarse-grained sediments. *Sedimentology*, **22**, 157-204.

Maarleveld, G.C. 1976. Periglacial phenomena and the mean annual temperature during the last glacial time in the Netherlands. *Biuletyn Peryglacjalny*, **26**, 57-78.

Maarleveld, G.C. 1981. Summer thaw depths in cold regions and fossil cryoturbation. *Geologie en Mijnbouw*, **60**, 347-352.

Mackay, J.R. 1956a. Deformation by glacier-ice at Nicholson Peninsula, N.W.T.. *Arctic*, **9**, 218-228.

Mackay, J.R. 1956b. Notes on oriented lakes of the Liverpool Bay area, Northwest Territories. *Revue Canadienne de Géographie*, **10**,169-173.

Mackay, J.R. 1963. *The Mackenzie Delta area, N.W.T.* Geographical Branch, Department of Mines and Technical Surveys, Canada, Memoir **8**, 202p.

Mackay, J.R. 1966. Segregated epigenetic ice and slumps in permafrost, Mackenzie Delta area, N.W.T. *Geographical Bulletin*, **8**, 59-80.

Mackay, J.R. 1970. Disturbances to the tundra and forest tundra environment of the western Arctic. *Canadian Geotechnical Journal*, **7**, 420-432.

Mackay, J.R. 1971. The origin of massive icy beds in permafrost, western arctic coast, Canada. *Canadian Journal of Earth Sciences*, **8**, 397-422.

Mackay, J.R. 1972a. The world of underground ice. *Annals of the American Association of Geographers*, **62**, 1-22.

Mackay, J.R. 1972b. Offshore permafrost and ground ice, southern Beaufort Sea, Canada. *Canadian Journal of Earth Sciences*, **9**, 1550-1561.

Mackay, J.R. 1973. Problems in the origin of massive icy beds, Western Arctic, Canada. In: *Permafrost: The North American Contribution to the Second International Conference*. National Academy of Sciences, Washington, D.C. p. 223-228.

Mackay, J.R. 1974a. Reticulate ice veins in permafrost, Northern Canada. *Canadian Geotechnical Journal*, **11**, 230-237.

Mackay, J.R. 1974b. The rapidity of tundra polygon growth and destruction, Tuktoyaktuk Peninsula-Richards Island area, N.W.T.. In: *Current Research, Part A*, Geological Survey of Canada, Paper **74-1A**, p.391-392.

Mackay, J.R. 1975a. Relict ice wedges, Pelly Island, N.W.T.. In: *Current Research, Part A*, Geological Survey of Canada, Paper **75-1A**, p.469-470.

Mackay, J.R. 1975b. The stability of permafrost and recent climatic change in the Mackenzie Valley, N.W.T.. In: *Current Research, Part B*, Geological Survey of Canada, Paper **75-1B**, p.173-176.

Mackay, J.R. 1976. Pleistocene permafrost, Hooper Island, Northwest Territories. In: *Current Research, Part A*, Geological Survey of Canada, Paper **76-1A**, p.17-18.

Mackay, J.R. 1977. Changes in the active layer from 1968 to 1976 as a result of the Inuvik fire. In: *Current Research, Part B*, Geological Survey of Canada, Paper **77-1B**, p.273-275.

Mackay, J.R. 1978. Freshwater shelled invertebrate indicators of paleoclimate in northwestern Canada during late glacial times: Discussion. *Canadian Journal of Earth Sciences*, **15**, 461-462.

Mackay, J.R. 1979. Pingos of the Tuktoyaktuk Peninsula area, Northwest Territories. *Géographie physique et Quaternaire*, **33**, 3-61.

Mackay, J.R. 1980. The origin of hummocks, western Arctic coast, Canada. *Canadian Journal of Earth Sciences*, **17**, 996-1006.

Mackay, J.R. 1981. Active layer slope movement in a continuous permafrost environment, Garry Island, Northwest Territories, Canada. *Canadian Journal of Earth Sciences*, **18**, 1666-1680.

Mackay, J.R. 1983. Oxygen isotope variations in permafrost, Tuktoyaktuk Peninsula area, Northwest Territories. In: *Current Research, Part B*, Geological Survey of Canada, Paper **83-1B**, p.67-74.

Mackay, J.R. 1984. The direction of ice-wedge cracking in permafrost: downward or upward? *Canadian Journal of Earth Sciences*, **21**, 516-524.

Mackay, J.R. 1985. Permafrost growth in recently drained lakes, western Arctic coast. In: *Current Research, Part B*, Geological Survey of Canada, Paper **85-1B**, p.177-189.

Mackay, J.R. 1986a. Fifty years (1935 to 1985) of coastal retreat west of Tuktoyaktuk, District of Mackenzie. In: *Current Research, Part A*, Geological Survey of Canada, Paper **86-1A**, p.727-735.

Mackay, J.R. 1986b. The permafrost record and Quaternary history of Northwestern Canada. In: (eds J.A. Heginbottom and J-S Vincent) *Correlation of Quaternary Deposits and Events Around the Margin of the Beaufort Sea*, Geological Survey of Canada Open File Report **1237**, p.38-40.

Mackay, J.R. 1986c. The first 7 years (1978-1985) of ice wedge growth, Illisarvik experimental drained lake site, western Arctic coast. *Canadian Journal of Earth Sciences*, **23**, 1782-1795.

Mackay, J.R. 1988. Catastrophic lake drainage, Tuktoyaktuk Peninsula area, District of Mackenzie. In: *Current Research, Part D*, Geological Survey of Canada, Paper **88-1D**, p.83-90.

Mackay, J.R. 1989. Massive ice: some field criteria for the identification of ice types. In: *Current Research, Part G*, Geological Survey of Canada, Paper **89-1G**, p.5-11.

Mackay, J.R. 1990. Some observations on the growth and deformation of epigenetic, syngenetic and anti-syngenetic ice wedges. *Permafrost and Periglacial Processes*, **1**, 15-29.

Mackay, J.R. 1992a. The frequency of ice-wedge cracking (1967-1987) at Garry Island, western Arctic coast, Canada. *Canadian Journal of Earth Sciences*, **29**, 236-248.

Mackay, J.R. 1992b. Lake stability in an ice-rich permafrost environment: examples from the western Arctic coast. In (eds R.D. Robarts and M.L. Bothwell) *Aquatic Ecosystems in Semi-arid Regions: Implications for Resource Management*, N.H.R.I. Symposium Series **7**, Environment Canada, Saskatoon, p.1-26.

Mackay, J.R. and Dallimore, S.R. 1992. Massive ice of the Tuktoyaktuk area, western Arctic coast, Canada. *Canadian Journal of Earth Sciences*, **29**, 1235-1249.

Mackay, J.R. and Lavkulich, L.M.1974. Ionic and oxygen isotopic fractionation in permafrost growth. In: *Current Research, Part B*, Geological Survey of Canada, Paper **74-1B**, p.255-256.

Mackay, J.R. and Matthews, J.V. Jr. 1983. Pleistocene ice and sand wedges, Hooper Island, Northwest Territories. *Canadian Journal of Earth Sciences*, **20**, 1087-1097.

Mackay, J.R., Rampton, V.N. and Fyles, J.G. 1972. Relic Pleistocene permafrost, western Arctic, Canada. *Science*, **176**, 1321-1323.

Mathews, W. H. and Mackay, J.R. 1960. Deformation of soils by glacier ice and the influence of pore pressure and permafrost. *Royal Society of Canada, Transactions*, **LIX**, Series III, Section 4, 27-36.

McCulloch, D.S. and Hopkins, D.M. 1966. Evidence for an early recent warm interval in northwestern Alaska. *Geological Society of America Bulletin*, **77**, 1089-1108.

McDonald, B.C. and Shilts, W.W. 1975. Interpretation of faults in glaciofluvial sediments. In: (eds A.V. Jopling and B.C. McDonald) *Glaciofluvial and glaciolacustrine Sedimentation*, Society of Economic Paleontologists and Mineralogists, Special Publication **23**, p.123-131.

McKee, E.D. and Bigarella, J.J. 1972. Deformational structures in Brazilian coastal dunes. *Journal of Sedimentary Petrology*, **42**, 670-681.

McKenzie, G.D. and Goodwin, R.G. 1987. Development of collapsed glacial topography in the Adams Inlet area, Alaska, USA. *Journal of Glaciology*, **33**, 55-59.

Miall, A.D. (ed.) 1978. *Fluvial Sedimentology*. Canadian Society of Petroleum Geologists Memoir **5**, Calgary, 859p.

Miall, A.D. 1985. Architectural-element analysis: a new method of facies analysis applied to fluvial deposits. *Earth Science Reviews*, **22**, 261-308.

Michel, F.A. 1990. Isotopic composition of ice-wedge ice in northwestern Canada. In: *Permafrost Canada: Proceedings of the Fifth Canadian Permafrost Conference*, Collection Nordicana, Centre d'études nordiques, Université Laval, Cité Universitaire, Québec, Canada, National Research Council of Canada, p.5-9.

Michel, F.A. and Fritz, P. 1982. Significance of isotope variations in permafrost waters at Illisarvik, N.W.T. In: (ed. H.M. French) *The R.J.E. Brown Memorial Volume, Proceedings of the Fourth Canadian Permafrost Conference*, National Research Council of Canada, Ottawa, p.173-181.

Michel, F.A., Fritz, P. and Drimmie, R.J. 1989. Evidence of climatic change from oxygen and carbon isotope variations in sediments of a small arctic lake, Canada. *Journal of Quaternary Science*, **4**, 201-209.

Mills, P.C. 1983. Genesis and diagnostic value of soft-sediment deformation structures: a review. *Sedimentary Geology*, **35**, 83-104.

Morgenstern, N.R. and Nixon, J.F. 1971. One-dimensional consolidation of thawing soils. *Canadian Geotechnical Journal*, **8**, 558-565.

Müller, F. 1962. Analysis of some stratigraphic observations and radiocarbon dates from two pingos in the Mackenzie Delta area, N.W.T.. *Arctic*, **15**, 278-88.

Murton, J.B. and French, H.M. 1993. Sand wedges and permafrost history, Crumbling Point, Pleistocene Mackenzie Delta, Canada. In: *Permafrost: VIth International Conference Proceedings*, July 5-9 1993, Beijing, China (in press).

National Wetlands Working Group, 1988. *Wetlands of Canada*. Ecological Land Classification Series, No.**24**. Sustainable Development Branch, Environment Canada, Ottawa, Ontario, and Polyscience Publications Inc. Montreal, Quebec, 452p.

Nekrasov, I.A. and Gordeyev, P.P. 1973. *The North-east of Yakutia*. Guidebook, Permafrost: Second International Conference, Yakutsk, USSR Academy of Sciences Yakutsk, 46p.

Nelson, R.E. 1982. *Late Quaternary Environments of the Western Arctic Slope, Alaska.* Unpublished PhD Thesis, University of Washington, Seattle, 146p.

Nemec, W. and Steel, R.J. 1984. Alluvial and coastal conglomerates: their significant features and some comments on gravelly mass-flow deposits. In: (eds E.H. Koster and R.J.Steel) *Sedimentology of Gravels and Conglomerates*, Canadian Society of Petroleum Geologists, Memoir **10**, p.1-31.

Nisbet, E.G. 1989. Some northern sources of atmospheric methane: production, history and future implications. *Canadian Journal of Earth Sciences*, **26**, 1603-1611.

Paterson, W.S.B. 1981. *The Physics of Glaciers*. Pergamon Press, Oxford, 380p.

Paul, M.A. and Eyles, N. 1990. Constraints on the preservation of diamict facies (melt-out tills) at the margins of stagnant glaciers. *Quaternary Science Reviews*, **9**, 51-69.

Pécsi, M. 1969. Genetic classification of slope sediments. *Biuletyn Peryglacjalny*, **18**, 15-27.

Permafrost Subcommittee, Associate Committee on Geotechnical Research, 1988. *Glossary of Permafrost and Related Ground-ice Terms*. Associate Committee on Geotechnical Research, National Research Council of Canada, Ottawa, 156p.

Péwé, T.L. 1954. Effect of permafrost upon cultivated fields. *United States Geological Survey, Bulletin* **989-F**, 315-351.

Péwé, T.L. and Sellmann, P.V. 1973. Geochemistry of permafrost and Quaternary stratigraphy. In: *Permafrost: North American Contribution, Second International Permafrost Conference, Yakutsk, U.S.S.R.* National Academy of Science Publication **2115**, p.166-170.

Péwé, T.L., Church, R.E. and Andresen, N.J. 1969. Origin and palaeoclimatic significance of large scale polygons in the Donnely Dome area, Alaska. *Geological Society of America Special Paper* **109**, 87p.

Pissart, A., Vincent, J-S. and Edlund, S.A. 1977. Dépôts et phénomènes éoliens, sur l'île de Banks, Territoires du Nord-Ouest, Canada. *Canadian Journal of Earth Sciences*, **14**, 2462-2480.

Pollard, W.H. and French, H.M. 1980. A first approximation of the volume of ground ice, Richards Island, Pleistocene Mackenzie Delta, Northwest Territories, Canada. *Canadian Geotechnical Journal*, **17**, 509-516.

Popov, A.I. 1956. Le thermokarst. *Biuletyn Peryglacjalny*, **4**, 319-330.

Popov, A.I. 1978a. Cryolithogenesis, the composition and structure of frozen rocks, and ground ice (the current state of the problem). *Biuletyn Peryglacjalny*, **27**, 155-169.

Popov, A.I. 1978b. Cryolithogenesis. In: *USSR Contribution, Second International Conference on Permafrost*, Yakutsk, U.S.S.R. National Academy of Sciences, Washington D.C. p.181-184.

Popov, A.I. and Katasonov, E.M. 1978. Genesis, composition and structure of permafrost and ground ice. In: *USSR Contribution, Second International Conference on Permafrost*, Yakutsk, U.S.S.R. National Academy of Sciences, Washington D.C. p.713-724.

Popov, A.I., Rozenbaum, G.E., Kuznetsova, T.P., Tumel', N.V., Shpolyanskaya, N.A. Krylova, V.A. and Yanpol'skaya, S.N. (Faculty of Geography, Moscow State University) 1985b. *Map of Cryolithology of the U.S.S.R.* scale 1: 4,000,000. Ministry of Higher and Secondary Special Education of the U.S.S.R. Moscow. (Text translated into English by Secretary of State, Ottawa, Bureau No.**2643327**)

Popov A.I., Rozenbaum, G.E. and Tumel, N.V. 1985a. *Cryolithology.* Izdalielstova Moskovskogo Universitieta, 238p. (in Russian)

Porsild, A.E. 1938. Earth mounds in unglaciated Arctic northwest America. *Geographical Review*, **28**, 46-58.

Rampton, V.N. 1974. The influence of ground ice and thermokarst upon the geomorphology of the Mackenzie-Beaufort region. In: (eds B. D. Fahey and R.D. Thompson) *Research in Polar and Alpine Geomorphology*, Proceedings of the Third Guelph Symposium on Geomorphology, Geo-Abstracts, Norwich, p.43-59.

Rampton, V.N. 1982. *Quaternary Geology of the Yukon Coastal Plain*. Geological Survey of Canada Bulletin, **317**, 49p.

Rampton, V.N. 1988. *Quaternary Geology of the Tuktoyaktuk Coastlands, Northwest Territories*. Geological Survey of Canada, Memoir **423**, 98p.

Rampton, V.N. and Bouchard, M. 1975. Surficial geology of Tuktoyaktuk, District of Mackenzie. *Geological Survey of Canada, Paper* **74-53**.

Rampton, V.N. and Mackay, J.R. 1971. Massive ice and icy sediments throughout the Tuktoyaktuk Peninsula, Richards Island, and nearby areas, District of Mackenzie. *Geological Survey of Canada, Paper* **71-21**, 16p.

Reading, H. G. 1986. Facies. In: (ed H.G. Reading) *Sedimentary Environments and Facies*. Blackwell, Oxford, p. 4-19.

Reineck, H.-E. and Singh, I.B. 1980. *Depositional Sedimentary Environments*. Springer-Verlag, Berlin, 551p.

Reinson, G.E. 1984. Barrier-island and associated strand-plain systems. In: (ed. R.G. Walker) *Facies Models*, Geoscience Canada Reprint Series 1, Ainsworth Press, Kitchener, Ont. p.119-140.

Ritchie, J.C. 1984. *Past and Present Vegetation of the Far Northwest of Canada*. University of Toronto Press, Toronto, 251p.

Romanovskii, N.N. 1973. Regularities in formation of frost fissures and development of frost-fissure polygons. *Biuletyn Peryglacjalny*, **23**, 237-277.

Romanovskii, N.N. 1985. Distribution of recently active ice and soil wedges in the U.S.S.R.. In: (eds M. Church and O. Slaymaker) *Field and Theory: Lectures in Geocryology*, University of British Columbia Press, Vancouver, p.154-165.

Rose, J. and Allen, P. 1977. Middle Pleistocene stratigraphy in south-east Suffolk. *Journal of the Geological Society of London*, **133**, 83-102.

Rose, J., Boardman, J., Kemp. R.A. and Whiteman, C.A. 1985a. Palaeosols and their interpretation of the British Quaternary stratigraphy. In: (eds K.S. Richards, R.R. Arnett and S. Ellis) *Geomorphology and Soils*, George Allen & Unwin, London, p.348-375.

Rose, J., Boardman, J., Kemp. R.A. and Whiteman, C.A. 1985b. The early Anglian Barham Soil of eastern England. In: (ed. J. Boardman) *Soils and Quaternary Landscape Evolution*, Wiley, Chichester, p.197-229.

Rust, B.R. and Nanson, G.C. 1989. Bedload transport of mud as pedogenic aggregates in modern and ancient rivers. *Sedimentology*, **36**, 291-306.

Rust, B.R. and Romanelli, R. 1975. Late Quaternary subaqueous outwash deposits near Ottawa, Canada. In: (eds A.V. Jopling and B.C. McDonald) *Glaciofluvial and Glaciolacustrine Sedimentation*, Society of Economic Paleontologists and Mineralogists Special Publication **23**, Tulsa, p.177-191.

Sellmann, P.V., Brown, J., Lewellen, R.I., McKim, H. and Merry, C. 1975. *The classification and geomorphic implications of thaw lakes on the Arctic Coastal Plain.* Alaska, U.S. Army, Cold Regions Research and Engineering Laboratory, Hanover New Hampshire Research Report **344**, 24p.

Sharp, R. 1942. Periglacial involutions in north-eastern Illinois. *Journal of Geology*, **50**, 113-133.

Shaw, 1977. Till body morphology and structure related to glacier flow. *Boreas*, **6**, 189-201.

Shaw, J. 1979. Genesis of the Sveg tills and Rogen moraines of central Sweden: a model of basal melt out. *Boreas*, **8**, 409-426.

Shaw, J. 1982. Melt-out till in the Edmonton area, Alberta, Canada. *Canadian Journal of Earth Sciences*, **19**, 1548-1569.

Shaw, J. 1985. Subglacial and ice marginal environments. In: (eds G.M. Ashley, J. Shaw, N.D. Smith) *Glacial Sedimentary Environments*, Society of Economic Paleontologists and Mineralogists Short Course 16, SEPM, Tulsa, OK, p.7-84.

Shaw, J. 1987. Glacial sedimentary processes and environmental reconstruction based on lithofacies. *Sedimentology*, **34**, 103-116.

Shaw, J. 1988. Discussion: coarse-grained sediment flow facies in a large supraglacial lake. *Sedimentology*, **35**, 527-529.

Sher, A.V., Kaplina, T.N., Giterman, R.E., Lozhkin, A.V., Arkhangelov, A.A., Kiselyov, S.V. Kouznetsov, Yu. V., Virina, E.I. and Zazhigin, V.S. 1979. *Late Cenozoic of the Kolyma Lowland*. Tour XI Guidebook, XIV Pacific Science Congress, August 1979, Khaborovsk, Academy of Sciences, USSR, Moscow, 115p.

Shilts, W.W. 1978. Nature and genesis of mudboils, central Keewatin, Canada. *Canadian Journal of Earth Sciences*, **15**, 1053-1068.

Shur, Yu. L. 1988. The upper horizon of permafrost soils. In: *Permafrost, Fifth International Conference, Proceedings, vol. 1*, Tapir, Trondheim, p.867-871.

Shumskii, P.A. 1964. *Ground (subsurface) Ice*. National Research Council of Canada, Technical Translation **1130**, 118p.

Smith, M.W. 1976. *Permafrost in the Mackenzie Delta, Northwest Territories*. Geological Survey of Canada, Paper 75-28, 34p.

Smith, M.W. 1986. The significance of climate change for the permafrost environment. In: (ed. H. M. French) *Climate Change Impacts in the Canadian Arctic*, Proceedings of a Canadian Climate Program Workshop, March 3-5 1986, Geneva Park, Ontario, p. 67-81.

Soloviev, P.A. 1973. *Alass Thermokarst Relief of Central Yakutia*. Guidebook, Permafrost: Second International Conference, Yakutsk, USSR, 48p.

Sparks, B.W., Williams, R.G.B. and Bell, F.G. 1972. Presumed ground-ice depressions in East Anglia. *Proceedings, Royal Society London*, Series A, **327**, 329-42.

Stearns, S.R. 1966. *Permafrost (perennially frozen ground)*. US Army Cold Regions Research and Engineering Laboratory, Cold Regions Science and Engineering Monograph **1-A2**, 77p.

Strunk, H. 1983. Pleistocene diapiric upturnings of lignites and clayey sediments as periglacial phenomena in central Europe. In: *Permafrost: Fourth International Conference, Proceedings*, Fairbanks, Alaska, U.S. National Academy Press, Washington, D.C. p.1200-1204.

Swift, D.J.P., Niedoroda, A.W., Vincent, C.E. and Hopkins, T.S. 1985. Barrier island evolution, middle Atlantic shelf, USA, part 1: shoreface dynamics. *Marine Geology*, **63**, 331-361.

Tedrow, J.C.F. 1969. Thaw lakes, thaw sinks and soils in northern Alaska. *Biuletyn Peryglacjalny*, **20**, 337-345.

Thorson, R.M., Clayton W.S. and Seeber, L. 1986. Geologic evidence for a large prehistoric earthquake in eastern Connecticut. *Geology*, **14**, 463-467.

Tomirdiaro, S.V. 1982. Evolution of lowland landscapes in northeastern Asia during late Quaternary time. In: (eds D.M. Hopkins, J.V. Matthews Jr., C.E. Schweger and S.B. Young) *Paleoecology of Beringia*, Academic Press, New York, p.29-37.

Tomirdiaro, S.V. and Ryabchun, V.K. 1978. Lake thermokarst on the lower Anadyr' Lowland. In: *USSR Contribution, Second International Conference on Permafrost*, Yakutsk, U.S.S.R. National Academy of Sciences, Washington D.C. p.94-100.

Tsytovich, N.A. 1975. *Mekhanika Merzlykh gruntov (The Mechanics of Frozen Ground)*. Bysshaya Shkola Press, Moscow, 446p. (In Russian). Translation by Scripta Technica (eds G.K. Swinzow and G.P. Tschebotarioff), Scripta/McGraw-Hill, New York, N.Y. 1975, 426p.

Vandenberghe, J. 1983a. Ice-wedge casts and involutions as permafrost indicators and their stratigraphic position in the Weichselian. In: *Permafrost: Fourth International Conference, Proceedings*, Fairbanks, Alaska, National Academy Press, Washington D.C. p.1298-1302.

Vandenberghe, J. 1983b. Some periglacial phenomena and their stratigraphical position in the Weichselian deposits in the Netherlands. *Polarforschung*, **53**, 97-107.

Vandenberghe, J. 1988. Cryoturbations. In: (ed. M.J. Clark) *Advances in Periglacial Geomorphology*, John Wiley & Sons, Chichester, p.179-198.

Vandenberghe, J. and Broek, P. 1982. Weichselian convolution phenomena and processes in fine sediments. *Boreas*, **11**, 299-315.

Van der Hammen, T, Maarleveld, G.C., Vogel, J.C. and Zagwijn, W.H. 1967. Stratigraphy, climatic succession and radiocarbon dating of the last glacial in the Netherlands. *Geologie en Mijnbouw*, **46**, 79-95.

Van Loon, A.J. and Brodzikowski, K. 1987. Problems and progress in the research on soft-sediment deformations. *Sedimentary Geology*, **50**, 167-193.

Vialov, S.S. 1965. *Rheological Properties and Capacity of Frozen Soils*. U.S. Army, Cold Regions Research and Engineering Laboratory, Hanover, New Hampshire, Translation **74**, 1965, 219p.

Vincent, J.-S. 1983. *La géologie du Quaternaire et la géomorphologie de Lîle Banks, Arctique canadien*. Geological survey of Canada, Memoir **405**, 118 p.

Vincent, J-S. 1989. Quaternary geology of the northern Canadian Interior Plains. In: (ed. R.J. Fulton) *Quaternary Geology of Canada and Greenland*, Geological Survey of Canada, Geology of Canada, no. **1**, p.100-137.

Vincent, J-S., Carter, L.D., Matthews, J.V. Jr. and Hopkins, D.M. 1989. Joint Canadian-American investigation of the Cenozoic geology of the lowlands bordering the Beaufort Sea. In: (eds L.D. Carter, T.D. Hamilton and J.P. Galloway) *Proceedings of a cooperative workshop between earth Scientists from Canada and the United States of America*, U.S. Geological Survey Circular **1026**, p.7-9.

Van Vliet-Lanoe, B. 1991. Differential frost heave, load casting and convection: converging mechanisms. a discussion of the origin of cryoturbations. *Permafrost and Periglacial Processes*, **2**, 123-139.

Walker, R.G. 1992. Facies, facies models and modern stratigraphic concepts. In: (eds R.G. Walker and N.P. James) *Facies Models: Response to Sea Level Change*, Geological Association of Canada, p.1-14.

Walker, R.G. and James, N. P. (eds) 1992. *Facies Models: Response to Sea Level Change*. Geological Association of Canada, 409p.

Wallace, R.E. 1948. Cave-in lakes in the Nabesna, Chisana, and Tanana River valleys, Eastern Alaska. *Journal of Geology*, **56**, 171-181.

Washburn, A.L. 1980a. *Geocryology*. Wiley, New York, 406p.

Washburn, A.L. 1980b. Permafrost features as evidence of climatic change. *Earth Science Reviews*, **15**, 327-392.

Washburn, A.L. 1989. Near surface soil displacement in sorted circles, Resolute area, Cornwallis Island, Canadian High Arctic. *Canadian Journal of Earth Sciences*, **26**, 941-955.

Watson, R.A. 1980. Landform development on moraines of the Klutlan Glacier, Yukon Territory, Canada. *Quaternary Research*, **14**, 50-59.

West, R.G. 1977. *Pleistocene Geology and Biology*. Longman, London, 440p.

West, R.G., Dickson, C.A., Catt, J.A., Weir, A.H. and Sparks, B.W. 1974. Late Pleistocene deposits at Wretton, Norfolk: II. *Philosophical Transactions of the Royal Society of London*, **B267**, 337-420.

Whitten, D.G.A. and Brooks, J.R.V. 1972. *The Penguin Dictionary of Geology*. Middlesex, Penguin, 495p.

Williams, G.E. and Tonkin, D.G. 1985. Periglacial structures and palaeoclimatic significance of a late Precambrian block field in the Cattle Grid copper mine, Mount Gerson, South Australia. *Australian Journal of Earth Sciences*, **32**, 287-300.

Williams, J.R. and Yeend, W.E. 1979. Deep thaw lake basins of the inner Arctic Coastal Plain, Alaska. *United States Geological Survey Circular* **804-B**, B35-B37.

Williams, P.J. 1986. *Pipelines and Permafrost, Science in a Cold Climate*. Carleton University Press, Ottawa, 137p.

Williams, P.J. and Smith, M.W. 1989. *The Frozen Earth*. Cambridge University Press, Cambridge, 306p.

Williams, R.G.B. 1975. The British climate during the last glaciation: an interpretation based on periglacial phenomena. In: (eds A.E. Wright and F. Moseley) *Ice Ages: Ancient and Modern*, Geological Journal Special Publication **6**, Seel House Press, Liverpool, p.95-120.

Woodcock, N.H. 1991. Geologists and global warming. *Geoscientist*, **1**, 8-11.

Worsley, P. 1987. Permafrost stratigraphy in Britain: a first approximation. In: (ed. J. Boardman) *Periglacial Processes in Britain and Ireland*, Cambridge University Press, Cambridge, p.89-99.

Young, G.M. and Long, D.G.F. 1976. Ice-wedge casts from the Huronian Ramsey Lake Formation (>2,300 m.y. old) near Espanola, Ontario, Canada. *Palaeogeography, Palaeoclimatology, Palaeoecology*, **19**, 191-200.

Zoltai, S.C. and Tarnocai, C. 1975. Perennially frozen peatlands in the western Arctic and Subarctic of Canada. *Canadian Journal of Earth Sciences*, **12**, 28-43.

Zoltai, S.C. and Tarnocai, C. 1981. Some nonsorted patterned ground types in northern Canada. *Arctic and Alpine Research*, **13**, 139-151.